



Modelling Coastal Vulnerability

An integrated approach to coastal management
using Earth Observation techniques in Belize

Harry Cook

Swansea University

2023

Submitted to Swansea University in fulfilment of the requirements for the
Degree of Master of Science by Research in Earth Observation.

Copyright: The Author, Harry Cook, 2023.

Abstract

This thesis presents an adapted method to derive coastal vulnerability through the application of Earth Observation (EO) data in the quantification of forcing variables. A modelled assessment for vulnerability has been produced using the Coastal Vulnerability Index (CVI) approach developed by Gornitz (1991) and enhanced using Machine learning (ML) clustering. ML has been employed to divide the coastline based on the geotechnical conditions observed to establish relative vulnerability. This has been demonstrated to alleviate bias and enhanced the scalability of the approach – especially in areas with poor data coverage – a known hinderance to the CVI approach (Koroglu et al., 2019).

Belize provides a demonstrator for this novel methodology due to limited existing data coverage and the recent removal of the Mesoamerican Reef from the International Union for Conservation of Nature (IUCN) List of World Heritage In Danger. A strong characterization of the coastal zone and associated pressures is paramount to support effective management and enhance resilience to ensure this status is retained.

Areas of consistent vulnerability have been identified using the KMeans classifier; predominantly Caye Caulker and San Pedro. The ability to automatically scale to conditions in Belize has demonstrated disparities to vulnerability along the coastline and has provided more realistic estimates than the traditional CVI groups. Resulting vulnerability assessments have indicated that 19% of the coastline at the highest risk with a seaward distribution to high risk observed. Using data derived using Sentinel-2, this study has also increased the accuracy of existing habitat maps and enhanced survey coverage of uncharted areas.

Results from this investigation have been situated within the ability to enhance community resilience through supporting regional policies. Further research should be completed to test the robust nature of this model through an application in regions with different geographic conditions and with higher resolution input datasets.

Declarations

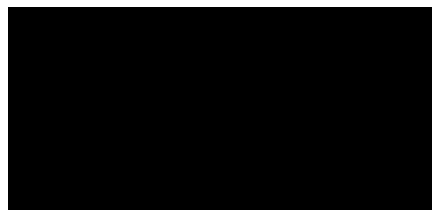
This work has not previously been accepted in substance for any degree and is not being concurrently submitted in candidature for any degree.

This thesis is the result of my own investigations, except where otherwise stated. Other sources are acknowledged by footnotes giving explicit references. A bibliography is appended.

I hereby give consent for my thesis, if accepted, to be available for photocopying and for inter-library loan, and for the title and summary to be made available to outside organisations.

The University's ethical procedures have been followed and, where appropriate, that ethical approval has been granted.

Signed:



Date: 05/05/2023

Contents

Abstract.....	ii
Declarations	iii
Acknowledgements.....	viii
List of figures.....	ix
List of tables.....	xii
List of abbreviations	xiii
PART I – INTRODUCTION	1
1. Modelling coastal vulnerability from space	1
1.1. Coastal areas in a changing climate	1
1.2. Case Study: Belize	3
1.3. Thesis aim	6
1.4. Thesis structure	7
PART II – LITERATURE REVIEW	8
2. Coastal hazards in Belize.....	8
2.1. The coastal zone	8
2.1.1. Physical environment.....	9
2.1.2. Anthropogenic activity.....	10
2.2. Managing coastal hazards in Belize	13
3. Coastal vulnerability in Belize	18
3.1. Geomorphology and geology	20
3.2. Oceanography.....	23
3.3. Topography	25
3.4. Wind exposure.....	26
4. Assessing vulnerability	27
4.1. The Coastal Vulnerability Index (CVI).....	27

4.2.	Limitations with the CVI.....	33
5.	Earth Observation (EO) in vulnerability mapping	35
5.1.	Sources	38
5.2.	Techniques	42
5.2.1.	Image classification	42
5.2.2.	Satellite Derived Bathymetry (SDB)	45
5.2.3.	Satellite altimetry	50
5.2.4.	Digital Elevation Models (DEMs).....	54
5.3.	Machine Learning	57
5.3.1.	Clustering algorithms.....	57
PART III – METHODS		62
6.	Methods	62
6.1.	Conceptual framework	62
6.2.	Data	66
6.3.	Primary data techniques	68
6.3.1.	Sentinel-2	68
6.3.2.	Supervised classification.....	69
6.3.3.	Satellite Derived Bathymetry (SDB)	70
6.4.	Secondary data techniques	74
6.4.1.	Digital Elevation Modelling (DEM).....	74
6.4.2.	Wave climatology modelling.....	75
6.4.3.	Wind intensity	75
6.4.4.	Tides.....	76
6.5.	Modelling approach.....	77
6.5.1.	Coastal sampling.....	77
6.5.2.	Assigning vulnerability groups with machine learning	79
6.5.3.	CVI Calculation	82

6.5.4. CVI Model Evaluation	82
PART IV – RESULTS	83
7. Characterisation of coastal vulnerability parameters.....	83
7.1. Geomorphology component.....	83
7.2. Marine slope component	87
7.3. Terrestrial slope component	92
7.4. Wave climatology component.....	93
7.5. Wind exposure component.....	97
8. Modelling of coastal vulnerability in Belize	99
8.1. Clustering of parameters	99
8.2. Spatial distribution of vulnerability.....	104
8.3. Validation of multi variate CVI model	108
PART V – DISCUSSION AND CONCLUSIONS	117
9. Uncertainties.....	117
9.1. Uncertainties in parameter derivation	119
9.1.1. Geomorphology component.....	119
9.1.2. Marine slope component.....	125
9.1.3. Terrestrial slope component.....	130
9.1.4. Wave climatology component	131
9.1.5. Wind exposure component	132
9.2. Uncertainties in the approach to modelling.....	136
9.2.1. Clustering.....	136
9.2.2. Scale.....	138
9.2.3. The CVI approach.....	139
9.2.4. Component assumptions	141
10. Analysis of vulnerable areas	143
11. Supporting policy: a use in Integrated Coastal Zone Management (ICZM)?.....	146

12. Recommendations.....	154
13. Conclusions.....	156
REFERENCES.....	159
APPENDIX.....	187

Acknowledgements

This thesis has been the result of two years of work. During this time, I have been fortunate enough to experience a great deal of support from a multitude of people without whom this thesis would not have been possible.

My profound thanks is extended to:

ARGANS Ltd. for supporting me with the initial project conception and for providing me with an experience and knowledge of Earth Observation through working across several marine projects. The technical experience in this role has provided me with the foundations to write this thesis and to which I am very grateful. I would specifically like to thank Jean Laporte for his technical advice and critical thoughts on my original project proposal.

My advisors at Swansea University – Professor Peter North and Dr Sietse Los – have been exceptional source of support and knowledge. This is especially appreciated through being largely provided remotely! Thank you for always being available for advice and support.

I am grateful also to Professor Eli Lazarus and Dr John Hiemstra for their time during my Viva exam. Their specialist expertise on Coastal Vulnerability and comments on the best ways to structure this thesis were certainly valued.

Finally, a big thanks to my family and friends who have listened to my many ramblings on vulnerability and have been a great source of encouragement for the last two years.

List of figures

Figure 1: Location of Belize and the Mesoamerican Reef Ecoregion.	4
Figure 2: Average annual occurrence of natural hazards in Belize (1980 – 2020).....	5
Figure 3: The coastal zone represents the area subjected to the interaction between land, sea and anthropogenic activity (Thia-Eng, 1993).	9
Figure 4: Areas of Belize affected by specific anthropogenic pressures (Verutes et al., 2016).	11
Figure 5: Extent of mangrove forest clearance from public EO data (Cherrington et al., 2020).	12
Figure 6: (a) Administrative districts in Belize. (b) Key stakeholders and their operating areas (Verutes et al., 2016).....	13
Figure 7: Location of Marine Protected Areas (MPAs), Belize (Graham et al., 2008).	14
Figure 8: Disaster Risk Management Cycle (Le Cozannet et al., 2020).....	15
Figure 9: Requirements for Earth Observation in decision frameworks for disaster management (Le Cozannet et al., 2020).....	16
Figure 10: Factors affecting coastal vulnerability (Noor & Maulud, 2022).....	19
<i>Figure 11: Schematic of the Belizean cross-shore habitats with corresponding bathymetry profiles (Guannel et al., 2016).</i>	<i>21</i>
Figure 12: Incident wave climate and distribution of coral impedance (McNeill et al., 2010).	23
Figure 13: Diurnal tidal range of the Caribbean Sea (Jevrejeva et al., 2020).....	24
Figure 14: Vulnerability groups and threshold ranges for each variable (Gornitz, 1990).....	28
Figure 15: (a) Distribution of vulnerability with respect to each parameter. (b) Increased accuracy resulting from the inclusion of weighted parameters in CVI assessment.....	30
Figure 16: Disparities to vulnerability assessments resulting from a difference in methods from Koroglu et al. (2019). (a) Lopez et al. (2016). (b) Thieler & Hammar-Klose (2000). (c) Shaw (1998). (d) Gornitz (1991).	32
Figure 17: The role of remote sensing in coastal monitoring programmes (Harvey et al., 2018).	36
Figure 18: Spatial and temporal resolutions of EO sensors (ESA, 2020).....	38
Figure 19: Appropriate spatial and temporal resolutions for analysis of coastal parameters (Phinn et al., 2010).....	40

Figure 20: Spectral band combinations of Sentinel-2 compared with Landsat (NASA, 2022).	41
Figure 21: Spectral endmembers of different land cover types (Kaab, 2014).	43
Figure 22: Random Forests decision tree architecture (Alshari & Gawali, 2021).....	45
Figure 23: Conceptual model of photon travel in SDB (ARGANS Ltd., 2019).....	47
Figure 24: Satellite Derived Bathymetry results in Guadeloupe against ground truth (red) using various sensors: Pleiades (blue), Sentinel-2 (purple) and Worldview-2 (turquoise) (Laporte, et al., 2020).	48
Figure 25: Light attenuation in open ocean and turbid coastal waters (NOAA, 2014).	49
Figure 26: Location of wave buoys (Dodet et al., 2020).	51
Figure 27: Principles of satellite altimetry for wave climate (Liang & Wang, 2019).	52
Figure 28: Validation of wave height derived from satellite altimetry against in-situ buoy measurements (Dodet et al., 2020).	53
Figure 29: Principles of DEM derivation (Japan Space Systems, 2016).....	54
Figure 30: Distinction between Digital Surface Models (DSMs) and Digital Elevation Models (DEMs) (Okolie et al., 2022).	55
Figure 31: Clustering workflow (Xu & Wunsch, 2005).....	58
Figure 32: KMeans clusters in the feature space of an image (Wikipedia, 2022).	59
Figure 33: KMeans clustering workflow (Hao, 2021).....	60
Figure 34: KMeans clustering for coastal vulnerability in Latin America and the Caribbean (Calil et al., 2017).	61
Figure 35: Workflow for the derivation of CVI using remote sensing and machine learning.	64
Figure 36: Belize study area. Key settlements (black) and management districts (gold) are labelled.....	65
Figure 37: SDB processing workflow.....	70
Figure 38: 1km coastal sample segments.....	77
Figure 39: Conceptual representation of feature space used in KMeans for (a) Coastal slope parameters, (b) Classification parameters, (c) Wave climate parameters.....	80
Figure 40: Random Forest classification maps for land cover (left) and benthic cover (right).	85
Figure 41: Spectral endmembers for each class defined.....	86
Figure 42: Physics-based Satellite Derived Bathymetry (SDB) model for Belize: (a) SDB DTM, (b) Study location, (c) SDB isobath model.	88
Figure 43: Temporal variation to cross-shore depth profiles for three image acquisitions.	89

Figure 44: Spatial variation to cross-shore depth profiles.	90
Figure 45: Validation of Merged SDB against Electronic Nautical Chart (ENC) contours. ...	91
Figure 46: ASTER Digital Elevation Model (DEM) for Belize.	92
Figure 47: WEVERYS modelled SWH at 20km resolution for the Yucatán Peninsula.	93
Figure 48: Magnitude and modal direction of wave climate from WEVERYS data.	94
Figure 49: Temporal variation of mean significant wave height (SWH).	96
Figure 50: Validation of WEVERYS predictions against in-situ buoy data from NOAA.	96
Figure 51: Exposure to increased wind speeds as expressed by the Saffir-Simpson Hurricane scale.	97
Figure 52: Relative vulnerability ranking of coastal segments for each parameter based on KMeans clustering.	102
Figure 53: Coastal vulnerability (CVI) in Belize using KMeans clustering.	105
Figure 54: Distribution of CVI values across vulnerability groups.	106
Figure 55: Distribution of vulnerability for individual CVI parameters based on the traditional Gornitz (1994) thresholds.	109
Figure 56: Coastal flood inundation Hazard, Belize (CHARIM, 2016).	111
Figure 57: Comparison of InVEST and KMeans results.	114
Figure 58: Copernicus land cover classification for Belize.	120
Figure 59: Belize National Marine Habitat Map (NMHM) and accuracy assessment (CZMAI, 2021).	122
Figure 60: Percentage of existing bathymetric survey coverage for Belize (IHO, 2022).	126
Figure 61: Quality of Sentinel-2 imagery. Note the presence of cloud cover, glint, suspended sediment and sediment movement.	129
<i>Figure 62: Distribution of wind speed and storm surge flooding impact (Markert & Griffin, 2014).</i>	<i>133</i>
Figure 63: Tracks of historical hurricane events.	134
Figure 64: Iterative process for the development of management strategies (Rosenthal et al., 2014).	148

List of tables

Table 1: Disparities to vulnerability thresholds in CVI studies (Koroglu et al., 2019).	31
Table 2: Comparison between resolutions of satellite sensors.	39
Table 3: Remote sensing techniques pertinent to the derivation of CVI parameters.....	42
Table 4: Comparison between ASTER and SRTM DEMs.....	56
Table 5: Overview of data sources used in this study.....	67
Table 6: Dates of Sentinel image acquisition for tiles T16QCE and T16QDE.	68
Table 7: Conceptual NumPy arrays produced to characterise coastal segment properties.....	78
Table 8: Conceptual NumPy array produced to characterise cluster centroid properties.....	81
Table 9: Conceptual NumPy array to rank cluster centroids based on the magnitude of each metric. Higher ranks will indicate a higher vulnerability.	81
Table 10: Confusion matrix accuracy assessments for image classifications.....	86
Table 11: Results of KMeans clustering and the designation of vulnerability groups based on similar geomorphic properties demonstrated by the centroids of each cluster.....	101
Table 12: Datasets used in the InVEST model.	114
Table 13: Impacts of Hurricane Keith (2000) by location (GFDRR, 2000).....	116
Table 14: Uncertainties in CVI estimation using remote sensing.....	118
Table 15: Comparison between Random Forest classification of Sentinel-2 against existing terrestrial and benthic maps for Belize.	125
Table 16: Hurricane storm surge extent for Belize City (NEMO, 2003).....	132
Table 17: Key stakeholders and relevant management issues in Belize.....	147
Table 18: Appropriate scales for the application of CVI modelling (Trigg & Smith, 2016).152	

List of abbreviations

AC	Atmospheric Correction	LUT	Look up Table
AHP	Analytical Hierarchy Process	MAR	Mesoamerican Barrier Reef
ASTER	Advanced Spaceborne Thermal Emission Reflection Radar	MAUP	Modifiable Areal Unit Problem
CDOM	Coloured Dissolved Organic Matter	MBES	Multi-Beam Echo Sounder
CHARIM	Caribbean Handbook on Risk Management	ML	Machine Learning
CMEMS	Copernicus Marine Environment Monitoring Service	MPA	Marine Protected Area
CMP	Coastal Management Plan	MSI	Multispectral Imager
CRS	Coordinate Reference System	MSP	Marine Spatial Planning
CVI	Coastal Vulnerability Index	NDVI	Normalised Difference Vegetation Index
CZMAI	Coastal Zone Management Authority and Institution	NDWI	Normalised Difference Water Index
DEM	Digital Elevation Model	NGO	Non-Government Organisation
DOP	Depth of Penetration	NIR	Near Infrared (spectral band)
DSAS	Digital Shoreline Analysis System	NMHM	National Marine Habitat Map
DSM	Digital Surface Model	NOAA	National Oceanographic and Atmospheric Administration
DTM	Digital Terrain Model	OLI	Operational Land Imager
EM	Electro-Magnetic (radiation)	RCP	Representative Concentration Pathway
ENC	Electronic Nautical Chart	RF	Random Forests
ENSO	El Niño Southern Oscillation	RGB	Red, Green, Blue (spectral bands)
EO	Earth Observation	RMSE	Root Mean Square Error
EPSG	European Petroleum Survey Group	RS	Remote Sensing
ESA	European Space Agency	SBES	Single-Beam Echo Sounder
GAR	Global Assessment Report on Risk Reduction	SDB	Satellite Derived Bathymetry
GDAL	Geospatial Data Abstraction Library	SIDS	Small Island Developing State
GDP	Gross Domestic Product	SMP	Shoreline Management Plan
GEBCO	General Bathymetric Chart of the Ocean	SLR	Sea Level Rise
GIS	Geographical Information System	SOM	Self-organising map
IBTrACS	International Best Track Archive for Climate Stewardship	SRTM	Shuttle Radar Topography Mission
ICZM	Integrated Coastal Zone Management	SST	Sea Surface Temperature
InVEST	Integrated Valuation of Ecosystem Services and Trade-offs	SWH	Significant Wave Height
IOP	Inherent Optical Properties	ToA	Top of Atmosphere
IPCC	Intergovernmental Panel on Climate Change	UNDP	United Nations Development Programme
IQR	Inter-quartile range	UNESCO	United Nations Educational, Scientific and Cultural Organization
IUCN	International Union for Conservation of Nature	UTM	Universal Transverse Mercator
LAC	Latin America and the Caribbean	USGS	United States Geological Survey
LAI	Leaf Area Index	VHR	Very High Resolution
LAT	Lowest Astronomical Tide	WGS	World Geodetic System
LiDAR	Light Detection and Ranging	WMO	World Meteorological Organization
LULC	Land Use Land Cover		

PART I – INTRODUCTION

1. Modelling coastal vulnerability from space

1.1. Coastal areas in a changing climate

Coastal environments are dynamic and complex networks which are subject to diverse pressures (Masselink et al., 2020). Ecosystems in this transitional region are highly productive and co-dependent due to their contributions to ecosystem services (Beatley et al., 2002). This has led to the World Wildlife Fund’s living planet index to suggest the economic value of the Blue Economy represents twenty percent of global nature; an equivalent of \$24 trillion. Due to their ecological productivity, these areas are often densely populated. An estimated twenty-three percent of the global population lives within 100m of the shoreline (Harvey & Nicholls, 2008).

Coastal areas also act as the buffer between terrestrial and oceanic regions. The converging of natural forces in these regions presents natural hazards. Hazards refer to processes with the ability to cause damage to people, livelihoods or the environment. The ability to manage them is critical for anthropogenic development in resource rich areas coastlines (Adger et al., 2005). Interdependency of coastal ecosystems provide the vital services that ensure these communities are protected from marine forces and extreme weather events through the absorption of wave energy.

Storm surges are a specific coastal hazard. Formed as the result of high winds coincident with low barometric pressures characteristic of poor weather systems, these events are manifested as a rise in water level above the normal astronomical tide (Bryant, 2005). These are often accentuated through human and geographic factors. These include wind direction, storm intensity, coastal morphology, bathymetry and tidal state and disproportionately affect low-lying areas of coast (Belfiore, et al., 2009). These hazards are frequently occurring, rapid-onset events which are often highly destructive. Damage to infrastructure is often the result of inundation and erosion.

An identification of areas more vulnerable to these impacts is paramount for the protection of resources and populations and provides a metric to understand the disparities between the impacts of a hazard (Cutter, 2012). This can be evaluated in distinct segments through index-based approaches and was pioneered by Gornitz (1991) through the Coastal Vulnerability

Index (CVI). The CVI quantifies the impact of coastal flooding using six parameters; geomorphology, coastal slope, sea-level change, significant wave height, shoreline change rates and tidal range. These approaches have been extended for application to coastlines globally (Abuodha & Woodroffe, 2010; Thieler & Hammar-Klose, 2000) and represents thirty percent of all coastal vulnerability studies (Cogswell et al. 2018).

The CVI highlights vulnerable areas and associates these with contributing facets to provide a useful tool for risk management. Through a relative vulnerability analysis, the CVI aids rational decision making by providing a clear indication for where conflicted management authorities should invest their limited resources. However, current CVI results require expert judgement in the computation of indices. The coastline is divided into vulnerability groups based on the geotechnical conditions at a point. These groups are assigned through static thresholds and are determined by an expert dividing the range of conditions observed over the whole study area (Koroglu et al., 2019). Due to the diverse nature of coastal geographies, these are often only relevant for specific areas and require expensive in situ survey campaigns to produce. This causes a bias to categorisations and hinders their transferability for implementation globally. This distorts the distribution and range of assessments (Gibb et al., 1992) and demonstrates the need to reduce subjective expert assessments and provide a method to rank systems based on their local conditions.

Innovative Earth Observation (EO) approaches using satellite imagery provide an efficient solution to these problems. This thesis presents the first national-scale analysis of coastal vulnerability using an automated approach to CVI using remote sensing. As a result of the dimensionality in the CVI, a machine learning based approach to classification has been employed to determine vulnerable regions that demonstrate similar environmental conditions. CVI variables have been derived using freely available data from remote sensing sources to alleviate the cost constraints and suboptimal requirement for expert knowledge or training. The method represents a modified version of the CVI approach suitable for a first-pass assessment of vulnerability which may identify areas of interest for additional local scale studies. A classification of coastal hazard distribution into representative groups is fundamental for assessing spatial variability. Developing best practices ensures this is legible and transferable at large scales.

1.2. Case Study: Belize

In this study, the CVI method has been modified for application in the Latin American and Caribbean (LAC) region. Here storms and hurricanes were attributed to 50.2% of deaths and 40% of damages from natural disasters in the period of 1972 to 2010 (Calil et al., 2017). Amplified storm climates with global climate change leads to a greater probability of coastal flooding due to an increase of storm intensity and frequency. Therefore, management authorities require reliable and regular information to protect populations from risk (Marcos & Woodworth, 2017).

Many countries in this region represent Small Island Developing States (SIDS). These are regions where a significant proportion of their natural resources come from the ocean. Due to this socio-economic dependency, these areas are disproportionately vulnerable to climate change (Nurse et al., 2014). Sustainable development is impeded through amplified natural disasters and inundation. Urgent management priorities are required to aid decision making to increase the resilience of these areas. The cost of inaction is severe – this is estimated \$2 billion by 2050 in the Caribbean alone. It is a region where SIDS lack geopolitical standing or resources to facilitate these studies (Rhiney, 2015).

Situated on the eastern extent of the Yucatán Peninsula, the SIDS of Belize represents an area exposed to such hazards (figure 1). Rapid urbanisation is a significant problem because of mass migration to exploit the thriving tourism economy. This sector represents 41% of national income (Nature Conservancy, 2021) and has resulted in 45% of the population living within 1.5km of coastline (Simpson et al., 2012). Coastal migration has led to anthropogenic pressures which threaten the wider functional ecosystem, such as intense development and inadequate infrastructure. Poor infrastructure will also act to increase risk and reduce adaptive capacity in the event of a natural disaster. An understanding of the trends to ecosystem dynamics resulting from these natural resource-based industries is critical to ensure their longevity.

Furthermore, a proximity to the Mesoamerican Barrier Reef (MAR) provides a considerable source of biodiversity to the region. This remains the longest continuous reef system in the western hemisphere and holds the status of UNESCO World Heritage site due to the variety of reef structures which provide significant habitats for endangered species such as: marine turtles and manatees (UNESCO, 2018). In 2009, external pressures (including: removal of mangrove cover and unsustainable coastal development) resulted in the inscription of this region to the UNESCO '*List of World Heritage in Danger*'.

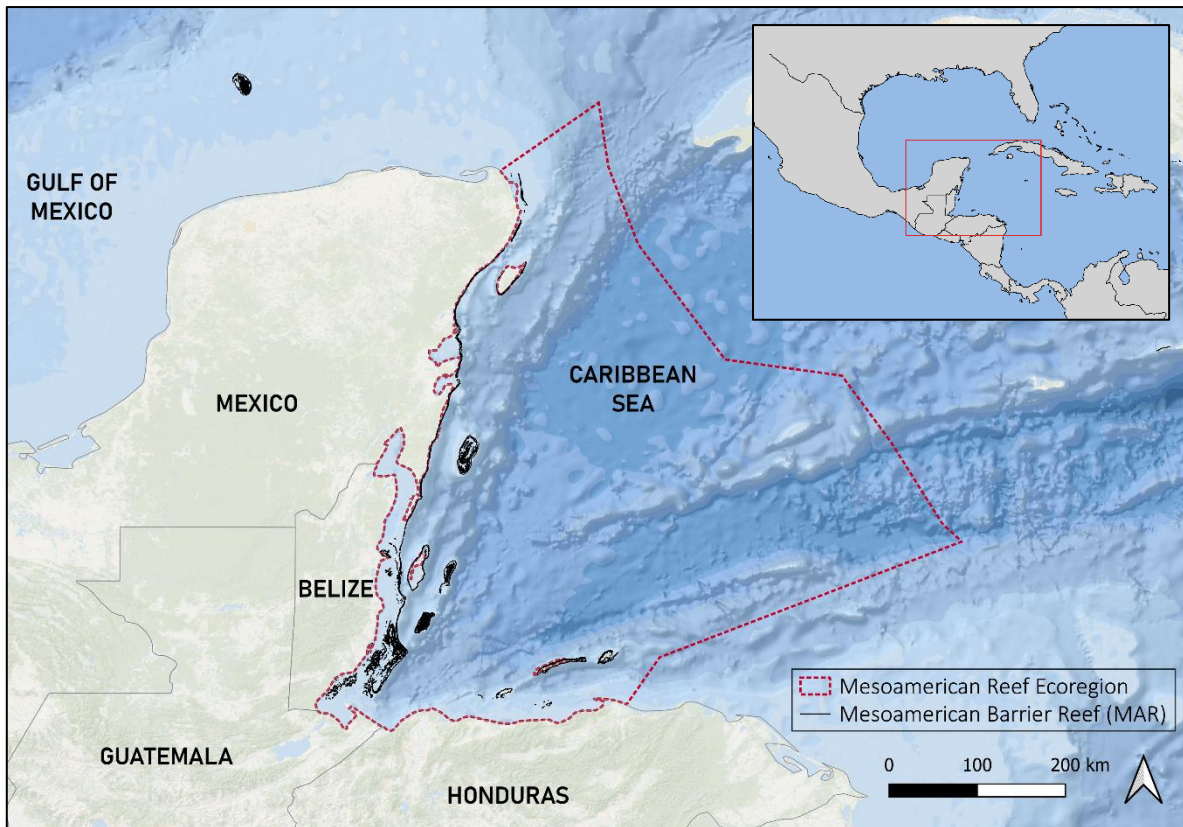


Figure 1: Location of Belize and the Mesoamerican Reef Ecoregion.

Implementation of an Integrated Coastal Zone Management (ICZM) plan in 2016 provided an outline for strategies to mitigate these pressures. These included the moratorium of oil exploration and allocation of marine protected areas (MPAs) which have contributed to the MAR being removed from the ‘*in danger list*’. This decision is met with controversy due to the continued decline of reef health and is scrutinised for being the result of geopolitical pressure rather than scientific evidence (Murray, 2021). Significant issues need to be managed to prevent further degradation of the MAR ecosystem and the natural protection it provides. The need for an integrated and efficient approach to targeted management is pivotal.

Belize is a country prone to hurricane storm surges. Fourteen storm events occurred from 1931 to 2010 and adversely affected the tourism and agricultural industries (figure 2). The low-lying terrain further enhances the risk of flooding from these events. The World Bank (2021) suggests that \$2.7 trillion of private investment is required to deploy appropriate innovation to enhance the adaptive capacity. This investment is difficult to acquire due to the uncertain causality of observations made. Geospatial data provides a pivotal role in quantifying vulnerability and resolving the complex relationships between hazards and ecosystems. An

implementation of data derived from satellite imagery presents exciting technological developments to ensure the provision of consistent, efficient and reliable monitoring (Blaschke et al., 2011).

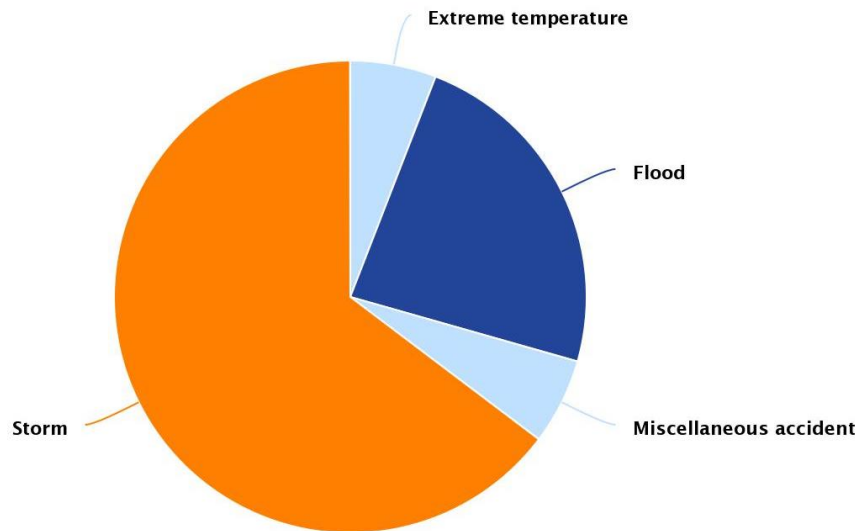


Figure 2: Average annual occurrence of natural hazards in Belize (1980 – 2020).

Belize provides a useful case study for the assessment of vulnerability from satellite data for several reasons. As a dynamic area experiencing rapid change, updated assessments are a prerequisite for informed coastal management. These have not been updated since 2016. Satellite images provide an avenue for this, especially as Caribbean waters are optically clear – this is a prerequisite for benthic assessment and satellite derived bathymetry (Hedley et al., 2012). Although, regular image acquisition can be difficult due to heavy cloud cover in the wet season. Moreover, the MAR presents a strong conservation focus to ensure the UNESCO categorisation and ecosystem productivity is retained. An incomplete ICZM strategy has meant the regulation of development and marine protected areas has been difficult. This should be enhanced with more robust approaches to aid management decisions. These issues pertinent in Belize are emblematic of SIDS and present transferability to the adversities they also endure.

1.3. Thesis aim

This thesis seeks to develop an Earth Observation (EO) based approach to evaluate coastal vulnerability in Belize. The method should be suitable for use in Integrated Coastal Zone Management (ICZM) to enhance resilience to climate change. This will be addressed through the following objectives:

1. Identify and quantify the spatial variability of factors relevant to coastal vulnerability, using EO sources.
2. Synthesise parameters into a bespoke (and semi-automatic) Coastal Vulnerability Index model using machine learning.
3. Validate the model through a comparison with historical data and existing vulnerability assessments for Belize.
4. Situate results in the context of Integrated Coastal Zone Management with recommendations for application in Belize.

1.4. Thesis structure

This thesis is structured across six parts. Each part is subdivided by chapters which represent issues pertinent to each geophysical parameter. A summary is outlined below.

Part One: Introduction – an overview on the contextual positioning of the project and outline of study aims and objectives.

Part Two: Literature Review – four chapters; the former providing a synthesis of the pressures present in the coastal zone and the current state of coastal management in Belize. This is followed by an overview of the methods for evaluating vulnerability to hazards and concludes with an evaluation of the role of remote sensing in coastal management.

Part Three: Methods – approaches employed for data acquisition, processing and modelling.

Part Four: Results – this section presents the results from parameter derivation using satellite data and validates the performance of the machine learning model in Belize.

Part Five: Discussion and Conclusions – a critical evaluation on the reliability of modelled vulnerability and the limitations of the approach. This is situated within a focus on coastal management.

This section ends with the conclusions of the study and presents appropriate recommendations for the successful integration to management strategies.

PART II – LITERATURE REVIEW

This section introduces specific coastal hazards in Belize through the characterisation of the coastal zone with respect to physical and anthropogenic activities. The management applications of these hazards are considered and vulnerability assessments are proposed as a metric for managing these problems. An analysis of how this is measured and the limitations of this approach are subsequently evaluated. Finally, Earth Observation approaches are assessed to combat these shortcomings with existing methods. This aims to create a comprehensive understanding of requirements and limitations to the successful implementation of effective risk assessment strategies.

2. Coastal hazards in Belize

2.1. The coastal zone

Belize has a coastline which covers an extent of over 380km (Guannel et al., 2016). An analysis of the specific hazards in the coastal zone requires a comprehension of the spatial distribution of forcing parameters and the degree of protection they might provide. Contrasting definitions for what constitutes a coastal region makes the scale over which to conduct this analysis difficult to isolate with precise boundaries. The coastal zone can be defined from a physical perspective as the coincident area of land and sea which are affected by their proximity to each other (Sorenson & McCreary, 1990). Alternatively, the coastal zone has been defined as the extent of which anthropogenic land-based activities have measurable influence on marine ecology (CMSER, 2009).

A holistic definition is appropriate for the complete characterisation of these regions including both physical and anthropogenic factors contributing to vulnerability. Benoit and Comeau (2005) suggest these are interface territories that are influenced physically, economically and socially by the interaction between land and sea (figure 3). Greig et al. (2013) takes this further to suggest these are also areas where adaptive management is required to ensure the human well-being.

The Belizean Coastal Zone has been described in the following section with respect to its human and physical characteristics (composed of terrestrial and marine environments). This provides a foundation for the parameters which might affect the disproportionate distribution of vulnerable areas.

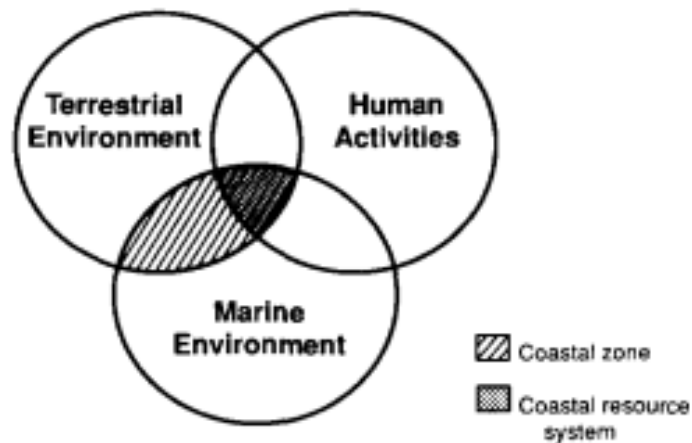


Figure 3: The coastal zone represents the area subjected to the interaction between land, sea and anthropogenic activity (Thia-Eng, 1993).

2.1.1. Physical environment

Climate is a significant hazard in the Caribbean region. The World Bank ranks 167 countries based on their climate risk and Belize retains the 8th place position. Climatic conditions in Belize are classified in the Köppen climate system as “Am” which indicates a tropical monsoon climate (Murray et al., 2003). Belize lies within the hurricane belt and is vulnerable to hurricane trajectories during the Atlantic hurricane season lasting from June to November. Threats from Hurricanes are the principle natural hazard due to their rapid parity for destruction.

In the period since 1930, Belize has been subject to 16 hurricanes with 8 of these causing damage or fatalities (NEMO, 2016). If less intense systems, such as tropical storms, are also considered then this includes an additional 17 events. Hurricane hazards include intense winds and low-pressure systems which can result in storm surges. Impacts of such events are accentuated by the area’s low topography and are increasing with current rates of environmental degradation and SLR due to climate change. These are further amplified through the situation of populations in disaster prone regions.

Although exposed, the coastal zone provides access to an abundance of resources useful to industry. This is demonstrated by Hurricane Keith (2000) – which caused the worst damage to the country – through the loss of 45% of the Gross Domestic Product (Jordan et al., 2016). In fact, during the 20th century the country’s capital city, Belize City, had been devastated twice by hurricanes. In 1970, the capital was moved eighty kilometres inland to Belmopan to enhance the resilience of administrative authorities from hurricane events. This act demonstrates the severity of vulnerability in this country – few governments would create a new capital city as a resilience strategy (Karlsson et al., 2015).

Belize is vulnerable to extreme climatic events (Karlsson and Mclean, 2020). In addition to hurricanes, the region is influenced by the El Niño Southern Oscillation (ENSO). This phenomenon of climatic variability is present within the Pacific Ocean but affects the Caribbean through teleconnection patterns. ENSO events are irregular but occur predominantly over a 2–5-year period. During ENSO periods, the Caribbean is subject to increased rainfalls and modified storm climates. Sustained trade winds can also bring higher wind generated wave climates and increase flooding risk.

2.1.2. Anthropogenic activity

In addition to the physical hazards of the coastline, the integrity of the coastal zone is further threatened by anthropogenic influences. In addition to the global patterns of anthropogenically driven climate change, the Blue Economy provides a substantial source of income to Belize. This attracts a large proportion of the country’s population and industry. These activities can lead to pressures acting to change the dynamics of the region; the distribution of areas most affected by individual pressures are shown in figure 4. Two significant practises provide significant contributions to the economy which paradoxically threaten the health of the region they are dependent on: agriculture and tourism (Rosenthal et al., 2014).

The agricultural industry employs 20% of the Belizean population (Verutes et al., 2016). Farmland faces threats due to salinisation from seawater intrusion and will increase in most vulnerable areas as sea levels rise. Farming practises also rely heavily on pesticides which can enter the ocean through runoff. A mutual protection of this source of revenue along with the natural ecosystem is fundamental.

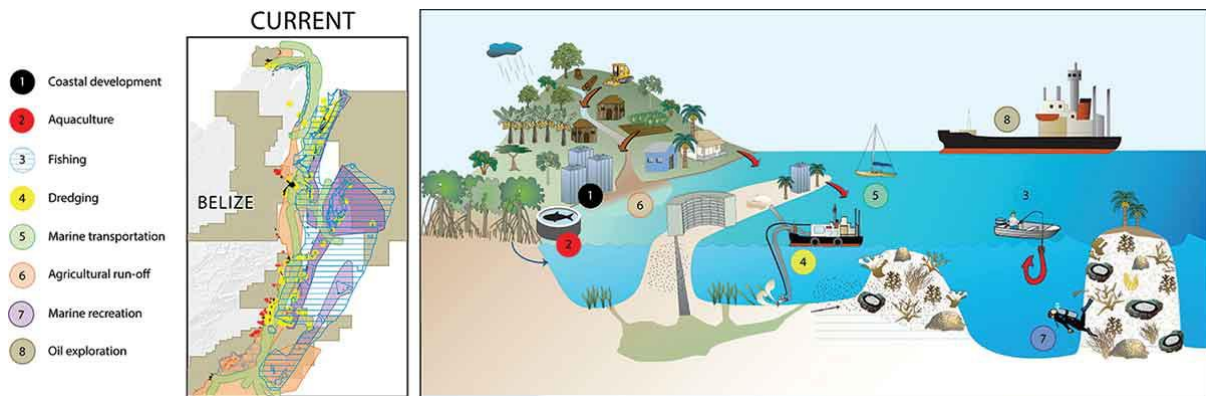


Figure 4: Areas of Belize affected by specific anthropogenic pressures (Verutes et al., 2016).

Population density is one of the principal threats to biodiversity loss. Tourism contributes to almost half the national economy and resulted in rapid urbanisation of coastal zone. The world-class status of MAR has attracted global tourists and investment; 80% of coastal land has been purchased by foreign investors (Moreno, 2005). In the period from 2000 – 2017, the coastal town of San Pedro’s population increased by 432% (SIB, 2017). This process of rapid urbanisation can be seen as unsustainable and has led to several impacts. Fuelled by urbanisation, areas closest to population centres have experienced a rate of mangrove deforestation of 3.6% a year (figure 5) which removes important ecosystems to protect against flooding. In addition, rapid urbanisation has resulted in inadequate infrastructure which has led to eutrophication of the water column from wastewater pollutants. Increased nutrients are detrimental for the health of corals and mangroves.

Moreover, the discovery of crude oil reserves has added pressure to the preservation of the region. Many of these reserves are coincident within existing marine protected areas (MPAs). These pressures had been identified by UNESCO in 2009 and resulted in the MAR becoming listed as a “*World Heritage Site in danger*”. Poor coordination of government agencies has contributed to the inability for the Coastal Zone Management Authority and Institute (CZMAI) to operate effectively and increased the pressure to ensure these are managed appropriately (Gibson, 2011).

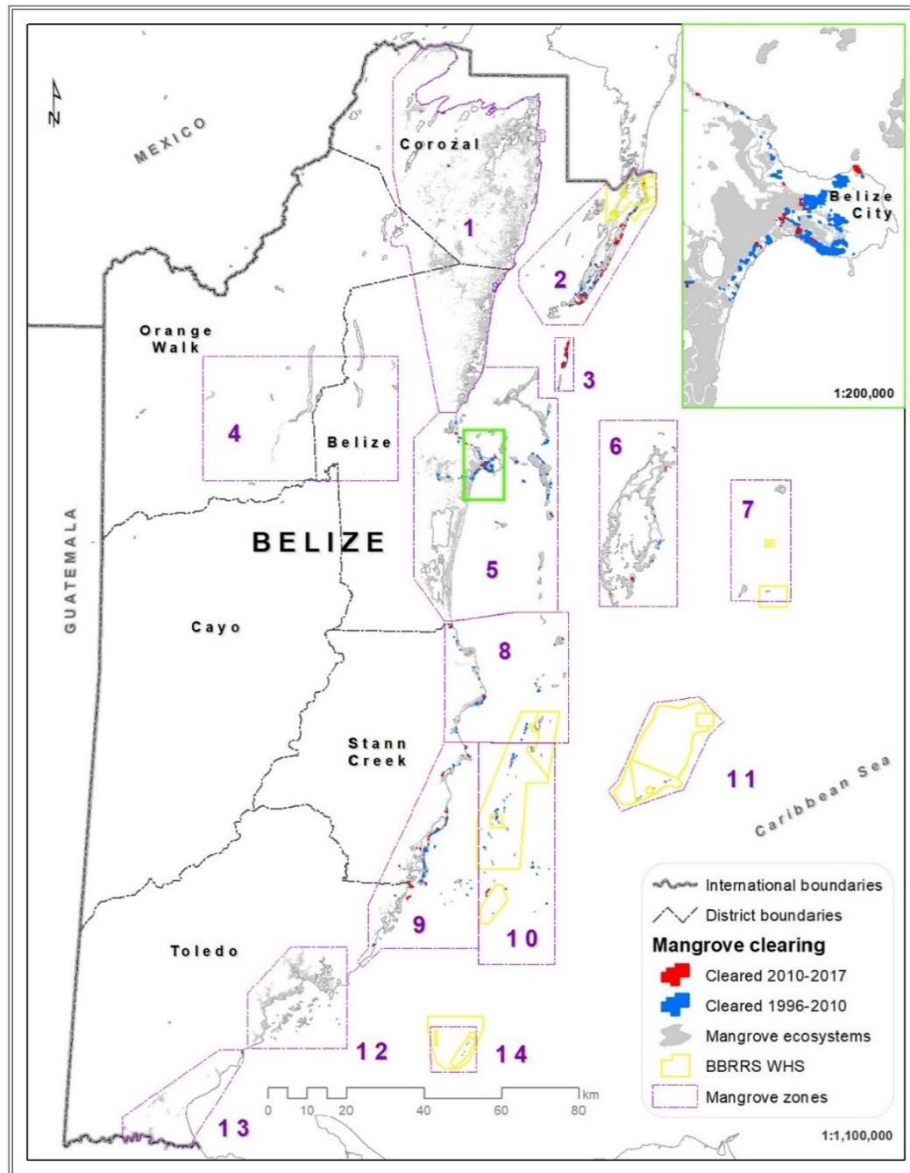


Figure 5: Extent of mangrove forest clearance from public EO data (Cherrington et al., 2020).

2.2. Managing coastal hazards in Belize

Coastal hazards are addressed through the Coastal Zone Management Act of 1998 which acknowledges the requirement of multi-sectoral planning to sustain ecosystem integrity and promote quality of life (Verutes et al., 2016). This legislation requires the implementation of an Integrated Coastal Zone Management (ICZM) strategy to identify and reduce the impacts of hazards at a subnational scale. ICZM is a holistic approach to addressing complex management issues to enhance resilience and encourage sustainable development. This is achieved through maintaining the function of ecosystem services, reducing conflicts in resource allocation and encouraging multisectoral development. This plan was accepted in 2016 and implemented by the CZMAI through the explicit consideration of multiple stakeholders (CZMAI, 2016). Stakeholders in Belize are outlined in figure 6 and present complex challenges to evaluate compromises between investment and environmental impact (Maguire et al., 2012).

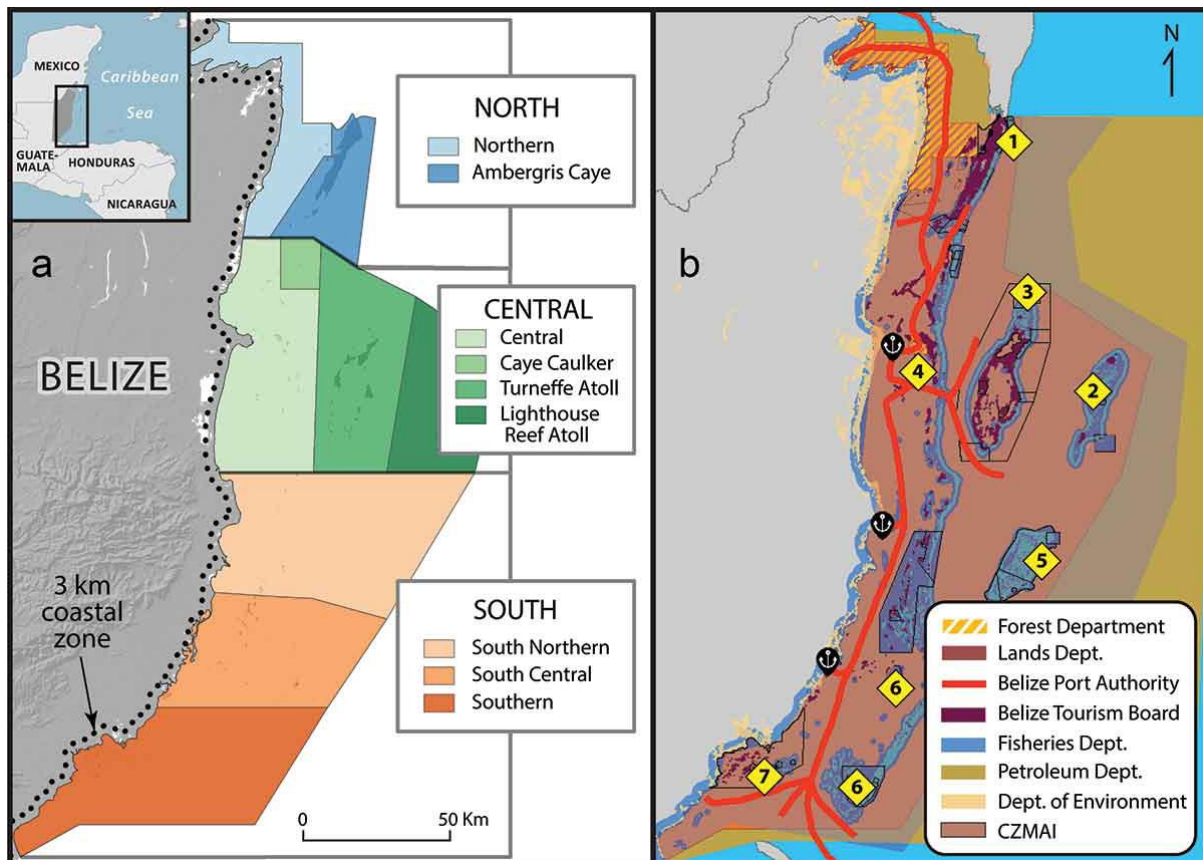


Figure 6: (a) Administrative districts in Belize. (b) Key stakeholders and their operating areas (Verutes et al., 2016).

Management strategies are administered over zones based on geographic and cultural features (figure 6). Development guidelines are produced for each region depending on their suitability. This marks a significant improvement for management of development. Coordination between regions is required for effective management through adoption of the Coastal Management Plan (CMP) which will assist in regulating uncontrolled development and unsustainable tourism.

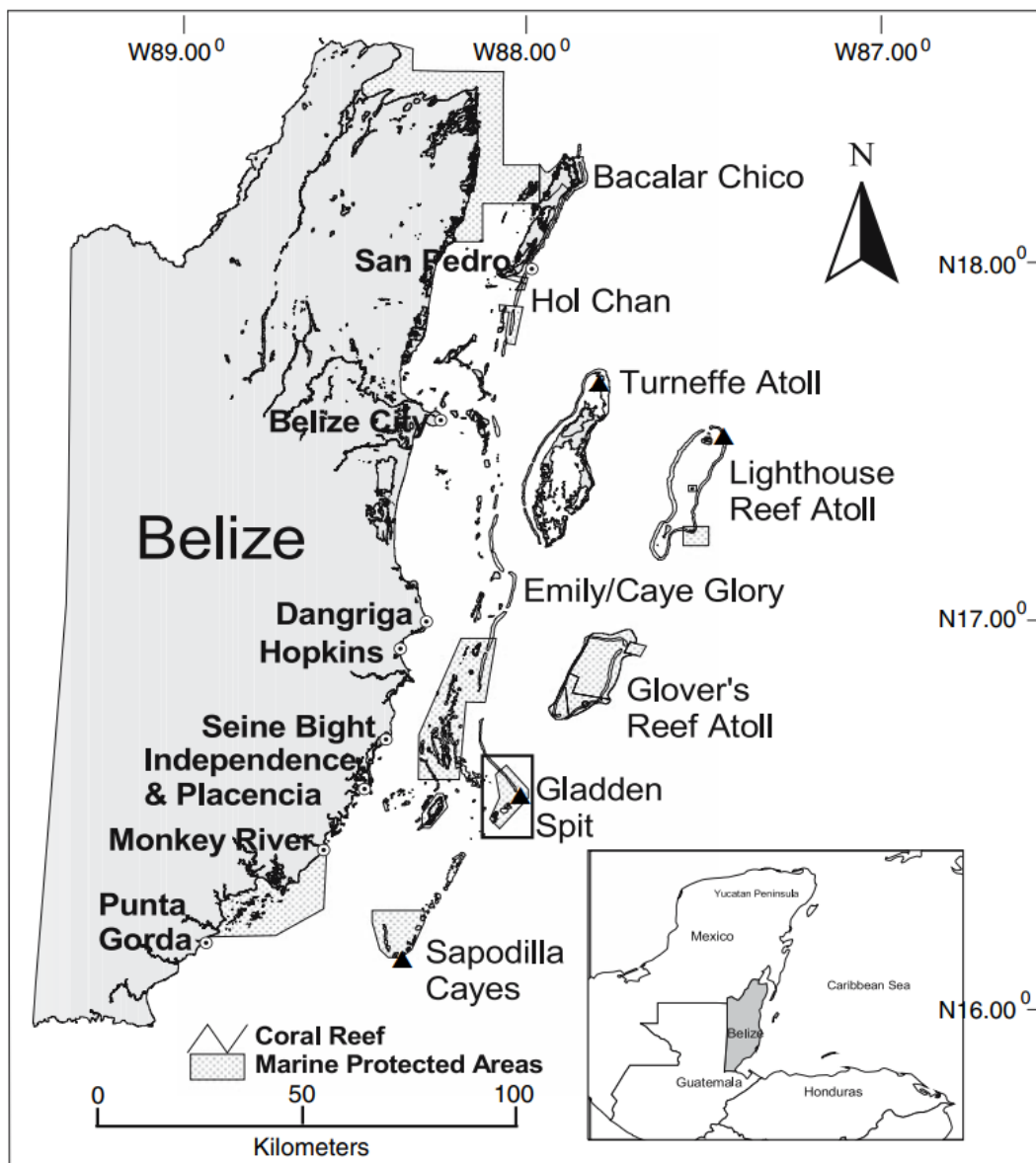


Figure 7: Location of Marine Protected Areas (MPAs), Belize (Graham et al., 2008).

The CMP emphasises the need for efficient planning to aid sustainable development. Graham et al. (2008) suggest a significant strategy for achieving this has been the designation of marine protected areas (MPAs). These are areas of sensitive marine habitats which are protected to prevent exploitation and ensure sustainable use (figure 7). MPA designation has been shown to increase reef quality and provide stronger protection from storm events. These benefits have encouraged a coordination of activities within MPAs under the integrated management process (Cho, 2005). Other management approaches have included the instigation of an oil moratorium and special development areas but these are not as well versed as MPAs.

Risk mitigation is also considered by the CMP. The Disaster Risk Management Cycle provides a reference framework for the mitigation of risk (figure 8). This cycle consists of four components: prevention, preparedness, response and recovery. A focus of management budgets is typically given to crisis response given the immediate impact to save lives and this often neglects vulnerability mapping (Le Cozannet et al., 2020). However, reactive approaches are often less effective than those that are integrated within coastal zone management (Nicholls & Small, 2002). Hence, proactive approaches are best suited for enhancing resilience. Nicholls and Klein (2005) suggest this includes enhancing the assessment of vulnerable systems.

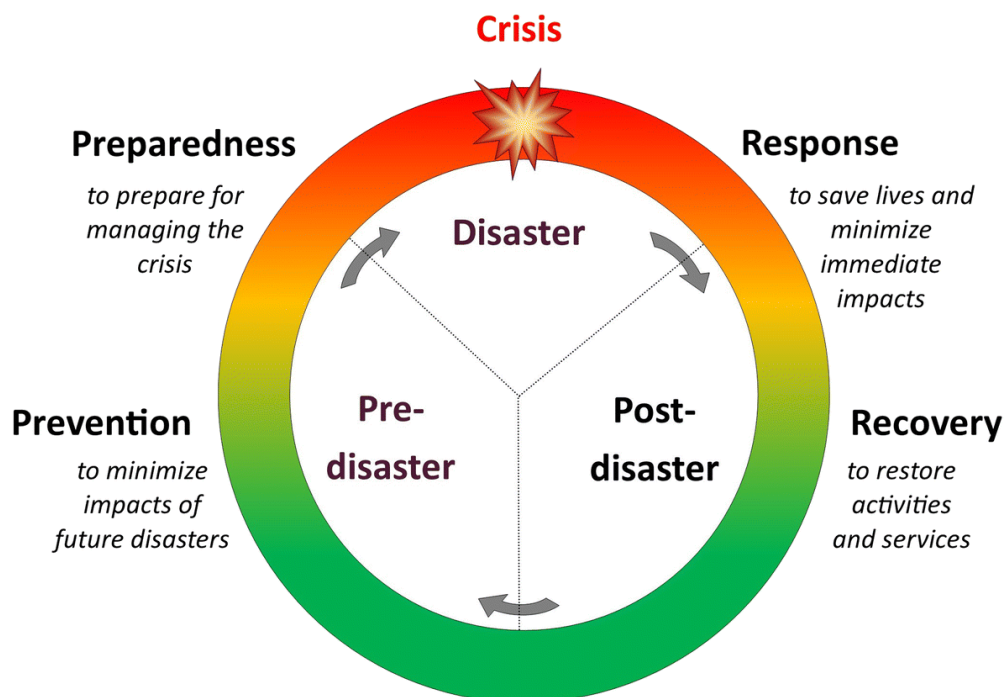


Figure 8: Disaster Risk Management Cycle (Le Cozannet et al., 2020).

In the context of climate change, risks are continually evolving through time and emphasises the need for reviewing mitigation strategies (Stammer et al. 2019). Hazard mitigation requires access to maps demonstrating the spatial distribution of geographical settings to characterise physical vulnerability (figure 9). Access to this information allows stakeholders (such as local governments, industries, disaster response NGOs and residents) to make informed decisions. The modelling of vulnerability can help to support preventative actions through a definition of land-use policies which limits exposure to hazards and facilitates the optimisation of resource allocation to highly vulnerable areas.

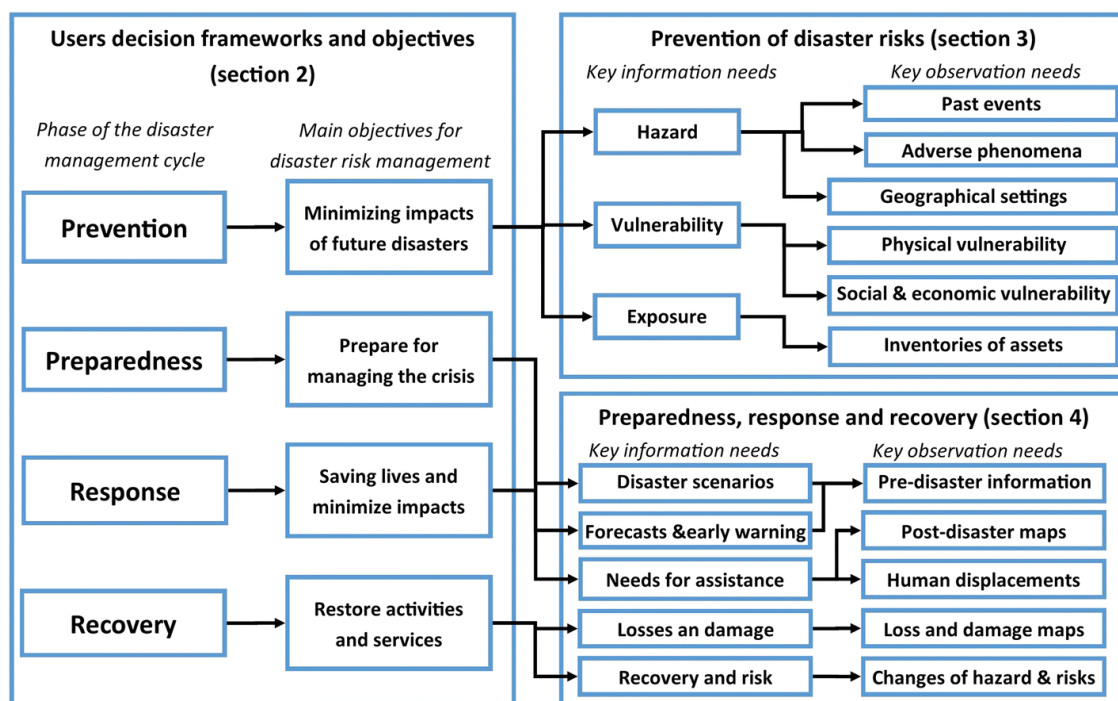


Figure 9: Requirements for Earth Observation in decision frameworks for disaster management (Le Cozannet et al., 2020).

As a SIDS, Belize is a country that possesses limited government resources and a small population. Therefore, the ability to enforce these strategies is limited through financial and personnel restrictions (Salichon et al., 2007). Underlying inefficiencies in the ICZM framework act to inhibit enforcement regulations. Many management policies are outdated and require revision to achieve this. This requires cost-efficient strategies which are reliable and spatially coherent. The ICZM will seek to facilitate this through alternative approaches for enforcement including public participation and education (Gibson et al., 1998).

A scarcity of tools and limited synthesis of existing data makes it difficult to develop defensible approaches that identify shared priorities among stakeholders. The Natural Capital Project used the InVEST model to provide spatial estimates of changes to ecosystem services and their effect on vulnerability from storms (Arkema et al., 2014). These models provide tailored reports for at localised planning region scales but are limited by the quality and scarcity of input data. This results in a high uncertainty (Sharp et al., 2016). These should be improved regularly and using updated technology.

The deficiency of effective modelling should be combated through a cost-efficient method of mitigating infrastructure and ecosystem damage from storm events are required to locate areas that are more vulnerable. This can promote further land management controls to discourage further development.

3. Coastal vulnerability in Belize

The characteristics of the Belizean coastal zone demonstrate several human and physical parameters which act to influence the exposure of the coastline to coastal hazards. Such concerns about coastal hazards and disasters have become closely linked to risk and vulnerability. To quantify the degree of vulnerability present in an area, an understanding of the differences between these subjective terms is required. Hazards, risks, disasters, and vulnerabilities each have a subtly different focus, but the terms are occasionally used interchangeably (Cutter, 2012).

The IPCC (2012) define vulnerability as “*the degree to which a system is susceptible to, and unable to cope with, adverse effects of climate change, including climate variability and extremes*”. The definition incites three facets: exposure, sensitivity and adaptive capacity. Exposure refers to the disposition to a natural system. Sensitivity suggests the degree to which an area might be impacted. While adaptive capacity provides an indication of a region’s resilience and ability to evolve to maintain key functions.

Vulnerability is often considered a product of the distribution to hazard exposure to inform decision-making on mitigation (Muler and Bonetti, 2014). This requires an assessment of physical factors but also requires an extension to outline the degree of adaptive capacity for appropriation in resilience assessments. Otherwise, socio-economic factors which are relevant to vulnerability are neglected (Cardona et al., 2014). This is often challenging as there is little consensus on consistent social indicators for vulnerability when compared to physical geography.

Lloyd et al. (2013) provides distinction between vulnerability and risk. Vulnerability outlines the degree to which factors that contribute to causing a hazard are present but this is not a direct measure of the hazard. Hence this metric is incapable in being considered in probabilistic terms. Risk provides the probability a hazard will have adverse effects to a population and is traditionally evaluated through hindcast analysis of impacts from historical events (Kearney, 2013). Another distinction stems from risk analysis purporting to describe the social and economic consequences in addition to physical aspects. Through the inclusion of both aspects, vulnerability assessments can be extended as a measure of susceptibility useful in risk analysis (Boruff et al., 2005).

Scale is a predominant factor in vulnerability studies. Spatial scale can influence whether national, regional or local pressures are considered. Yoo et al. (2011) suggest the spatial scale

is often too broad at regional scales or too fine at localised regions and shows a requirement for specific impact assessments that are not global climate studies. Localised studies provide contextualised assessments of vulnerability and are difficult to apply with climate projections as these are not produced with an appropriate spatial resolution (Romieu et al., 2010). This can be achieved through spatial analysis for the identification of segments which have propensity to be vulnerable to a hazard (Bonetti et al., 2013).

For this thesis, vulnerability is defined as the geophysical susceptibility to storm-induced coastal flooding. The severity of impacts has been characterised with respect to the geographical constituents. As a result, resilience assessment of risk is not evaluated.

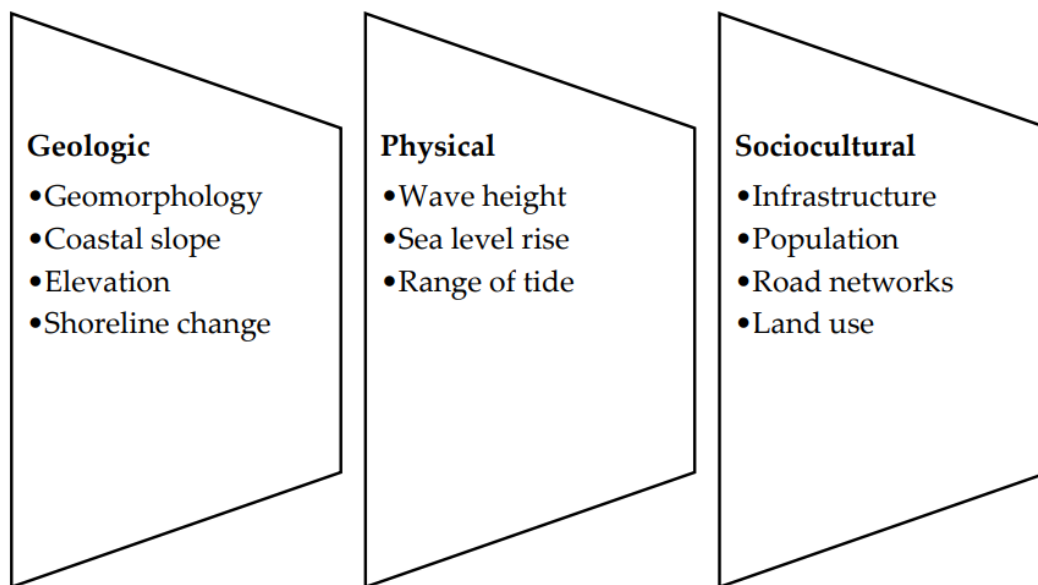


Figure 10: Factors affecting coastal vulnerability (Noor & Maulud, 2022).

Coastal hazards contribute to vulnerability and have a multivariate nature. These are often the combination of multiple processes which characterise a compound event. The vulnerability to such an event is dependent on physical and geological constituents of the coastline (figure 10). When considering storm surges, the most relevant factors have been suggested to be geomorphology, oceanography, topography and wind exposure. Sociocultural factors do not change the exposure to a hazard but act to modify the social vulnerability to a population. An understanding of the importance of each factor is vital for effective vulnerability assessments. These have been discussed in turn, with respect to Belize.

3.1. Geomorphology and geology

Geomorphology is applied widely in vulnerability assessments to describe the variation in natural landforms present in the coastal zone (Pethick and Crooks, 2000). Each landform will have a relative parity for resistance to flooding. The unique combination of processes provides specific morphologies which can act to accentuate the effects of storm surges. This is represented by the pathway component of the Source-Pathway-Receptor model (Holdgate, 1980).

Guannel et al. (2016) demonstrate how healthy coastal ecosystems provide a source of coastal protection from storm events in Belize; the distribution of such habitats is shown in figure 11. Consideration should be made for the distribution of geomorphology as a proxy for wave attenuation. Coastal habitats act to reduce incident wave energy from between 35 and 71% (Narayan et al., 2016). Coral reefs and saltmarshes provide the most coastal protection and act to reduce wave height by up to 88 and 70%, respectively. Seagrass beds and mangroves also offer protection to the degree of 36% and 30%. Conversely, exposed seafloor, unconsolidated coastlines and urban areas are likely to have a higher degree of vulnerability to flooding. These observations show how the design of greenbelts can be an efficient approach for coastal protection (Koch et al., 2009).

Wetlands consisting of mangrove dominate the terrestrial coastline and extend 200m landward (this represents 3.4% of Belize's land area). Mangroves are a dominant example of a saline ecosystem present within the tidal range in Belize. Incident wave energy is reduced through the bottom friction of roots and is enhanced in areas of dense canopy close to the surface of water. Sediment stabilisation occurs through the establishment of roots and further reduces erosion. McIvor et al. (2016) show that as little as one-hundred metres of mangroves can reduce incident wave energy by up to sixty-six percent. As a result, mangroves provide a strong ability to reduce the vulnerability of an area.

Benthic habitats refer to ecological regions on the seabed. The Mesoamerican Barrier Reef will act to reduce vulnerability in Belize through moderating wave height to dissipate wave energy (Quataert et al., 2015). Wave reduction capacity is the result of the ratio of reef width and depth relative to wave height. The most effective dissipation occurs on reefs twice as wide as the wavelength. At their most effective, corals can dissipate wave energy through a reduction of wave height of 88% (Ghiasian et al., 2021).

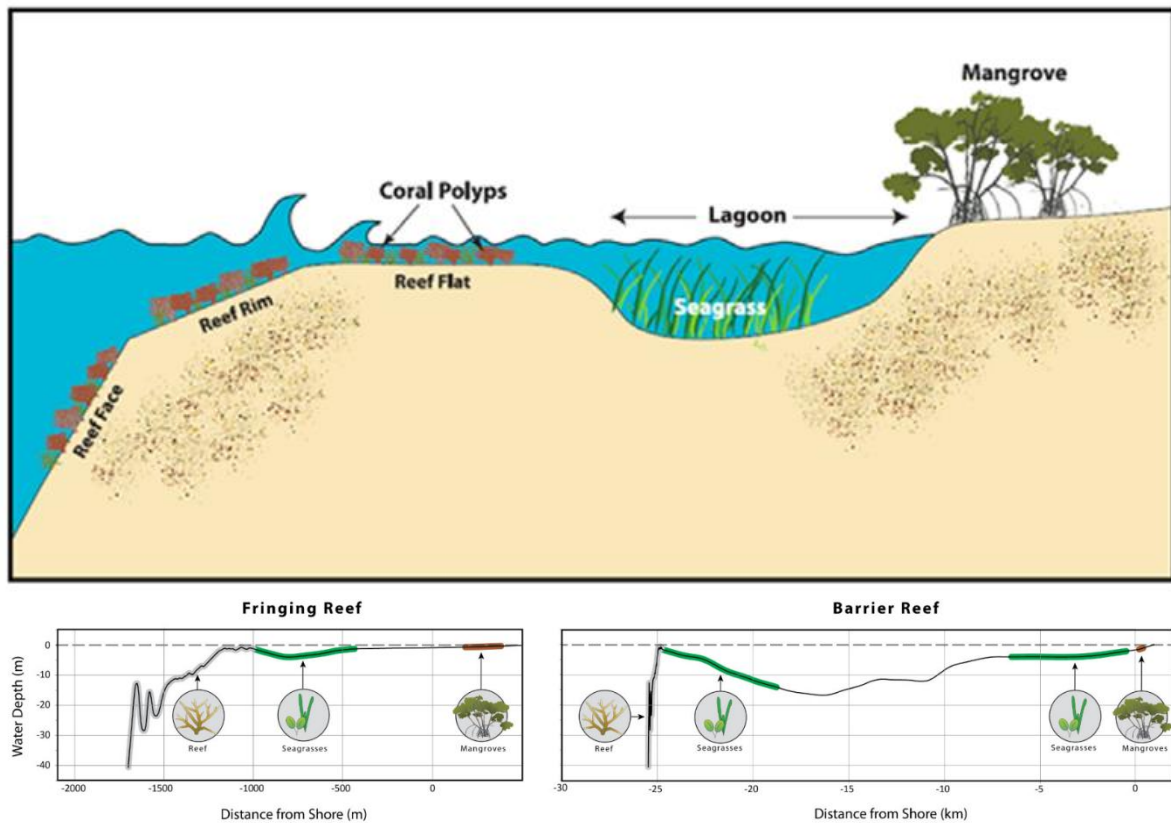


Figure 11: Schematic of the Belizean cross-shore habitats with corresponding bathymetry profiles (Guannel et al., 2016).

Offshore morphology in Belize demonstrates a steep continental shelf to the coral reef. The reef provides protection but this is variable along the coastline due to the diverse reef structures. The MAR is divided from the mainland by a shallow lagoon (5-20m deep), which extends up to twenty-five kilometres, and encompasses many isolated island territories, including: Ambergris Caye, Lighthouse Reef and the Turneffe islands.

This lagoon is populated by seagrass beds covering an area of approximately 6km in width between the depths of 1 and 13 metres. Seagrass will act to slow the rate of water flow through capturing silt and sand in their leaves. Much like mangroves, once established their roots provide stability for underlying sediment to reduce erosional transport and provide a buffer to the coastal zone (De Dominicis et al., 2023). The optimum conditions for enhanced seagrass defence occurs in shallow waters. Increased water levels with global sea level rise reduces energy dissipation in seagrass and reefs. The 6km area covered by seagrass in Belize has the capacity to reduce wave height by 1.5cm; albeit less so than reef structures.

Geology will affect the landforms observed. Shoreline recession rates can differ by a factor of ten based on their geological constituents (Brooks et al., 2012). Away from the Mayan Mountains, the coastal zone of Belize exhibits a limestone geology characteristic of sandy coasts. The rate of recession for unconsolidated sands can change by a factor of one hundred when compared to hard rock. Sandy coasts often possess shallow gradient slopes which facilitates the landward penetration of waves and increases the vulnerability to hazards (Poate et al., 2018). Sediment transport can lead to more complex systems than hard-rock geologies with the growth of features including nearshore sandbars providing additional protection. Beach morphology is dynamic and will alter the protection that is provided (Barbier et al., 2011).

Urban areas, including Belize City and San Pedro, are often built on coastal floodplains due to their fertile soil providing a source for agriculture and picturesque natural morphology ideally suited for exploitation from the tourist industry. Hence, these areas are often densely populated whereby social impacts of hazards are most heavily affected. Coastal flooding exposure is likely to increase in urban areas due to increased run off from impermeable surfaces resulting in slower water drainage and more surface water. This can also lead to secondary effects including local drainage failure which will exacerbate the natural effects of flooding (Cea & Costabile, 2022).

A consideration of each of these habitats individually undermines the role that multiple habitats have in moderating wave climate. An improvement to the quantification of these drivers is paramount to characterise the extent of protection to Belize. Pressures in the coastal zone have capacity to influence the health of these ecosystems and hence the degree of protection they provide. In Belize, these specific challenges include direct impacts such as habitat fragmentation and the coastal squeeze caused by rapid urbanisation. Indirect factors including pollution and increased nutrients in the water can also lead to degradation and drastic alterations to ecosystem structure and function. These factors demonstrate the importance of considering these ecosystems in coastal planning in Belize (Hale et al., 2009).

3.2. Oceanography

Wave climate represents the parameter of oceanography with strongest capacity for coastal flooding (Ghiasi et al., 2021). Significant Wave Height (SWH) is a measure of the average height of the highest third of surface waves. This metric is of interest because high waves represent a significant chance of overtopping and inundation. Furthermore, these higher waves are attributed to increased power and erosional capacity through the wave equation:

$$F = \frac{\rho g^2 H_s^2 T}{64\pi}$$

where F = wave energy flux (F), ρ represents the density of salt-water, g is the acceleration due to gravity, H_s representing significant wave height and T demonstrating wave period.

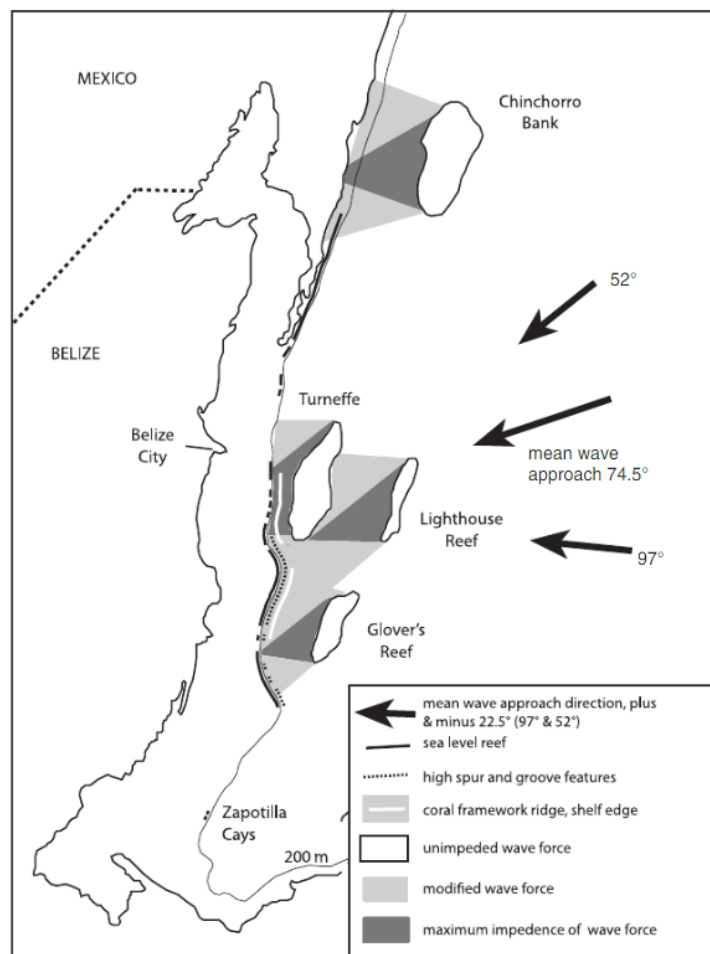


Figure 12: Incident wave climate and distribution of coral impedance (McNeill et al., 2010).

Two components can act to enhance the influence of wave propagation in coastal zones: water level and tidal currents or surges (Peregrine and Jonsson, 1983). Water level transforms waves through shoaling and refraction in shallow water which can reduce wave height through bottom friction. Tidal currents impact the generation of waves and ease of propagation. The tidal level is significantly accentuated in surge conditions (Horsburgh and Wilson, 2007). These are exacerbated by rising sea levels through increasing efficiency of wave transmission in deeper inshore waters.

Wave conditions may be impacted by climatic phenomena such as the El Niño-Southern Oscillation (ENSO). ENSO represents a global climatic pattern of ocean surface warming through circulation patterns. Inclement warmer waters increase the probability of tropical cyclone production through the temperature gradient resulting in strong winds. This contributes to a seasonal variability of wave climate (often with higher wave energy and incident wave direction shifts) and atmospheric forcing in the tropics (Pereira & Klumb-Oliveira, 2015).

McNeill et al. (2010) provide a thorough overview of the offshore topography of Belize. Bathymetry of the forereef is seen to drop rapidly to several thousand metres close to shore (figure 11). This suggests wave energy is not impeded by barrier reefs or through bottom friction until they are close to land. Figure 12 shows the degree of protection afforded by each reef system with respect to dominant incident wave direction. This steep reef morphology provides a significant contributor to oceanographic characteristics; including a diurnal microtidal range of less than 0.5m (figure 13).

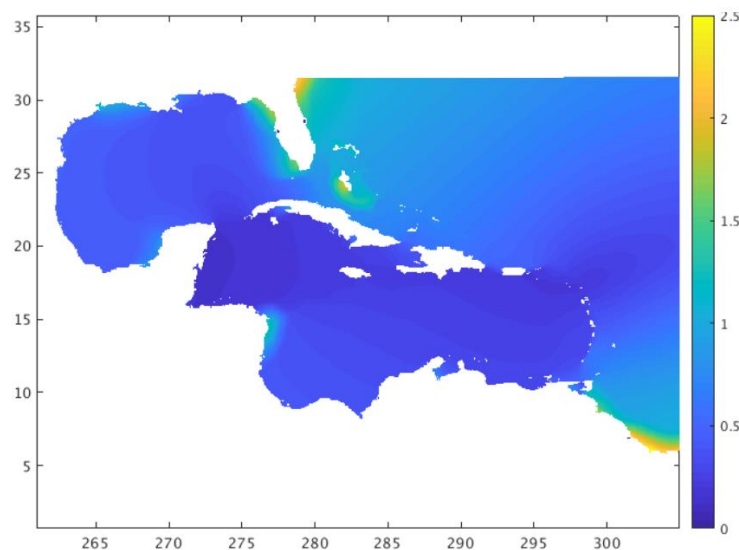


Figure 13: Diurnal tidal range of the Caribbean Sea (Jevrejeva et al., 2020).

3.3. Topography

Topography represents the elevation of terrestrial surfaces and the gradient of offshore bathymetry. When combined these represent the coastal slope and provide a significant driving process behind the dissipation of wave energy. This is a proxy for inundation capacity. The distinct lack of accurate bathymetric mapping over coastal areas poses a prominent issue to produce functional risk assessments in Belize as 48% of the country has not been surveyed. A robust understanding of the seabed is essential to understand the propagation of energy dispersed from oceanic forces and has a direct impact on navigation, commerce, geo-hazards and marine habitats (Traganos, et al., 2018).

Study of the complex dynamics of offshore bathymetry can highlight vulnerabilities to coastal areas and is pivotal to effective management. The properties of the ocean floor can elucidate physical processes acting to alter the coastal morphology contributing to coastal risk. This can include the variation of natural barriers to sea level rise and hurricane storm surges whose genesis and propagation can have substantial impact on the modification of morphology (Chiocci, et al., 2011).

Furthermore, constant anthropogenic pressure from competing areas of the Blue Economy act to change the bathymetry of nearshore waterways indicating these regions are not static environments. Dredging has occurred to provide for shipping and navigation demands. This has included an increase of channel depth; aquaculture changing benthic habitats through unsustainable fishing practices; and over tourism physically damaging reef structures (Gibson, 2011). These practices change the seabed structure with implications for sub-aquatic ecosystems by causing rapid changes to benthic morphology. These environments are inherently dynamic therefore there is a requirement to keep renewed assessments of the seafloor to understand the processes of sediment transport, erosion and deposition which act to alter the coastal morphology and present new hazards.

Belize is characterised by a low terrestrial topography because over half the land area has a elevation lower than two-hundred metres (Murray et al., 2003). Coastal extents in the south of the county are dominated by mountainous terrain (derived from the Maya Mountain range) but these are found inland. This area of igneous rock is particularly resistant to coastal erosion and flooding. In the northern regions, however, the limestone lowlands are covered by mangroves and swamps indented by lagoons. Hence, these coastal regions are subject to flooding.

3.4. Wind exposure

Storm surges represent a meteorologically driven parameter of ocean climate and are synonymous with strong winds. SWH has been shown to be influenced by the combination of wind speed, duration and fetch but the precise process of energy transfer between the atmosphere and sea is complex and not fully understood (Janssen, 2004).

A characterisation of windspeed can aid in prediction of severity of flooding events as, when these events are coincident with high tide, extreme water levels generate high surges and are exhibited as storm tides. Locally generated waves occur through the influence of wind and will significantly alter sea level and runup (Stockdon et al., 2006). Understanding windspeeds is important as wind generated waves are not self-sustaining and subside when wind drops. Clarity on whether increased water levels is the result of storm surges or wind driven wave effects and hence there is a requirement for wind to be included in vulnerability assessments.

Hurricane frequency and intensity metrics are used as a measure of hurricane impact. A measure of frequency is important to characterise the recovery period between events to demonstrate the adaptive capacity and aid in estimations of resilience. The Saffir-Simpson wind scale represents a widely used method to rate hurricanes on a scale of one to five based on their sustained wind speed. The International Best Track Archive for Climate Stewardship (IBTrACS) database provide an archive of tropical cyclone events occurring in the Caribbean over the last thirty-two years to characterise hurricane climatology (Knapp et al., 2010).

4. Assessing vulnerability

4.1. The Coastal Vulnerability Index (CVI)

The assessment of vulnerability aims to quantify the individual contributions from each factor impacting the disparate variation of exposure along the coast. This can provide a legible and comparable metric for analysis. Due to the subjective nature of vulnerability (and of the parameters being measured) assessments are situated within the epistemological assumptions of the study. This can provide contrasting results based on the approach utilised (Koroglu et al., 2019).

Several approaches to mapping vulnerability have been produced through index-based, GIS based and dynamic computer modelling methods. This section will focus on index-based methods as these are the most abundant. Their abundance is due to their ability to indicate clear spatial disparities and merge multi-variate parameters. This analysis provides a proxy for systematic processes that cannot be directly measured to analyse patterns in their distribution (McIntosh & Becker, 2019). Thirty percent of studies on coastal vulnerability have adopted this method and demonstrates the robust nature of this method (Cogswell et al., 2018).

A popular approach to mapping vulnerability is the Coastal Vulnerability Index (CVI); an extension of the coastal hazards database developed by Gornitz (1991). A reflection of the physical vulnerabilities in coastal areas is produced whereby parameters are quantifiably compared and directly equated with physical effects. In the original method, six variables are qualified with respect to their susceptibility to coastal flooding; (1) geomorphology, (2) coastal slope, (3) sea-level change, (4) shoreline change rate, (5) mean tidal range and (6) significant wave height. These variables have been utilised in various studies (Nageswara Rao et al., 2008; Pendleton 2004) and applied globally (Abuodha & Woodroffe, 2010).

Gornitz (1994) later modified the CVI to incorporate climatological variables to model effect of hurricanes and severe storms through the addition of parameters including annual tropical storm probability, hurricane frequency-intensity index and mean hurricane surge. These variables are particularly pertinent in the Caribbean region. There is an abundance of analysis incorporating sea level risk and storm surges, however, wave data has only been used by a few studies (Toimil et al. 2017).

Marine and terrestrial variables are not coincident. This requires a sampling strategy to aggregate these parameters and determine their combined effects at a specific point on the coastline. Koroglu et al. (2019) suggest using a 1km x 1km sample grid that extends from a point on the coastline as an appropriate method to characterise coastal conditions.

VARIABLE	Ranking of coastal vulnerability index				
	Very low	Low	Moderate	High	Very high
	1	2	3	4	5
Geomorphology	Rocky, cliffed coasts Fiords Fiards	Medium cliffs Indented coasts	Low cliffs Glacial drift Alluvial plains	Cobble beaches Estuary Lagoon	Barrier beaches Sand Beaches Salt marsh Mud flats Deltas Mangrove Coral reefs
Coastal Slope (%)	> .2	.2 – .07	.07 – .04	.04 – .025	< .025
Relative sea-level change (mm/yr)	< 1.8	1.8 – 2.5	2.5 – 2.95	2.95 – 3.16	> 3.16
Shoreline erosion/ accretion (m/yr)	>2.0 Accretion	1.0 – 2.0	-1.0 – +1.0 Stable	-1.1 – -2.0	< - 2.0 Erosion
Mean tide range (m)	> 6.0	4.1 – 6.0	2.0 – 4.0	1.0 – 1.9	< 1.0
Mean wave height (m)	<.55	.55 – .85	.85 – 1.05	1.05 – 1.25	>1.25

Figure 14: Vulnerability groups and threshold ranges for each variable (Gornitz, 1990).

A measure of vulnerability is quantified in the CVI method through a ranking system (figure 14). Values from one to five represent an increasing degree of vulnerability to a specific parameter which facilitates the use of qualitative and quantitative measurements. Static thresholds are defined to differentiate these groups based on supporting observations and are often subjective and site specific (Koroglu et al., 2019). These values are assigned for a section of the coastline; thus, at each sample point a measure of vulnerability for each parameter should be made. These values are input into the CVI equation (calculated as the square root of the product mean) to give a single value indication for combined vulnerability. The mean square root method is used to dampen extreme range due to sensitivity to small changes in factors. This relative scale is broken down into sections representing classes of severity using the percentile approach.

$$\text{Coastal Vulnerability Index (CVI)} = \sqrt{\frac{V_{\text{Geomorphology}} * V_{\text{Slope}} * V_{\text{SLR}} * V_{\text{Shoreline}} * V_{\text{Tides}} * V_{\text{Waves}}}{6}}$$

Equation 1: Coastal Vulnerability Index (CVI).

This approach has been employed by the United States Geological Survey (USGS) to determine vulnerability at a national scale and have demonstrated the application of this approach for easily identifying spatial patterns in most vulnerable areas (Thieler and Hammar-Klose, 2000). A key distinction of this method is the consideration of tidal forces. Gornitz (1994) posits that high tidal ranges are associated with most vulnerable areas through stronger currents and sediment transportation. However, Thieler and Hammar-Klose (2000) argue that micro-tidal environments are consistently closer to high tide and subsequently at the greatest risk to storm events.

The CVI can be applied to any spatial-temporal scale depending on data availability. McLaughlin and Cooper (2010) have studied impacts of spatial scale in depicting vulnerability at three scales: national, local authority and site levels. As resolution increased, variables which operate over larger coastal scales become obsolete and a greater level of detail is required to provide distinction. This demonstrates how the scale of a study might provide different outcomes and conflicting assessments of vulnerability.

The ability to implement at regional scales is constrained by the availability of consistent datasets across these large areas. Amendments to the methodology, particularly in the derivation of variable typology and thresholds, will be required to compensate for a variation of characteristics in different regions. The traditional CVI thresholds apply specifically to the Gulf of Mexico and will not be comparable to the range of conditions present in other areas (Thieler & Hammar-Klose, 2000). This means numerical values will differ such that vulnerability remains the same across a whole region because the entire coast falls within one vulnerability group. Numerical values may represent high vulnerability in one region and a moderate assessment in another area of the globe. As a result, this approach has not yet been applied in Belize.

To provide comparison of CVIs globally, national-scale studies should be implemented using bespoke vulnerability groups. This requires a prior understanding of the variation present on the coast. Aboudha and Woodroffe (2010) applied this approach to seven beaches in Eastern Australia and demonstrate how thresholds should be adapted using source data for successful implementation in new areas.

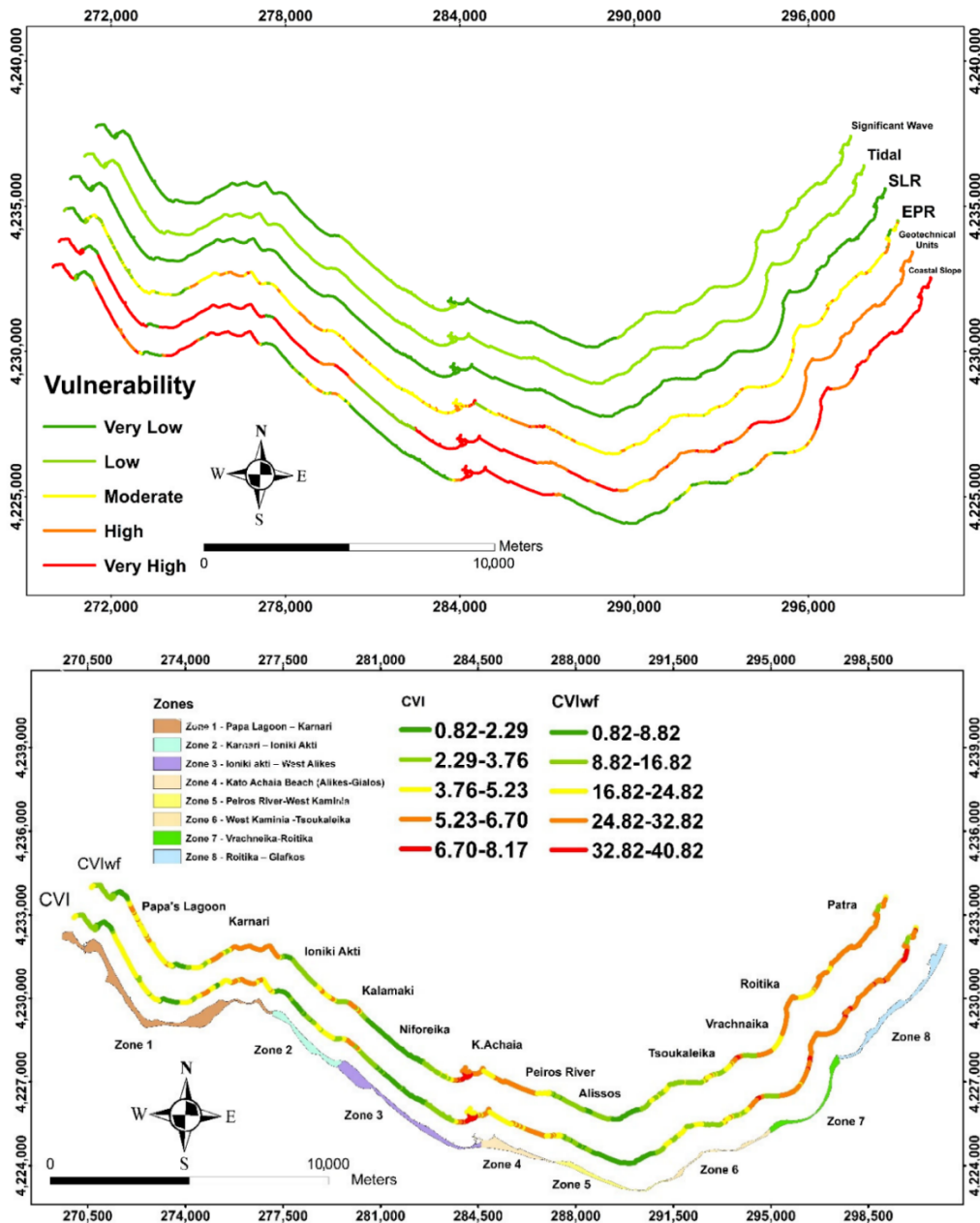


Figure 15: (a) Distribution of vulnerability with respect to each parameter. (b) Increased accuracy resulting from the inclusion of weighted parameters in CVI assessment.

An index-based approach provides merit for the identification of priority vulnerable areas or systems but are lacking in a more detailed quantitative assessment with the corresponding adaptation measures. The resulting CVI metric can be broken down into individual component risk scores before compiling into the overall CVI (Abuodha & Woodroffe, 2010). This will allow for the identification of controlling factors in modulating vulnerability. Figure 15 shows the overall effect of each parameter on CVI which can be used to identify areas most prevalent for management.

Table 1: Disparities to vulnerability thresholds in CVI studies (Koroglu et al., 2019).

Variable	Unit	CVI Reference				Coastal Vulnerability Index Ranking				
		Lopez et al., 2016	Thieler and Hammar-Klose, 2000	Shaw et al., 1998	Gornitz, 1991	Very Low	Low	Moderate	High	Very High
						1	2	3	4	5
Geomorphology	-	X				Rocky/hard cliffs (little erosion)	Embankments	Cliffs subject to erosion, Vegetative shores (pond or lake type)	Soft shores (beach rocks), Soft shores (mine-waste sediment), Soft shores (heterogeneous category grain size)	Small beaches, Developed beaches, Soft, non-cohesive sediments, Artificial beaches, Soft beaches (uncertain category grain size)
	-		X		X	Rocky, cliffed coasts, Fjords, Fiards	Medium cliffs Indented coasts	Low cliffs, Glacial drift, Alluvial plains	Cobble beaches, Estuary Lagoon	Barrier beaches, Sand beaches, Salt marsh, Mud flats, Deltas, Mangroves, Coral reefs
Land form	-			X		Fiords, high rock cliffs, Fiards	Moderate and low rock cliffs	Beach, unconsolidated sediment over bedrock	Barrier, bluffs, salt marsh, peat, mud flat, delta, tombolo	Ice-bonded sediment, Ice-rich sediment, Ice shelf, Tidewater glacier
Coastal slope	%	X				> 12	8-12	4-8	2-4	<2
	%		X			> 1.9	1.3 - 1.9	0.9 - 1.3	0.6 - 0.9	< 0.6
Relief	m			X	X	>30	21-30	11-20	6-10	0-5.0
Relative sea-level change	mm/yr	X				< -1.21	0.0-1.5	1.5-3.9	3.9-9.7	> 9.7
	mm/yr		X			-1.21 - 0.1	-1.21 - 0.1	0.1 - 1.24	1.24 - 1.36	> 1.36
	mm/yr			X		> -5.0	-5.0 to -2.0	-19 - 2.0	2.1 to 4.0	>4.0
	mm/yr				X	< -1.0	-1.0-0.9	1.0-2.0	2.1-4.0	> 4.0
Variable	Unit	CVI Reference				Coastal Vulnerability Index Ranking				
		Lopez et al., 2016	Thieler and Hammar-Klose, 2000	Shaw et al., 1998	Gornitz, 1991	Very Low	Low	Moderate	High	Very High
						1	2	3	4	5
Shoreline erosion/accretion	m/yr	X			X	> + 1.0	1.0 - 2.0	-1.0 - +1.0	-1.1 - -2.0	< - 1.0
	m/yr		X			> 2.0	1.0 - 2.0	-1.0 - +1.0	-1.1 - -2.0	< - 2.0
Shoreline displacement	m/yr			X		> + 0.1	0.0	-0.1 - -0.5	-0.6 - -1.0	>-1.0
Mean tide range	m	X				> 6.0	4.1 - 6.0	2.0 - 4.0	1.0 - 1.9	< 1.0
	m		X		X	<0.50	0.5-1.9	2.0 - 4.0	4.1-6.0	>6.0
	m				X	<1.0	1.0-1.9	2.0-4.0	4.1-6.0	>6.0
Wave climate	$H_{s0.5}^2/H_{s10m}$	X				< 0.65	0.65 - 0.75	0.75 - 1.0	1.0 - 1.5	> 1.5
Mean wave height	m		X			< 1.1	1.1 - 2.0	2.0 - 2.25	2.25 - 2.60	> 2.60
Maximum wave height	m			X	X	0-2.9	3.0-4.9	5.0-5.9	6.0-6.9	>6.9
Geology					X	Plutonic, Volcanic, High-medium grade metamorphics	Low grade metamorphics, Sandstones and conglomerates, Metamorphic rocks	Most sedimentary rocks	Coarse, poorly sorted, unconsolidated sediments	Fine, consolidated sediment, ice
Rock Type				X		Plutonic rocks, high-grade metamorphic & volcanic rocks	Metamorphic rocks	Most sedimentary rocks	Poorly consolidated sediment	Unconsolidated sediment, ice

Moreover, a shortcoming of this approach is the inability to include weighted parameters and not all components have the same importance on impacting vulnerability. The inclusion of the CVI_{WF} metric in figure 15 acts to address this through the inclusion of weighted parameters to improve the accuracy of the model (Boumboulis et al., 2021).

Distinction of the threshold values can provide conflicting results. Koroglu et al. (2019) reviewed four approaches to CVI, including those by Gornitz and Thieler and Hammar-Klose, and suggests that the mean CVI value varied by 25% (figure 16). Despite using the same method and datasets describing equivalent parameters, the difference to thresholds and methods of data aggregation presents significant differences in results. Table 1 summarises the range of physical variables used in this study and demonstrates the key requirement for strategies which facilitate comparability between outputs for coasts in different areas. Wolters and Kuenzer (2015) suggest this may be achieved through clearer definition of dominant processes and specification of approach to ranking variables.

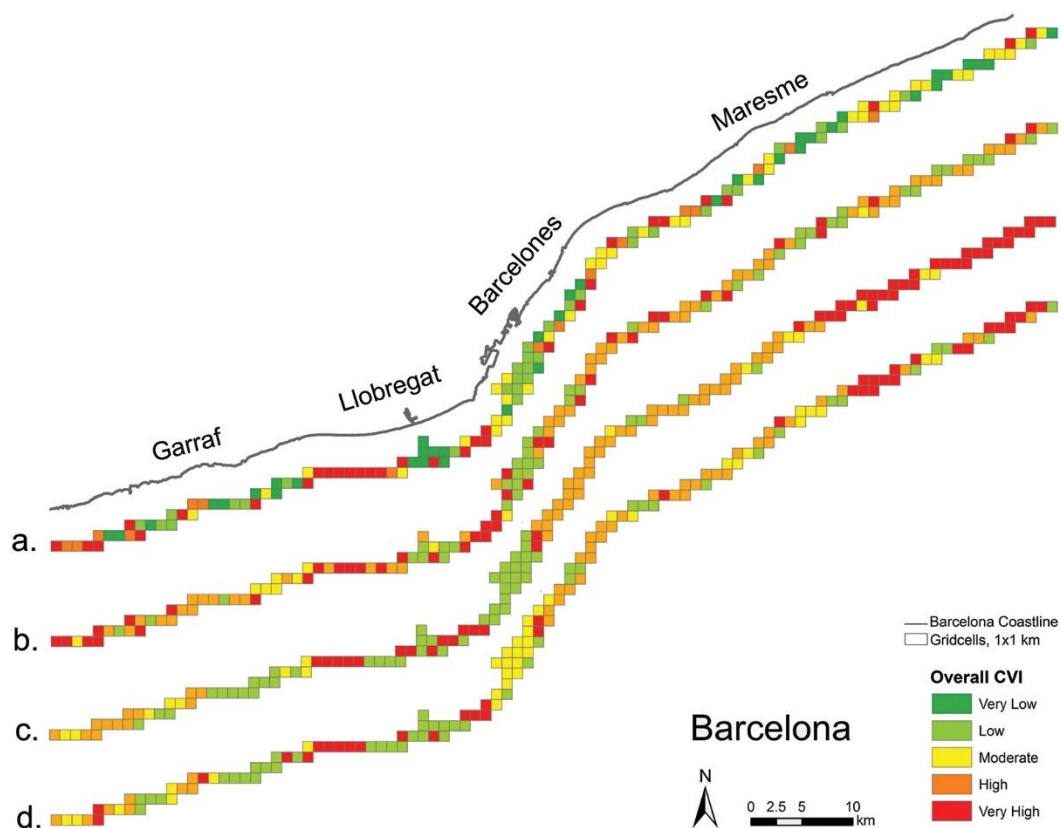


Figure 16: Disparities to vulnerability assessments resulting from a difference in methods from Koroglu et al. (2019). (a) Lopez et al. (2016). (b) Thieler & Hammar-Klose (2000). (c) Shaw (1998). (d) Gornitz (1991).

4.2. Limitations with the CVI

Coastal vulnerability indices of this nature are limited to physical parameters and provide an ineptitude for the consideration socio-economic aspects (including economic damages and number of people impacted in the assessment of vulnerability). This does not conform to the definition of risk from Kearney et al. (2013) and will require supplementary information on social factors to be implemented within resilience building. Anthropogenic activities are presented as a significant driver of environmental degradation with communities lacking in economic resources the most susceptible (Malone and Engle 2011). Therefore, a holistic approach to incorporate social considerations (in addition to physical parameters) will shift the focus from what is vulnerable to who. This identifies areas of danger as well as impact to critical infrastructure, the people and communities and is crucial for resilience planning (Tragaki et al. 2018). Parameters relating to socio-cultural conditions are hard to define without prior contextual information and engagement with local communities which this preliminary study is lacking.

An index-based approach provides a robust method for planning adaptation strategies to climate change. However, these results require expert analysis to avoid bias in clustering. Despite this, consistency between the selection of parameters and the distinction of vulnerability groups is poor (Koroglu et al., 2019). Although many of these parameters can be quantified, the evaluation of their contribution to vulnerability is subjective. The opinion of many researchers will conflict in the categorisation and ranking of variables and result in different approaches for the same parameter; as shown in table 1.

Furthermore, extensive field campaigns are often required to characterise the specific dynamics of systems to reinforce the distinction of risk categories. Although Gornitz defines a threshold, these have been shown to be incompatible with other areas of the world due to differing coastline geographies. Therefore, information about the range of geomorphic conditions present in the coastline must be established through a physical measurement campaign. This presents a series of interrelated issues: scale, time and financial investiture.

Variables have been considered over a range of spatial and temporal scales in previous studies. This produces variations to categorisation of parameters. Gargiulo et al. (2020) suggest that a high spatial resolution is crucial for effectiveness. Furthermore, temporal considerations are important as the index approach provides a static assessment for one point in time and does not account for physical and anthropogenic coastal processes which are highly dynamic. Variables

which vary in magnitude regularly over space and time require repeat assessments. If thresholds must be reconstructed from survey information each time an assessment should be made, this will become a cost prohibitive approach.

Koroglu et al. (2019) demonstrate a lack of coordinated focus between localised surveys and threshold delimitation. Jackson et al. (2014) suggests a need for global protocols for data collection to prevent this. Furthermore, in areas where access for surveys is impractical only a small percentage of coastline can be surveyed leading to data gaps. This demonstrates an advantage to autonomous remote sensing surveys and image analysis (Beijbom et al., 2012).

5. Earth Observation (EO) in vulnerability mapping

Remote Sensing is the indirect acquisition of physical characteristics from reflected or emitted EM radiation and covers technologies which range from airborne sensors to satellites (Campbell and Wynne, 2011). These techniques aid in the establishment of long-term baselines and are underexploited due to the relative infancy on space-borne observations (Nagendra, 2013). Data records are large and are constantly increasing. This facilitates the design of monitoring programmes through a repeated qualification of natural parameters. An important prerogative of coastal management agencies is to prepare for natural hazards. This requires large scale and repeated qualification of coastal morphologies – a void which Earth Observation (EO) data can fill (Ostfeld, 2005).

Issues with scale and cost in the CVI approach are ideally suited for EO techniques. The frequency and consistency of in situ measurements are often inadequate to discern meaningful patterns given the high variability of terrestrial and marine coastal processes (Andrefouet, 2001). Accelerated development in coastal areas coupled with limited resources for research in tropical regions creates situations where conservation decisions must be based on limited data (Roberts, 2002). Therefore, there is a need for data-efficient tools that integrate spatial ecology and epidemiology.

For the CVI to provide useful implementation in Belize, CVI thresholds must be adjusted to the conditions present in the area. This requires a complete evaluation of the relevant geotechnical conditions in the region. Data collection can be achieved through supplementing fieldwork with Earth Observation data to enhance the planning process with more cost-effective methods and data processing techniques (Harvey et al., 2018). The role of EO in monitoring programmes is shown in figure 17.

Covering the whole 380km of Belize's coastline would be a vast undertaking and prohibitively expensive if surveyed in situ, especially for a SIDS. A consideration for the scale at which a study is undertaken is important as geographical processes often operate over entire coastal regions which cover hundreds of kilometres. Satellite imagery is one of the only technologies available to measure pressures at sufficiently large scales and capture widespread or subtle changes (Hedley et al, 2016). This is achieved through a simultaneous study of extensive regions to establish spatial patterns at a high spatial resolution and facilitates the quick surveying of a coastline. As a result, processing time and mobilisation costs involved with fieldwork are reduced (Ostfeld, 2005). Therefore, repeat surveys can be performed regularly

and updated based on changes to the dynamic coastal conditions in areas which have previously been inaccessible to survey vessels.

Satellites often have high temporal resolutions meaning data is acquired regularly. This allows monitoring on a frequent basis or rapidly after a disaster event (Green et al, 1996). Regular acquisition is especially pertinent in Belize as mobile sediment and fast rates of urbanisation produce particularly dynamic areas. The clear coastal water in the Caribbean makes this area ideally suited to the evaluation of coastal properties – particularly those of the seabed due to the increased penetration capacity of EM radiation through water column in clear waters (Louvart et al., 2022).

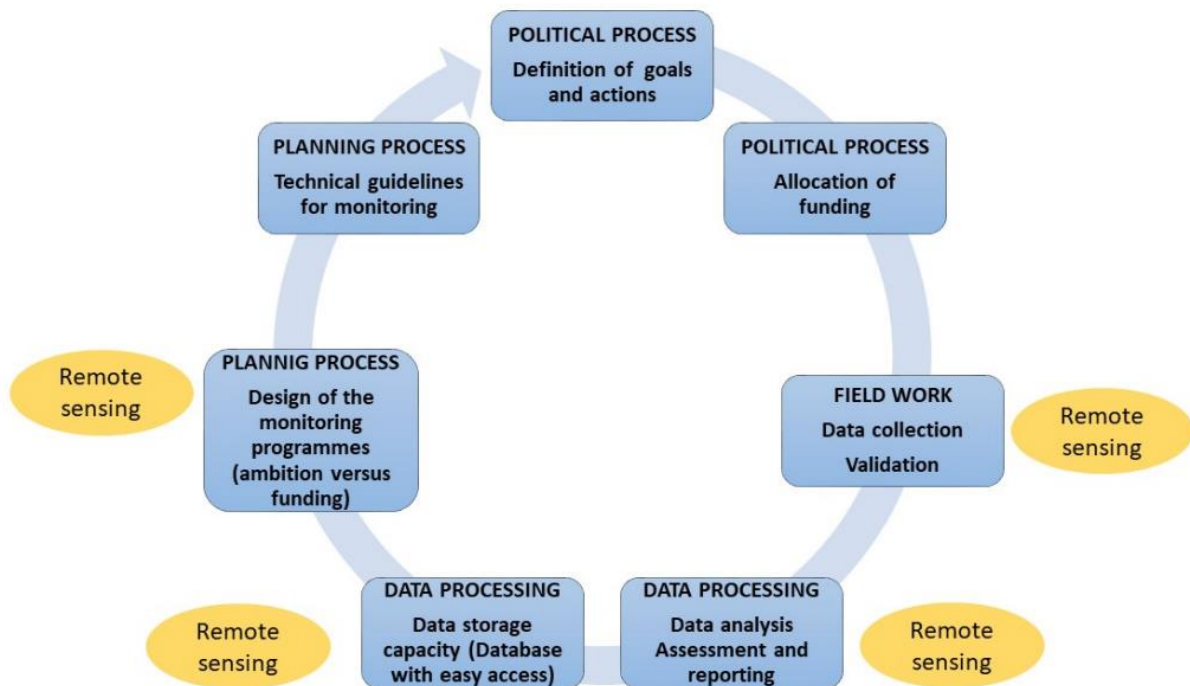


Figure 17: The role of remote sensing in coastal monitoring programmes (Harvey et al., 2018).

In addition to the physical sampling of areas, the ability to map processes from high resolution satellites provide the most cost-effective solution. Although the same level of detail and precision cannot be provided as a field campaign, the statistical capacity for characterising patterns is increased through large data quantities. Mumby et al. (2004) suggest just twenty seconds of remote acquisition time is equivalent to six days of field survey. This represents a significant cost saving of open-source satellite data. As surveys can encompass large sections of management budgets, the minimisation of expenditure here provides more resources for the implementation of physical protection measures. The dissemination of vast quantities of data from satellite archives demonstrates a radical change to management. With less resources required for processing and integration of differing datasets, time can be spent more effectively in other areas of the programme. Despite this, Le Cozannet et al. (2020) argue that the potential for remote sensing in the prevention of natural disasters remains underutilised.

5.1. Sources

A vast array of satellite constellations are available for Earth Observation (figure 18). Properties of sensors depend on their applications and will offer differing spatial and temporal resolutions (Campbell and Wynne, 2011). Open-source sensors (such as Sentinel-2 and Landsat) have the benefit of a huge timeseries of archive imagery beneficial for repeat assessments. Commercial sensors (such as Worldview) often have higher spatial resolution and increased revisit periods. However, this comes at the cost of data becoming voluminous and expensive at large scales. In addition, commercial sensors do not routinely capture data due to the size of images and require tasking. A focus will be placed on open-source optical sensors for this study due to their extensive application in studies of coastal areas and large data catalogue available.

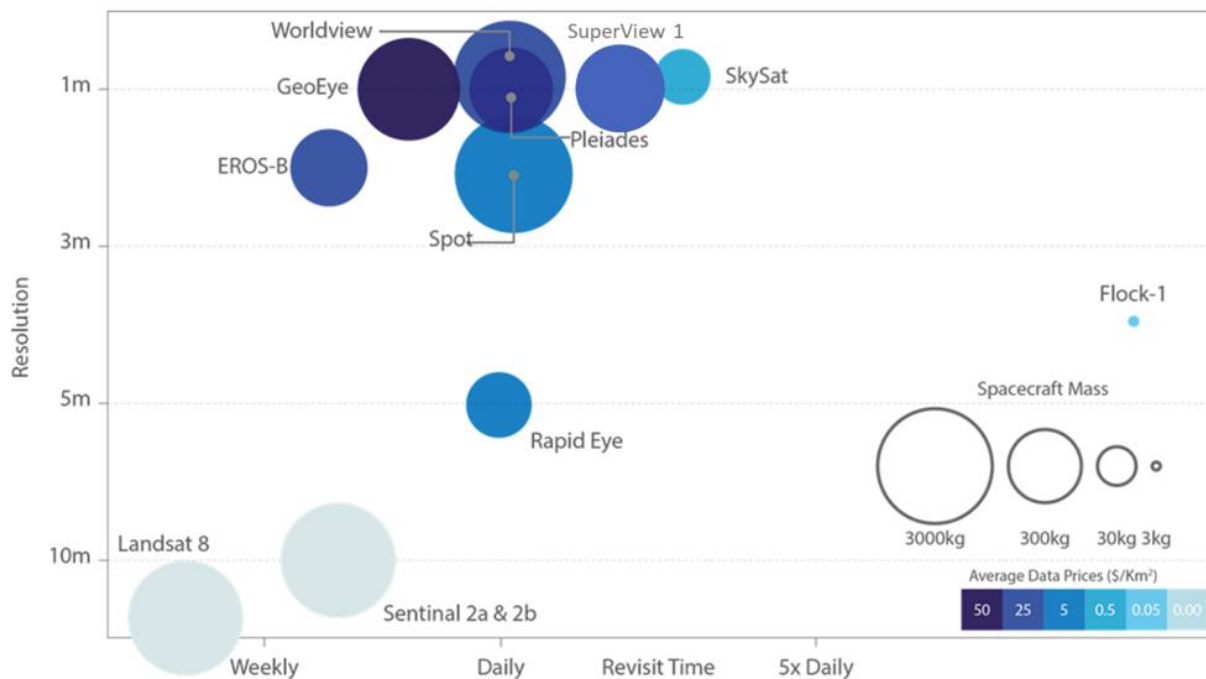


Figure 18: Spatial and temporal resolutions of EO sensors (ESA, 2020).

In order to sequester the abundance of sensors, a key consideration should be made as to their respective resolutions. Within remote sensing, resolution refers to the ability to distinguish an object through four number separate parameters; these include spatial, spectral, temporal and radiometric properties (table 2).

There is often a trade-off between resolutions due to constraints on data volumes and satellite providers (Gamon et al., 2020). Therefore, studies require an understanding as to which resolution is the most influential for their phenomena of interest. A tendency exists to prefer sensors with the highest spatial resolution; however, these may not always be the most appropriate. For example, WorldView-2 may have a superior spatial resolution of two metres but is hindered by its four spectral bands (which cover only the RGB and NIR segments of the spectrum). This would limit the distinction of species which present distinct patterns of spectral response.

Table 2: Comparison between resolutions of satellite sensors.

Resolution	Definition	Sentinel-2	Landsat	WorldView-2
Spatial	A measure of the smallest object that may be resolved by the sensor. Represented by pixel size.	10-60m	30m	2m
Spectral	Ability of a sensor to characterise the EM spectrum. Represented by the number of spectral bands.	12 bands (0.44-2.2 μ m)	8 bands (0.45-12.50 μ m)	8 bands (0.45-1.0 μ m)
Temporal	Revisit period for image acquisition.	2 – 5 days	16 days	1.1 days
Radiometric	The number of bits representing the data recorded in a pixel	12 bits	16 bits	11 bits

Phinn et al. (2010) provide an overview for the relevant scales at which to undertake analysis for different parameters (figure 19). Within the context of coastal vulnerability, this suggests a higher spatial resolution is required for parameters including land cover and bathymetry. Coarser scales are more appropriate to describe wave climate and atmospheric forces, however, these should be provided with a much finer temporal resolution. The temporal resolution used for analysis should be finer for climatic products as these are not static and change will occur rapidly. This is opposed to gradual variations seen with land cover. Figure 19 fails to capture the impacts of spectral resolution. However, Hedley et al. (2012) show the spectral confusion of heterogenous areas in land cover mapping and suggests low spectral resolutions provide a limiting factor.

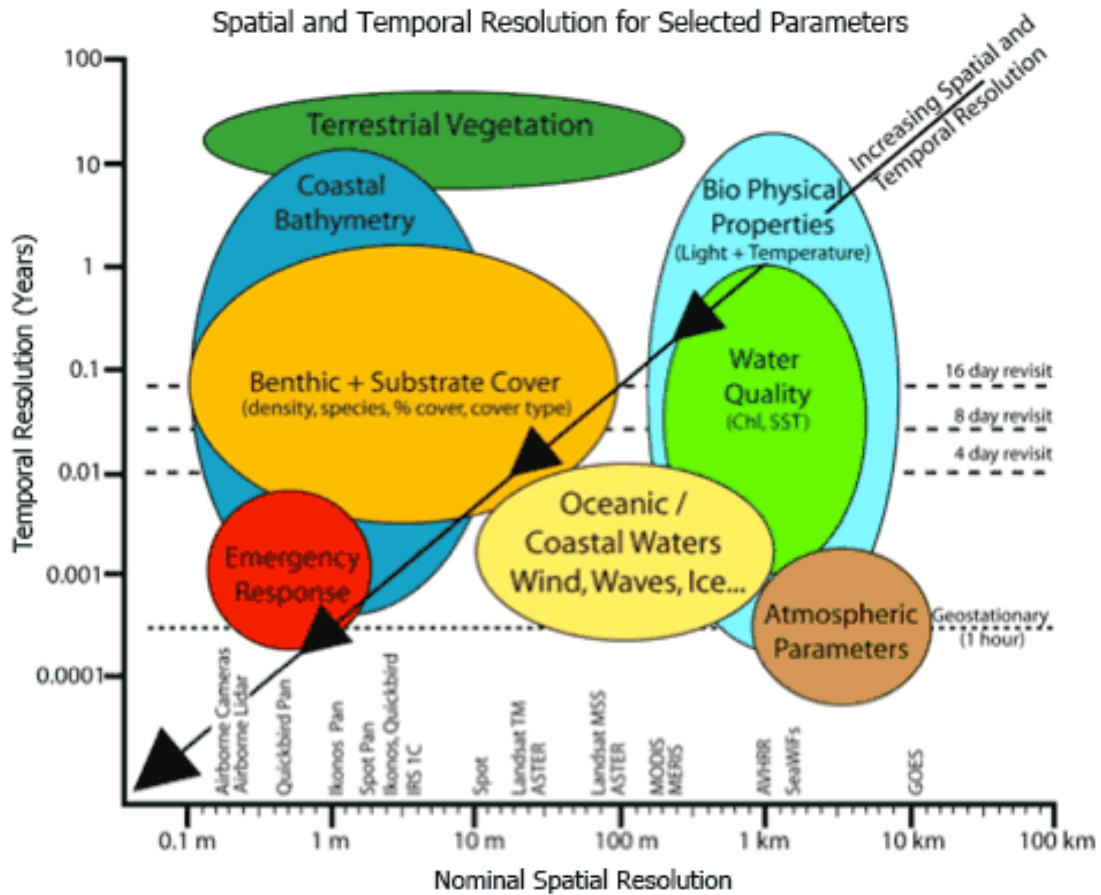


Figure 19: Appropriate spatial and temporal resolutions for analysis of coastal parameters (Phinn et al., 2010).

Sentinel-2 is a widely available open-source sensor. This twin satellite mission is part of the European Space Agency (ESA) Copernicus; a suite of satellites that are intended to monitor the environment. Designed primarily for terrestrial modelling, Sentinel-2 produces an image over a single point on the earth’s surface every five days at the equator (ESA, 2020). The Multispectral Imager (MSI) instrument provides a high spatial resolution in the ten to sixty metre range. Additionally, the MSI provides a narrow coastal band in the blue wavelengths of the spectrum (443nm) and an enhanced signal-to-noise ratio which makes it ideally suited for water applications, especially in the coastal zone (figure 20) (Tulloch et al., 2013). Therefore, based on the observations of Phinn et al. (2010), the high spatial and spectral resolution of Sentinel-2 should be deemed sufficient at elucidating the coastal parameters relationships. Moreover, the five-day temporal resolution is adequate for the observation of most coastal conditions with the exception of climatic and atmospheric parameters. These should be supplemented with additional remote sensing datasets.

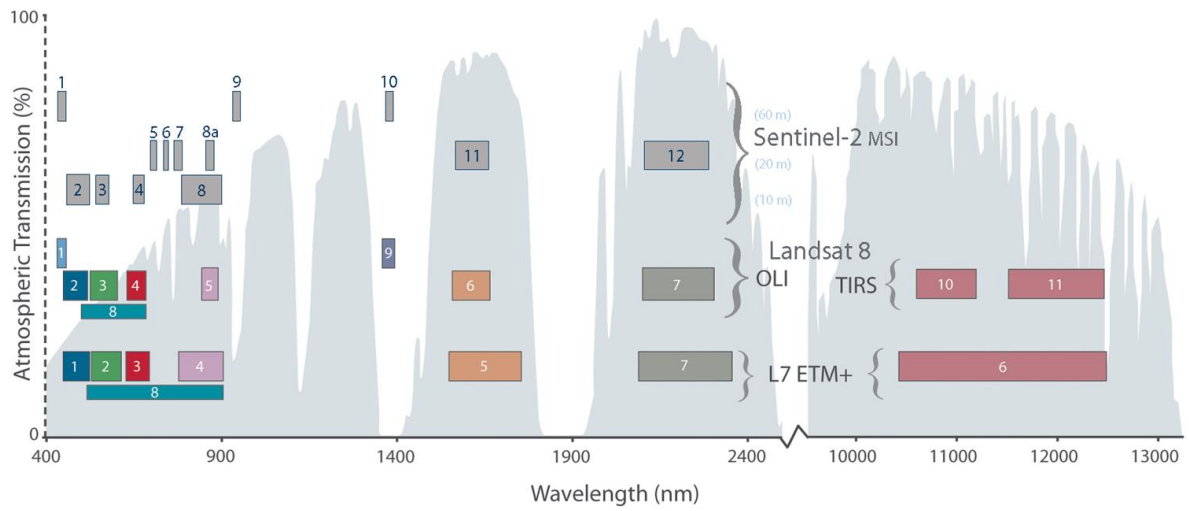


Figure 20: Spectral band combinations of Sentinel-2 compared with Landsat (NASA, 2022).

5.2. Techniques

Raw satellite data can be processed to characterise the parameters pertinent to coastal vulnerability using a range of methods (table 3). In this section, each technique has been critiqued in turn to evaluate the merits of the approach and how these may be integrated to coastal vulnerability studies. EO techniques in this section seek to provide information about the range of geomorphic conditions present in the coastline. Previously these have been either incomplete or outdated and present a limitation to the application of the CVI in Belize.

Table 3: Remote sensing techniques pertinent to the derivation of CVI parameters.

Parameter	Remote Sensing Technique
Geomorphology	Image classification
Marine coastal slope	Satellite Derived Bathymetry (SDB)
Terrestrial coastal slope	Digital Elevation Models (DEM)
Wave climate	Satellite Altimetry and wave modelling

5.2.1. Image classification

Optical remote sensing using passive sensors produces images containing data across a range of spectral wavelengths. The objects observed will possess different spectral properties and can influence their interaction with electromagnetic radiation. Therefore, these can be differentiated due to their distinct solar reflectance values (Tempfli et al., 2009). The combination of reflectance values across the spectrum is known as a spectral endmember (figure 21).

Land Use Land Cover (LULC) classification is the process of appointing discrete classes to pixels which can be separated and categorised based on their spectral responses. This is particularly useful in monitoring geomorphology of coastal zone. This approach has been used in coastal studies to map changes to terrestrial (Doyle et al., 2021) and benthic habitats (Poursanidis et al., 2019). LULC models have been applied in Belize with accuracies ranging from 60% to 92.6% (Meerman & Sabido, 2004; Doyle et al., 2021). These have typically focussed on monitoring wetland change and are tailored towards the identification of mangroves. Therefore, there is a need to update these classifications to reflect the range of geomorphologies present in the region.

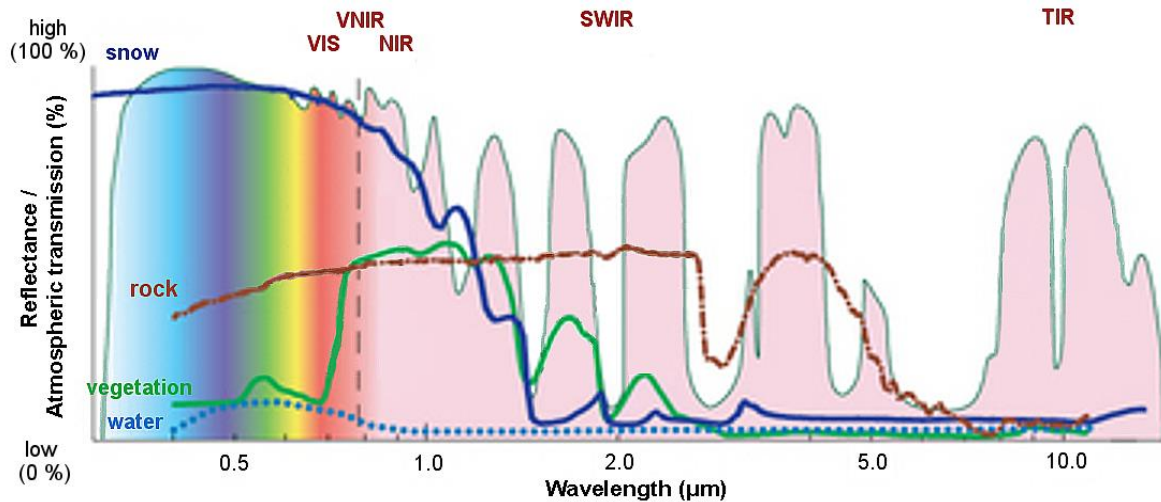


Figure 21: Spectral endmembers of different land cover types (Kaab, 2014).

When considering the use of classification models in geomorphic mapping, Kennedy et. al (2021) suggest that a spatial resolution of 10 – 100m is required to capture the diversity of landforms. The quality of the classification is dependent on the extensiveness of spectral endmembers and can be enhanced with additional layers (Yu et al., 2014). Specific remote sensing indices, such as Normalised Difference Vegetation Index (NDVI), can utilise ratios between bands significant for certain land cover types and added to classification models to improve accuracy through the capacity for class differentiation. Hence, the accuracy of existing classifications in Belize can be enhanced through the application of more spectral bands in the analysis. Previously, these have only included four spectral bands (CZMAI, 2021).

Supervised classification methods are dependent on user selected training data. The selection of good quality training samples, which fully characterise the variability of class signatures, is paramount. Training sample size presents a larger impact on classification accuracy than the algorithm used for processing (Huang et al., 2002). Large and accurate training samples are consistently important across any algorithm employed (Lu and Weng, 2007; Li et al., 2014). Doyle et al. (2021) have shown that the specific tailoring of training samples can be used to assess land use to a 90% accuracy. This is an improvement to an unsupervised approach which provides an approximate accuracy of 62.5% (Nurdin et al., 2019).

Class imbalance of training samples can lead to bias in models. If imbalanced class samples are used then relatively rare classes will be underrepresented relative to their true proportions in final model due to their smaller proportions of the training set. Blagus and Lusa (2010) found

that Random Forests and Support Vector Machine classifiers were influenced by imbalanced training data and should be avoided using an equalized stratified random sampling design (Stehman and Wickham, 2011). In the situation where a small training sample is provided or the quality of training pixels are uncertain, an algorithm robust to these uncertainties should be used. Ensemble decision tree methods, including Random Forests (RF), are robust to these inconsistencies.

The classification accuracy of individual classifiers is case dependent. With limited ground truth data on geomorphology in Belize, selecting data using a purely EO-based approach will result in uncertainties to the training data. This is because the pixels provided to train the model have not been validated on the ground and so may contain incorrect or multiple endmembers. Therefore, RF is a reasonable choice for this study to mitigate these inaccuracies.

RF provides a popular choice of classifier (Nurdin et al., 2019). RF represents an ensemble classifier which utilises large number of decision trees with random subset of training data (figure 22). Each tree uses a small sample and so is less correlated making overall ensemble more reliable. In order to decrease the correlation between trees, Rodríguez-Galiano et al. (2012) posits that a large number of trees should be used with a small number of random predictor variables available at each node. An advantage of the RF approach is the ability for optimisation to require lower computational resources compared to other classifiers. This is especially prevalent with large training samples. In coastal areas, the Random Forest classifier has performed well and provided superior results to Support Vector Machines (Pal & Mather, 2005).

RF classifications can be applied at a per pixel or object-based scale (Weih and Riggan, 2010). At a pixel level, spectral information is only analysed for an individual pixel in turn and its surrounding values are ignored and a class assigned to every pixel of an image. Conversely, object-based approaches utilise an aggregation of neighbouring pixels containing similar spectral properties which yields a class prediction for groups of pixels this often requires pre-processing of images to segment pixels into groups.

Object-based approaches often yields superior results (Nurdin et al., 2019). This is due to pixel-based methods exclusively considering pixel independent classification and result in limitations of mixed trait classification. Through the combination of pixels, spectral and spatial information is included concurrently and results in more accurate and reliable results (Pandey et al. 2019). Prior to object-based classification, an image must be divided into segments. The

segmentation algorithm employed for this can have strong influence over the outcome of classification and should be considered carefully.

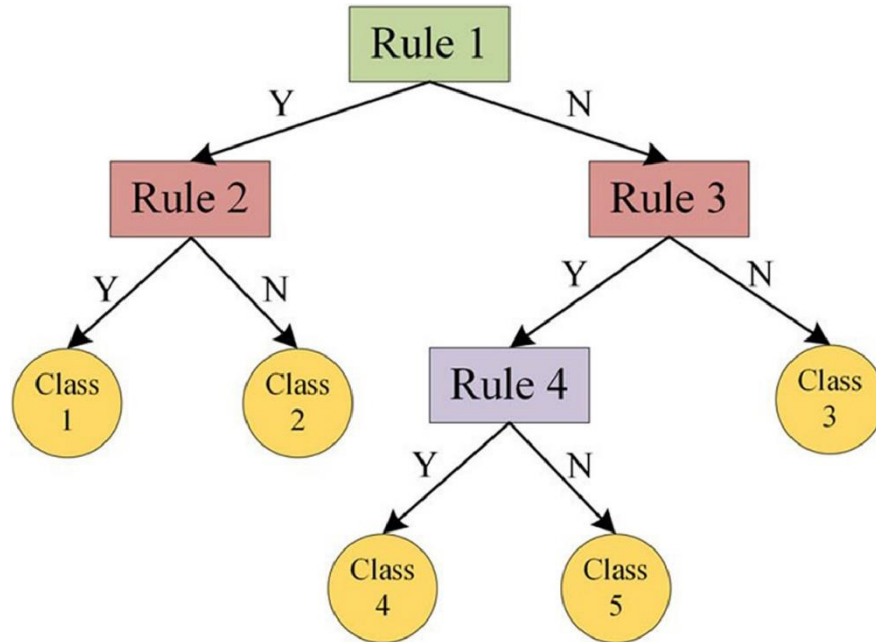


Figure 22: Random Forests decision tree architecture (Alshari & Gawali, 2021)

Hence, the ability of a classifier to faithfully represent an environment is dependent on the quality of ground truth data to train models, the intricacy of user pre-processing and classification algorithm employed.

5.2.2. Satellite Derived Bathymetry (SDB)

Studies of the coastal zone, including the modelling of coastal risk assessments, require the availability of updated bathymetric data of high (10m) to very high resolution (2m) (Wöfl, et al., 2019). Coastal processes are not currently captured by existing coarse bathymetry datasets for Belize due to their limited spatial and temporal resolutions (IHO, 2022). Enhancing the assessment of bathymetry can aid in the measurement of how morphometric parameters vary through time to enable proper Marine Spatial Planning (MSP) and sharing of coastal waters (Foley et al., 2010).

Traditional methods for bathymetric surveys consist of a small craft equipped with Single Beam (SBES) or Multi-Beam Echo Sounders (MBES) for regional high-resolution mapping. A typical MBES survey would expect to produce a vertical precision of two centimetres (Aykut et al., 2013). This approach can be prohibitively expensive without substantial funding and inefficient as survey craft are impeded by their draught and can be prohibited from operating over protected areas. As a result, hazardous areas can often be under-represented due to the high risks involved with surveying; this is especially evident in developing regions. Furthermore, mapping campaigns can be time intensive which is not a viable option for the regular mapping required for the assessment of risk after hurricane events.

In recent years, efficient technologies have facilitated the prolonged and regular mapping of the seafloor through innovations in Satellite Derived Bathymetry (SDB) serving to fill the gaps. Optical satellite imagery serves to enhance spatial and temporal continuity where surveys are limited. At a coarser spatial resolution than afforded by MBES surveys, satellites act to combat the time and economic resources required for traditional surveys while collecting enough data to elucidate prominent contour features of the seabed.

SDB provides an assessment of the depth of the seafloor in shallow coastal waters using space-borne multispectral sensors. Sensors will measure the seafloor reflectance through a utilisation of the upwelling signal of light (figure 23). The depth of the water column is established through a relationship between the intensity of upwelling reflectance recorded by the sensor and the depth (Hedley, et al., 2012).

Passive remote sensing sensors estimate SDB through surface reflectance. The most popular approach proposed by Lyzenga et al. (2006) utilises depth invariant indices but requires a preliminary classification of seabed to account for bottom reflectance. These models have since been refined by Hedley et al. (2012) to encompass a more thorough adaptive lookup table approach.

A physics-based model inversion approach to SDB will derive a depth estimate at each pixel using equations governing the propagation of photons through the water column. An assessment at each pixel will allow large areas to be surveyed very quickly with minimal resource requirement. A physics-based approach can be applied without the presence of known data points to train the inversion model. This is particularly useful in areas (such as Belize) which are lacking in existing depth data (Casal, et al., 2020).

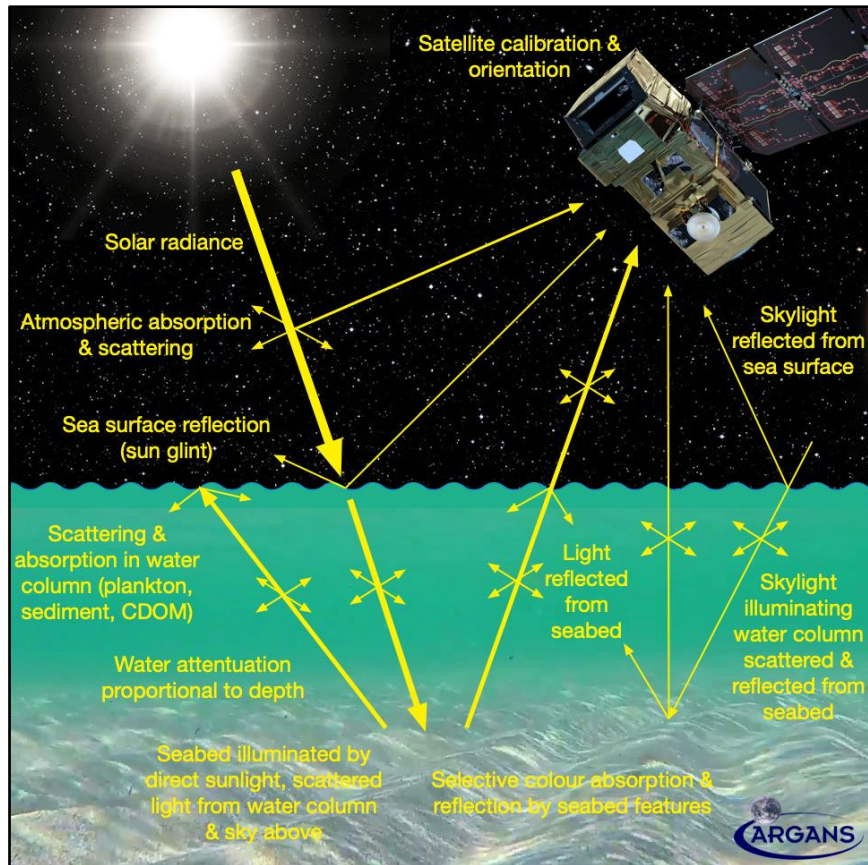


Figure 23: Conceptual model of photon travel in SDB (ARGANS Ltd., 2019).

Although there is no obligation for SDB models to utilise insitu bathymetric data, the assessment of the accuracy of a model is limited without this (Headley et al., 2012). Furthermore, the availability of in situ data can be utilised to calibrate parameters used in imperfect estimations of atmospheric conditions for the image to ameliorate effects of data bias. Traganos et al. (2018) show that the vertical uncertainty of SDB models recorded using Sentinel-2 is $\pm 3\text{m}$ but can be improved to $\pm 1.5\text{m}$ through training algorithms with appropriate data. Therefore, the ability to evaluate the performance of these models is limited by the data available for evaluation.

Moreover, the accuracy of SDB models is dependent on sensors and algorithms employed (Ashphaq et al., 2021). A trade off exists between spatial, spectral and temporal resolutions and there is a focus on the requirement for very high-resolution (VHR) data amongst the hydrographic community. Laporte et al. (2020) refute this suggestion due to the reduction in image quality, absence of orthorectification and significantly increased processing requirements. Model quality can be adversely impacted over water in VHR imagery due to a

high signal to noise ratio increasing the impact of anomalies from ocean glint (figure 24). The expense of commercial VHR data and poor relative frequency of acquisition further contradicts the benefit of using SDB for regular and cheap monitoring. Sentinel-2 is, however, suggested as a viable alternative through the improved propagation of noise and environmental uncertainties.

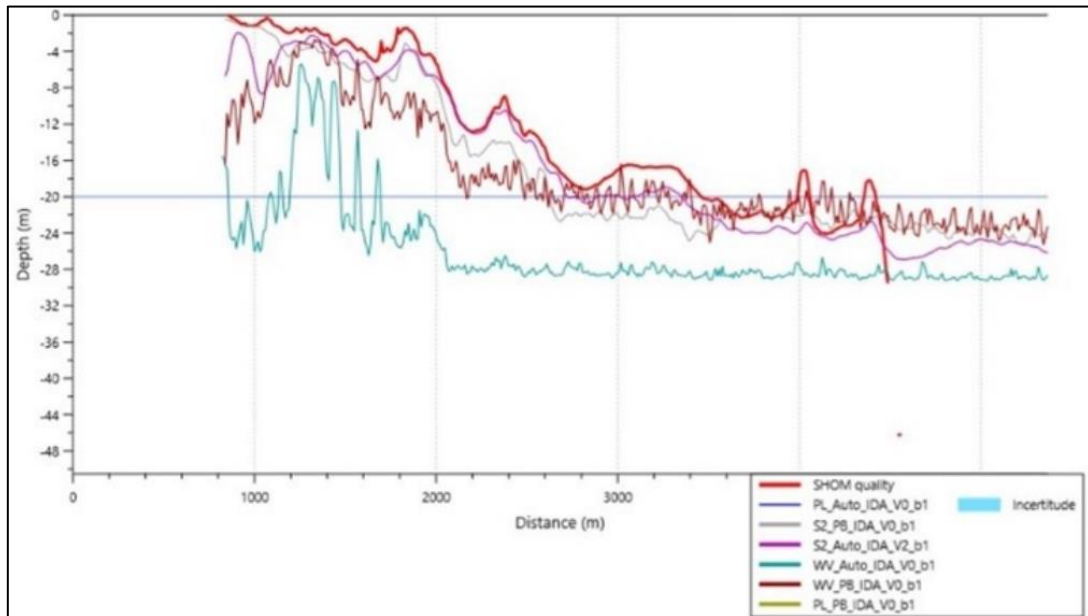


Figure 24: Satellite Derived Bathymetry results in Guadeloupe against ground truth (red) using various sensors: Pleiades (blue), Sentinel-2 (purple) and Worldview-2 (turquoise) (Laporte, et al., 2020).

SDB relies on the relationship between reflected solar radiation and sea depth. However, this is not consistent in water columns of differing clarity (NOAA, 2014). Solar radiance will enter the water column as white light which is absorbed at different rates in relation to its wavelength (figure 25); hence the spectrum of light observed within the water column will change rapidly with increasing depth. In the clear ocean the red wavelengths will be attenuated at the fastest rate; this results in a blue hue. However, in more turbid coastal waters dissolved organic material will result in increased absorption in the blue spectrum which can shift the light spectrum towards the red wavelengths.

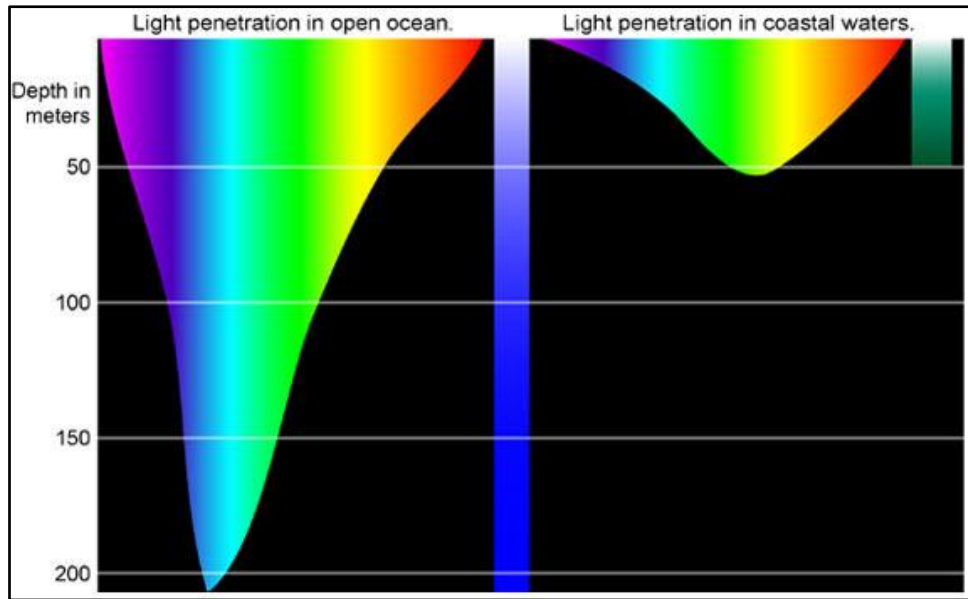


Figure 25: Light attenuation in open ocean and turbid coastal waters (NOAA, 2014).

Furthermore, the penetration capacity of light in water can be influenced by the seabed characteristics as geologic composition can impede the concentration of reflected light (Louvart et al., 2022). Coastal areas that have large concentrations of sand deposits on the seafloor, for example, will reflect more radiation than the equivalent seabed consisting of seagrass or algae. Typically, coastal waters constitute more turbid environments with an abundance of Coloured Dissolved Organic Matter (CDOM), such as phytoplankton, and suspended sediments also impeding the penetration of EM radiation.

As the results acquired through SDB rely on the reflectance of solar radiation from the seabed, accurate data acquisition is limited to a maximum of thirty metres in clear coastal areas due to these patterns of attenuation (Louvart et al., 2022). The effective cut off is dependent on the inherent optical properties of the water at each site and is generally likely to be less than this extent. This limits the use of SDB in coastal mapping to the nearshore area.

The properties of SDB suggest that it could be a viable tool for survey planning and regular coastal monitoring, especially for national hydrographic offices with limited resources, however. Misra and Ramakrishnan (2020) demonstrate the application of SDB to aid management of the marine environment. Coastal erosion impacts were assessed through the mapping of geomorphological changes to the seabed. This study achieved a RMSE value of less than one metre with the highest inaccuracies observed at deeper depths. These uncertainties emphasise the intrinsic decrease of accuracy with depth and presents its relevance for use in

shallow water coastal areas. SDB results were useful to management agencies through enabling a reduction to the number of repetitive in-situ surveys required.

5.2.3. Satellite altimetry

Characterising the variability in sea state conditions is a high priority in the assessment of vulnerability to coastal communities and is a key parameter in the CVI. Therefore, the accuracy of wave height derivation is vital. The World Meteorological Organisation (WMO, 2018) detail the requirements for wave height derivation accuracy at 5-10% (or 10-25cm), however, for applications in coastal regions this is required to be higher and presents significant challenges.

One such challenge is that long term time-series data from observations is required and is often limited. Traditionally this information would be acquired from in-situ moored data buoys (Dodet et al., 2020). These work under the premise that the measured buoy motion can be converted into wave motion based on hydrodynamic characteristics. However, this can produce over estimations of up to 56% in high winds due to the mean tilt of the buoy (Bender et al., 2010). Furthermore, these buoys are sparse and their distribution uneven (figure 26). Wave data is derived from buoys in the coastal margins of North America and Europe but present large data gaps for the rest of the global ocean. This is particularly prevalent in the tropics (Ardhuin et al., 2019). Wave buoy data is sparse and discontinuous leading to systematic errors on a regional basis and in extreme storms within the datasets.

The limitation of sparse data coverage is reduced through historical hindcasting (Liang & Wang, 2019). Wave climate is determined in this method through running ocean response models for historical periods, a prominent example of which is the Copernicus Marine Environment Monitoring Service (CMEMS) WAVERYS model (Law-Chune et al., 2021). WAVERYS provides a comprehensive record of global ocean significant wave heights (SWH) from 1993 to 2020 at a three hourly resolution. Although satellite data is ingested into these models, hindcast models often rely on insitu observations for validation. The complimentary use of both datasets in WAVERYS have provided an accuracy of SWH derivation at 8.7% (Law-Chune et al., 2021).

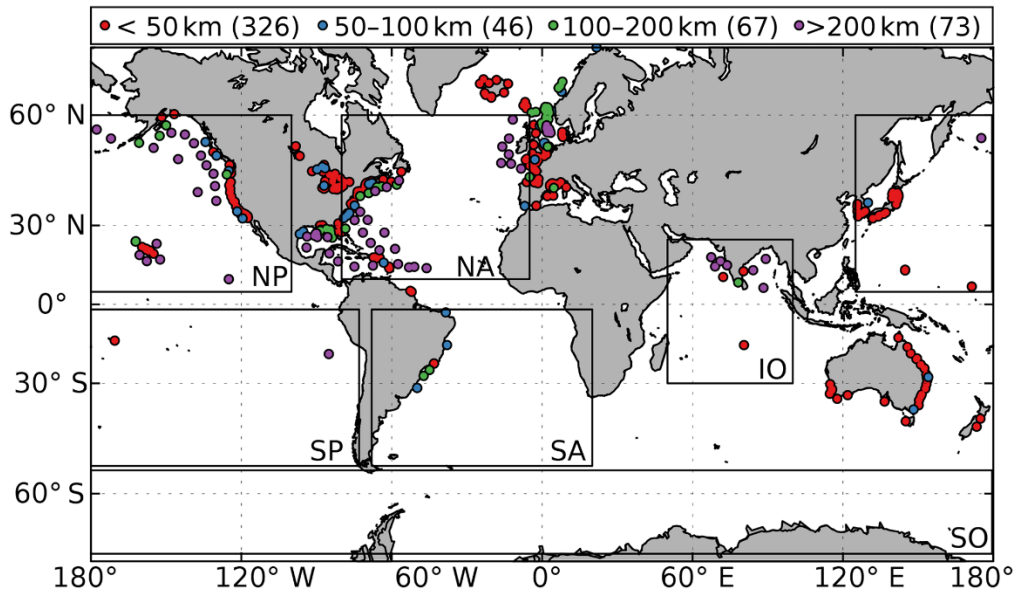


Figure 26: Location of wave buoys (Dodet et al., 2020).

Satellites are employed in the derivation of sea state through nadir-orientated altimeters and synthetic aperture radar (Collard et al., 2005). Data quality is dependent on calibration to combat instrument bias and drift (Ribal & Young, 2019). Radar altimetry works under the principle that pulses emitted from the sensor are reflected by the sea surface at nadir and are subsequently recorded as a function of time (figure 27). The time can provide an indication of distance between the instrument and incident surface and facilitates the derivation of wave height.

Satellite data can be acquired over larger volumes and hence sample more extreme sea states than traditional wave buoys (Hanafin et al., 2012). Although it is impeded by the short time series, extending 30 years in the case of WAVEYYS. This makes it difficult to establish any multi-annual fluctuations of wave height, including North Atlantic oscillations. Inconsistent representation can bias trends and result in inappropriate statistical weighting applied to observations which are strongly affected by a climatic mode (Timmermans et al., 2020). This should be considered in Belize, a country subject to the ENSO.

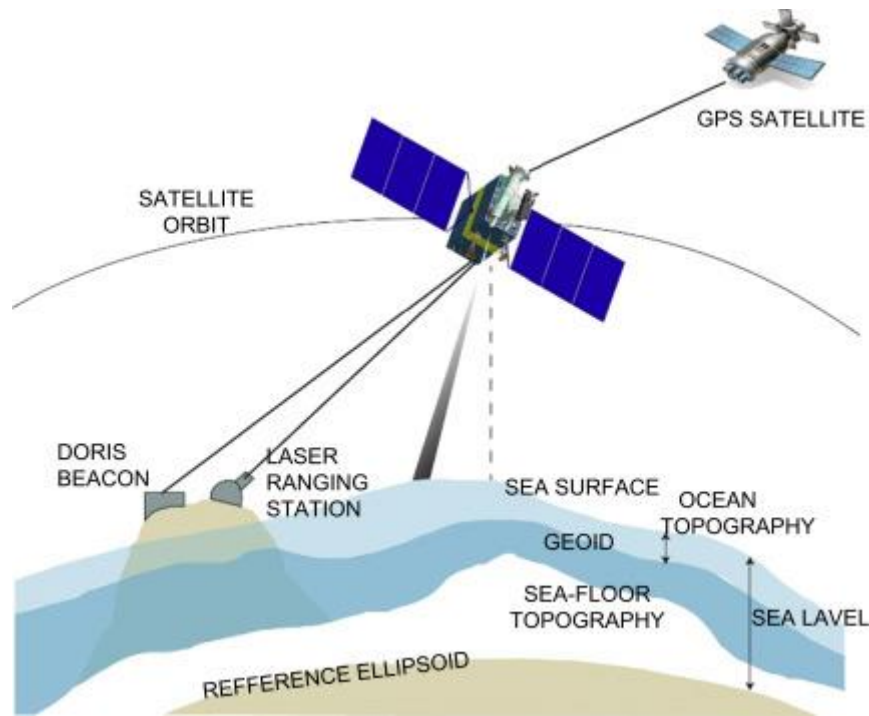


Figure 27: Principles of satellite altimetry for wave climate (Liang & Wang, 2019).

WAVERYYS is also limited by the spatial sampling of 0.2-degree grids. Smaller scales will be desirable for applications in the coastal zone due to the refraction of waves over shallow bathymetry and tidal currents modifying wave height. The issue with fine spatial resolutions in the coastal zone is the contamination of altimeter signals close to land which can cause data loss or accuracy reduction (Law-Chune et al., 2021). A sparse pattern to altimeter sampling can provide bias to the modelled wave condition and is prevalent in extreme conditions (Jiang, 2020).

Comparisons between altimeter data and in situ measurements showed much better agreement when coastal buoys (<200 km) were discarded from the analysis with figure 28(a) demonstrating a higher RMSE and bias. This is attributable to land shading and refraction which modify SWH over short distances (Dodet et al., 2020). In addition, coastal backscatter results in inconsistencies with satellite footprints close to the coastline and stronger variation of wave properties in the coastal zone. This is as a result of tidal currents, bathymetric refraction and coastal winds and invalidates the assumption of homogeneity in sample grids. Altimetry is particularly useful in remote ocean areas or regions which lack infrastructure to populate hindcasting models. Jiang (2020) suggests a hybrid approach which incorporated both altimetry and reanalysis models.

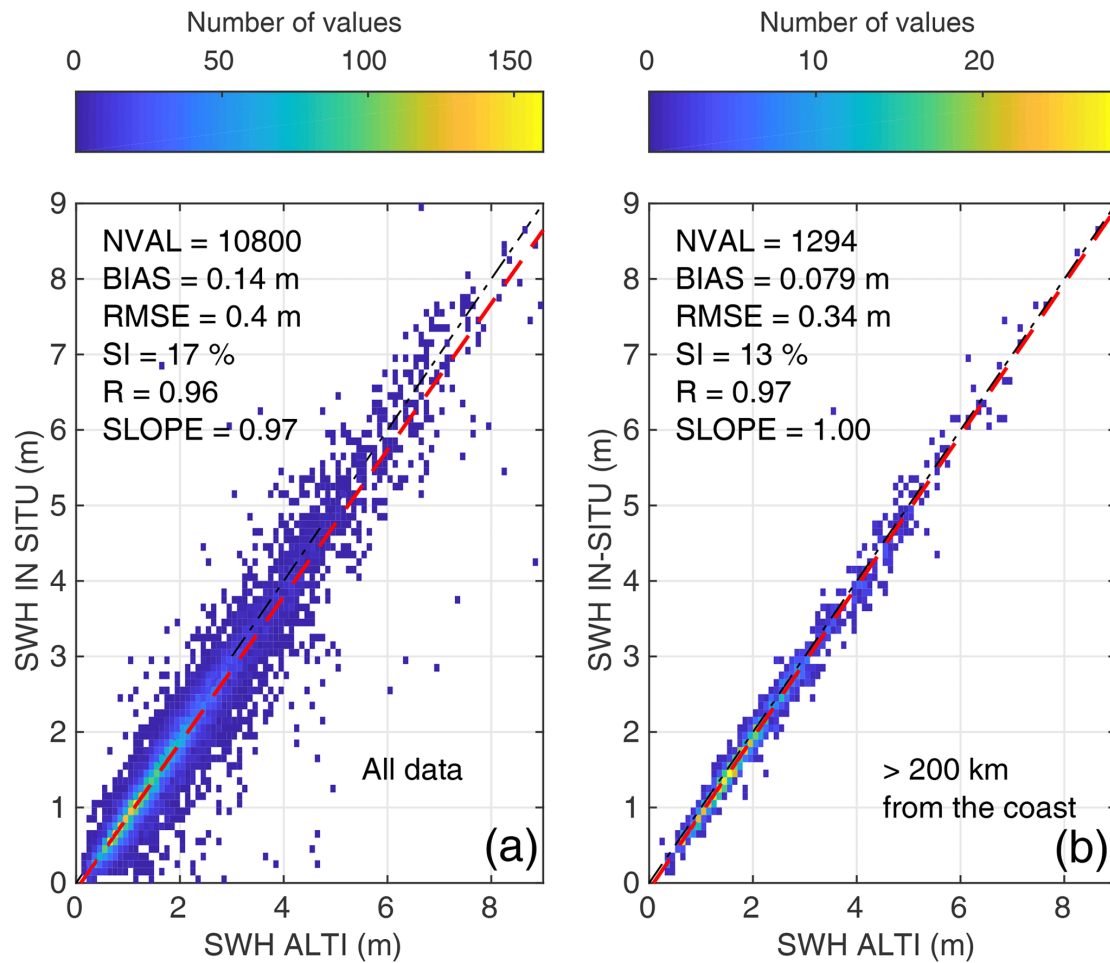


Figure 28: Validation of wave height derived from satellite altimetry against in-situ buoy measurements (Dodet et al., 2020).

The trajectory of hindcast modelling likely to continue with Surface Water Ocean Topography mission (Morrow et al., 2019) and the extension of the Sentinel-1 constellations with Sentinel-1C & 1D launching in 2022 and 2023 with modified wave mode of two incidence angles for improved swell sampling demonstrating a robust and sustainable approach to wave height derivation with prediction accuracy set to increase in coming years.

5.2.4. Digital Elevation Models (DEMs)

An understanding of topographic variability facilitates the characterisation of the interplay between dynamic earth systems (Wilson, 2018). The CVI requires an assessment of coastal topography as a proxy for the inundation capacity of surge water. Digital Elevation Models (DEMs) represent gridded rasters which can provide elevation data for this purpose. These are often provided as global products and derived from the remote sensing approaches of photogrammetry or interferometry. DEMs of this nature offer high positional accuracy with improved speed of data acquisition for areas that are difficult for survey access (Fuss, 2013).

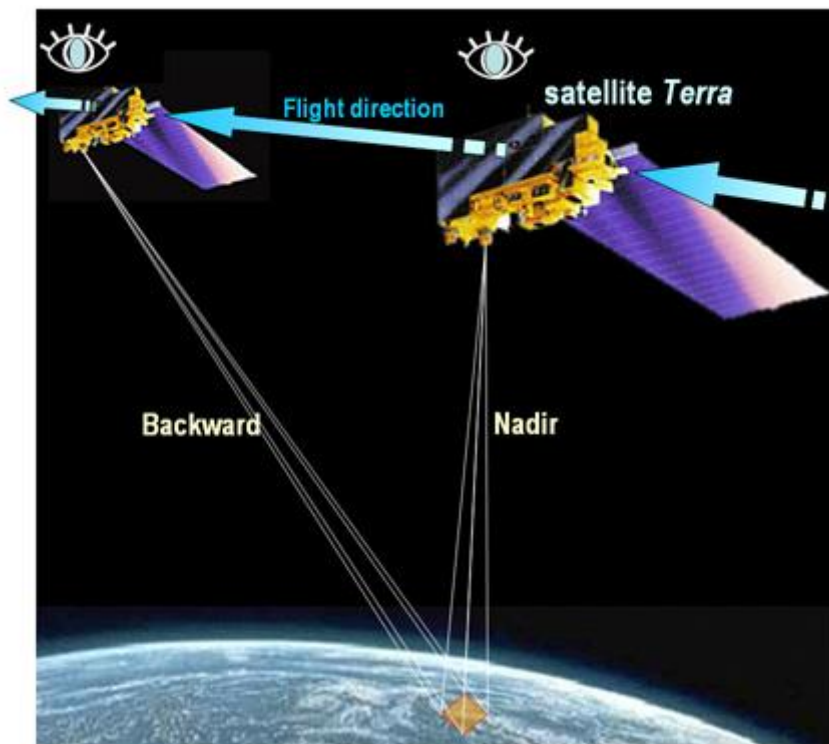


Figure 29: Principles of DEM derivation (Japan Space Systems, 2016).

A photogrammetric concept for deriving topography from satellites involves a stereo image acquisition (figure 29). This consists of two images acquired at nadir and off-nadir angles for the same region. The stereo image product represents a Digital Surface Model (DSM) and accounts for natural and artificial features (such as trees and buildings). This must be converted to a DEM which represents the bare-earth surface referenced to a vertical datum (Okolie et al., 2022). This pre-processing is achieved through morphological filtering to mask non-terrain features (Ismail et al., 2013). A distinction between DSM and DEM can be seen in figure 30.

DEMs are preferable for use in assessing flood risk because this represents the underlying coastal morphology and is not impeded by buildings or tree canopies which would infer a disproportionality lower vulnerability (Wilson, 2018). Belize has a low-lying topography and a gentle gradient. Therefore, the DEMS used must be reliable and robust to areas with subtle variations in their elevation. A DEM produced through this approach is the ASTER global DEM and provides regular topographic assessments at a 30m resolution (Japan Space Systems, 2016).

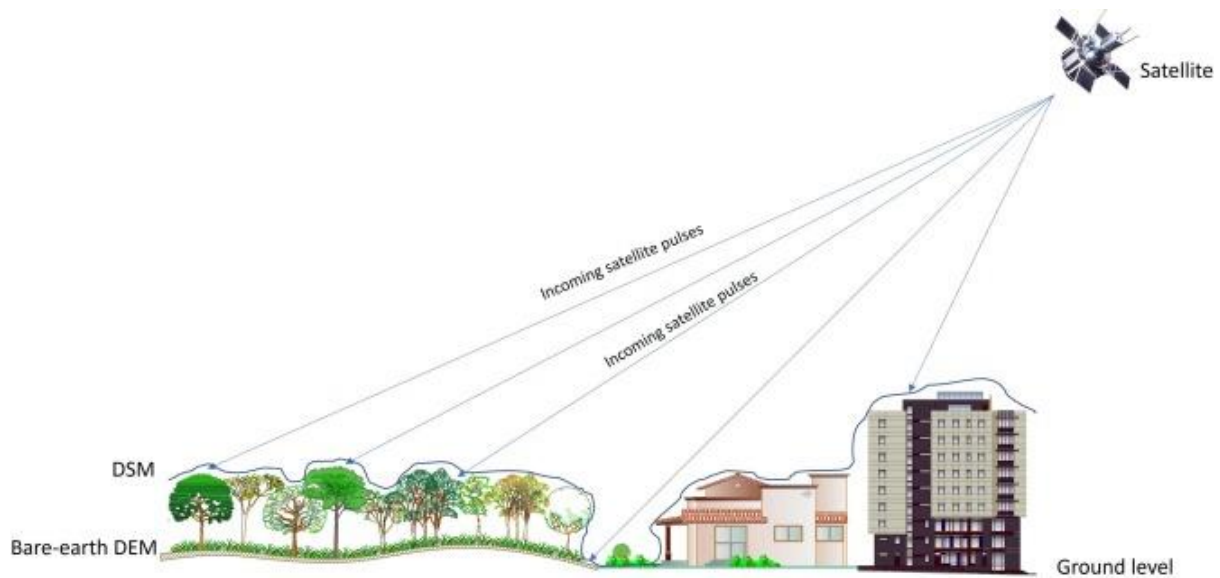


Figure 30: Distinction between Digital Surface Models (DSMs) and Digital Elevation Models (DEMs) (Okolie et al., 2022).

Conversely, interferometric-based approaches have also been employed in the generation of elevation models. The Shuttle Radar Topography Mission (SRTM) was launched in 2000 and uses multiple radar images captured at the same time to create a DEM (Werner, 2001). This dataset is only available over a 90m spatial resolution for the year 2000 which presents issues for data relevance, especially in coastal areas subject to dynamic changes.

Hayakawa et al. (2008) provide a comparison of the performance of photogrammetry and interferometric approaches. ASTER is shown to produce superior results in low elevations due to a higher spatial resolution and less missing data from a continued image acquisition. The vertical accuracy of ASTER is recorded as less than half that of SRTM (Farr et al, 2007). A full comparison of which can be seen in table 4.

Errors in derivation of DEMs are likely to extend from spatial sampling and interpolation methods (Guo et al., 2010). These processing techniques can insight bias. Measurement error may occur due to sensor noise which can produce speckle noise in the models. In addition, the age of data will cause inconsistencies because of land cover changes. The outdated nature of the SRTM further suggests ASTER will provide more suitable results in Belize; a region where rapid urbanisation is constantly changing the morphology of the coastal zone.

To minimise these issues for flood mapping, topographic data should be acquired recently and provide high vertical accuracies. A large-scale assessment of topography is beneficial for coastal vulnerability assessments to determine low-lying areas as these are associated with highly vulnerable categories with low coastal slopes. Therefore, ASTER can be seen to provide superior results for this application.

Table 4: Comparison between ASTER and SRTM DEMs.

	ASTER	SRTM
Source	Stereo image photogrammetry	Synthetic Aperture Radar on board space shuttle
Acquisition period	2000 – Present	2000 (11-day mission)
Spatial resolution	30 metres	30 metres for United States 90 metres globally
Vertical accuracy	7 metres	16 metres
Spatial coverage	Global	60 degrees North to 56 degrees South
Gaps to coverage	N/A	Areas with steep topography

5.3. Machine Learning

Satellite data techniques can fill the gaps in data extents through efficiently surveying the coastline at a large scale. Another problem presented by the CVI, however, is the inability to automatically scale for application in new coastal regions or environments. Currently, this requires a manual adaptation of thresholds which divide the coastline into segments of relative vulnerability. This incites a subjective bias to the qualification.

The analysis of data through machine learning (ML) is rapidly becoming a new paradigm in remote sensing through the ability to process large quantities of data without the interference of humans (Lary et al., 2018). ML allows for automation of complex tasks and provides multifaceted merits including modelling and image classification.

In the context of modelling, unsupervised ML models involve the training of algorithms with an unlabelled dataset to learn independently to identify patterns in similar features within the dataset (Xu & Wunsch, 2005). Therefore, user guidance based on contextual information is not required. This allows for the discovery of unknown patterns in datasets and a more flexible approach to model automation. Unsupervised ML can be applied to several situations given an abundance of data but is particularly useful in the clustering of data.

An application of ML to automate the detection of thresholds will reduce the subjective bias of hard defined boundaries and facilitates the automatic scaling to adapt the method for new environments (Calil et al., 2017). This is based on the conditions seen in an image rather than hard defined boundaries to subsets of a parameter (some of which may not even be present in the study area). This provides a consistent metric for grouping variables and will be comparable for conditions which may change in multiple images or in new regions of the globe.

5.3.1. Clustering algorithms

Clustering through ML will enable the division of coastal segments into groups representing a relative parity for vulnerability. This is based on whether similar geotechnical properties are demonstrated and have been evaluated in each EO parameter. Clustering involves the grouping of uncategorised objects based on their similar features to find natural distributions in the data (Xu & Wunsch, 2005). A typical clustering workflow is shown in figure 31 where a key consideration should be given to the clustering algorithm chosen.

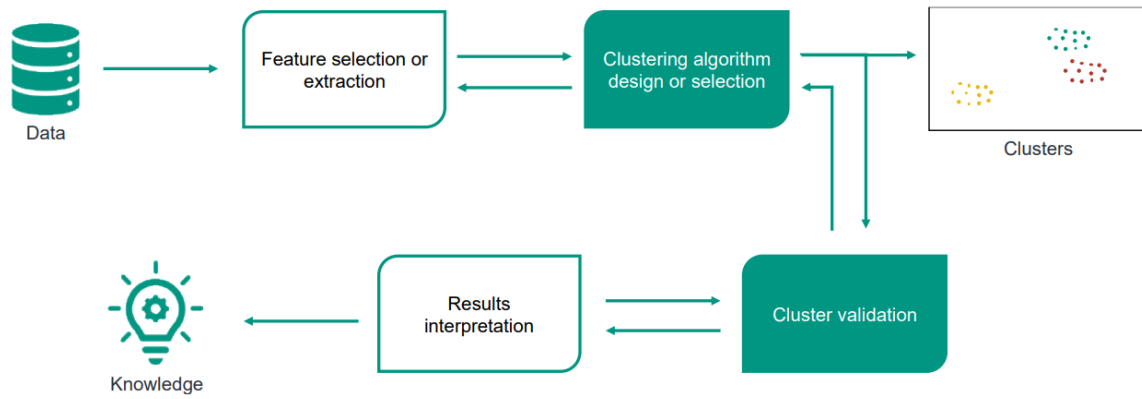


Figure 31: Clustering workflow (Xu & Wunsch, 2005).

The KMeans algorithm uses a partitional approach to distribute discrete data into a specified number of clusters with k representing the number of pre-determined groups (Ahmed et al., 2020). Partitional clustering splits the data based on an iterative location of datapoints to assign clusters based on similar properties; the quality of partitioning is enhanced with more iterations. The granularity of which can be adjusted through number of clusters chosen. The algorithm constructs a feature space based on pixel values to determine the distribution of groups (figure 32). In the context of remote sensing, each dimension of the feature space will represent a spectral band in an image or an individual parameter of a model.

The KMeans workflow is outlined in figure 33. Clusters are assigned through the dropping of centroids. This is an iterative process which repeats a pre-determined k -number of iterations with a new cluster centre being dropped for each. With every iteration, the distance of the clusters shifts and the distance between the dropped centroid and surrounding datapoints is assessed. An optimal centroid location is determined through minimising the Euclidean distance to surrounding points and clusters are assigned to data points with closest to a centroid (Ahmed et al., 2020). This process continues until there is no more movement in the centroid of each cluster or until the stopping criterion is met. Iterating this process with different random centroids ensures groups are well separated and present a greater intra-cluster similarity than inter-cluster similarity.

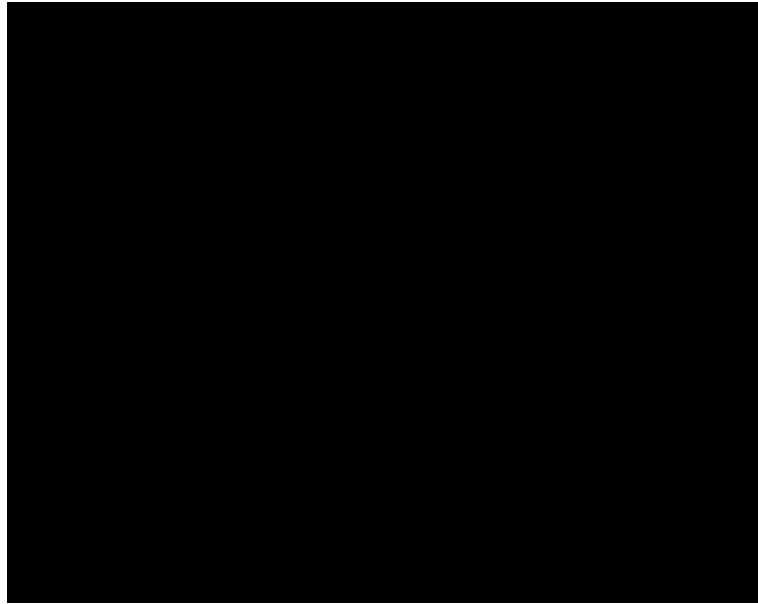


Figure 32: KMeans clusters in the feature space of an image (Wikipedia, 2022).

This method is effective at computing clusters synchronously and is simple to implement with a low computational intensity (Jain, 2010). However, KMeans encounters limitations through the initialisation of parameters in the inability to propose optimal number of clusters – these are defined by user and provide suboptimal results if not appropriately defined to sufficiently split the group (Rathore et al., 2018). The number of iterations to obtain a suitable distribution is also unknown and must be defined by the user, overcompensation can increase memory requirements and processing time.

Furthermore, KMeans is sensitive to outliers and can skew clusters through the forcing of data points which are far from the centroid into the group (Saxena et al., 2017). Moreover, datasets with large variations to their magnitude will present extreme values which results in narrower confidence intervals. These datasets should utilise a univariate index to account for this prior to clustering (Rueda et al., 2017).

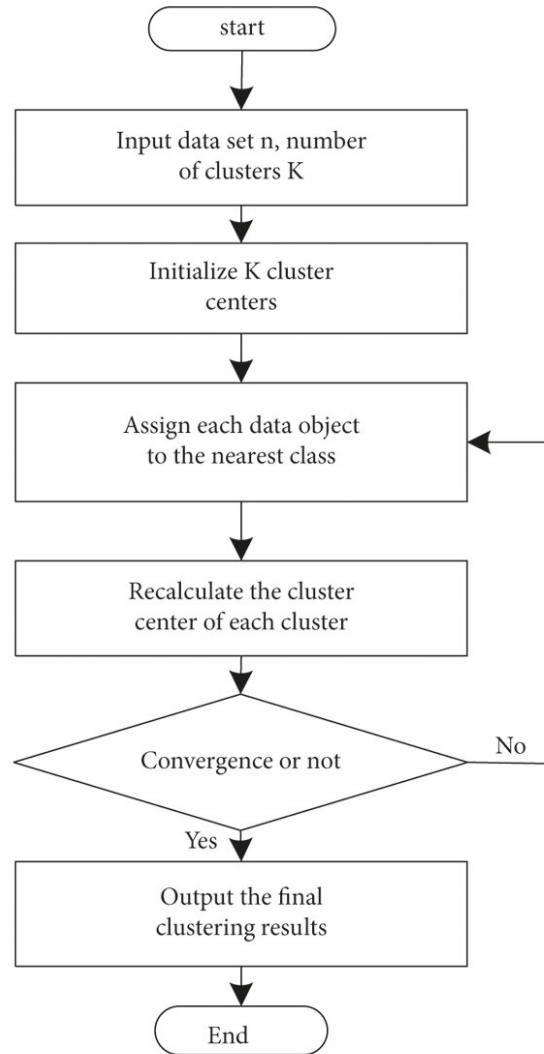


Figure 33: KMeans clustering workflow (Hao, 2021).

Calil et al. (2017) demonstrates the application of ML clustering to the identification of coastal risk hotspots with an emphasis on Self-Organising Maps and KMeans (figure 34). This study classified over 50,000km of coastline into nine distinct clusters based on coastal hazard, geographic exposure and socioeconomic vulnerability. Coastal hazard in this context was limited to the assessment of wave energy, storm surge, El Niño and cumulated cyclone winds. This method has shown merit for the processing of large-volume, multidimensional and multivariate data with a high computational efficiency to assess coastal risks to Latin America and the Caribbean on a comparative scale. Clustering is applied prior to the calculation of vulnerability indices to facilitate the simplification of analysis by categorising multivariate data based on similar attributes and allows for drivers of coastal risks to be traced back to individual clusters. These hotspots can be easily identified to show where consistent reduction strategies

might be applied. Calil et al. conclude by suggesting higher resolution and smaller scale studies are needed with a focus on coastal risk reduction. Localised case studies, such as that of Belize, will provide an extension of this approach in specific coastal zones.

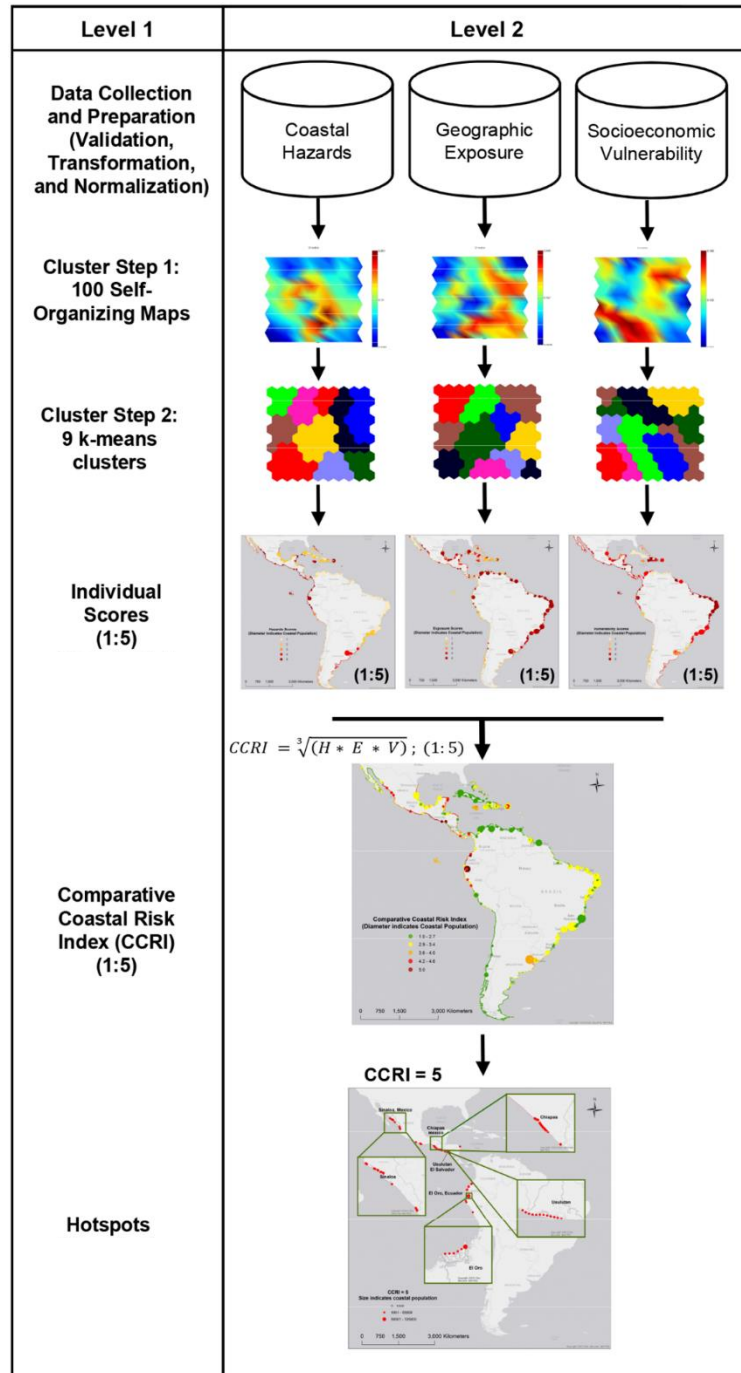


Figure 34: KMeans clustering for coastal vulnerability in Latin America and the Caribbean (Calil et al., 2017).

PART III – METHODS

This section outlines the methodology employed in this study and the approach to the integration of remote sensing and machine learning within vulnerability studies.

6. Methods

6.1. Conceptual framework

Coastal vulnerability has been assessed through the traditional index-based approach. The Coastal Vulnerability Index (CVI) has been evaluated using the corresponding indicators of geomorphology, coastal slope, wave climate, wind speed and tidal range. These have each been derived using satellite remote sensing techniques to address the issue of expensive field surveys required to characterise the coastal zone. Satellite images have been taken from the last five years provide an indication of current conditions scenario for vulnerability.

Traditionally, the CVI metric incorporates shoreline change as a measure of erosivity of the coastline pertinent to vulnerability. Abuodha (2010) suggests this provides an indication of coastal response to storm surges as opposed to physical characteristics purporting to vulnerability and therefore was omitted from this study. Current rates of shoreline retreat for Belize are estimated at -0.49m/yr (Azueta et al., 2020) which is below the accuracy of current remote sensing (RS) derived methods which are dependent on the RS sensor used and must exceed half a metre per year (Luijendijk et al., 2018). Luijendijk et al. (2018) demonstrate the accuracy of vector shoreline data derived from Sentinel-2 is between one and five metres. This approach is more suitable to coastline experiencing higher erosivity and should be considered when evaluating vulnerability in such locations.

Another parameter within the CVI framework is the rate of sea-level rise (SLR). Vulnerability has not been assessed with respect to this variable due to the homogenous effect of SLR in the region of interest. The global rate of SLR is 1.8mm/yr and is classified as a very low vulnerability. This rate reflects a eustatic change apparent to all shorelines. An incorporation of this dataset would provide a constant quantity and not illustrate disparities along the coastline corresponding to SLR. A dataset representing heterogenous changes for Belize does not yet exist.

The framework proposed in this study (figure 35) revolves around the application of machine learning (ML) to cluster parameters into groups of similar geomorphic conditions. Each group will possess similar parity for vulnerability. This removes the need for the static thresholds shown in the vulnerability table (figure 14). The thresholds outlined by Gornitz are not appropriate to evaluate relative risk along coastlines around the world, coastlines with little variability will often all fall into one risk class and does not help isolate areas which may be disproportionately at risk. Derivation of appropriate thresholds will require technical insight to survey the coastline and divide observations into specific classes. These are instead evaluated whenever the model is run based on the conditions seen in an image. This provides a globally scalable approach as vulnerability is provided relative to other clusters.

KMeans is a method of machine learning to group dimensional datasets. This has been used in this study to cluster segments of the coastline into vulnerability groups which contain similar properties. Due to the lack of spatial concurrence between marine and terrestrial variables in the CVI, parameters are sampled to provide generalised conditions across a one-kilometre gridded samples (Koroglu et al., 2019). The KMeans classifier facilitates the analysis of these large and multidimensional datasets at a low computational cost. Outputs of the model will consist of raster maps demonstrating vulnerability with respect to each parameter and an overall combined CVI value map with larger cell values representing an increased degree of vulnerability.

A number of advantages are achieved through using this approach. The first is the easy identification of hotspots which can be traced to individual parameters demonstrating coastal vulnerability drivers. These clusters present similar conditions which can be attributed to consistent management strategies. Furthermore, the redundancy of in-situ data results in a scalable approach to new locations without the need for prior study. This results in a cost effective and repeatable approach.

This preliminary study will focus on the Northern and Central Belize coastal management districts due to their dense populations and low topography (figure 36).

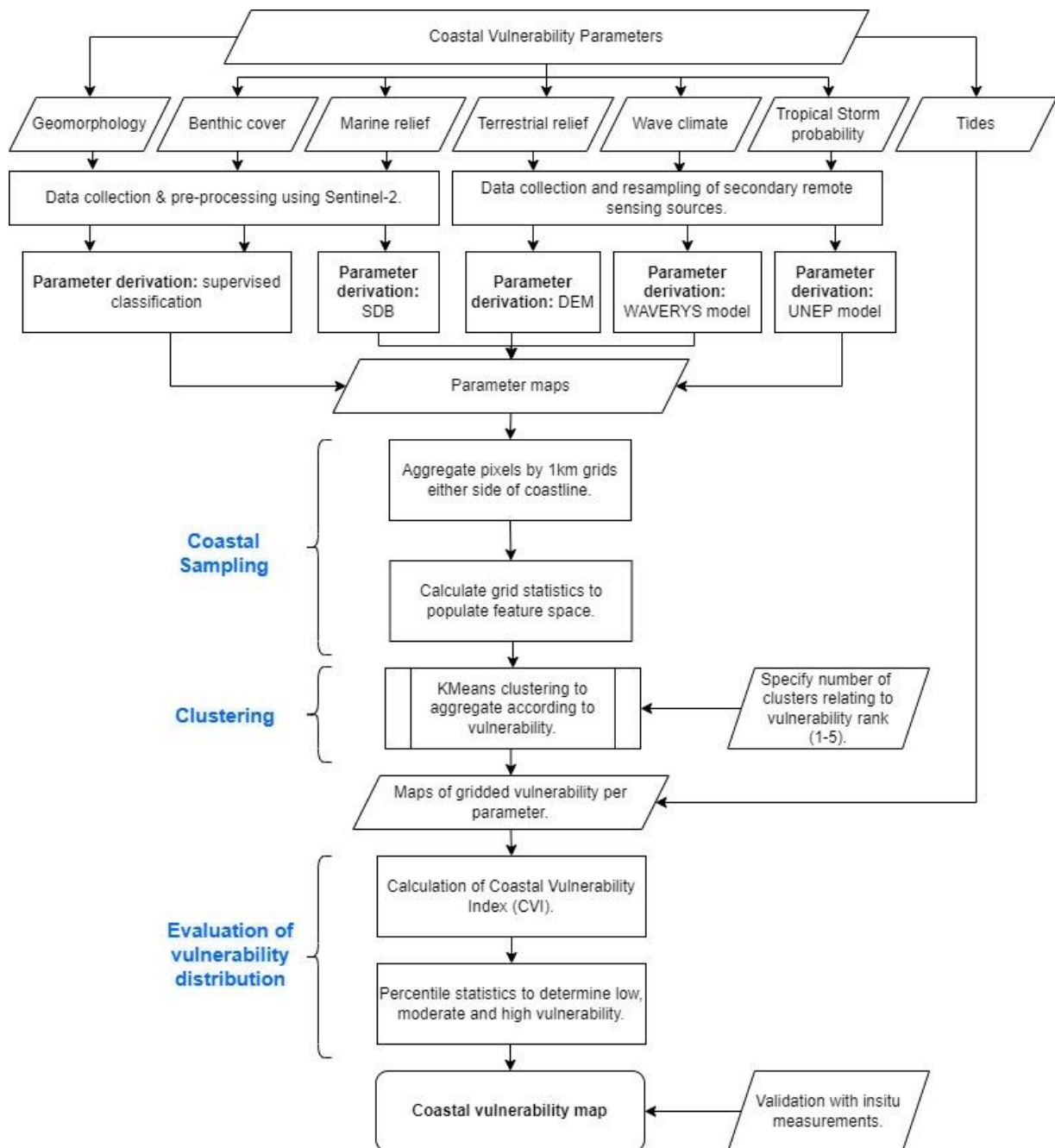


Figure 35: Workflow for the derivation of CVI using remote sensing and machine learning.

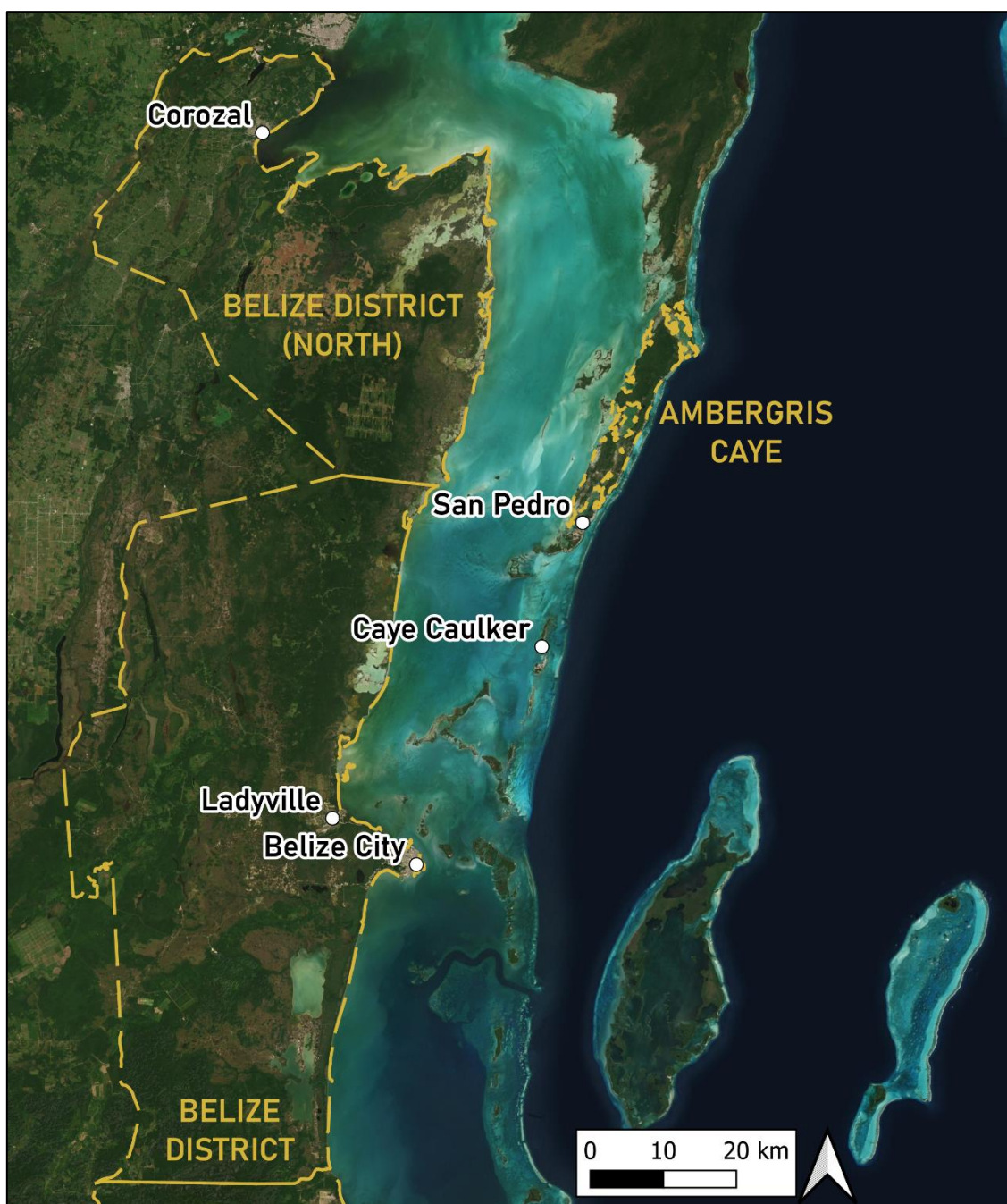


Figure 36: Belize study area. Key settlements (black) and management districts (gold) are labelled.

6.2. Data

To provide characterisation of the coastal zone, key coastal parameters have been quantified using a range of remote sensing techniques. These have been split into two broad groups based on the datasets utilised in their derivation.

Sentinel-2 forms the basis of the optical remote sensing approach and has been used to evaluate parameters based on the emission and absorption of spectral radiation. This technique is specifically useful for the differentiation of spectral responses and is well suited to classifications and SDB.

In addition to Sentinel-2, open-source remote sensing datasets have been employed to characterise other environmental conditions utilising several RS techniques, including altimetry and thermal emission.

An overview of datasets and corresponding methodology can be found in table 5.

Table 5: Overview of data sources used in this study.

Application	Dataset	Type	Processing	Temporal Resolution		Spatial Resolution	Coordinate Reference System	Source
				Available	Sampled			
Land & Benthic Cover	L2A Sentinel-2	Optical multispectral GEOTIFF	Object-based supervised classification	2-5 days 2015 – Present	11/2017 – 06/2020	10m	EPSG: 32616	(Copernicus, 2022)
Bathymetry	L1C Sentinel-2	Optical multispectral GEOTIFF	Physics based inversion model for SDB	2-5 days 2015 – Present	11/2017 – 06/2020	10m	EPSG: 32616	(Copernicus, 2022)
Terrestrial Elevation	ASTER Global DEM	Thermal emission optical GEOTIFF	Mosaicked tiles	2000 – Present	N/A	30m, resampled to 10m	EPSG: 4326	(USGS, 2019)
Wave Climate	WAVERYS Hindcast model	Model using satellite altimetry NETCDF	Sampled monthly maximum SWH and translated to coastal segment	1993 – 2020	09/2015 – 01/2017	21km	EPSG: 4326	(Piollé et al., 2020)
Wind Exposure	UNEP Global Risk Data Platform (Cyclone Intensity), derived from NOAA IBTrACS product	Hindcast observations on storm trajectories GEOTIFF	None	1969 – 2009	N/A	10km, resampled to 10m	EPSG: 4326	(Knapp et. al, 2010)
Tidal range	Tide gauge data	Open access in-situ measurement	None	N/A	N/A	N/A	N/A	(PSMSL, 2001)

6.3. Primary data techniques

The following section outlines the methodology for quantifying coastal variables using the optical multispectral sensor onboard Sentinel-2.

6.3.1. Sentinel-2

In 2015, the European Space Agency (ESA) launched the twin optical satellite mission Sentinel-2 as part of the Copernicus programme. The Multispectral Instrument (MSI) payload affords a high spatial resolution of ten metres in the visible bands. A spatial resolution of ten metres reduces glint on the water surface as returning signal is more homogenous which results in a less signal to noise ratio in the model than the equivalent VHR sensor while still possessing capacity to elucidate contours of bathymetry.

In addition, thirteen spectral bands encompass the EM spectrum from visible (443nm) to Short Wave Infrared wavelengths (2190nm) which aids the detailing of light transmissibility in water. Coordination between two satellites in a sun synchronous orbit provides a temporal revisit time of five days at the equator. This regular coverage produces a large database of imagery which can be especially useful in areas where adverse weather may prevent clear image acquisition. Finally, the georectification and orthorectification of products produce a reduce geometric biases to enhance positional accuracy. Fourteen Sentinel-2 images have been used in this study across seven acquisition dates. These cover the tiles T16QCE and T16QDE (table 6).

Table 6: Dates of Sentinel image acquisition for tiles T16QCE and T16QDE.

20171118	1628GMT
20181203	1628GMT
20190924	1628GMT
20191118	1628GMT
20200102	1628GMT
20200122	1628GMT
20200206	1628GMT

6.3.2. Supervised classification

Geomorphology is pertinent to expressing the degree to resistance to erosion and provides a proxy for the inundation potential of floodwater through their capacity to dissipate wave energy. This parameter will affect both the marine and terrestrial environment and has been evaluated in the form of a land cover classification and benthic sea floor cover assessment.

In both instances, these classifications have been derived using atmospherically corrected Level 2 Sentinel-2 images. A time series approach has been used to merge individual scene acquisitions layers to create cloud free composite images through maximum value of NDVI (Corbane et al., 2020). This approach provides a superior spatial resolution to the existing CORINE open-source land cover map with a one-hundred metre positional accuracy.

Data fusion of reflectance and spectral indices was used to produce an image composite which would enhance disparities between spectral features. Pre-processing was required to calculate an additional to an NDVI index layer, using the Near-Infrared and red bands. Hence, the classified images contained seven spectral bands (B01, B02, B03, B04, B05, B08 and NDVI).

Image composites were classified by means of an object-based supervised classification using a bespoke Python script. A pixel-based approach was deemed inappropriate for this study due to the levels of noise produced in thematic mapping over large scales (Whiteside et al., 2011). Both an unsupervised and supervised approach were considered but the supervised approach has been seen to show superior accuracy. Each image was segmented using the Shepherd segmentation algorithm (Shepherd et al., 2019).

The machine learning algorithm used to perform the classification was chosen to be Random Forests (RF). RF fits several decision tree classifiers on data sub-samples and uses averaging to improve the predictive accuracy. Predictions from each tree are averaged across all the decision trees to provide a better performance than individual trees. The data used to train supervised models has a large impact on output quality. If training samples are small or possess uncertain quality then a classifier that is robust to these problems should be used – this includes RFs (Huang et al., 2002). Due to the lack of ground truth data for Belize, the quality of training pixels selected have an increased degree of uncertainty and hence RF should be chosen.

Six distinct spectral classes were assigned to models over land (urban, mangroves, wetland, agriculture, forest and water) and five assigned over water (coral, bare substratum, sand, seagrass, deep water). Terrestrial classes were defined based on recommendations from the Ministry of Natural Resources in Belize (2020) who classify the region using cropland, grassland, forest, settlements and wetlands. Malthus and Mumby (2003) suggests appropriate benthic classes in Belize are corals, bare substratum dominated, seagrass dominated and sand dominated. A deep-water class was added for areas where the seabed could not be distinguished. Training data for each of these classes was generated by sampling a hundred pixels for each class.

In order to provide an assessment of the accuracy of the classification models a confusion matrix was applied. The validation data required to achieve this includes an indication of the actual land cover type. This has been provided through higher resolution imagery including the open-source Planet base map imagery of the site. A sample of fifty points were produced across each class in this assessment.

6.3.3. Satellite Derived Bathymetry (SDB)

The following section outlines the approach to calculating bathymetry using a physics-based model inversion method. The processing workflow is shown in figure 37.

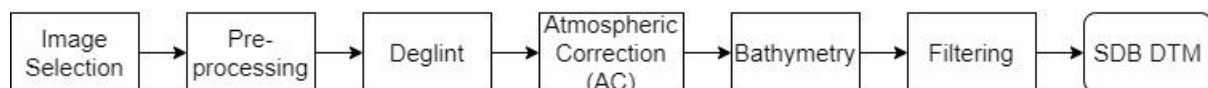


Figure 37: SDB processing workflow.

Pre-processing & image selection

The large catalogue provided by Sentinel-2 gives the opportunity to select imagery based on favourable environmental conditions. Accuracy of the final model is dictated by the quality of the image used. As a result, each image in the timeseries has been inspected to consider the presence of high suspended sediment loads, ocean glint or high cloud cover and only images demonstrating low concentrations will be processed. One image will produce one digital terrain model.

As a result of the intense cloud cover in the wet season in tropical latitudes preventing the acquisition of useful images; all images used in this study have been acquired in the dry season to assess the impacts of the previous year's hurricane season.

Once a repository of images had been selected, masking of anomalous features is completed by hand per image to remove pixels which might impede on the reliability of bathymetry estimated and to decrease processing requirements. These include pixels over land, boats, and clouds.

Deglint

A glint correction will reduce the noise resulting from the sun's reflectance on wave crests. Training samples have been selected in each image over deep water to include pixels with and without strong glint. From this sample, glint can be quantified through a regression calculated utilising NIR bands.

$$R'_i = R_i - b_i (R_{NIR} - Min_{NIR})$$

In this equation, R_i represents the pixel value per band, B_i is the product of the regression slope and R_{NIR} is the difference between the pixel NIR value and the Min_{NIR} value (the ambient level).

Atmospheric correction

This study has utilised Level-1C Top of Atmosphere (ToA) reflectance products using a timeseries based approach to employ specialist assessments for atmospheric corrections. Each of the Top of Atmosphere (ToA) Sentinel products have been translated to surface reflectance to accommodate for atmospheric reflection and transmission. This correction is homogenous across the image extent and is defined by:

$$P'_i(x, y) = [P_i(x, y) - S_i] * m_i$$

Where $P_i(x, y)$ is the input value in band i and $P'_i(x, y)$ is the atmospherically corrected value. The values for S and M represent subtraction values and multipliers, respectively. These are estimated from the image by constraining the values that may be plausible in terms of a radiative transfer model of the atmosphere, and the same water column model used in generation of bathymetry. Therefore, rather than an independent AC it may be better considered

a radiometric alignment with the water column model. To monitor the quality of the atmospheric correction, tests were carried out over points of known depth in deep and shallow water to ensure the estimated bathymetry was correct before proceeding.

Bathymetry

The forward model of spectral remote sensing reflectance ($R_{rs}(\lambda)$) used in this study is based on the parameters of the water column and sea bottom properties (Hedley et al., 2009):

$$R_{rs}(\lambda) \approx f(P, G, X, H, e_1, e_2, m, \lambda)$$

The parameters P, G, X and H characterise the water column phytoplankton, the coloured dissolved organic matter (CDOM), particulate backscatter, and depth, respectively. Bottom reflectance has been defined as a linear mix of two endmember reflectance spectra indexed by e_1 and e_2 . The spectral endmember model used for this study incorporates the bottom reflectance spectra of sand, coral, dead coral, macroalgae and seagrass in tropical waters. Individual pixels in the satellite image are subject to an adaptive look up table method for model inversion to associate the input values with the model to provide the closest spectral correspondence with the image reflectance. This approach allows for the bounded ranges of validity for parameters and a per-pixel uncertainty estimate to be established. Uncertainty is propagated by inverting each pixel in a deep water setting twenty times with a random spectral error term added to the pixel reflectance derived from the covariance matrix.

To further reduce the impact of noise and glint anomalies and provide enhanced depiction of bathymetric contours, the individual models are passed through a smoothing filter to convert each pixel into the mean value of a window encompassing an area of 5 x 5 adjacent pixels.

A consideration should be made as to the influence of tidal forces when each image is acquired as the instantaneous water level at the time of image acquisition is unlikely to coincide with that of chart datum (Lowest Astronomical Tide (LAT)). In the case of Belize, tidal forces have been considered negligible and hence no additional corrections will be accounted for to translate results to chart datum levels.

Full utilisation of the Sentinel-2 repository is facilitated with a time-series merge. Pixel values for each individual Digital Terrain Model (DTM) will be statistically merged to produce one map which attempts to characterise the general representation of bathymetry through statistical uncertainty weighted average analysis to reduce the impact of anomalies such as suspended sediment and cloud cover.

While the hydrographic coverage in Belize is limited, a validation of SDB models has been performed against existing Admiralty Electronic Nautical Charts (ENCs) where available. Three ENCs were utilised in this study covering the approached to Belize City, these have the references: GB400522, GB389330 and GB300662.

6.4. Secondary data techniques

The following section outlines the methodology for quantifying coastal variables using open-source remote sensing datasets.

6.4.1. Digital Elevation Modelling (DEM)

The gradient of the coastal slope over land and water will impact the degree of inundation due to storm surges as well as the potential speed of shoreline retreat (Nageswara Rao et al., 2008). To characterise this over terrestrial areas, the slope has been assessed using orthometric height from altimetry data from the Terra satellite. This open-source dataset has been pre-processed to provide indication of elevation at a thirty-metre resolution in the coastal zone.

Elevation data for this study is derived from stereo-pair images collected by the Advanced Spaceborne Thermal Emission and Reflection Radiometer (ASTER) instrument (USGS, 2019). This dataset was chosen due to its superior resolution and recent acquisition dates and is currently the DEM of choice for national studies in Belize. The Shuttle Radar Topography Mission (SRTM) DEM was considered, however, is only provided at a ninety-metre spatial resolution across the globe so was discounted.

The ASTER DEM is generated using a regular grid and provided in GEOTIFF format. Topographic data is projected on the 1984 World Geodetic System (WGS84) Earth Gravitational Model (EGM96) geoid.

Each scene encapsulates an area of approximately 100 square kilometres. For this study, four scenes have been selected to cover Belize (N18W089, N18W088, N17W089 and N16W089). These have been mosaicked into one single GEOTIFF and resampled to ten metres using the Python library GDAL. In addition, null data values over water were removed and the resulting raster reprojected to EPSG:32616. This is to ensure spatial congruency across data layers with differing spatial resolution and projections.

6.4.2. Wave climatology modelling

Wave climate conditions have been characterised using the open-source WAVERYS hindcasting model (Law-Chune et al., 2021). This dataset extends from 1993 to 2020 and is compiled using altimeter data with insitu recordings from several satellite missions, including the Topex series and Sentinel-3. This dataset contains a significant wave height (SWH) product which is gridded at a 0.3-degree resolution over a global projection.

The WAVERYS model has produced global merged multi-sensor time-series of gridded satellite altimeter SWH with a temporal resolution of three hours. This was deemed too fine for the purposes of long-term climatic monitoring. To reduce data volumes, the highest recorded monthly SWH was sub-sampled over an 18-month period. This was aggregated into a multiband GEOTIFF and reprojected to the local coordinate reference system (EPSG:32616).

Due to the coarse spatial resolution, the extent of the dataset does not extend to within one kilometre of the coastline. Due to this, pixels along the coast have been resampled to contain the value of the closest pixel with recorded data. Therefore, SWH is more representative of the offshore wave conditions rather than in the coastal zone. Finally, the pixel size has been resampled to ten metres to allow direct comparison with other data layers.

In-situ tide gauges are sparse on the Yucatán Peninsula and will not represent the wave conditions in Belize. WAVERYS provides a peer-reviewed method to indication of more precise wave climate across the coast and was used due to its low biases to SWH measurements of only three centimetres.

6.4.3. Wind intensity

Hurricane wind speed can be a driving force behind storm surges due to wind generated wave run-up. This is a particularly relevant parameter in Belize due to hurricane winds. The windspeeds associated with hurricanes have been included to these represent the vulnerability in the most severe scenario.

The impact of tropical storm intensity has been evaluated in this study using the United Nations Environment Program (UNEP) Global Risk Data Platform. The UNEP raster dataset was developed as part of the Global Assessment Report on Risk Reduction (GAR) and provides an estimation of global tropical cyclone buffer footprints generated from 2534 cyclonic events

over the period 1970 – 2009. The UNEP model has been used to evaluate wind hazard analysis in the north Atlantic and indicates a reliable dataset for this study (Cardona et al., 2014).

The impact of cyclones is recorded in the Saffir-Simpson categories which characterises hurricane frequency and intensity through a scale of 1-5 in increasing severity. This dataset has been derived using historical hindcast observations from the International Best Track Archive for Climate Stewardships (IBTrACS); a record of global tropical cyclone tracks used to assess distribution, frequency and intensity (Knapp et al., 2010). Windspeeds have been converted to the Saffir-Simpson scale through GIS modelling to take into consideration the movement of the cyclones through time.

As this is a global dataset, the raster is first acquired WGS1984 (EPSG:4326) projection. To enhance the spatial precision for Belize, this is reprojected to the local coordinate reference system (EPSG:32616). Pixels are subsequently resampled to a ten-metre spatial resolution.

6.4.4. Tides

Tidal forces are associated with inundation hazards. As suggested in section 3.2., tidal forces in Belize are minimal with a mean diurnal range of 0.125m. This suggests that this region experiences a micro tidal climate. Koroglu et al. (2019) suggests that unless the analysis is completed at a large spatial scale (where tidal range will vary substantially) then this parameter does not add significant information to discriminate more vulnerable areas. In the case of this study, tidal forces have been considered as homogenous along the coast.

There is conflicting opinion in the literature with regards to the impact of micro-tidal climates on coastal vulnerability. According to Gornitz (1991) and Shaw et al (1998) coastal zones with a high tidal range should be considered more vulnerable, as a macro tidal range is typically associated with stronger tidal currents, and thus deem micro tidal areas to be of low vulnerability. On the other hand, Thieler and Hammler-Klose (2000) suggest micro tidal areas are of greatest vulnerability due to the sea level always residing close to the high tide line. Therefore, in storm surges flooding is more likely to occur (Pendleton, 2004).

Since this study has a focus on vulnerability against storm surges, tidal forces have been assumed to have a high risk in the CVI model and possess the equivalent high-risk class for all segments along the coastline.

6.5. Modelling approach

6.5.1. Coastal sampling

Each coastal parameter will occur exclusively over either the terrestrial or marine environments hence raster layers will not be spatially coincident. As a result of this, the data must be sampled and aggregated along the coastline. The extent of the coastline is determined from the vectorised shoreline produced using an NDWI index mask.

A 10m resolution is deemed to be too fine for analysis as processes of interest operate over a much larger scale than this. Hence, a larger scale of aggregation is chosen through the application of a 1km buffer (figure 38). This buffer extends in all directions from a point on the coastline resulting in 215 cells on 1km x 1km. This will give an indication of coastal vulnerability at each 1km segment of the coastline.



Figure 38: 1km coastal sample segments.

Each data layer is loaded into a bespoke Python script and resampled to the 1km grid using the coastline shapefile. In order to characterise the prominent environmental conditions that persist in this area, a spatial aggregation of pixel values has been applied in two approaches: grid statistics and grid pixel count.

Sample cell statistics were calculated for the coastal slope (terrestrial and marine) and wave climate layers. The metrics calculated for each cell were the mean, median, standard deviation, minimum and maximum values. In the case of wave climate, the coarse resolution prevented variation in pixel values at a 1km scale, so these statistical metrics were calculated used across a time series of eighteen images to characterise conditions with respect to temporal variation as opposed to spatial variation in the grid.

For the classification layers, the use of statistics would not be an appropriate metric to characterise the variation in conditions due to the independent and arbitrary designation of class values. Conditions were assessed through the prominence of landforms occupying that grid through pixel count of class.

This process results in a single value for each metric per grid. A multidimensional NumPy array is constructed containing pixel stats or pixel counts depending on the layer. The conceptual structure of this array is demonstrated in table 7.

Table 7: Conceptual NumPy arrays produced to characterise coastal segment properties.

Coastline Sample Grid Number	Grid Statistics				
	Mean	Median	Standard Deviation	Minimum Value	Maximum Value
x					
x + 1					

Coastline Sample Grid Number	Grid Pixel Count					
	1 – Urban	2 – Mangrove	3 – Agriculture	4 – Mudflats	5 – Forest	6 – Water
x						
x + 1						

Hurricane intensity did not require any sampling as Saffir-Simpson categories naturally divides data into 5 clusters. These clusters correspond to increasing severity and can be easily adapted to the context of vulnerability. Tidal range also did not require sampling as this was considered equivalent for each coastal cell.

6.5.2. Assigning vulnerability groups with machine learning

The NumPy array containing coastal samples must be grouped with respect to cells containing similar conditions to demonstrate exposure. Traditionally these groups would be ranked with a specific vulnerability value and defined using a static range of thresholds. This is a major limitation of the Gornitz (1994) method as these values cannot be scaled to new environments and require prior knowledge of the geomorphic conditions present to define.

Machine learning has removed the requirement for thresholds to be defined manually. In this case, the vulnerability ranking becomes a dynamic and relative scale based on areas where similar geotechnical conditions are observed in the image. Python has been used to develop a script which takes pixel values from individual parameter layers and groups these along the coastline using clusters suggesting underlying patterns.

The KMeans classifier is an unsupervised machine learning clustering technique which classifies a given dataset into a pre-determined number of groups. This method learns iteratively to assign a K group to each data point based on its features. A feature space is constructed with axis relating to pixel values of each input layer and a series of points are dropped at random extents and over a defined number of iterations within this space. The distance to surrounding points is then established. Clusters are determined through the minimum distance to each centroid seed.

Wind speed intensity data did not require clustering through this method as the Saffir Simpson scale is a labelled dataset and already divides the dataset into five clusters. In addition, tidal forces were not clustered using KMeans as these were considered homogenous along the coastline.

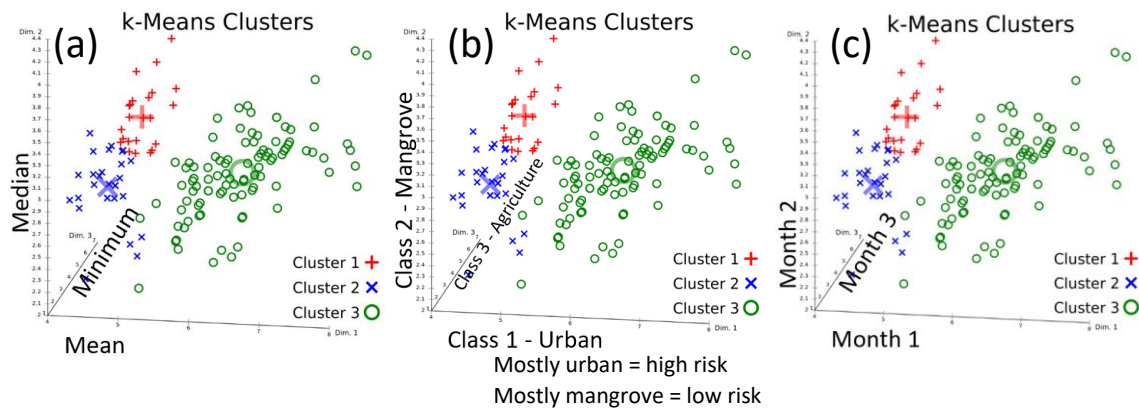


Figure 39: Conceptual representation of feature space used in KMeans for (a) Coastal slope parameters, (b) Classification parameters, (c) Wave climate parameters.

In the CVI model developed, a feature space is constructed for the remaining parameters of coastal slope, geomorphology and wave climate to determine five distinct vulnerability groups (figure 39). These groups are determined using a generalisation of predominant conditions for each 1km coastal sample grid which can be grouped with others along the coastline. The feature space for each parameter is constructed with dimensions corresponding to the columns in table 7. Data points in the feature space represent the values for each metric in coastal segments. As the number of dimensions in the feature space increases, the scalability decreases therefore a low dimensionality should be used. Number of iterations chosen to be three hundred as suggested by Calil et al. (2017).

In the case of coastal slope, a 5-dimensional feature space axis is created consisting of the statistical metrics of mean, median, standard deviation, minima and maxima. A higher weight was assigned to the mean to emphasise the importance of this metric in describing conditions. For geomorphology, the feature space represents the pixel counts for each class in the 1km coastal grid. As a result, the feature space is 6-dimensional for land and 5-dimensional for benthic representing each class present. As the resolution of wave data is too coarse to have multiple pixel values within the coastal grids, the feature space instead contains eighteen dimensions constructed from a single value of wave height for each coastal grid.

Table 8: Conceptual NumPy array produced to characterise cluster centroid properties.

Cluster	Cluster Centroid Values				
	Mean	Median	Standard Deviation	Minimum Value	Maximum Value
x x + 1					

Once similar clusters are established, these must be related to a degree of vulnerability. Vulnerability is assigned to each of the five clusters through a determination of the cluster centroids for each group (table 8). These centroids are used to provide an indication of the generalised conditions represented by a cluster. Centroids are ranked for each dimension based on the magnitude of values observed against other clusters (table 9). In the case of wave climate, higher magnitude cluster centroids demonstrate higher classes of vulnerability and are ranked accordingly. Each statistic is ranked individually as a cluster may not demonstrate the same rank across each metric. These ranks are summed with the lowest ranks demonstrating the lowest vulnerability clusters.

Table 9: Conceptual NumPy array to rank cluster centroids based on the magnitude of each metric. Higher ranks will indicate a higher vulnerability.

Cluster	Cluster Centroid Rank				
	Mean	Median	Standard Deviation	Minimum Value	Maximum Value
x x + 1	Ranked values per metric based on comparison of magnitudes in each cluster.				

This approach affords the benefits of being a simple and computationally efficient workflow to process. As a result, this clustering is quickly scalable to large datasets and can easily adapt to new examples.

6.5.3. CVI Calculation

Once the relative vulnerability has been assigned to each of the parameters detailed above, the arrays containing information for each layer are overlaid and Coastal Vulnerability Index (CVI) calculated over coincident pixels. The following formula for CVI has been used, reflecting the seven parameters evaluated:

$$CVI = \sqrt{\frac{a * b * c * d * e * f * g}{7}}$$

<i>a = Land Cover Classification</i>	<i>e = Wave Height</i>
<i>b = Benthic Cover Classification</i>	<i>f = Wind intensity</i>
<i>c = Bathymetry</i>	<i>g = Tidal range</i>
<i>d = Terrestrial Relief</i>	

Once the CVI for each pixel is established, vulnerability groups are derived using quartiles. Diez et al. (2007) suggest there are alternative approaches to define the index values at which to place thresholds. The choice of which can determine sensitivity levels and result in contrasting impressions of the degree of vulnerability (Nageswara Rao et al., 2008). In this study, quartiles were used consistent with that applied by Thieler and Hammar-Klose (2000). The first quartile representing low vulnerability, the central quartiles representing moderate to high vulnerabilities and values in the upper quartile show severe vulnerability groupings. The resulting vulnerability map is exported as a GEOTIFF at 1km pixel resolution.

6.5.4. CVI Model Evaluation

A model evaluation has been performed against previous studies. The distribution of vulnerability is first compared against existing flood maps in Belize. The model has also been evaluated against the existing exposure model for Belize; InVEST. This provides a quantitative indication for the level of agreement. These models have both been qualitatively compared against impacts from historical hurricane events.

PART IV – RESULTS

Section seven outlines the results for each satellite derived parameter used in the derivation of the CVI. This is followed by a consideration of the ability for the KMeans CVI model to determine vulnerable areas and suggestions for its place in ICZM.

7. Characterisation of coastal vulnerability parameters

7.1. Geomorphology component

Two supervised classifications were produced for this study, over the marine and terrestrial environments, using an object-based approach. Figure 40 demonstrates the geomorphological variation along the coastal zone.

In the terrestrial classification, there is clear definition of urban areas including: Belize City (365000, 193000), San Pedro (395000, 197000) and Caye Caulker (385000, 196000). The surrounding Cayes present a dominance of mangrove and mudflat classes with sparse fragmented areas of forest; likely resulting from misclassification. In the mainland, mangroves are typically seen to be present in the southern regions below Belize City. Mudflats are prevalent in the northern landward areas and correspond with areas of sandy seabed.

Furthermore, the marine classification demonstrates a northern bias for sand with large extents present to the west of Ambergris Caye. Sand is also prevalent in mid latitudes and can demonstrate the impact of suspended sediment through plumes and river discharge surrounding Belize City. This region is typically comprised of bare substratum with sparse seagrass assemblages and is reflected between coordinates 1950000 to 1980000. A section of the Mesoamerican Barrier Reef subtends the region from north to south and has been identified by a high density of coral benthic types, however, coral is particularly subject to misclassification especially in areas close to the coast. Deep water has been well represented in areas where the seabed cannot be seen. This is prevalent to the east of barrier reef and through deep water approach channel to Belize City. This model produces a much more fragmented classification with high levels of noise.

Within the 1km coastal buffer, 50.9% has been identified as mudflats, 8.1% of pixels are classified as urban, 23.2% demonstrate mangroves and the remaining 17.7% show forest or fresh water. Within the 1km coastal buffer, 21.3% of pixels classified as sand, 16.8% demonstrate bare substratum, 15.3% showing seagrass, 40.8% deep water with the remaining 5.8% characterising coral reefs.

Each model has had their overall accuracy quantified and the resulting confusion matrices can be seen in table 10. A total of 500 points were compared with very high resolution (VHR) Planet base map imagery. The terrestrial classifier performed better than that of the seabed with accuracies of 70.4% and 61%, respectively. The kappa statistic is a measure of how similar pixels classified by random forest classifier match the ground truth. In the terrestrial classification a value of 0.63 was achieved and 0.51 in the marine. This suggests a substantial and moderate correlation (Koch et al., 2009). Sand and mangrove classes have likely been underestimated due to low producer accuracies of 48.31% and 48.68%. Sand also has the highest user accuracy which conversely suggests a strong parity for classification.

Endmember spectral response curves for each class are shown in figure 41. The urban class demonstrates a high reflectance from the bright surfaces typical of anthropogenic construction. Classes representing vegetation experience a spike in band 8 which reflects the increased reflectance of near infrared wavelengths in photosynthesis. Benthic classes show a reduced degree of separability than terrestrial class and have tightly clustered reflectance values with similar trends across wavelengths. These characteristics make the individual endmembers harder to distinguish and disproportionately affects higher wavelengths.

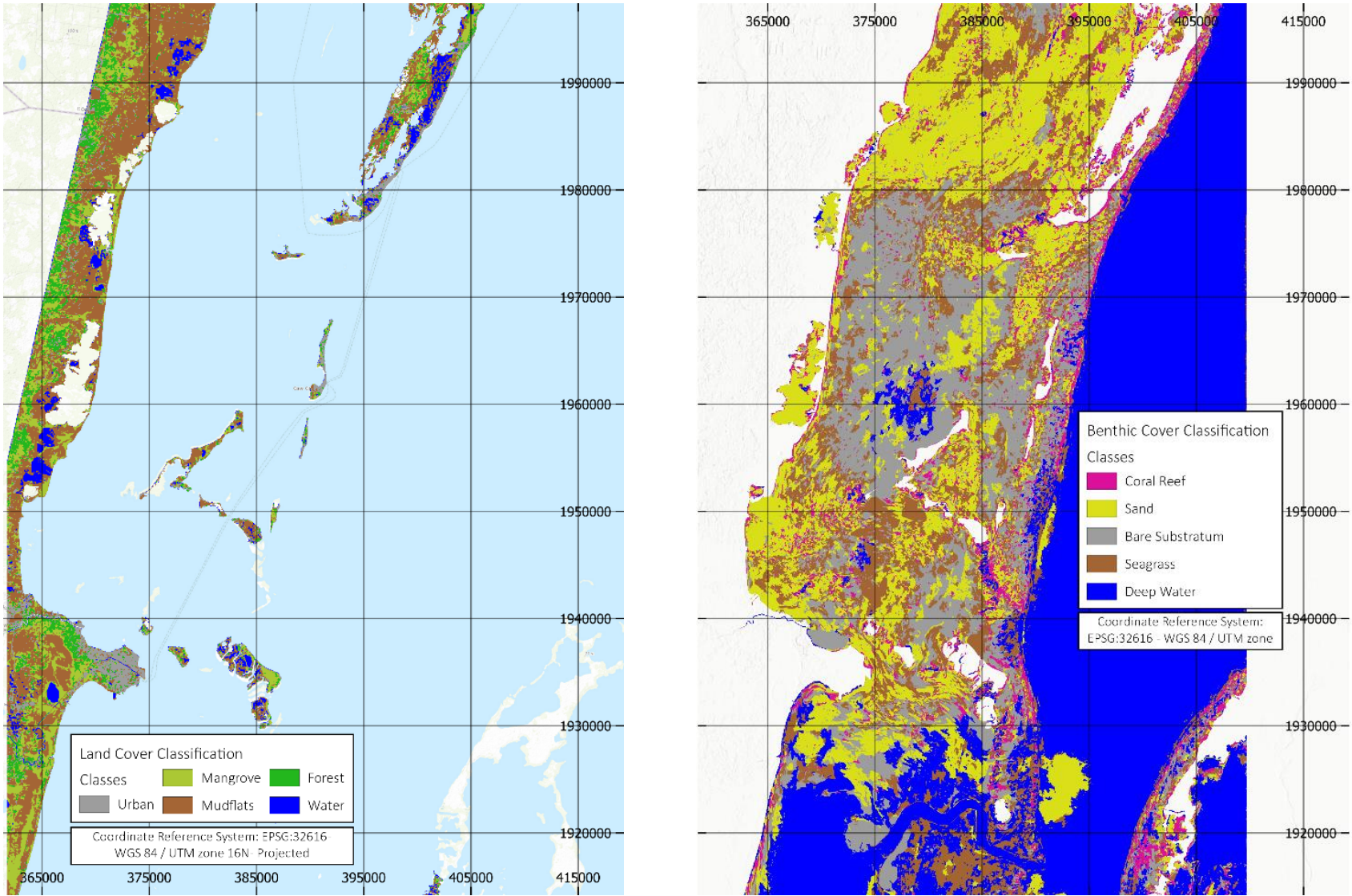


Figure 40: Random Forest classification maps for land cover (left) and benthic cover (right).

Table 10: Confusion matrix accuracy assessments for image classifications.

		Actual					Totals	User %
		Urban	Mangrove	Mudflat	Forest	Water		
Predicted	Urban	30	12	5	3	0	50	60.00
	Mangrove	2	37	7	4	0	50	74.00
	Mudflat	0	13	34	0	3	50	68.00
	Forest	1	10	3	36	0	50	72.00
	Water	3	4	3	1	39	50	78.00
	Totals	36	76	52	44	42	250	-
Producer %		83.33	48.68	65.38	81.82	92.86	-	70.4

kappa statistic 0.63

		Actual					Totals	User %
		Coral	Sand	Substrate	Seagrass	Deep Water		
Predicted	Coral	19	19	5	4	3	50	38.00
	Sand	0	43	3	4	2	50	86.00
	Substrate	4	13	29	3	1	50	58.00
	Seagrass	7	5	8	30	0	50	60.00
	Deep Water	0	9	4	4	33	50	66.00
	Totals	30	89	49	45	39	252	-
Producer %		63.33	48.31	59.18	66.67	84.62	-	61.111

kappa statistic 0.5149

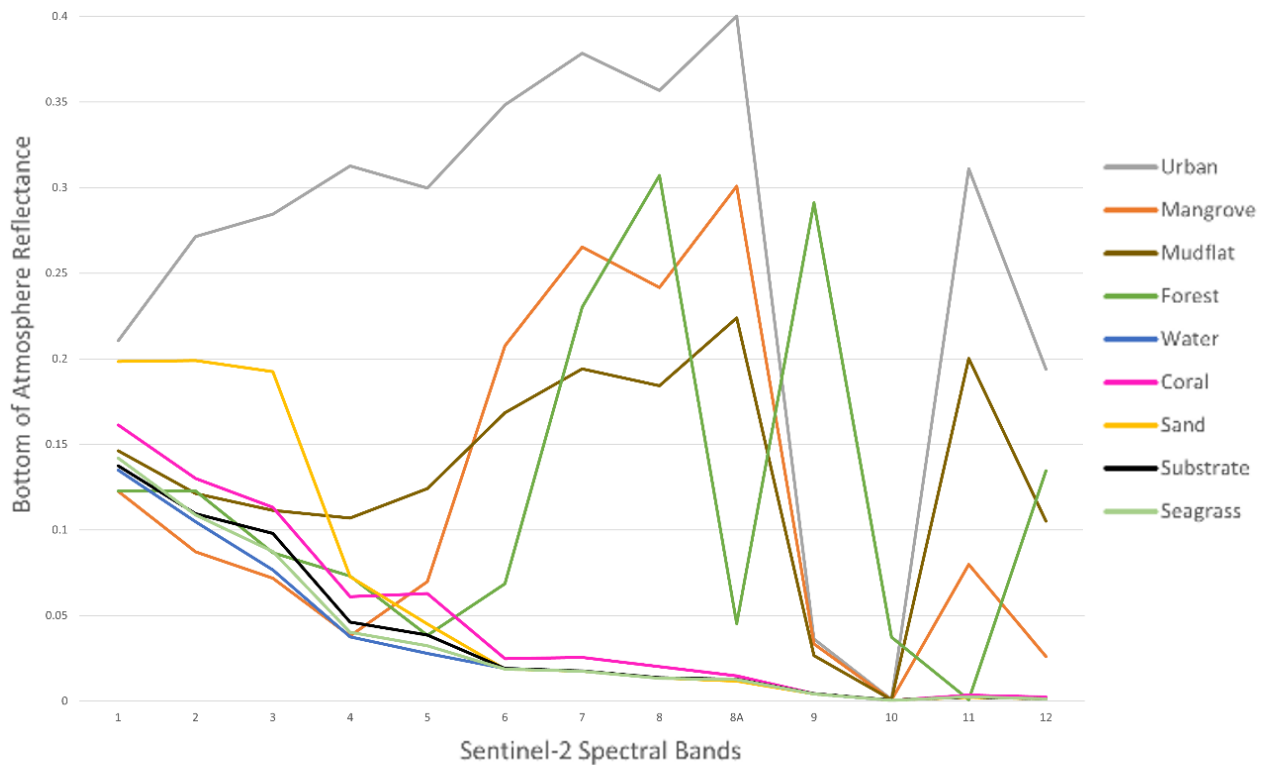


Figure 41: Spectral endmembers for each class defined.

7.2. Marine slope component

Satellite Derived Bathymetry (SDB) has been provided using an uncertainty weighted average of pixels from seven models (figure 42). At a regional scale, the general bathymetric conditions show the shallowest water in the north of the image. These conditions typically occur above a latitude of 17.8 degrees and are sheltered by Ambergris Caye. In the south, below latitudes of 17.4 degrees, the bathymetry is deeper. This includes the lagoon sheltered by the barrier reef with a well characterised deep water approach channel. Western extents along the shoreline represent a gentle slope of shallow water with the 5m contour occurring 5km from the coastline. The eastern extent of the model shows a steep gradient along the Mesoamerican Barrier Reef; this is particularly prevalent close to shore near Ambergris Caye.

SDB profiles experience temporal variation due to the images used in their derivation (figure 43). Three transects for 2018, 2019 and 2020 show the variable conditions; 2020 demonstrates a particularly deep model, high variation can be seen in 2019 suggesting mobile sediment and gaps in time series exist in 2018 through presence of cloud. Uncertainties in model LUT generation span from different conditions in image acquisition. This will affect model performance and highlights issues with taking one image in isolation. Moreover, these observations demonstrate the significance of merging individual models to establish a full characterisation of bathymetry.

The RMSE of individual SDB models ranged between 4.86m and 6.88m (with a mean RMSE of 5.57m) for each date. Although not directly comparable, due to variations of image conditions, these errors are similar to those demonstrated by Kanno (2013) and Lyzenga et al. (2006). The time-series merging of multiple SDB models has been shown to be effective in improving the accuracy of models through reducing the RMSE to 4.88m. However, RMSE metric still appears high. This is due to the RMSE being calculated over the whole model which provides bias towards inaccuracies with deep water. Through considering RMSE at each depth contour, the model provides good accuracy to the 20m contours with low RMSEs of 3.00m, 2.375m and 3.713m at 2m, 5m and 10m contours, respectively. This increases to 6.305m and 13.967m for 20m and 30m depths.

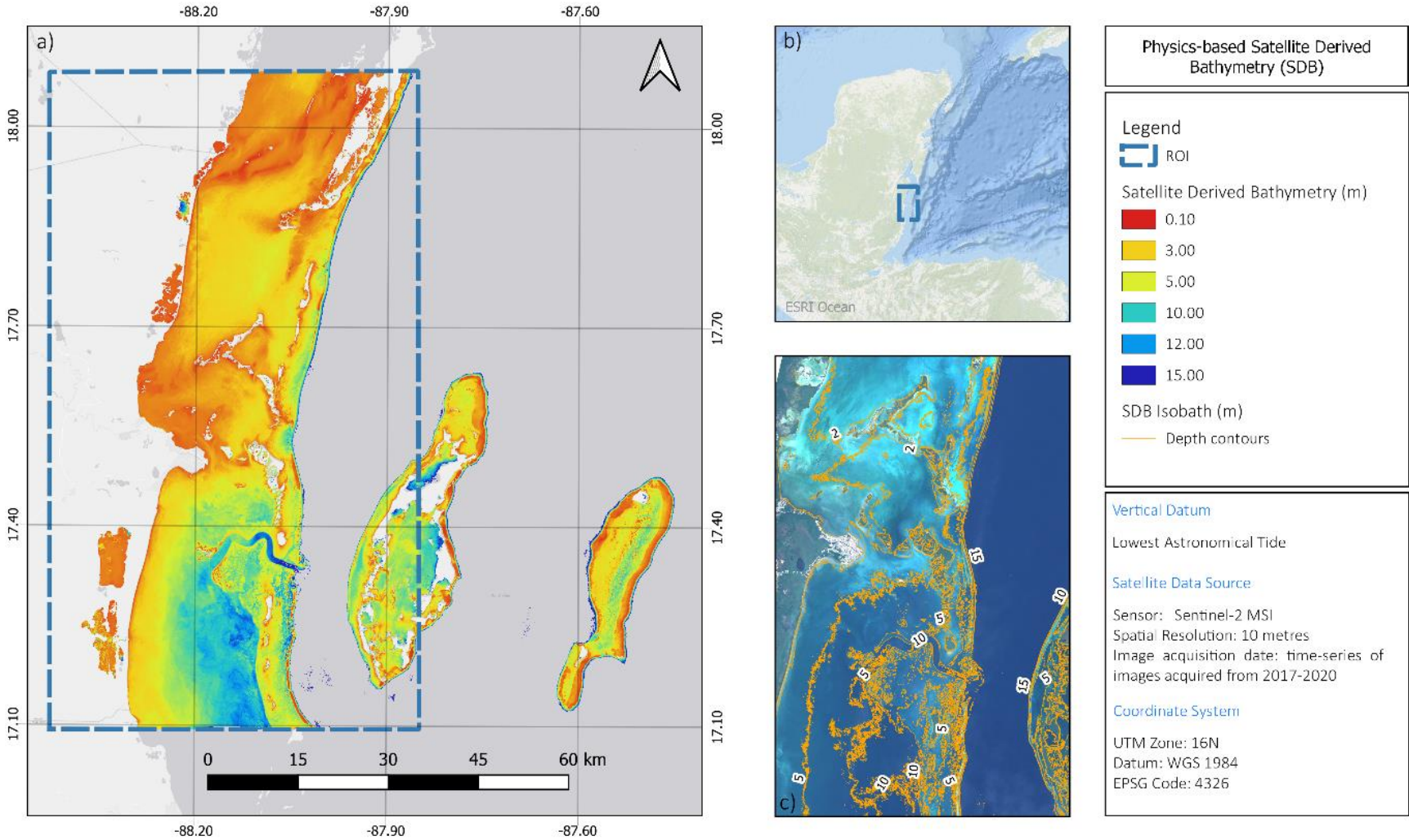


Figure 42: Physics-based Satellite Derived Bathymetry (SDB) model for Belize: (a) SDB DTM, (b) Study location, (c) SDB isobath model.

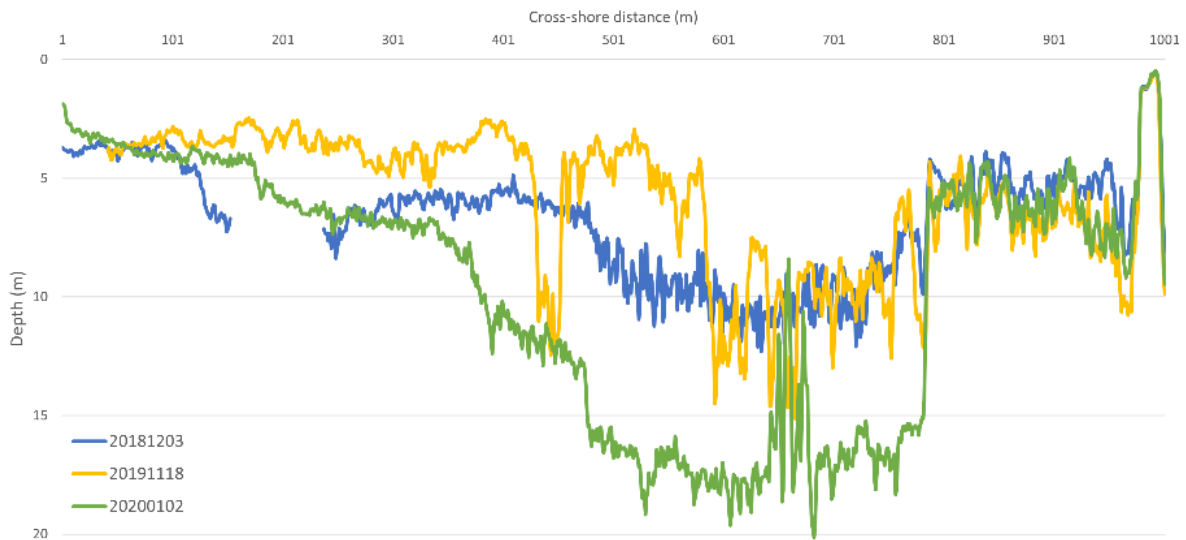


Figure 43: Temporal variation to cross-shore depth profiles for three image acquisitions.

Figure 44 shows the variable gradient along the coastline. Profile one shows bathymetry in the north punctuated by shallow areas of offshore sandbars created by sediment mobility. This is evident at 6km offshore with a depth of 0.4m. At this distance, these features are not captured by coastal sample. This gradient fluctuates within a 2.5m range.

Past the shelter of Ambergris Caye, profiles two and three show shallow slopes in the south of 0.3% and 0.005%. The slope remains shallow under 5m until 20km offshore where a steep coastal shelf is experienced in both cases with a gradient of 3.4% and 5.6%, respectively. The negligible gradients (0.3%) of SDB profiles which are present in the lagoonal areas demonstrate the lowest risk for flooding in the traditional framework. This covers much of the coastal waters within 1km of the coastline with the shallowest areas in the north. Differences in transects show this region is not static and provides sediment mobility. These profiles show a marked drop off (5.6%) to deep water regions in the eastern extents of the model. This steep gradient suggests a high level of exposure to storm events and will affect the regions of Ambergris Caye and outermost Caye islands significantly. Moreover, strong wave energies from storm events have the potential to alter already mobile sediments rapidly. Hence, regular assessments are important to provide actionable intelligence.

Validation has been performed through comparison with existing depth contours from Electronic Nautical Charts (ENCs). A random sample of points are allocated along each ENC isobath and are compared with the coincident pixel value of the SDB model (figure 45). Median values for each contour show good agreement in shallow water (3.04 for 2m, 5.65m for 5m and 9.58m for 10m) with the error due to underestimation increasing in deep water (17.33m for 20m and 17.24m for 30m). The interquartile range is also low for 2 – 5m contours (2.02m and 1.74m). This increases to 4.92 at 10m.

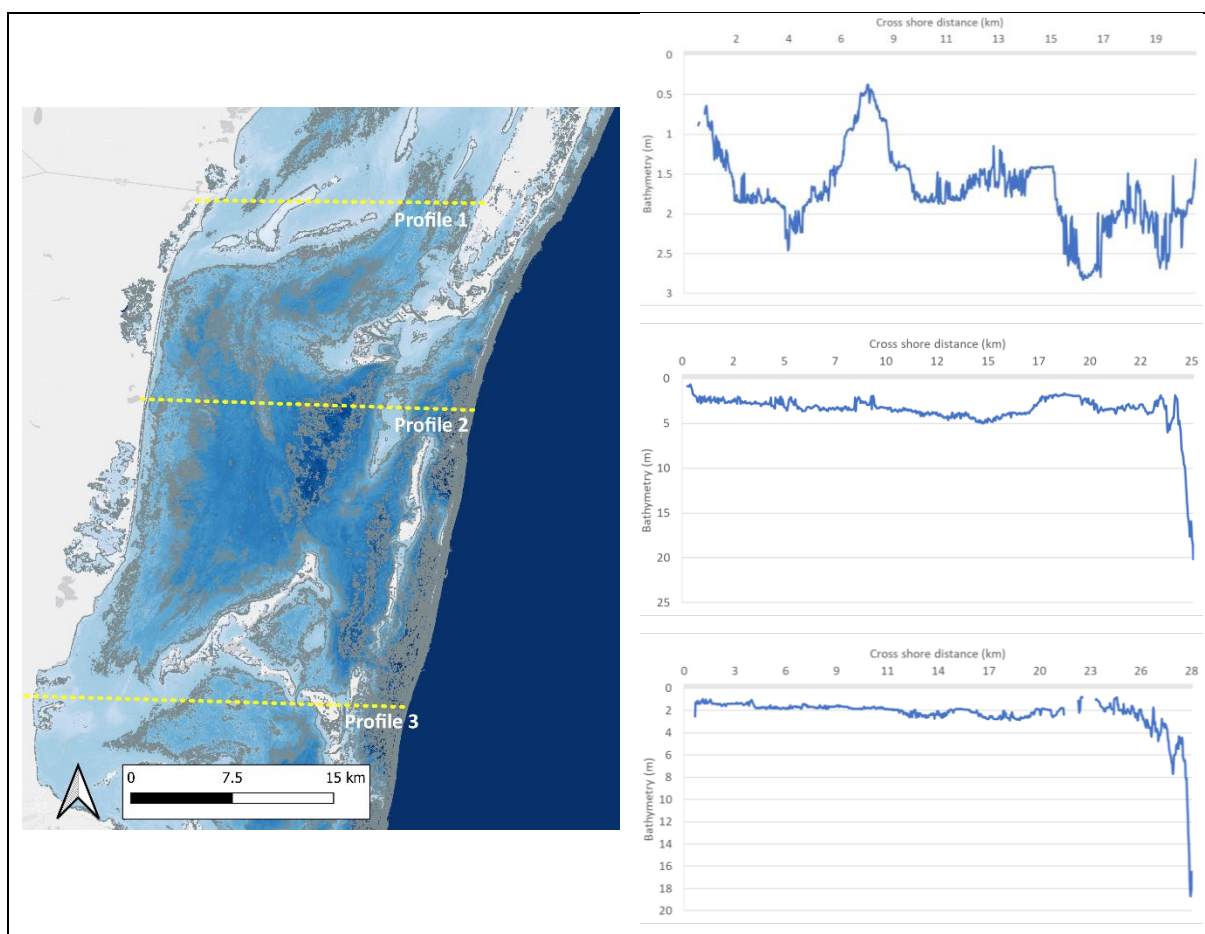


Figure 44: Spatial variation to cross-shore depth profiles.

Results show an overestimation of shallow water up to the 5m contour, with strong accuracy from 5 – 10m. After this point, the range is high and suggests a cut off depth for SDB with data being valid up to the 15m contour.

Features have been missed to north of Belize City due to sediment plumes from the mouth of Belize River. Conversely, coral head features have been identified in SDB to the south of channel which are not present in ENC and are visible in the RGB satellite image.

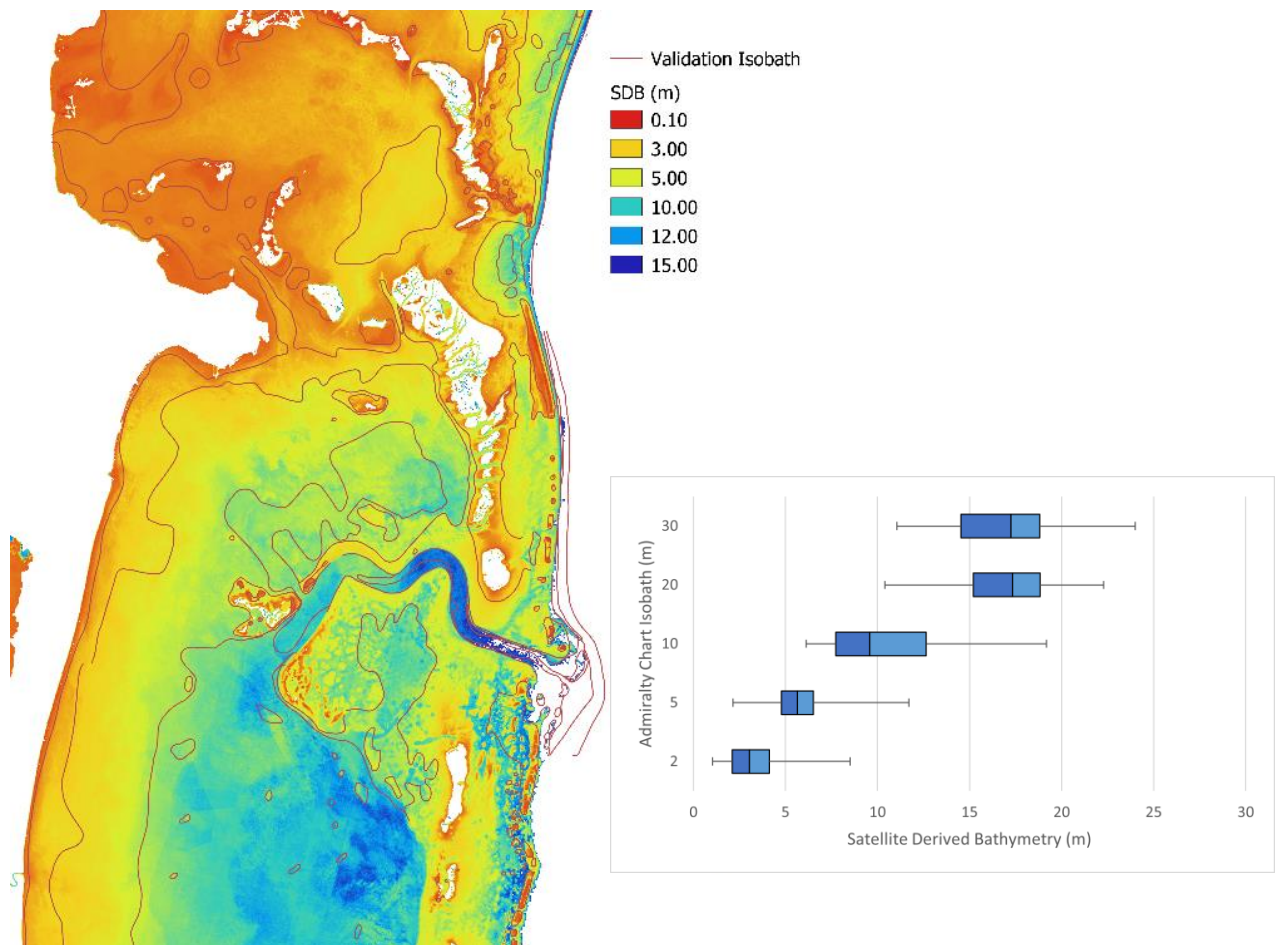


Figure 45: Validation of Merged SDB against Electronic Nautical Chart (ENC) contours.

7.3. Terrestrial slope component

The topography of Belize has been quantified through analysis of data from ASTER (figure 46). Belize's coastal region can be described as low-lying because all areas of the coast presenting an elevation under ten metres. The lowest elevation regions can be found offshore in the caye islands and the highest elevation is clustered to the south of Belize City. The CZMAI suggest the regions that are most susceptible to inland flooding are to the very north of Belize City and westward of Ambergris Caye (Azqueta et al., 2020). This area is coincident with mangrove classes present in the RF classification. Elevation values vary by only a couple of metres along the coastline and demonstrates largely homogenous conditions.

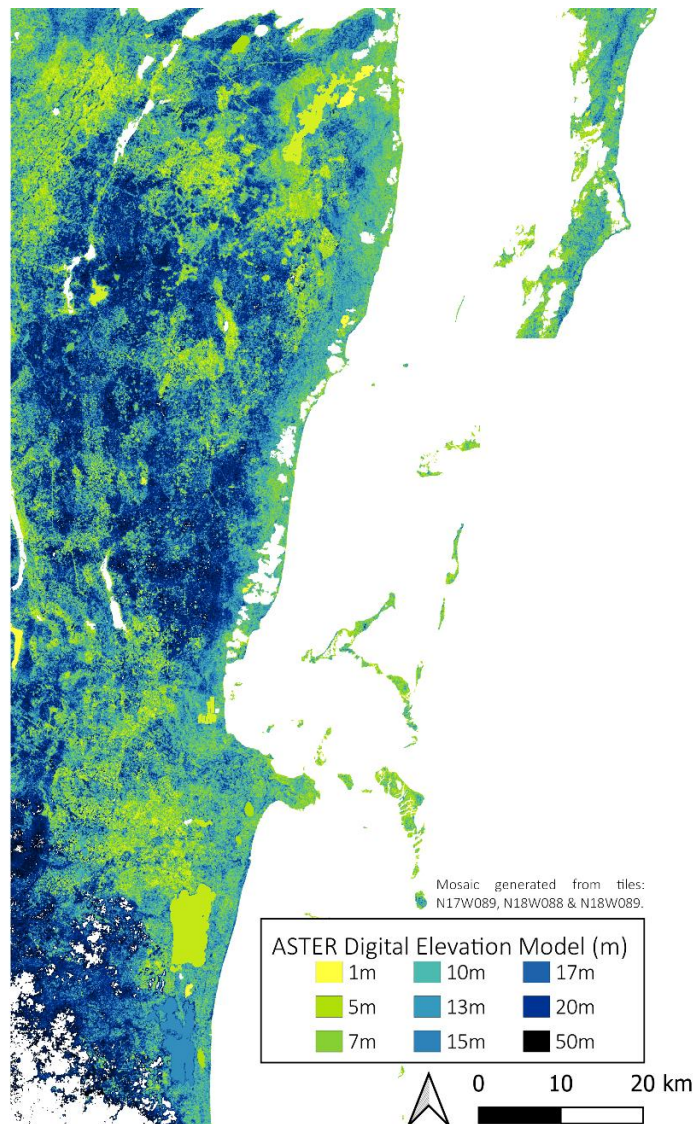


Figure 46: ASTER Digital Elevation Model (DEM) for Belize.

7.4. Wave climatology component

Figure 47 shows estimates for the mean wave conditions over the sampled eighteen-month period. Due to limitations of data provision close to the coast, conditions at the coastline were estimated through receiving values for significant wave height (SWH) based on closest pixel. Consequently, this describes the wave climate conditions approximately 20km offshore and before they have broken on the shallower continental shelf. Mean SWH demonstrates modal conditions and is, therefore, not the best metric for storm induced vulnerability. The maximum recorded wave height is a more representative measure to simulate the strongest wave conditions and has been used within the CVI every month.

The maximum recorded wave height of 2.3 metres was recorded in January 2016 and the minimum recorded wave height was recorded at 0.6 metres in September 2015; these occurred at northern and southern latitudes, respectively. This suggests a diminishing wave energy trend from south to north which is corroborated by other hindcast models, including SWAN (Orejarena-Rondón et al., 2021).

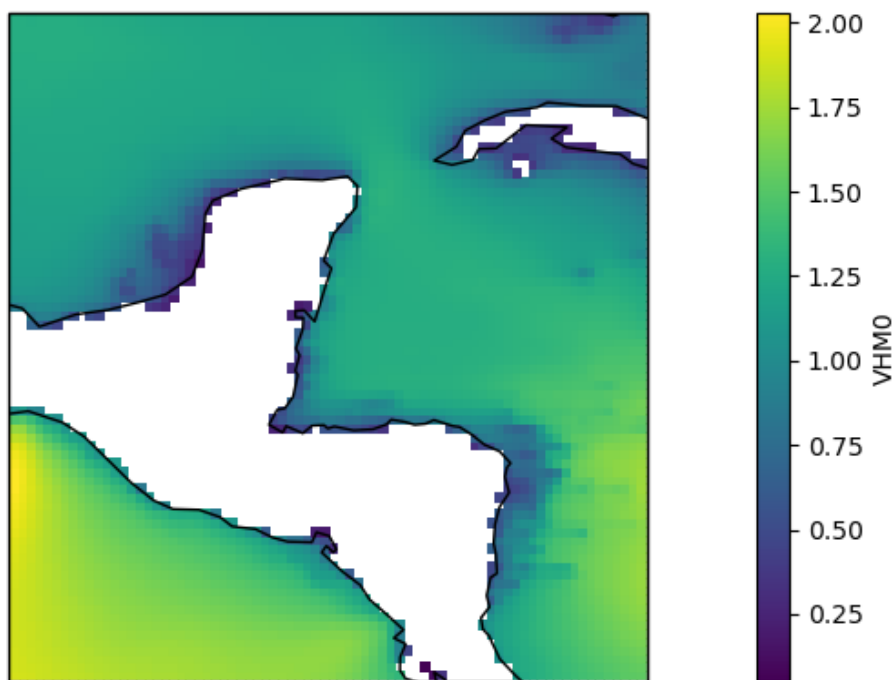


Figure 47: WEVERYS modelled SWH at 20km resolution for the Yucatán Peninsula.

Figure 48 shows the prevailing wave direction and magnitude. A gradient of increasing magnitude is evident southward along the eastern edge of the Yucatán Peninsula. This suggests high wave energy conditions. Higher magnitude waves will demonstrate faster speeds of propagation and cause an increase to kinetic energy. Swell is generated from the North Atlantic with an easterly incidence angle, which is perpendicular to the coastline of Belize, and suggests incident waves will transfer the maximum wave energy. These conditions diminish as the current flows around the Yucatán Peninsula.

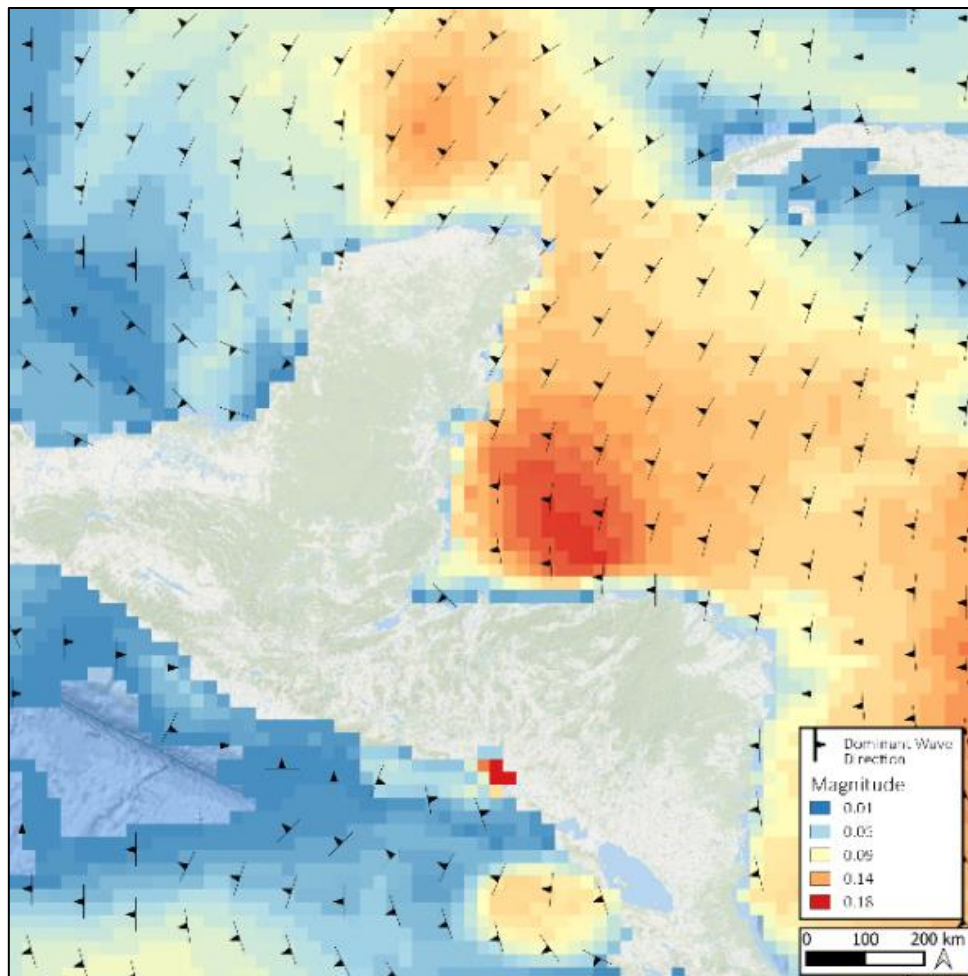


Figure 48: Magnitude and modal direction of wave climate from WAVERYS data.

Due to the coarse spatial resolution of this dataset, clustering was achieved through the analysis of sustained wave climate conditions over time. Figure 49 demonstrates the temporal variation in SWH. This time-series has been constructed from the multi-dimensional dataset through averaging all data values present on a single date. SWH can be seen to be highly variable and fluctuates around median height of 1.1m. A consideration of temporal trends enables the evaluation for the likelihood of strong wave energy incident on the coast and their return period. This is used in an assessment of vulnerability to determine the spatio-temporal extent at which an area will experience a high energy event.

Despite the limited temporal extent of the dataset, there appears to be a distinct pattern of periodicity of inter-annual periods that show higher SWH. The height of waves in the wet season appears greater with January often experiencing the highest energy conditions. This is after the end of the Atlantic hurricane season (November). The precise return interval of which is unclear, however, due to the limited temporal extent of the data. This makes it difficult to provide any statistical indication of this relationship as only two annual cycles are captured. Data with longer temporal extents are required to establish these fluctuations further.

Seasonal patterns are punctuated with infrequent climatic events. In August 2016, an anomalous increase in recorded SWH is seen. This event is attributable to Hurricane Earl which made landfall in Belize on 4 August and brought waves of up to 4.7m. These magnitudes have not been captured by this dataset due to the use of the mean and spatial-temporal sampling. During the hurricane season, the lowest mean wave climate is observed but is punctuated by the largest extreme waves.

Furthermore, figure 49 provides evidence to suggest strongest wave conditions are coincident with ENSO events and is supported by increased wave heights during this period. The 2015-16 ENSO is one of the strongest on record. During this time, unusually high SWHs were seen in satellite images and linked to flooding in South America (Masoero, 2016). During the warming ENSO phase, the strength of trade winds increases and becomes more consistent. This leads to larger wind generated waves. Münnich and Neelin (2005) describe the correlation between ENSO and SWH suggesting a statistically significant relationship and lag times of up to four months. This relationship suggests a strong indication for ENSO driving climate in MAR, however, a longer temporal dataset is required to establish the trend of ENSO events.

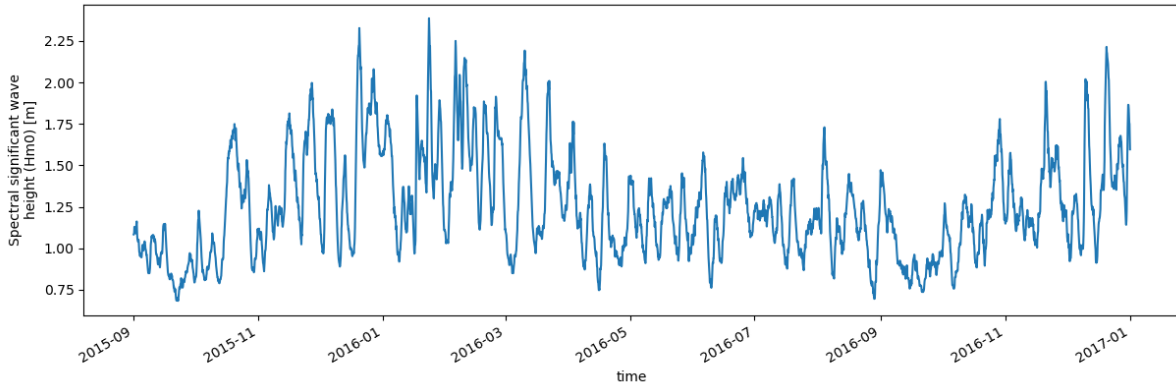


Figure 49: Temporal variation of mean significant wave height (SWH).

Validation of wave data results is achieved through evaluation against wave buoy data in the Caribbean Sea. The buoy used for validation is NOAA Station LLNR 80 situated in the Yucatán basin. Figure 50 demonstrates in-situ wave heights are well characterised by the WEVERYS model. The correlation coefficient (R) is 0.6 suggesting a good relationship between observed and predicted wave heights. It is evident that high energy waves are systematically under-represented. Under-representations of this nature are a known limitation of wave modelling.

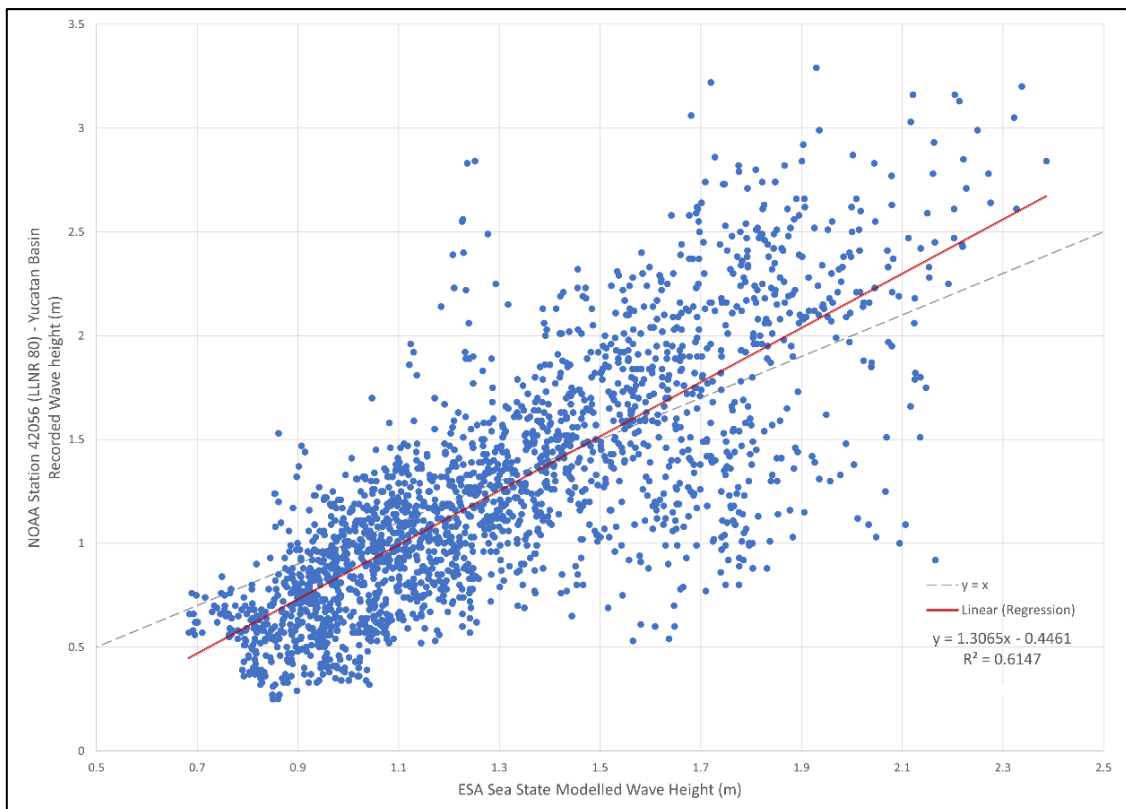


Figure 50: Validation of WEVERYS predictions against in-situ buoy data from NOAA.

7.5. Wind exposure component

Figure 51 represents the spatial distribution of coastal exposure due to hurricane winds. This has been generated from existing data produced by the UN Environment Program (UNEP). The Saffir-Simpson scale shows a visualisation of the annual accumulated and sustained windspeed of storm tracks derived from IBTrACS dataset. 2594 historical tropical cyclones are characterised by this dataset from the period 1969 to 2015.

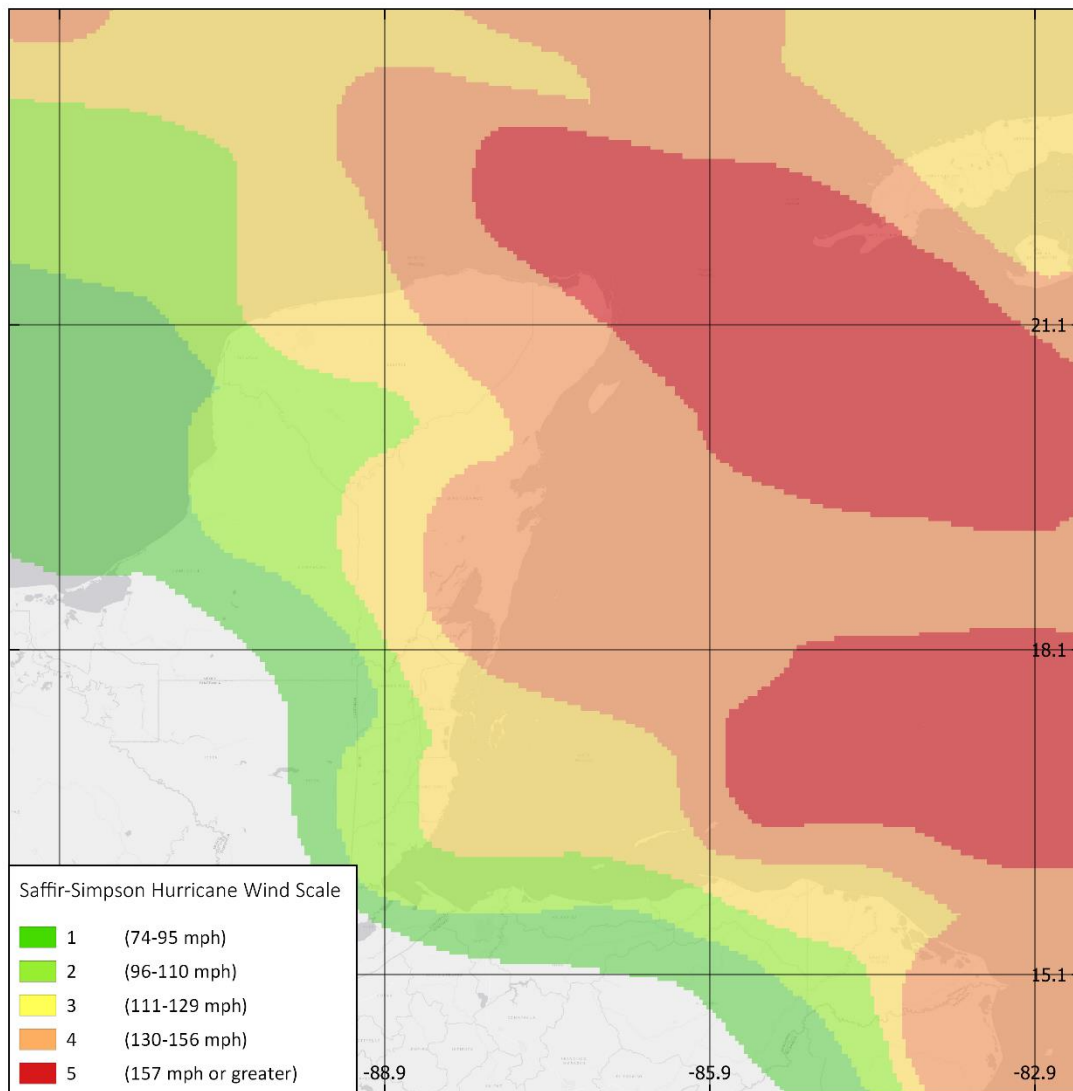


Figure 51: Exposure to increased wind speeds as expressed by the Saffir-Simpson Hurricane scale.

The distribution of wind speed demonstrates a northern bias. The highest vulnerability to hurricane winds occurs above a latitude of 21-degrees and shows a diminishing trend towards the Gulf of Honduras. This area is particularly susceptible due to the situation in the path of several tropical storm tracks. Strongest winds can be seen over open ocean and significantly lose power inland; this is the result of wind shear.

The whole Belize region falls within two distinctions of windspeed: class three and four. These classes represent the 111-129mph and 130-156mph ranges, respectively. The boundary of conditions can be seen to occur at the tip of Ambergris Caye coincident with the town of San Pedro. There is little variability due to wind exposure; this is not surprising as Phinn et al. (2010) suggest atmospheric parameters will vary over scales of one to ten kilometres.

8. Modelling of coastal vulnerability in Belize

8.1. Clustering of parameters

Machine learning clustering techniques were used to delineate segments of the coastline which exhibit similar characteristics. Clustering was performed through an application of the KMeans algorithm over 215 coastal sample grids. Each of which has been assigned a vulnerability score from one to five. The application of this approach has been shown for the classification of coastal areas by Calil et al. (2017).

Quantitative variables have been assigned clusters based on the ranking of centroid statistics. These represent the generalised conditions present in the coastal sample. In the case of waves and SDB, higher centroid values suggest a greater risk. Whereas for the DEM, the lowest values represent the highest risk group. Centroid statistics have not been used to rank the qualitative variables present in the geomorphology component. Instead, the proportional abundance of each class has been evaluated to represent the dominant land cover types in that cluster.

Cluster characteristics and thresholds are outlined in table 11. As the feature space contains multiple dimensions for each parameter, cluster centroids have been simplified to show only the mean centroid statistic. This figure shows the coastline has been well segmented into areas of similar conditions. These values differ significantly from those defined by Gornitz (1994) and present an automated method for the adaptation of thresholds to new coastal regions.

An indication of the spatial distribution of vulnerability clusters for each parameter is shown in figure 52. As suggested by Calil et al. (2017), the ability to track causes of vulnerability in the final model back to individual clusters or parameters is an advantage of clustering prior to the calculation of the CVI index. KMeans has provided a distinct distribution of parameters along the coastline to demonstrate segments with similarities. The spatial trends are largely reflective of the vulnerability for each parameter.

Coastal segments that demonstrate a consistently high risk across parameters have been identified. These areas include Caye Caulker and Ambergris Caye. In the case of Caye Caulker, the only low vulnerability is attributed to the geomorphology parameter. This is due to the dominance of mangroves and seagrass. The seaward side of Ambergris Caye demonstrates low vulnerability with respect to elevation and wave climate but is otherwise subject to medium to high vulnerability across all parameters.


Conversely, areas of low vulnerability are less apparent due to a lack of consistent coincidence between each parameter. Areas demonstrating a spatially consistent low risk are situated in the northern extent of the mainland coastline. This covers the lagoonal area of Belize District North. In this region, a low risk from land and marine geomorphology is observed but a very high risk is associated with the low topography (a characteristic often associated with mangrove dominated areas).

In figure 52(d), the clustering of DEM values show a significant proportion of the coastline at the highest risk with 34% of the coastline attributed to this cluster. KMeans clustering will differentiate groups in the feature space based on the proximity of points to centroids (Jain, 2010). Therefore, the distribution of points across clusters will not always be equal and is demonstrated by the percentage distributions in table 11. This is prevalent in parameters which have low range of values or with uneven distributions as low and high clusters will be disproportionately affected by extreme outliers (Rueda et al., 2017).

The data populating the CVI demonstrate variation over several spatial scales. The most spatial variability to clustering occurs with respect to land cover and the least variability occurs in wind exposure. Geomorphology varies over a ten-metre spatial resolution – the minimum pixel size of datasets – and thus provides an increased degree of heterogeneity in and between individual coastal samples. This results in variation to vulnerability clusters over a smaller spatial scale.

As an indication of an initial national-scale study, the comparatively low-resolution datasets for some parameters is adequate. This will identify broad areas of vulnerability which can be prioritised with further detailed studies (López Royo et al., 2016). The CVI clusters can efficiently assess the impact of individual physical factors acting over a range of scales. These can be used to identify hotspots and provide targeted management information. This information can be used to detail the areas which are more vulnerable but also what parameter they are vulnerable to. This will provide an indication as to where to target initial management resources in that area and will be vital for sustained, large-scale coastal zone planning.

Table 11: Results of KMeans clustering and the designation of vulnerability groups based on similar geomorphic properties demonstrated by the centroids of each cluster.

		Vulnerability Cluster									
		1		2		3		4		5	
		Cluster centroid attributes	% coastline segments	Cluster centroid attributes	% coastline segments	Cluster centroid attributes	% coastline segments	Cluster centroid attributes	% coastline segments	Cluster centroid attributes	% coastline segments
Parameter	Land	Mangroves with sparse forest assemblage	15.3	Agricultural & mangroves	24.2	Mudflats & agriculture	26.1	Mudflats with sparse mangroves and urban	14.4	Predominantly urban areas	20.0
	Benthic	Coral with sparse sand	20.5	Seagrass with sparse deep-water areas	36.3	Rocky areas with sparse sand and coral	28.8	Sand with limited coral	10.7	Deep water	3.7
	SDB	1.361m	31.6	1.608m	21.4	1.775m	19.5	2.942m	12.6	7.348m	14.9
	DEM	4.937m	24.2	4.632m	12.1	3.339m	15.7	1.819m	14.0	0.907m	34.0
	Waves	0.508m	24.7	0.858m	8.8	1.203m	24.2	1.213m	37.6	1.472m	4.7
	Wind	74-95mph	0.0	96-110mph	0.0	111-129mph	79.1	130-156mph	20.9	>157mph	0.0
		<div style="display: flex; justify-content: space-between; align-items: center;"> Low Vulnerability  High Vulnerability </div>									

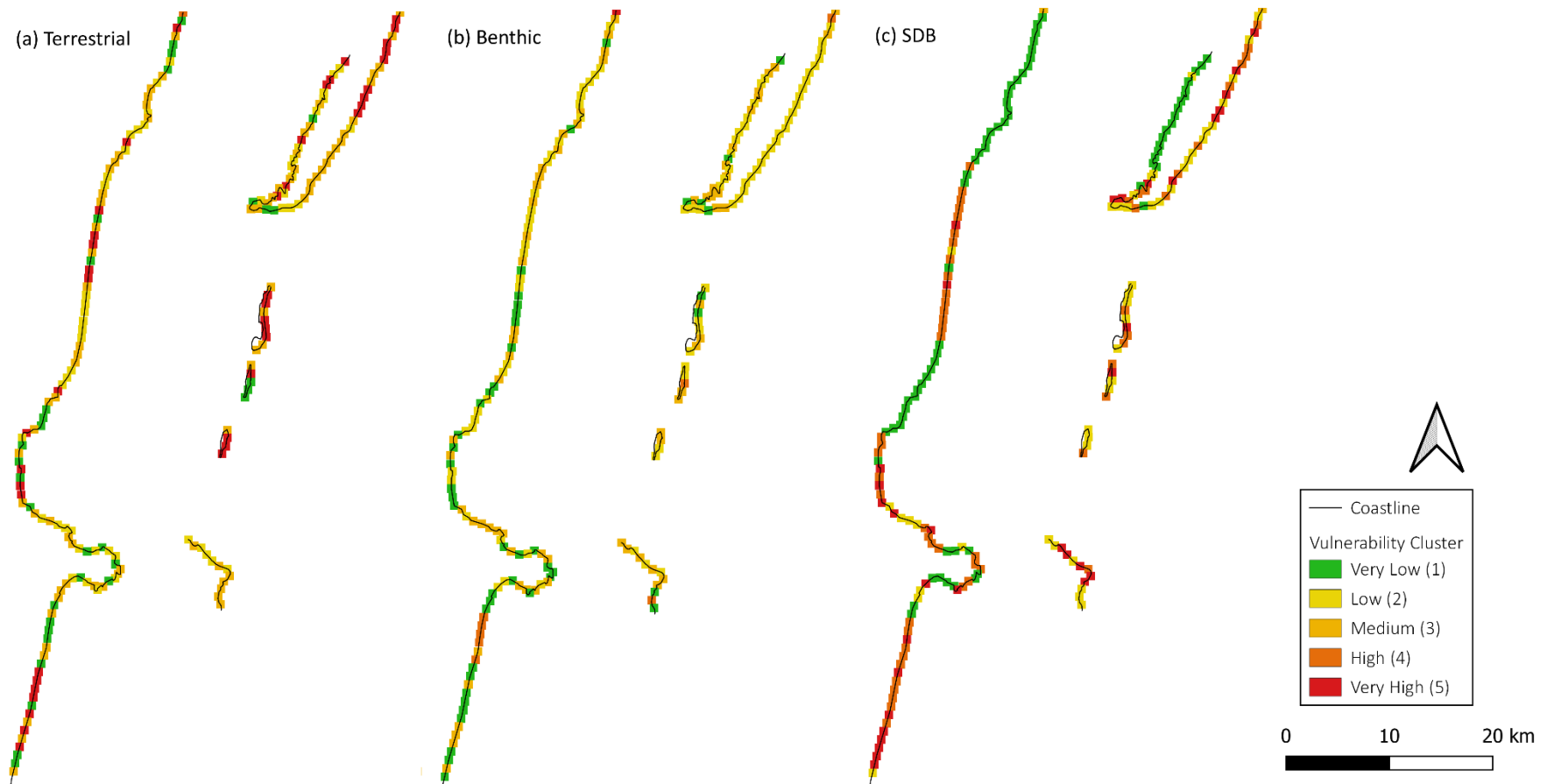


Figure 52: Relative vulnerability ranking of coastal segments for each parameter based on KMeans clustering.

(a) Terrestrial geomorphology (b) Benthic geomorphology (c) Marine coastal slope



Figure 52: Relative vulnerability ranking of coastal segments for each parameter based on KMeans clustering.

(d) Terrestrial coastal slope (e) Wave climate (SWH) (f) Wind exposure

8.2. Spatial distribution of vulnerability

The Coastal Vulnerability Index (CVI) is given for Belize using KMeans clustering in figure 53. The range of CVI values is between 3 and 48 with a standard deviation of 8.77. These metrics were divided into categories of low, moderate, high and severe based on the following quartiles:

1. Low	CVI	3 – 7	22% coastline
2. Moderate	CVI	8 – 12	26% coastline
3. High	CVI	13 – 21	33% coastline
4. Severe	CVI	22 – 48	19% coastline

Figure 54 shows the distribution of CVI values amongst vulnerability classes around the sample mean. The deviation of values is not normally distributed with a skewness mean of 0.84. The mean CVI is 14.46 and median 12.00, this range is comparable to other CVI studies (López Royo et al., 2016; Pendleton, 2010). Cogswell et al. (2018) posit that the CVI equation is sensitive to the percentile division of vulnerability classes because of skewed index values. As a result, the translation of index values into vulnerability percentiles is subjective and subject to opinion (Füssel and Klein, 2006). This instates a user bias in the demonstration of vulnerability.

The bell curve distribution of CVI tails off at the two extremities. Therefore, dividing the values based on quarterly percentiles would incite bias as the high skewness value supports a dense cell distribution around the moderate vulnerability class. The interpretation of skewness stats provides the justification of defining vulnerability classes through the natural breaks approach (Koroglu et al., 2019). This ensures the model provides the most effective indication for targeted planning as the disproportionately vulnerable areas should be adequately highlighted.

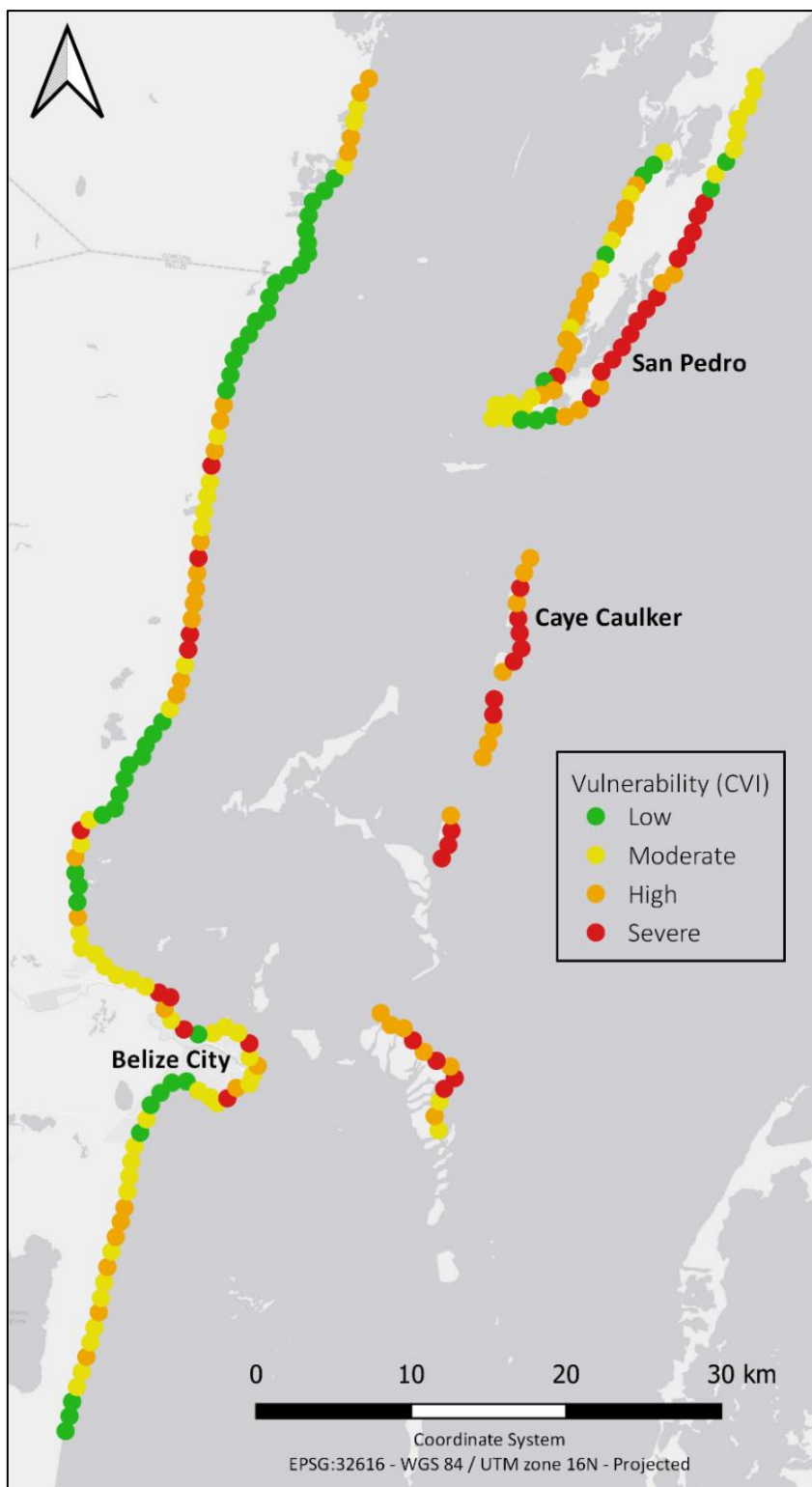


Figure 53: Coastal vulnerability (CVI) in Belize using KMeans clustering.

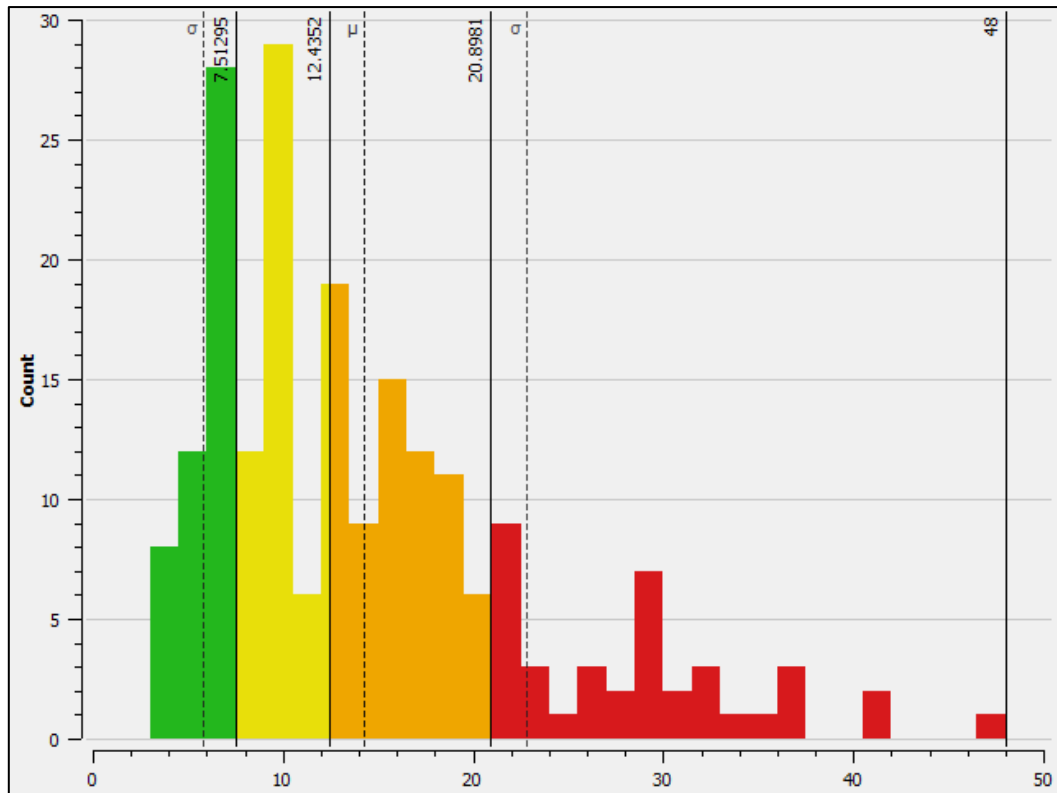


Figure 54: Distribution of CVI values across vulnerability groups.

The distribution of most vulnerable regions accounts for 19 per cent of the coastline. A seaward bias is demonstrated through significant concentrations in the east. In this thesis, processes have been quantified which contribute to vulnerability. Areas with the highest vulnerability have been seen to include Ambergris Caye and Caye Caulker. The highest CVI value of 48 is seen in Caye Caulker. These coastal sections are typical of low-lying regions with a steep marine coastal slope and high energy waves. Land-use is a mix of urban and mudflat classes surrounded by bare substratum under water. Coastlines of this nature have been demonstrated to be subject to adverse effects of inundation and ecosystem loss (Nicholls et al., 2007). This is supported by the observations of Lane et al. (2013) who suggests these regions demonstrate cumulatively higher storm surges.

Several severe vulnerability hotspots contain concentrated population centres, including San Pedro and Caye Caulker; these areas have a population of 1,767 and 11,778, respectively. Further regions of high vulnerability can be seen in parts of Belize City – including the area coincident with Sir Barry Bowen Municipal Airport – and would account for an additional vulnerable population of 57,310. These areas are known to have significant flooding impacts (NEMO, 2016).

An exception to the seaward trend is found at the northern-most and southern-most extents of Ambergris Caye; which are classified as low risk. A low wave climate with a dominance of mangroves, coral and seagrass clusters combine for a low CVI score. This observation should be contextualised against other significant policies implemented in Belize. In the south, this region contains the Marco Gonzalez Archaeological Reserve (which accounts for significant forest and mangrove land use in the area) and is surrounded by the Hol Chan Marine Reserve – a government defined marine protected area (MPA). In the north, the MPA of Bacalar Chico Marine Reserve intersects areas of lower risk. These areas are protected and carefully managed which likely contributes to a lower terrestrial vulnerability and are evidenced by dominant land uses in geomorphology clusters.

Low and moderate risk areas represent 48% of the coastline. Such areas include the town of Ladyville (population: 5,468) where coastal segments demonstrate CVI values of less than 12. Although, historical evidence indicates that storm events have had significant impacts here in the past (NEMO, 2016). The lowest CVI value of 3 is seen in the lagoonal area of Belize District North. These areas exhibit low vulnerability due to the dominance of mangroves and inland lagoonal areas. Low vulnerability areas should not be disregarded by management policies as these are reflected through the protection provided by land use practices in the area. Therefore, the maintenance of functional habitats provides a pressing management priority.

8.3. Validation of multi variate CVI model

Vulnerability is an inherently intrinsic characteristic which provides difficulty for absolute quantification or validation (Roy and Blaschke, 2013). Performance of the KMeans CVI model has been evaluated against other relevant studies in the region. This has formed an integral part of validation and testing. Validation has been performed against: the traditional approach employed by Gornitz, national flood models, existing vulnerability models and impacts of historical hurricane events. Direct comparison between these studies will be impractical due to the differences in resolution, derivation methods and approach to designation of composite vulnerability groups. The approach for comparison of separate modelling approaches suggested by Perini (2016) has been appropriated.

Traditional CVI Thresholds

Figure 55 shows the process of sensitivity testing through a comparison of CVI assessments obtained using the original thresholds defined by Gornitz (1994). This figure demonstrates poor contributions to the CVI variance from terrestrial elevation, bathymetry and wave climate as these are homogenous along the coastline. Identifying the whole coast as a high vulnerability is not a helpful metric for prioritising management targets.

A high degree of variability in the CVI stems from the qualitative parameters of terrestrial and benthic coverage. The resulting vulnerability level is difficult to interpret as, despite all classes ranking highly, percentiles will differentiate the data values. Variation to the degree of vulnerability will be subject to the changes in geomorphology identified. This parameter requires subjective definition and pixels are more likely to fall within discrete class bands than those with numerical thresholds.

These parameter ranges are defined with respect to the northern Gulf of Mexico and are not comparable to ranges in other localities (Pendleton, 2010). Even though this is an area not too geographically detached from Belize, these discrepancies demonstrate the requirement for adapting thresholds to regional-specific studies. Machine learning takes away need for careful deliberation of thresholds to allow rapid and automatic deployment at scale in new areas. To this degree, the KMeans model is effective at improving upon the assessment of vulnerability to provide distinction along coast for each parameter. This can be used to provide actionable intelligence for decision makers.

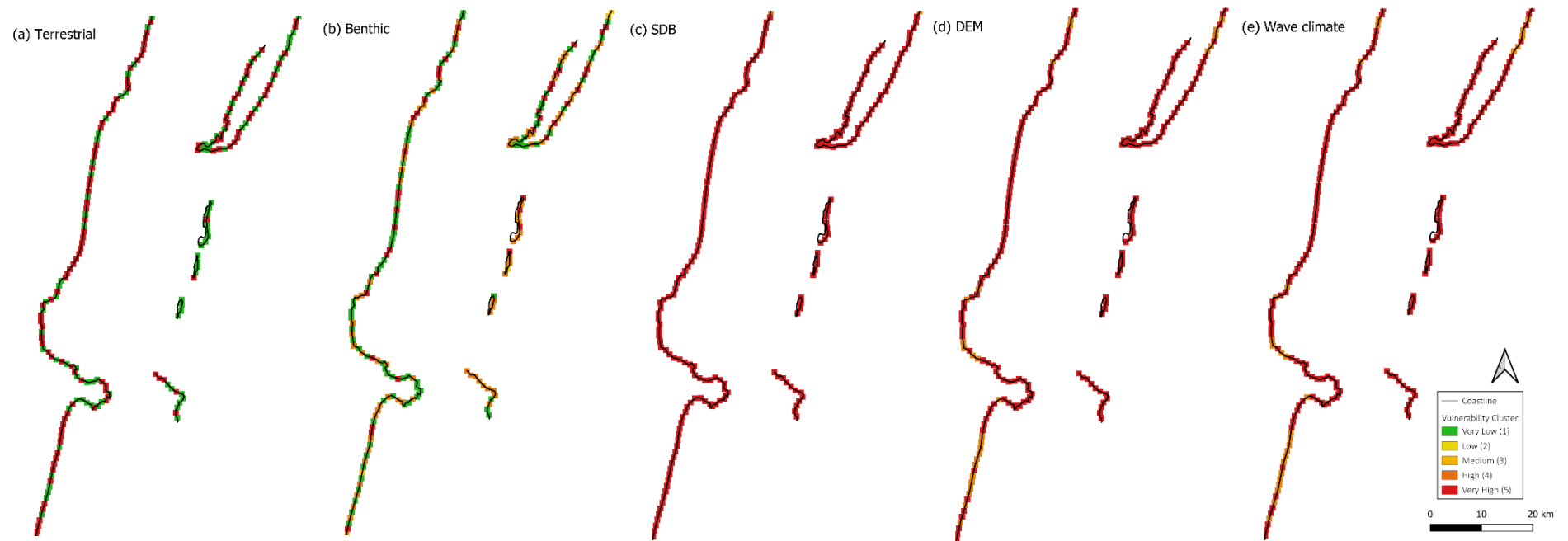


Figure 55: Distribution of vulnerability for individual CVI parameters based on the traditional Gornitz (1994) thresholds.

Mullick (2018) also suggests these thresholds ignore the spatial variability present in global coastlines and that thresholds based on data distribution are more appropriate. KMeans has reduced the complexity of the computational framework and reduced the qualitative and quantitative uncertainty. This is a major obstacle for studies with limited budgets in national-scale assessments (European Environment Agency, 2011).

National Flood Models (Caribbean Handbook on Risk Information Management, CHARIM)

The current flood assessments utilised within ICZM for Belize are produced by CHARIM through hydraulic modelling and topographic consideration at a national scale. Figure 56 shows the extent of coastal flooding modelled for each Saffir-Simpson category. In this study, offshore islands have not been included due to lack of data but are deemed very high risk.

The spatial distribution of flood extent shows almost 100% of the coastline would be flooded in a category one hurricane. This is except for Belize City and some sporadic southern-most regions. The worst flooding occurs in Belize City is corroborated by the two high severity hotspots seen in figure 53. In addition, the penetration of flood water extends further in the north of the coastline suggesting these areas are more vulnerable to storm surges. This was an area that was assessed as holding a low risk to storm surge in the CVI assessment.

Disparities are likely stemming from the consideration of multiple variables in the CVI. The northern extent of the coastline is inherently low lying but the impacts of land use in this area are neglected in the CHARIM assessment. Furthermore, the elevation derived in this model is limited by the coarse 90m resolution of the SRTM DEM used and will provide an overestimation of flood extents. This demonstrates an advantage of utilising the ASTER DEM to improve the relief component with higher resolution data.

The CVI method in this thesis further combats the lack of data availability in rural areas and provides an indication of flood vulnerability for the entire region.

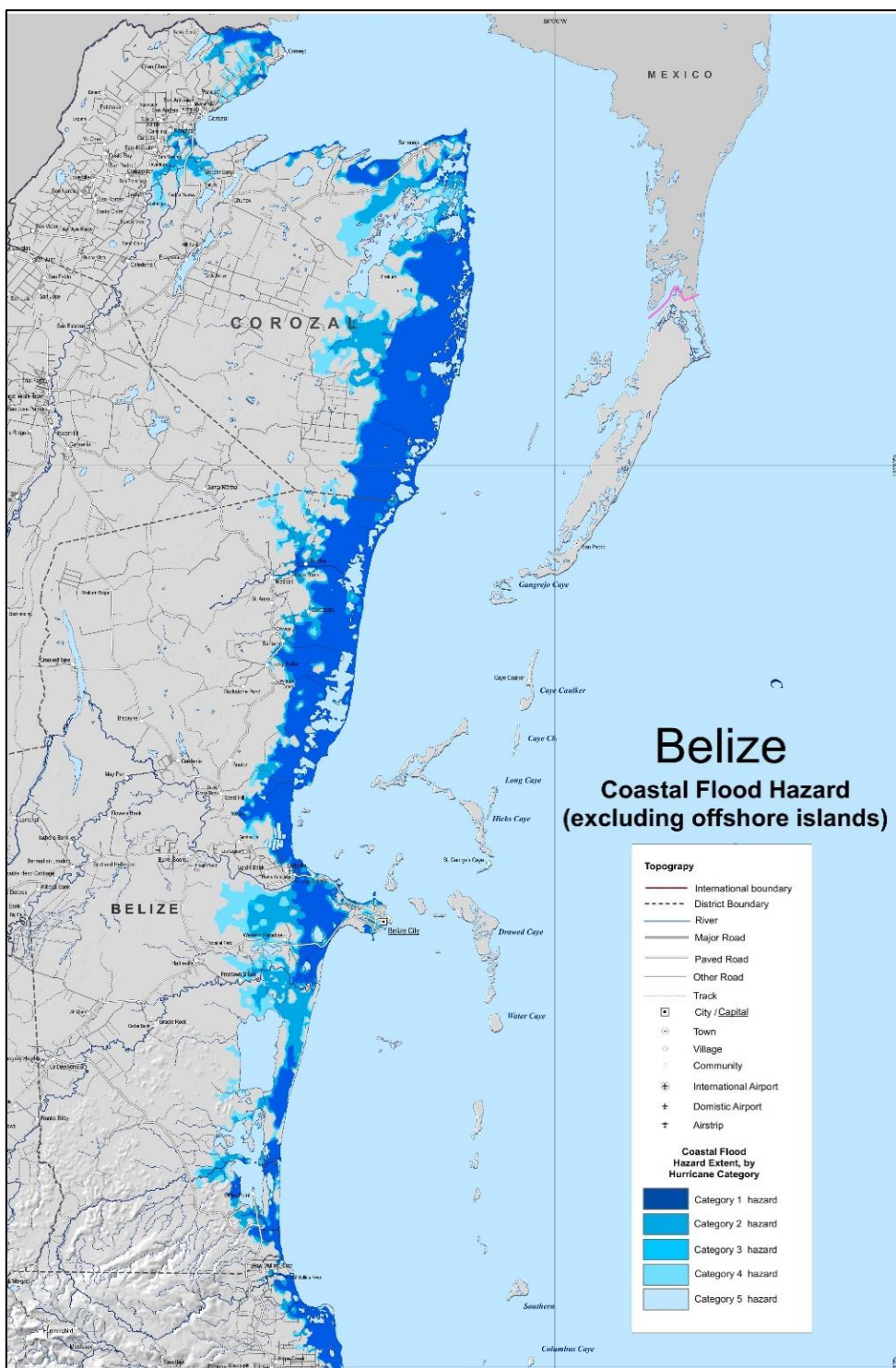


Figure 56: Coastal flood inundation Hazard, Belize (CHARIM, 2016).

InVEST Exposure Model

In addition to the CVI equation, subsequent index-based assessments have been made of the coastal zone. The Integrated Valuation of Ecosystem Services and Tradeoffs (InVEST) model, developed as part of the Natural Capital Project, calculates the exposure index for a coastal segment through the combination of six ranked bio-geophysical variables. Based on the ranking schema defined by Thieler and Hammar-Klose, this model defines vulnerability of variables based on statistical groups rather than static thresholds. These groups are provided by quartiles and result in hard boundaries which cannot represent clusters of similar conditions. This approach has been used by Hopper and Meixler (2016) to model changes to vulnerability over time and represents the primary approach for vulnerability mapping in Belize.

$$EI = (R_{\text{Geomorphology}} R_{\text{Relief}} R_{\text{Habitats}} R_{\text{Wind}} R_{\text{Waves}} R_{\text{Surge}})^{1/6}$$

Equation 2: InVEST Exposure Index (EI).

Figure 57 shows an exposure assessment based on the InVEST model; a geographically scalable approach to vulnerability through thresholding coastal characteristics using percentiles. This model has been validated previously (Onat et al., 2018; Ballesteros & Esteves, 2021) and is currently accepted for use in ICZM for Belize.

Variability in the relative vulnerability assessment of InVEST show a good corroboration with KMeans. 54.0% of coastal segments fall within one vulnerability class of each other while only 4.65% of segments show a significant difference of three classes. InVEST demonstrates a high clustering of mid-vulnerability values which tend to underestimate the extremities with the least vulnerable regions accounting for 5% of the coastline and highest severity covering 13%. Both studies demonstrate a good agreement of high vulnerability regions for the outermost cayes, however, the severity is seen to be less in InVEST and especially at the south of Ambergris Caye.

Due to differences in the scale of data used and the complex approaches to modelling, discrepancies should be expected between the two models. A key distinction is the large disparities seen in the northern extents of the mainland. This is the same region as demonstrated

by the CHARIM flood map and suggests the KMeans model is under-representing the severity of vulnerability in this area. This is an area demonstrating high proportions mudflat landforms and can be attributed to the difference in parameter weighting in the two models. InVEST suggests mudflats retain the maximum exposure class while these landforms prominently feature in the moderate to high clusters in KMeans. This provides an indication of the bias stemming from the subjective ranking of qualitative classes rather than the results of clustering processes. Discrepancies such as this suggests the value of an expert assessment to defining cluster groups which may be prone to subjective uncertainties to ensure these are appropriate.

Prior to modelling, input datasets are also derived from different sources and have inconsistent spatial resolutions (table 12). KMeans will show more changes to vulnerability within small spatial scales which will not be apparent in InVEST due to its poorer resolution. The InVEST model is likely to overpredict the extent of flooding because of the low spatial resolution of these datasets. Furthermore, these are unlikely to properly represent small topographic features across the 1km coastal segments.

Despite inequivalent modelling approaches, the identification of vulnerable spots is consistent with results produced by InVEST (which aims to fulfil the requirements of mapping the value of natural goods and services) and demonstrates robustness for both methods. Although, the similar trends observed may not provide an indication of model reliability and requires ground truth to increase the confidence of this assessment.

Although both models act to assess spatial distribution of vulnerability, the differences observed show that CVIs must be adequately used to be a useful tool in identifying coastal areas at risk. Different approaches may indicate a contrasting vulnerability for a given area which will result in critical repercussions to management decisions (Koroglu et al., 2019). Due to these disparities, it is crucial to analyse the bias and uncertainties resulting from the modelling approach to isolate the cause of differences. This includes an understanding of each component's contribution to the overall vulnerability for context as to how these differences will spatially vary.

Table 12: Datasets used in the InVEST model.

InVEST Parameter	Dataset	Resolution
Bathymetry	GEBCO	100m
DEM	USGS (SRTM30)	10m
Wave climate	Wavewatch III	18,600m
Geomorphology	Allen Coral Atlas benthic coverage	25m
Mean Sea Level	Permanent service for mean sea level (PSMSL)	N/A

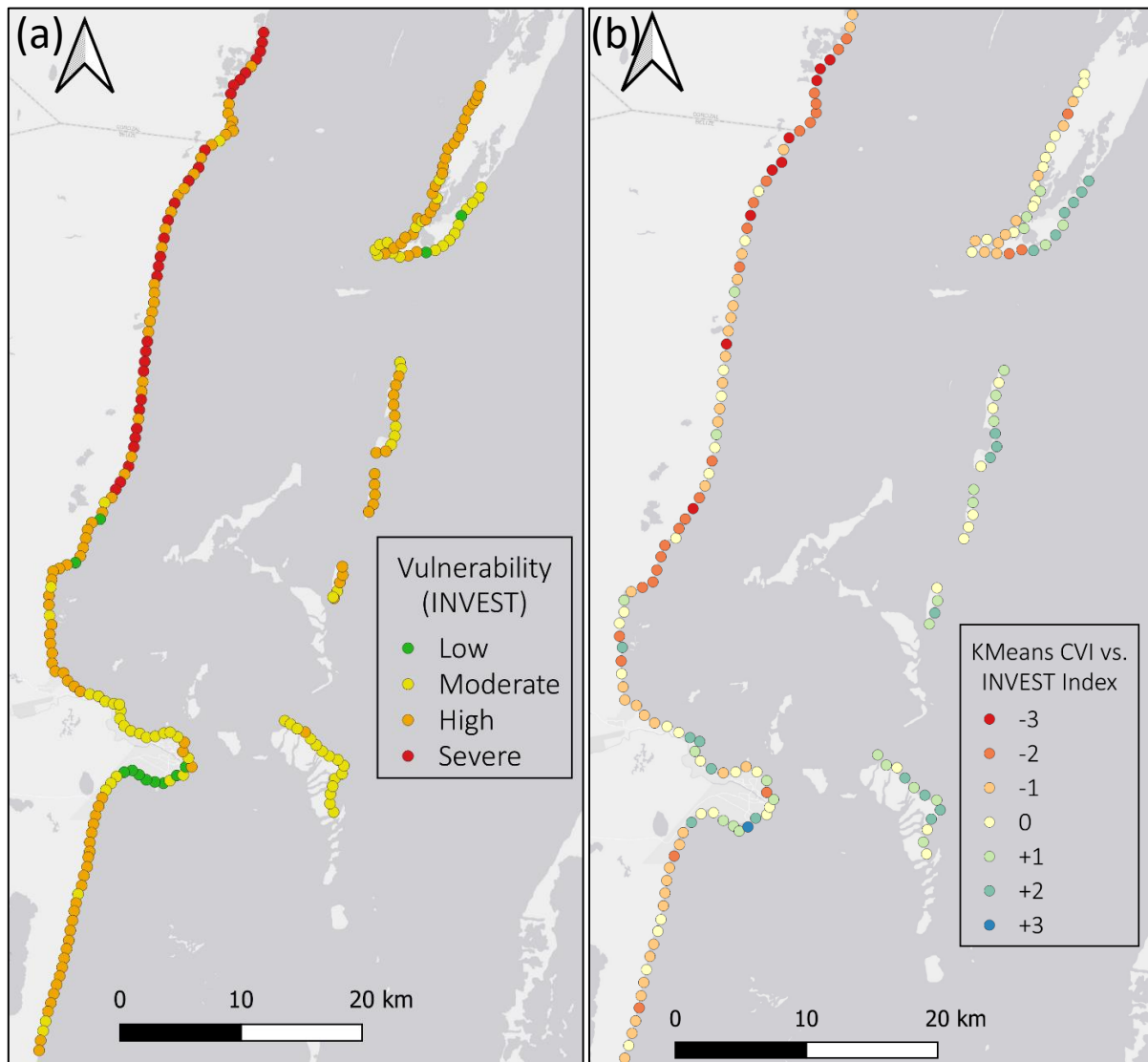


Figure 57: Comparison of InVEST and KMeans results.

(a) InVEST modelled assessment of vulnerability in Belize. (b) Difference between KMeans and InVEST vulnerability assessments.

Previous Hurricane Events in Belize

Bertin et al. (2014) suggest flood hazard maps are generally not tested against survey information after a storm event. Hence, in addition to the comparison with InVEST, vulnerability maps produced for this study have been validated against areas affected by historical events. As spatial maps showing physical flood inundation are sparse, this was achieved through comparison of damage assessments and anecdotal evidence from reports provided for significant events in recent years as a proxy for flood damage.

Hurricane Earl provides capacity for comparison due to its widespread impacts and intersection with the time-series availability of Sentinel-2 imagery used in this study. This suggests conditions observed in the imagery are likely to represent conditions present at the time of the event. Anecdotal evidence is available but can be further validated using SAR imagery from Sentinel-1 – which can provide imagery acquired within a week of the event – to map the extent of flooding (Uddin et al., 2019).

Earl made landfall in Belize as a category one hurricane on 4th August 2016 and primarily impacted the districts of Belize City and Belize Rural (containing Ambergris Caye and the outer-lying islands). A nine-foot surge was seen in San Pedro which caused damage to houses and businesses; including 56% of National Hotel Stock and \$30,000 in damages to households.

On the eastern coast of Ambergris Caye, 227 of 252 docks were impacted and 135 of which were destroyed. Likewise, in Caye Caulker 49 of 54 docks were affected. These damages amounted to \$14 and \$2 million, respectively. This was sufficiently greater than the \$470,000 of dockland damage occurring in the commercial area of Belize City – a factor of four times less! Adverse impacts also resulted due to flash flooding in the Cayo district inland. This is not captured by this model, however, as these impacts did not occur in the vicinity of the coast and are likely the result of rainfall rather than storm surges (NEMO, 2016).

Moreover, an indication of the spatial distribution of damage can be seen more extensively by Hurricane Keith in 2000. Table 13 demonstrates the total population affected by the hurricane. A significant proportion of the regional populations were affected in San Pedro and Corozal (66.7% and 42.5%). This supports areas that have been outlined to have the highest vulnerability in the model. Although Corozal experiences a significant affected population, only \$80 of damages is experienced here which is likely the result of low population density and dominance of agriculture. Caye Caulker and Belize City also experience the highest concentration of damage.

Table 13: Impacts of Hurricane Keith (2000) by location (GFDRR, 2000).

		Location				
		Belize District	Belize City	Caye Caulker	San Pedro	Corozal District
Number affected (as of 11 October 2000)	Total population (2000)	62,729	49,059	742	4,499	26,748
	Affected population	27,308	14,717	279	3,000	11,356
	Families affected	N/A	1,168	45	1,145	816
	Living in flooded areas	24,029	14,717	N/A	N/A	19,126
	Homeless	3,279	N/A	279	3,000	N/A
	High risk of health impairment	35,314	14,711	1,300	10,000	15,419
	Damaged houses	BZ\$2,761	N/A	BZ\$6,625	BZ\$10,280	BZ\$80
	Destroyed houses	BZ\$3,490	N/A	BS\$9,625	BS\$46,735	BZ\$80

Despite the different incidence tracks of these hurricane events, the areas experiencing the worst impacts are consistent. KMeans predictions have been shown to be consistent with qualitative observations and provides evidence for the application of the model at a regional scale. The seaward regions of the coast (including Ambergris Caye and Caye Caulker) show a better correspondence with the historical information than INVEST which suggests Ambergris Caye presents a low-moderate vulnerability.

The social impacts of storm surges are modulated by more than just the geographic components which are captured by the model. The CVI fails to capture elements (such as population density) which may influence these observations. Recording data following a storm event is fundamental to improve the methodology and identify whether the areas modelled represent true vulnerable areas. Although, Cote and Nightingale (2012) argue these modes of risk assessment are related to power relations as opposed to clear quantifiable values. The use of satellite estimations in the wake of hurricane events for impartial assessments is a beneficial approach to equalise this.

PART V – DISCUSSION AND CONCLUSIONS

This section provides an analysis of the value for Earth Observation data within CVI assessments. The initial chapter outlines the inherent uncertainties in deriving parameters from satellites and the modelling approaches employed. This is followed by a consideration for the implications of the KMeans CVI model results to determine areas which may be disproportionately vulnerable and are situated within the context of Integrated Coastal Zone Management (ICZM).

9. Uncertainties

Sources of uncertainty require comprehension to interpret the results of CVI studies and understand how to increase the accuracy and reliability of the model (Boumboulis et al., 2021). Due to the inclusion of novel remote sensing techniques in this study, sources of uncertainty span from the derivation and integration of parameters within the modelling process. Inherent uncertainties are associated with deriving variables from satellites and have been considered individually in respective sections. The ability to precisely derive parameters from satellite provide a more significant impact on model effectiveness than by the modelling process itself. Remote sensing is not a perfect substitute for in-situ measurements, however, this technique provides an effective method for quantifying parameters at scale and with a good degree of accuracy. A trade off should be considered between the benefits of accuracy, scale and cost required for geotechnical information in coastal management. When working at scale, highly accurate data will be costly – both in time and money.

An overview of the key limitations discussed in this section are shown in table 14. Due to limitations in derivation and modelling, a cautious approach must be taken when making any deductions from the model outputs as these can provide a false impression of the certainty of results. Caveats have been explicitly communicated to not waste resources or present misleading management concerns amongst stakeholders. Hence, the use of a relative CVI scale as opposed to absolute values is appropriate (Rosenthal et al., 2014).

Table 14: Uncertainties in CVI estimation using remote sensing.

Uncertainties in parameter derivation	Uncertainties in modelling
<ul style="list-style-type: none"> • Low spatio-temporal resolution. • Habitat quality not assessed. • Lack of observations for model calibration. • Qualitative measurements of habitats. • Inherent Optical Properties of the water column and Depth of Penetration (DoP) of solar radiation needed for SDB. 	<ul style="list-style-type: none"> • Compounded uncertainties resulting from individual parameter derivation. • Factors given same weight. • Scale of coastal sample – only captures 1km grid of coastal zone. • Over-simplification of dynamic coastal processes. • Variables with differing spatio-temporal scales. • Anthropogenic factors disregarded. • Lack of observations for model calibration and validation.

9.1. Uncertainties in parameter derivation

9.1.1. Geomorphology component

Uncertainties in establishing the extent of land and marine geomorphologies have stemmed from the process of image classification. Existing terrestrial classifications are provided for Belize with accuracies ranging from 60% to 92.6% (Meerman & Sabido, 2004; Doyle et al., 2021). These studies largely focus on changes to specific localised habitats, including mangroves, and so provide bespoke training samples for these habitats. The accuracy of the terrestrial RF model in Belize is substantial (70.4%), however, does not meet that of recent wetland studies. This can be attributed to a sub-standard quality of training data.

Complete national coverage is provided by the Copernicus Global Land Service; a global model at a 100m spatial resolution and an accuracy of 80.3% (figure 58). This global accuracy may not be applicable in localised studies. A coarse resolution of 100m is well suited for studies at large scales but can present errors when representing localised assessments. Phinn et al. (2010) suggest that 100m is the top end of the appropriate scale for vegetation mapping and the limit for appropriate benthic assessments. The 10m resolution of Sentinel-2 improves upon the quality and volume of data to show the diversity of habitat types and will provide a better indication of the exact proportions without diluting habitats at large scale. This is evidenced as 100m is too coarse to pick out sparse mangroves assemblages and thus would be missed in the Copernicus model.

In highly diverse regions, these 100m pixels will present a mixed-pixel problem through containing multiple land use types. This results in pixels containing combined contributions of spectral information and is compounded through an object-based analysis as clusters of pixels are chosen as training data and underrepresents data on spatially heterogeneous classes (Stehman & Wickham, 2011). Through utilising a higher resolution dataset in Sentinel-2, the distinction between classes becomes clearer. A 10m resolution shows an improvement to the estimated coverage of each class (table 11) but could be further enhanced through VHR imagery. Wang et al. (2016) suggests a spectral unmixing approach should be used further improve the accuracy of Sentinel-2 classifications through a decomposition of pixel spectra into a set of endmembers with corresponding abundance.

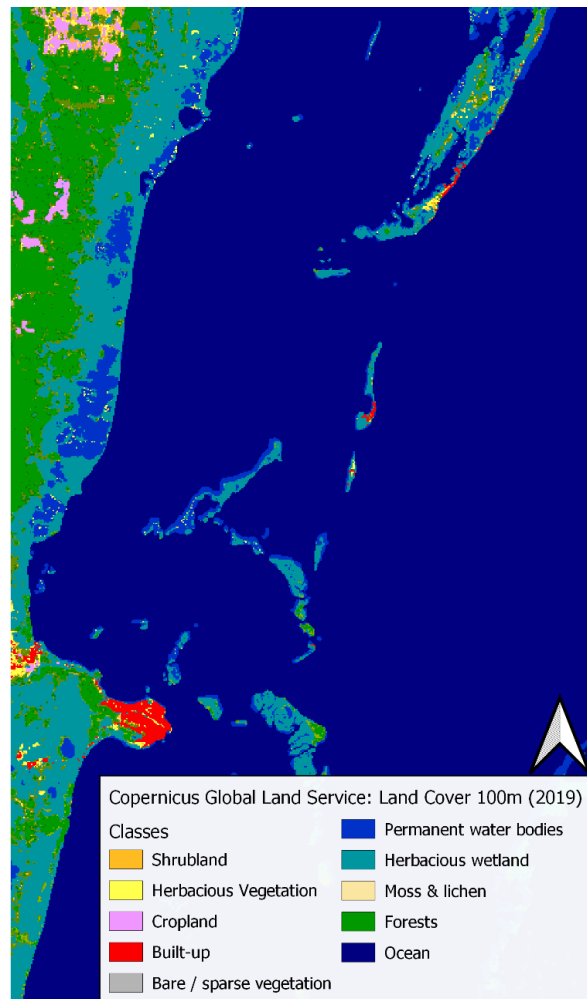


Figure 58: Copernicus land cover classification for Belize.

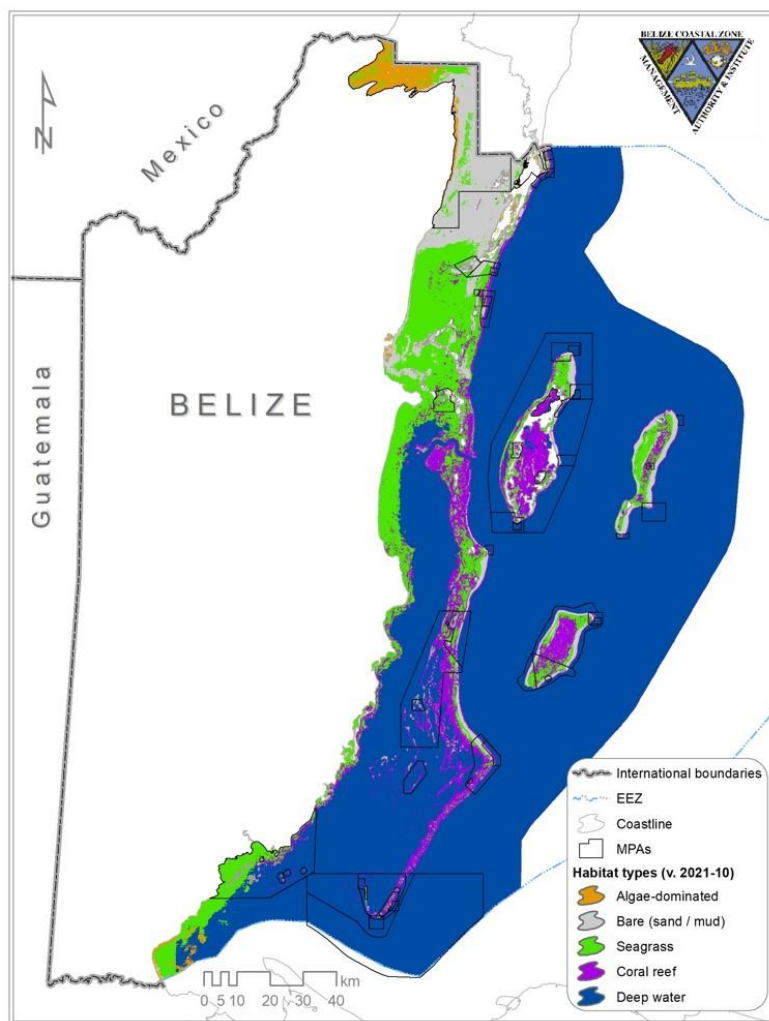
Benthic classifications exist as part of the CMP in Belize and have also employed a machine learning approach using Sentinel-2. Figure 59 shows the existing National Marine Habitat Map (NMHM) with a 58.7% accuracy. Several studies support similar accuracies for benthic mapping with comparable accuracies (58.2%; Poursanidis et al. 2019, 58.5%; Pottier et al., 2019). An improvement to the accuracy of the benthic map can be seen through the RF model provided in this thesis (61.1%). These accuracies are low and can be associated with a highly fragmented seascape where multiple benthic types can exist within one Sentinel-2 pixel. Higher spatial resolution imagery should also reduce these uncertainties.

Limitations of benthic mapping with current EO techniques were corroborated by the NMHM. The presence of the coastal aerosol band in Sentinel-2 is an advantage when downscaled to 10m as this provides deeper penetration of the water column and allows more habitats to be identified (Poursanidis et al., 2019). The biggest differentiation to benthic endmembers is

observed at lower wavelengths so an ability to provide more spectral information covering this part of spectrum is advantageous. Through using only four visible spectral bands in their classification, the NMHM is limited in the ability to separate classes. The RF model improved the accuracy using seven bands to increase the separability of endmembers and capacity for distinction between classes.

Despite representing a less diverse surface than the terrestrial classification, a reduced accuracy is observed for the marine model and is reflected by high levels of noise. The potential for misclassification extends from the endmembers observed in figure 41. These show a tight clustering of marine classes which demonstrate similar trends with minimal variation to their magnitude of reflectance. Distinctions between pixels become hard to distinguish without sufficient alterations in the magnitude of EM spectrum between classes. This is contrasted by the terrestrial classes which show high separability across spectral bands. Poor separability suggests that the clustering of marine classes is likely a result of reduced penetration capacity through the water column. The distinction between endmembers should be improved with an increased spectral resolution which may elucidate hidden patterns present within spectral bands of Sentinel-2. Hyperspectral sensors and drone surveys may provide a more suitable option if the highest levels of accuracy at local scales is desired.

Endmembers may also be supplemented through incorporating more spectral bands. In this study, the NDVI index was used to enhance the distinction of vegetated classes and has contributed to an increased accuracy. Other indices should be investigated for their influence. Choubin et al. (2017) show the benefit of including indices such as LAI and NDWI for the calibration of ML models for forested or water classes, respectively.



Producer classification dataset (revised 2021 NMHM)	User validation dataset (field survey data)						TOTAL	User accuracy
	Class	Algae	Bare	Seagrass	Coral	Deep water		
Algae		15	12	9	0	0	36	41.7%
Bare		6	44	53	25	0	128	34.4%
Seagrass		1	2	37	5	0	45	82.2%
Coral		0	1	21	103	0	125	82.4%
Deep water		0	0	0	5	0	5	-
TOTAL		22	59	120	138	0	339	-
Producer accuracy		68.2%	74.6%	30.8%	74.6%	-	-	58.7%

Figure 59: Belize National Marine Habitat Map (NMHM) and accuracy assessment (CZMAI, 2021).

The producer accuracy observed in the RF benthic model range from 26.7% to 93.6% (table 10). This broad range indicates a significant confusion between classes. Coral has a low producer accuracy of 63.3% and is often misclassified as seagrass. Inaccuracies in this class can be attributed to a high degree of spatial autocorrelation in training samples. Coral can only be seen in a narrow region of barrier reef which is hard to validate and often means samples

are tightly clustered. Data fusion provides a key solution to increase this distinction (Kulkarni and Rege, 2020). This should improve benthic mapping through a utilisation of supplementary data layers, such as bathymetry, which can provide additional parity for differentiation. Coral reefs occur in a distinct range of bathymetries and will differ from that of seagrass. An indication of depth will facilitate a contextualisation of the habitat. Fusion of optical and radar sources should also provide merit in mangrove identification due to the double bounce observed from these environments. This has led to classification accuracies of greater than 90% (Zheng and Takeuchi, 2020) although minimal research has utilised Sentinel-1 radar.

Classifier results are highly sensitive to size of training data sets. The proportion of training data should be representative of the landscape and provide minimal spatial autocorrelation (Millard & Richardson, 2015). Through a utilisation of the Sentinel-2 time series, an extensive repository of training data is provided due to a regular image acquisition. Through exploiting more training samples, this model has provided an improved accuracy over studies with in-situ validation samples. This was achieved over a small subsample of the full time-series available.

Training samples may also be improved through image pre-processing techniques including cropping the size of tile. Terrestrial and marine classifications were performed independently to limit invalid endmembers. This is especially useful in segmentation to provide specific training polygons and avoid confusion between similar land and water classes.

Furthermore, identified areas of noise can be reduced through a consideration of object-based segmentation approaches. As the first stage in the classification workflow, the choice of segmentation algorithm can provide significantly contrasting outputs. Gao et al. (2011) show how the use of different algorithms can lead to the over-segmentation of an image. This can result in noise, especially if training samples are poor. Optimal classification should be provided using a combination of approaches based on the area characteristics. Homogenous areas of forest cover in Belize are well-suited to object-based classifiers (Kamal and Phinn, 2011) but are less suited for areas of sparse seagrass. A hybrid-approach of pixel and object-based classifications would be beneficial to map complex environments (Wang et al., 2016).

An absence of in-situ data resulted in a reliance on user interpretation of the study site to produce classification training samples. As a result, the selection of high-quality training data was difficult and assumptions were made which may not reflect conditions on the ground as a result. A primary source of error in image classification extends from inadequate training data (Pal and Mather, 2005). Foody and Arora (1997) reinforce that the selection of high-quality

training data has a greater impact over model accuracy than the classification algorithm used. Ground control points over a small-scale sampling campaign could provide a useful and cost-effective supplement to validate classification models. This is useful as many land cover types are hard to discern at the 10m resolution, especially without a prior contextual understanding of the area. Although, in the case of the NMHM, these have been shown to have minimal impact to accuracy and could be avoided to cut costs if required.

The rate of land cover change is rapid and requires regular reassessment. Vegetation in Ambergris Caye has declined by 10.9% over the period from 2000 to 2017, while urban areas increased by 39% (Sweetman, et al., 2018). Such substantial land use change transforms the function of the coastal band. Satellite imagery facilitates numerous reassessments to compensate for these changes using a weekly acquisition of imagery. These rapid changes may suggest a relevance for the inclusion of a change detection product in the CVI, as opposed to a singular classification model, to determine the areas of the coast experiencing the fastest habitat loss. Although substantial change can be observed over terrestrial areas, these changes were not observed in marine reserves and suggests the success of MPAs as a management approach to limit degradation.

Table 15 shows the differences in the estimated area covered by each class from the three models and highlights the disparities to the degree of protection estimated. The different resolutions and class distinctions of these studies will be a contributing factor towards this. The RF classification models produced in this thesis have provided an updated assessment of coastal habitat condition with a substantial accuracy. In the case of benthic assessments, the quality of models has improved upon those from existing studies. This product can be used within the CVI or independently to support policy development and supports the value of habitat protection in addition to providing assessments for development opportunities in the Blue Economy.

Table 15: Comparison between Random Forest classification of Sentinel-2 against existing terrestrial and benthic maps for Belize.

Class	Copernicus Global Land Service		National Marine Habitat Map		Random Forest Classification (Sentinel-2)	
	Area (km ²)	%	Area (km ²)	%	Area (km ²)	%
Urban	14.23	2.0	N/A		45.82	8.1
Mangrove	23.59	3.3	N/A		131.25	23.2
Mudflat	371.07	51.2	N/A		287.84	50.9
Forest	296.90	40.9	N/A		68.10	12.0
Water	N/A		1,458.71	37.2	1,433.55	40.8
Coral	N/A		301.35	7.7	203.17	5.8
Sand (algae)	N/A		60.29	1.5	749.81	21.3
Substrate	N/A		523.99	13.3	589.76	16.8
Seagrass	N/A		1,572.51	40.2	537.96	15.3

9.1.2. Marine slope component

Traganos et al. (2018) suggests the accuracy of SDB models should be in the range of $\pm 3\text{m}$ and can be reduced to 1.5m through training data. The SDB models produced in this study meet this criterion up to the 10m contour; after which the IQR increases. However, these results do not meet the hydrographic standards (S-44 1b) for use in navigation as these require an accuracy of $\pm 0.5\text{m}$. Figure 45 illustrates a higher RMSE in deep water areas and indicates the underestimation of bathymetry here. Such areas should be masked from the final model to remove erroneous values. This approach is well suited for the sampling of coastal conditions within a kilometre of the shoreline as often these depths are shallower and will not exceed 5m . Depths of this magnitude provide lower uncertainties in SDB metrics.

ENCs have been used to provide reference for the calibration and validation of SDB models. There is good agreement shown between shallow water pixels and existing chart coverage. However, these observations should be taken critically as charted isobaths are difficult to validate against since these prioritise the reduction of grounding risk and therefore are depicted to be shallower than the true depths. More accurate validation should be performed with raw survey data. Furthermore, these charts are outdated with 48% of the country without systematic

survey data (figure 60). Charted coverage is not complete due to a limited ability to survey with echo sounders in shallow water; only the approach channel to Belize City and the southern inner channel are surveyed to modern standards (IHO, 2022). SDB models have allowed the first full coverage indication of bathymetry to be produced for the country. A robust, physics-based indication for bathymetry can now be provided for the 90% of the coastal zone which is not currently represented. This EO-based approach provides merit for the use in increasing the percentage of surveyed coverage.

Although, ENCs present limitations in their capacity for integration in SDB workflows, these represent consistent datasets which cover most of the globe. New models can be trained using ENCs with a consistent systematic bias to update outdated charts or supplement survey information in areas where this is absent.

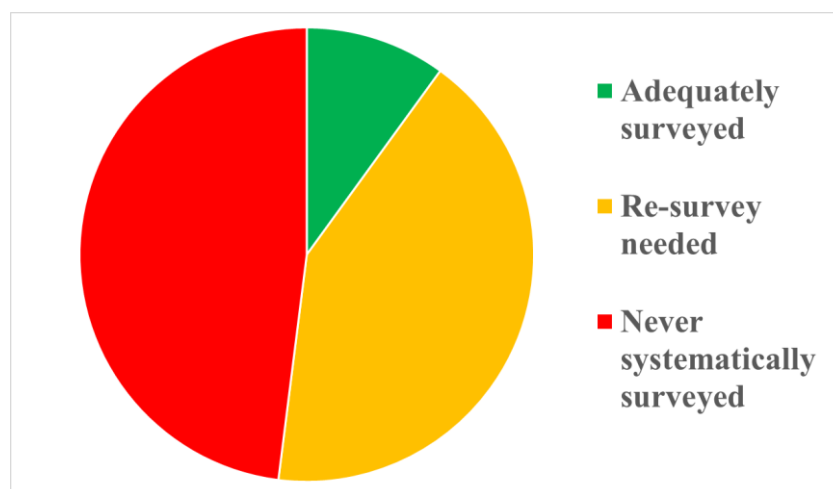


Figure 60: Percentage of existing bathymetric survey coverage for Belize (IHO, 2022).

The uncertainty in deep water provides an indication for reliable cut off depth for light attenuation; although this is seen to occur above 15m and is significantly outside the range of values seen in coastal samples. Hence, these uncertainties have minimal impediment to vulnerability results. After the 15m contour, figure 45 demonstrates an under representation of depth after this point. Traganos et al. (2018) suggests a cut off depth from Sentinel-2 occurs at 30.2m; almost double that seen in Belize. However, the observed attenuation of light is dependent on locality and environmental factors. The effect of turbidity, dissolved organic matter and clouds can all act to obscure the visibility of the water column. In the case of Belize,

suspended sediment plays a significant role. Through the application of the light attenuation curve and inherent optical properties (IOPs) of the water column, a Depth of Penetration (DoP) assessment can calculate the theoretical cut-off threshold after which the reflectance signal will become largely attributable to noise. This has been used as a supplementary method to SDB to provide validity as to whether the predicted depths fall within the feasible range based on the transmissibility of light in the specific IOP conditions present in each image (Louvard et al., 2022).

IOPs and clarity of the water column are closely linked to image quality. Figure 43 shows the high variability to transects and dependence on the quality of image used. Sentinel-2 provides the opportunity to exploit a large repository of images occurring every five days and increases the chance of acquiring images which reflect the best conditions. This is especially prevalent in areas limited by weather and hydrographic conditions. The diversity of conditions in Belize is shown in figure 61; cloud cover is a significant limiting factor in the regular acquisition of images and is often not absent. This can result in gaps to coverage if only one image is analysed.

Limited studies have utilised multi-temporal satellite images in SDB. These models are disadvantaged due to the loss of data from clouds and sediment. This study has supported the work of Caballero and Stumpf (2020) who show how merging analysis from multiple images provides a robust approach for the elimination of outliers. The RMSE of SDB was reduced by 12.4% through merging individual models. Sagawa et al. (2019) suggest the number of data points per pixel reduce missing or erroneous data. In this study, each pixel considers an average of seven data points and allows for erroneous results to be discarded. This is especially valuable for the highly variable range seen in deep water areas. The merge approach can also reduce changes to water column turbidity over the time-series and improves bathymetry by providing a considered assessment to the range of depths quantified. This is seen in the depth profiles for the northern lagoonal area. As such, the potential for application in both case 1 and case 2 waters is demonstrated.

Although uncertainty has been reduced through merging the time-series, errors are still present due to turbidity and are likely contributors to the high RMSE. Localised turbidity can be seen with sediment plumes observed at the mouth of Belize River and the lagoonal area behind Ambergris Caye. In these areas, it is a rarity that the seabed is not completely obscured. Areas of sustained sedimentation present shallower depth estimates than reality due to the obscured

seafloor and is prevalent in DTM to the west of the approach channel. More images should be used in the merge process to mitigate these anomalies.

Sentinel-2 images were acquired during the dry season (occurring September to February) which does not coincide with the hurricane season. This suggests the method is limited in its assessment for the derivation of bathymetry as this is likely to change immediately after a storm event due to re-suspension. It will be difficult to assess bathymetry immediately after a storm event due to sediment in the water obscuring the seabed and an increased prevalence of clouds. In these circumstances active sensors should be used for the derivation of bathymetry; these include promising new methods of satellite lidar bathymetry (Schwarz et al., 2019).

In order to transfer this approach to SDB globally, a consideration should be made as to the sensitivity to bottom habitat variability. Within the model inversion analysis, an endmember seabed reflectance model is included to characterise the natural reflectance observed by variations to benthic types. As SDB relies on the relationship between pixel brightness and estimated depth, variations to bottom types can influence the depth modelled (Hedley et al., 2009). Input reflectance spectra will be different for climates around the world. In several localities in Belize, the bathymetry has been observed as deeper than validation chart data. These have occurred in areas where bottom constituents are darker, rocky areas and hence led to over-estimations of depth. Observations of this nature indicate their importance in SDB modelling and show a need for benthic characteristics to be considered on an individual site basis.

Westley (2021) argues that the use of VHR imagery is beneficial in SDB assessments, however, model quality can be adversely affected due to the low signal to noise ratio. This increases the impact of anomalies such as ocean glint. Commercial VHR imagery is expensive and provides a relatively poor frequency of acquisition which is not suited for the regular and cheap monitoring solutions beneficial to coastal management authorities. Sentinel-2 has been presented as a viable alternative through the improved propagation of noise and uncertainties through merging multiple models.

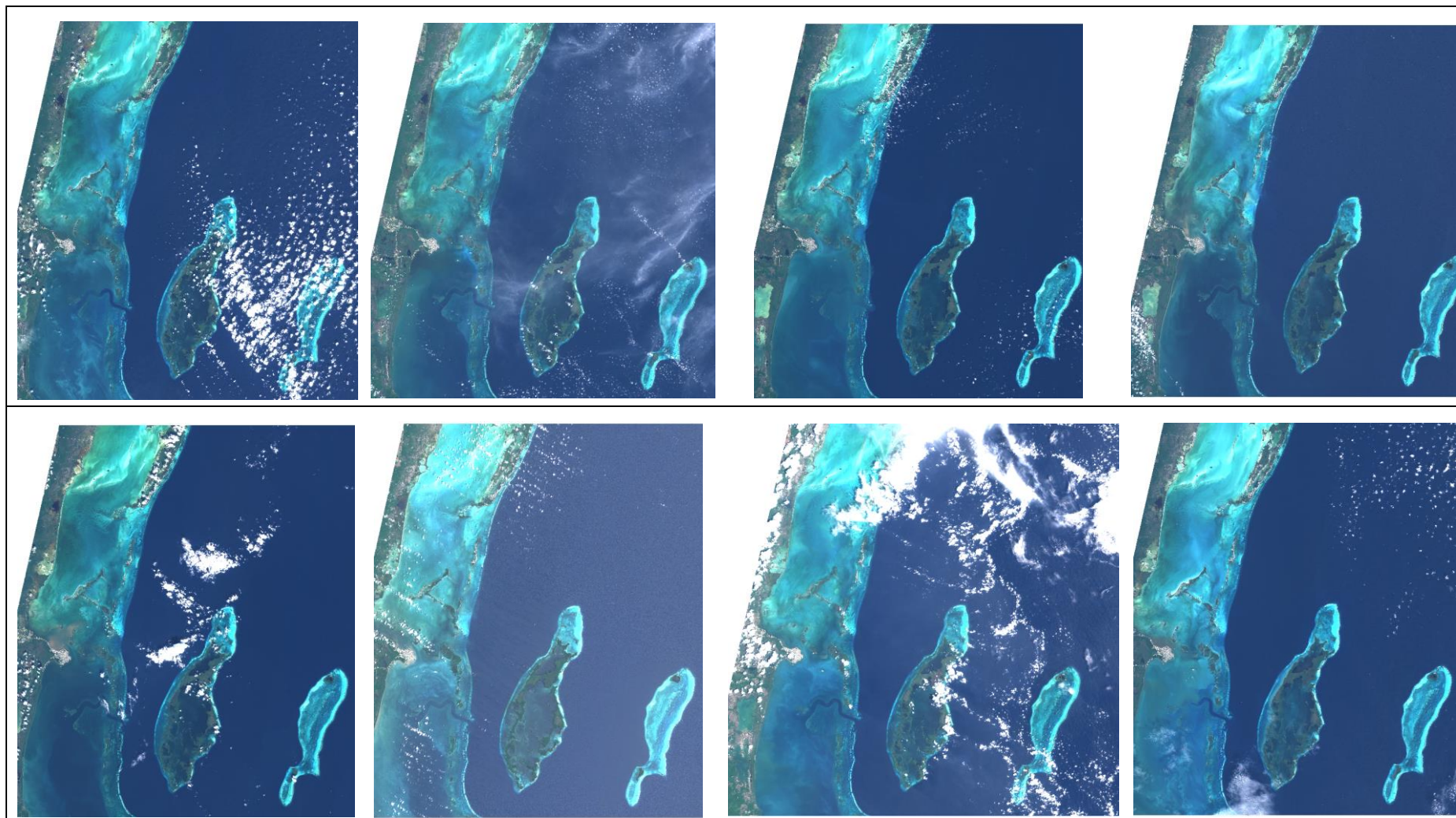


Figure 61: Quality of Sentinel-2 imagery. Note the presence of cloud cover, glint, suspended sediment and sediment movement.

An open-source archive of imagery presents a regular approach for time and cost-efficient seafloor mapping. Although not up to S-44 charting standards, this method is accurate and provides a valuable approach to indicate bathymetry in areas devoid of previous survey information. These models can be used to determine precise geographical regions which require further surveying at a higher vertical accuracy. The facilitation of more precise survey designs from preliminary SDB models will significantly reduce the cost required for surveys (Chenier et al., 2018). Standardizing this approach will allow for monitoring of seasonal or decadal changes across localised or global scales to provide quantitative indicators for use in effective management. It is preferable to derive this parameter directly over secondary sources, such as the GEBCO Seabed 2030 dataset, as these open access data archives are limited by a 100m resolution. This is well suited to unaltering deep sea regions but not sufficient to capture the complex nearshore bathymetry and will become dated in areas experiencing changes to their seafloor.

9.1.3. Terrestrial slope component

ASTER represents a widely used DEM with a robust accuracy providing better results than previous SRTM studies. However, Zhao et al. (2011) show the ASTER DEM demonstrates a negative bias for flat regions. This bias should be assumed negligible as the vulnerability assessment is looking at relative risk along the coast. Hence, the effect of which will be uniformly experienced. In coastlines with varied topographies, it is suggested to improve accuracy through the addition of the mean difference between SRTM3 and ASTER (Pakoksung and Takagi, 2021).

The elevation derived shows Belize to have a flat and low-lying topography. An infrequency to variability in conditions along coastline suggests that terrestrial elevation does not hold a vast contribution over the relative vulnerability as most areas will be affected to the same degree. The difference is the distance over which the low topography extends inland. This factor is not adequately covered by 1km coastal sample grids – despite these sampling strategies being a popular choice in studies seeking to evaluate flooding. Topography should be considered alongside offshore coastal slope in Belize as this is shown to vary significantly along the coast.

Although all areas can be seen to be low-lying, the impacts of such are not proportionately distributed. Anthropogenic activity acts to compound these flooding events by increasing

impermeable surfaces. This further supports the need for multivariate consideration. Tourism provides the central industry of Belize with 94% of resorts found within elevations of less than five metres (CZMAI, 2014). Analysis of land use can highlight areas of significant development to contextualise disparities to elevation risk. Areas of lower elevation are often coincident with areas of mudflats and mangroves identified in the RF classification. Cissell et al. (2021) suggest mangroves are often present in low lying areas and are regularly inundated. This multi-faceted nature of vulnerability demonstrates the importance of an integrated approach.

9.1.4. Wave climatology component

Systematic errors in WEVERYS data are well characterised in literature, including the under-representation of SWH (Timmermans et al., 2020). This analysis will focus on the pre-processing and data aggregation methods in extracting meaningful trends from the WEVERYS data used. It is important not to omit wave data from vulnerability assessments due to their ability to influence inundation. Hence, the limitations of the data must be fully established.

The WEVERYS model provides data on global wave climate and is well suited for analysis of patterns at a global scale but this resolution severely impedes the assessment of wave climate at regional scales. Data is provided in the global projection system UTM WGS 1984 and requires reprojection for integration with local datasets. Inconsistencies in the CRS of input layers will introduce bias in model outputs (Cao, 2017). The process of reprojection will always cause distortion at local scales due to the imposition of a 3D spheroid on a 2D plane.

Moreover, the coarse spatial scale of 20km presents a high variability in conditions within pixels. Data coverage does not extend to the coastline and thus the narrow shelf around the coastline is not adequately characterised. This compounds an underestimation of wave climate and is exacerbated by interference in altimeter readings from the disparity between the reflectivity of land and water. Resampling of data was required to provide an indication of conditions along the coast and will not accurately reflect true conditions in these areas.

Figure 50 shows good agreement with wave buoy measurements but this is valid for deep water conditions and not in the coastal zone. To refine the use of satellite derived wave data in localised studies, region specific models should be implemented; although the availability of which are sparse. Recent techniques have been proposed for deriving wave heights directly

from SAR imagery and would provide the most accurate and up-to-date localised wave assessments (Pramudya et al., 2019).

Finally, a temporal resolution of 3 hours is the highest resolution of all the parameters evaluated; this results in large volumes of data. Aggregation techniques have been critical to subsample these datapoints and establish trends at a relevant resolution.

9.1.5. Wind exposure component

Northern areas are the most vulnerable to high winds with the most exposed regions occurring above 18.1 degrees of latitude in the CVI model. Despite only demonstrating a difference of one Saffir-Simpson class, there are distinct differences to the degree of impact between classes. Devastating damage, including uprooted trees and roof tiling removed, occurs for class three. While catastrophic damage – with homes sustaining severe damage, most trees uprooted and widespread power outage – occurring for class four. Table 16 shows the disparities between surge extents for each hurricane category. A category four hurricane is likely to provide a 25% greater storm surge than category three and ability to flood an increased elevation inland. This would suggest Ambergris Caye is substantially more vulnerable to hurricane-induced flooding than the rest of the coast. A category three hurricane could have capacity inundate the whole of San Pedro to the top level of single storey buildings.

Table 16: Hurricane storm surge extent for Belize City (NEMO, 2003).

Hurricane Category	Storm Surge (metres)
3	4.1
4	5.5
5	7.4

Hurricane Earl struck Belize City in 2016. By the time Earl made landfall on August 4 2016, the depression had been degraded to a category one – the class demonstrating the lowest wind speeds. Despite this, Earl produced the most significant hurricane damage in ten years. Turneffe Atoll experienced surge heights of up to 1.8 metres which also impacted the northern areas of Belize City and Ladyville. In the north, lower surges of 1.22m were experienced (NEMO, 2016). These observations suggest that the incidence of hurricane events are not

proportional to the severity of impact. The UNEP dataset will provide merit to illustrate the disproportionate effects of windspeeds along coastline.

This is supported by observations by Markert and Griffin (2014) who suggest east coast of the Yucatán Peninsula – primarily Belize – is at the greatest risk of experiencing hurricane hazards (figure 62). These areas occur in the north of the peninsula and coincide with the strongest observed hurricane wind speeds.

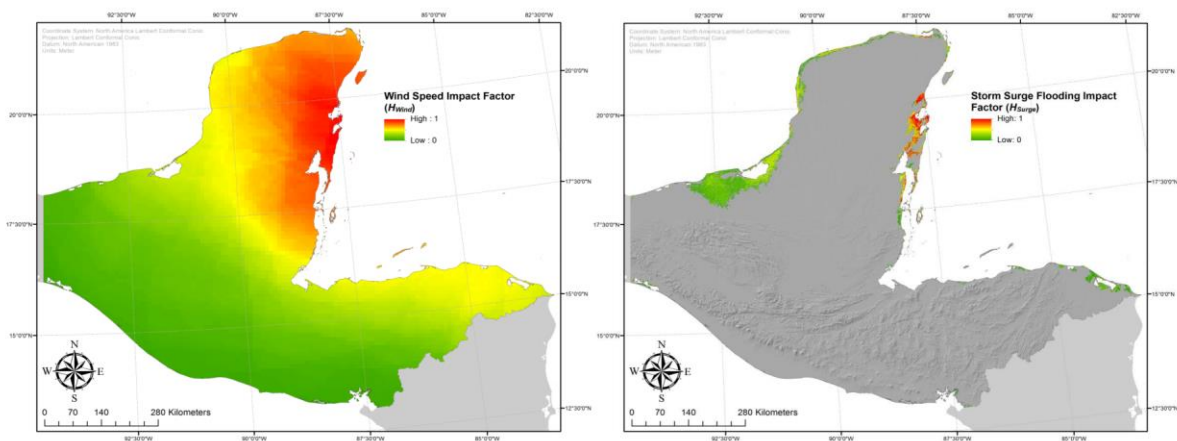


Figure 62: Distribution of wind speed and storm surge flooding impact (Markert & Griffin, 2014).

The impacts of Hurricane Earl (2016) suggest the Saffir-Simpson scale is a poor metric for the distinction of vulnerability. This metric quantifies the magnitude of wind speed and assigns this to a discrete class based on the properties observed. Therefore, the specific windspeeds are not retained and an indication of the broad class range of values is given. These classes have finite boundaries. Hence, consideration of values at the boundary between classes can result in a significant jump in perceived risk due to a windspeed difference of one mile an hour. The jump in category will show an increased vulnerability when the intensity is not excessively dissimilar. Without the provision of exact wind speeds, it is difficult to differentiate areas of coast within the same class. This covers most of the study area. A poor distribution of classes in Belize – only across two groups – presents large incremental distances with the ability for a high degree of variation within each category.

Uncertainties are also presented by the generalisation of trends at the coarse resolution of the dataset. The spatial resolution of the UNEP dataset does not provide sufficient clarity to discern the true intensities of wind speed along the coast. The localities induced by meso-climates will not be captured and may be impacted through the effect of complex topography (particularly prevalent from Maya Mountains).

On the other hand, an incorporation of windspeed analysis at a coarse scale increased the computational efficiency of clustering. The grouping of five distinct classes in the Saffir-Simpson scale makes clustering simple as these are naturally reflective of the five vulnerability groups required for the CVI. A trade-off has been made between a sufficient resolution to discern changes accurately and processing time through suggestions from Phinn et al. (2010).

Moreover, the highest magnitude windspeeds are saturated. Despite the actual maxima, a hurricane will be classed category five if it exceeds 156mph. This applied to thirty-seven hurricanes between 1851 and 2022 (with windspeeds up to 190mph recorded). This broad categorisation undermines the impact of the most severe events. More rigorous validation of this dataset would be required with in-situ wind gauges. Through the extrapolation of directional data from local weather stations, the variation of frequent exposure to anomalous wind speed by direction could be determined.

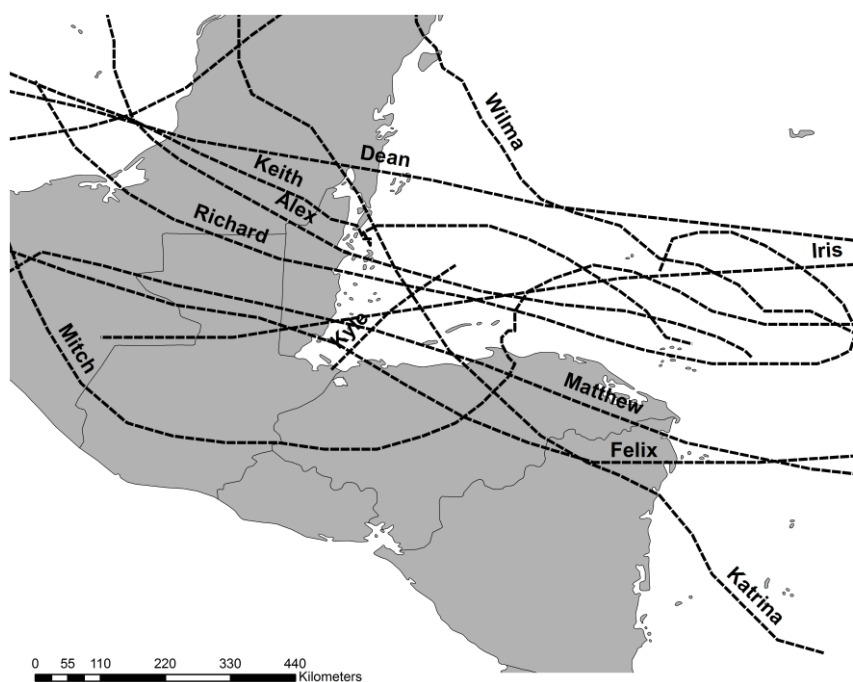


Figure 63: Tracks of historical hurricane events.

Furthermore, average hurricane wind speeds seek to compensate for a lack of sufficient local wind data to simulate these events at the coasts. Reanalysis models help to fill these gaps by analysing events over a two-hundred-year period. The average metric used in this dataset, however, provides an equal weight for each hurricane event and does not consider the incident direction. These will likely change with each pass. Through ignoring directionality in a modal model, the disparity of impact severity from different trajectories is not represented. Figure 63 shows that more hurricanes are impacting the south – although, the Saffir-Simpson scale suggests the severity of each is lower. With more incident tracks occurring in the south, there is more influence from erroneous events which can skew the average.

As a result, the consideration of the frequency and intensity of hurricane events should also be made. Through the effects of Hurricane Earl, it can be seen that category four winds are not needed for a damaging storm surge. Repetitive wind damage at lower exposures may provide just as significant influence on vulnerability as the magnitude of the event itself. For example, forests will adapt to disturbance through changes to species composition – this is a long-term recovery and varies greatly between species. Continual inundation will impede this process. In future studies, directional data should be extrapolated to add a weight to each event based on the direction and frequency at which strong winds are recorded.

9.2. Uncertainties in the approach to modelling

9.2.1. Clustering

Individual errors in each method of component derivation are compounded when aggregated into the CVI. For example, the classification accuracies of 70.4% and 61.1% and the RMSE of 4.88m in SDB measurements demonstrate errors to the derivation of conditions on the ground. These uncertainties will propagate to produce a conflated cumulative error for vulnerability in an area. Boumboulis et al. (2021) suggest methods for mitigating these satellite inaccuracies in coastal studies through the synergy of high-resolution satellite imagery and aerial photos. This approach has provided accurate results. One aerial flight will save six days of field survey (Mumby et al., 2004) – this still presents a considerable cost saving approach in addition to satellite imagery.

The spread of data values can influence the degree of effective clustering. In the case of the DEM parameter, very little variation is observed between cluster one and two and for groups three to four in wave climate. This implies a poor separation of classes and a degree of overlap between these categories. The number of classes have been dictated by the CVI method but five groups may not represent an appropriate number of classes for every dataset. Some parameters have a small variation to data values and are not well separated so the imposition of five groups in this range may relate to little actionable differences to vulnerability. It is important to ensure these subtle variations are adequately characterised as Lionello et al. (2021) show that a difference in 0.5 metres elevation can impede the inundation of small magnitude surges. Observations of this nature are especially useful in areas with uniformly low topography as there is a lack of data objectively dividing the range of elevation into five vulnerability intervals (Sekovski et al. 2020).

Furthermore, Rathore et al. (2018) shows that suboptimal results will be produced if the number of clusters defined does not sufficiently split the group. A much larger spread of values is observed for SDB than the DEM parameter; these are shown to be a highly skewed distribution due to the substantial jump in values at higher vulnerability groups. Rueda et al. (2017) suggests this should be compensated for through a box-cox transformation to normalise the data set – this will give all variables an equal weight despite their variation. However, the deterministic classification produced remains able to demonstrate the variability to parameters influencing storm surge risk at large scales.

In some cases, the maxima of cluster centroids occur at values significantly less than the maxima recorded in satellite-derived parameter maps. For example, the maximum SDB cluster centroid occurs at 7.384m whereas the maximum recorded SDB was 28.1m. This suggests that the coastal sample is too small to sufficiently capture the offshore topography or that these deep-water pixels have been saturated by shallower water across this sample size. This is especially prudent to areas of the coast with steep shelves near the shore.

The use of discrete classes for the geomorphology parameter will also present another source of bias. This is because clustering is based on the proportions of classes rather than continuous values. Through assigning a singular vulnerability score based on predominant land cover types will undermine the actual diversity present. This will conversely impede the assessment of coarse datasets, such as wave climate, due to the oversimplification of conditions. Therefore, higher resolution datasets are going to have more significance in determining the spread of variability along the coast in the final model. Errors in the characterisation of these parameters would result in substantial inaccuracies in the CVI model.

Furthermore, satellite data is limited by the capacity to describe observable spatial information. Earth Observation cannot directly provide value for the cultural or socioeconomic considerations pertinent to vulnerability. These are also not considered within the CVI framework. Impacts of this nature include the number of people affected or economic costs to damaged infrastructure. Satellites can use proxies such as housing density to provide indications for these issues but are not measured directly. This is a major constraint to CVI studies (Fernández-Macho et al. 2020).

Sustainable development will benefit from a detailed analysis of the degree of vulnerability with respect to a range of anthropogenic activities taking place in these areas. These limitations should be considered through incorporating additional indices which are able to represent complexity of the coastal system with a socio-economic focus. These should be utilised through the modification of the existing CVI equation to encompass parameters representing socioeconomics (Özyurt & Ergin, 2010). Understanding this will help to structure this research in the context of human resilience; a factor of interest to ICZM.

In the individual component maps, wave height can be seen to be greatest in Belize District North. As this is an area to the west of shelter provided by Ambergris Caye, such an observation seems illogical and reinforces the inconsistencies with sampling wave values from offshore at a twenty-kilometre resolution. The wave climate associated for this region will be unaffected

by these changes to coastal morphology. Directly adjacent to this region is the lowest wave climate cluster. This rapid gradient change suggests limitations to the clustering of waves. This parameter presents the most dimensional class with eighteen dimensions of feature space due to the sampled time series. A high dimensionality is indicative of the Hughes Phenomenon (Hughes, 1968). Clustering accuracy has been reduced due to an increased complexity providing a reduced separability of points. To reduce the influence of this phenomenon, the application of data normalisation should be applied prior to KMeans. Self Organising Maps (SOMs) have been suggested as an effective approach to extract patterns of high-dimensional data and identify correspondence between parameter values (Calil et al., 2017).

9.2.2. Scale

The Modifiable Areal Unit Problem (MAUP) represents a biasing effect occurring from the imposition of arbitrary units for spatial sampling of continuous geographic phenomena. Each continuous parameter has been generalised through the imposition of pixels or mapping units from satellite data. This aggregation of spatial patterns will produce conflicting results depending on the scale at which areal units are analysed (Dark & Bram, 2007).

Moreover, the division of coastlines into grids is a regular assessment approach to provide optimal results for vulnerability mapping (Cui et al., 2018). For example, Koroglu et al. (2019) used units of 1km grids, Abuodha and Woodroffe (2010) used 1.5km grids and McLaughlin and Cooper provide the CVI over 500m samples. Through the grouping of data by artificial boundaries, each study has yielded significant analytical differences.

Ecological zones are much larger than the grids sampled in this study and likely modulate patterns due to processes acting at different scales. The ability to identify significant differences in environmental conditions is a problem of the working scale. Changing the Euclidean length of samples will omit detail for coasts which exhibit irregular or highly variable shapes (Kovaleva et al., 2022). In this study, a 1km sample was kept as the most appropriate scale to provide scalability for this approach and mitigate the irregular fractionation of the coast.

However, this sample only considers an area of the coastal zone covering the closest 1km to the shoreline. This fails to capture the significant processes which occur in the offshore region and results in generalisation of the coastal zone. Juanes et al. (2016) suggests the measurement of variables up to 5km offshore demonstrate appropriate coastal conditions. The sampling of coastline segments could be modified to make best use of the 10m resolution of Sentinel-2

through a transect based approach to aggregation. This would encompass a 5km transect of pixel rows extending landward and seaward of a point on the coast to characterise the range of conditions present in the coastal zone. This approach is currently limited by the poor spatial resolution of wave climate datasets used in this study.

These observations highlight the disparities between the InVEST and KMeans models due to different resolutions of the studies. In the context of vulnerability studies, an insufficient scale derives generalisations which leads to inadequate or unnecessary responses detrimental to the ecosystem. Ju et al. (2021) suggest using a semi-variogram modelling approach to determine the optimal scales for interpolation of regional patterns as there are no single scales suitable for all requirements. Scale will provide a reflection of management priorities and can impact the influence of individual variables depending on the magnitude employed. This is limited by the sample length of the coastline and processing capacity.

Scale and resolution are intrinsically linked. The CVI provides a useful first pass at national scale assessments where uncertainty will result from the low resolution of spatiotemporal data. Datasets with a coarse resolution, such as the globally averaged wave climate, will not provide enough clarity to elucidate changes at local scales. A priority should be the downscaling of global climate models and increasing the modelling accuracy of SWH in coastal regions. This will be prudent for more-rigorous localised assessments to be performed in areas identified as being more vulnerable than average by the CVI – especially if there is a potential high risk to communities (Lopez et al., 2016).

9.2.3. The CVI approach

Limitations with the broader CVI method have been well outlined (Roukounis & Tsihrintzis, 2022). The CVI represents a synthesis of constituents within dynamic and complex coastal interactions. Limiting the inclusion of only geotechnical variables within a geometric mean provides an excessive generalisation of these processes. Although this study has quantified individual processes, the interaction between which has not been demonstrated. This acts to artificially deflate the degree of relative vulnerability in an area. These are ancillary at the regional scales used in this thesis but will have significant influence for localised studies.

Parameters are afforded equivalent weighting irrespective of their variation or parity for impact to vulnerability. In the case of this study, the model is biased towards the parameters with the finest spatial resolution due to their higher degree of variability across coastal grids. Increasingly, a weighted approach to CVI is being implemented (Boumboulis et al., 2021). The significance of each variable's contribution to vulnerability should be reflected using the Analytical Hierarchy Process (AHP) and weighted accordingly. The focus of the model should be rigidly defined as conflicting focal points will influence the weighting of parameters and the thresholds of vulnerability groups in each parameter.

Despite the introduction of new objective derivation techniques, qualitative measurements persevere in the model. This is primarily demonstrated by the geomorphology variables. Qualitative assessments limit the ability to quantify the role of an individual land cover type in modulating coastal hazards. Therefore, the assumption has been made that segments which are characterised by the same geomorphic clusters will behave in a similar way. This may not always be the case. Analysing on the proportion of the coast consisting of a particular habitat ignores the essential consideration of the degree of protection provided by healthy, functional habitats.

The volume, density, quality and fragmentation of the habitats will also provide capacity for inundation protection and are not considered in this study. Degraded ecosystems are likely to provide reduced ecosystem services to the efficiency assumed in the model. This includes a reduced capacity for modulating wave run-up which alters vulnerability and is especially prevalent for Belize. Cherrington et al., (2020) have shown how the deterioration of mangrove habitats impedes their capacity to prevent marine ingress.

There is a lack of observational data for the assessment of current storm surge hazards. A deficiency in observations limits the calibration of the model. Jevrejeva et al. (2020) suggest a relationship between model performance and the extent of observation gaps. Although limited for calibration, this CVI model helps to compensate for these gaps through an automated approach to parameter derivation using satellite images to provide continuous records quickly and efficiently. In addition, multiple images from the Sentinel-2 time-series were utilised in parameter derivation. This has represented the modal conditions present in Belize as opposed to the direct response to an individual event. This could be done through using specific images before or after an event to qualify change.

9.2.4. Component assumptions

The selection of parameters used to populate the index is subjective and the way in which parameters have been considered can produce conflicting results (Koroglu et al., 2019). Balica et al. (2012) posits that fewer variables are less reliable than more thorough inclusions to the CVI. This is because large variations in a single parameter are likely to produce significant influence on the final calculation. Moreover, Del Río and Gracia, (2009) suggest an approach with fewer variables will reduce redundancy if closely related parameters reflecting equivalent processes. In this study, only seven parameters were used based on those identified by Gornitz (1994). The number of parameters were limited due to the aim of providing an index which had a wide application and performed in conditions which might be different and should be updated easily without extensive survey campaigns (Villa and McLeod, 2002).

Although the number of parameters has been limited, the consideration of how each component has been perceived to modify vulnerability remains an area of potential uncertainty due to the subjective nature of the analysis. Micro-tidal forces in Belize, for example, have been deemed to present a high vulnerability due to the sea level always residing close to the high tide line (Thieler and Hammler-Klose, 2000). This is opposed to the traditional low vulnerability assigned to these areas by Gornitz. Pendleton (2004) suggests this state of tide means flooding is more likely to occur during storm surge. Since this study has a focus on vulnerability against storm surges in particular, the tidal forces have been considered as high-risk.

Habitats provide essential protection from coastal flooding; the degree of which is dependent on the target of the vulnerability assessment. Mangroves and coral reefs have been determined to provide the most protection from hurricanes. This contrasts with the original Gornitz assessment. This decision was made as De Dominicis et al. (2023) suggests that mangrove forests placed in front of coastal protection structures reduce the risk of overtopping and wave impact allowing for lower construction costs. However, these areas are delicate ecosystems and can be deemed to be the most susceptible to damage and degradation. A small alteration to their conditions or a significantly strong storm event can destroy the functional habitat – even if the ingress of water inland is reduced in the process. As the focal point of this study is the vulnerability to coastal flooding and not ecosystem health, these areas have been deemed to be the least vulnerable.

The comprehension of coastal slope has also deviated from the original comprehension. Gornitz suggests that shallower gradients present a higher degree of risk. In this study, the steeper gradients associated with the offshore coastal shelf have been deemed to provide the highest degree of vulnerability. Adams et al. (2002) show how the process of wave shoaling on steep continental shelves can result in an increase to wave amplitude as water propagates from deep to shallow water. This wave height is moderated significantly by tide and surge level. Shallower areas have been associated with the dissipation of wave energy due to bottom drag and wave breaking. As a result, these areas have been presented as a lower vulnerability.

Furthermore, Gornitz suggests that elevations lower than five metres are at a very high risk of flooding. This represents a significant proportion of the coastline. As this is the minimum threshold in Gornitz study, the entire coastline of Belize is characterised as the highest risk from elevation and does not help to identify areas which may be disproportionately susceptible. Although the terrestrial elevation is low, variations to topography are still present along the coastline. Therefore, there is a requirement to subset the highly vulnerable (<5m) vulnerability threshold defined by Gornitz to provide specific and actionable groups. Although these will vary across small scales, topographic changes will still present significant disparities. As a result, the consideration of actionable topography classes in the CVI assessment are required and are facilitated by KMeans.

10. Analysis of vulnerable areas

Vulnerable hotspots have been identified in the KMeans CVI model and the distribution of these areas has been discussed in the following section. This analysis aims to provide justification for the observed distribution through a contextualisation of results with wider coastal practises and provides the foundations for identifying issues or useful management practices.

Marine Protected Areas (MPAs) are shown to be coincident with areas of low vulnerability, including the Hol Chan Marine Reserve. Protecting marine habitats can enhance positive feedback to the wider coastal zone through provision of services including the protection of critical habitats and preservation of biodiversity which restricts the transmission of forcing factors. MPAs are vulnerable to anthropogenic exploitation along the coastline and demonstrate the connected nature of the coastal system (Cicin-Sain & Belfiore, 2005). The correlation between MPA location and low CVI values suggests the protection of coastal areas should be integrated into management strategies over large areas and embedded within integrated coastal management (ICM) strategies. Pressure to develop protection for more vulnerable areas of the coast could jeopardise productivity of MPAs and threaten the protective value they provide. Therefore, the linkages between MPAs and the extended coastal zone should be maintained and enhanced with institutional policies. It is essential for effective ICZM to incorporate the coordination of policies and strategies to develop productive relationships with those that have a stake in the conservation (Maguire & Fletcher, 2012).

Murray (2021) suggests an interdependence between sustainable coastal management and tourism in Belize leading to a conflict of management priorities. The Hol Chan Marine Reserve has become self-sustaining due to the implementation of a decentralised management approach funded entirely through tourism visitor fees. Paradoxical agendas exist between the maintenance of coastal protection and exploitation of tourism with the MAR representing the only UNESCO site in Belize so there is pressure to ensure the region retains prestige to tourists (Meskell, 2013). Tourism is the primary contributor to Belizean economic development and hence a focal point for the government (Diedrich, 2007). As a result, this can facilitate political support through pressure to increase the protection of natural areas and support the revenue accrued through tourism.

Moreover, an estimated 60% of tourists in Belize will visit Ambergris Caye. San Pedro has the highest concentration of visitor accommodation in the country with 75-80% of land purchased by foreign investors for development (Young, 2008). This region demonstrates the coincidence of severe vulnerability with high tourist concentrations. This would suggest an increased precedence for focused management in San Pedro due to the propensity for significant damage to property and livelihoods through the impact to the wider tourist economy. Scherer et al. (2014) suggest the prioritisation of coastal management should be based on the ability to solve socioeconomic problems. This is demonstrated by the significant international investment to these areas. A fine line must be struck, however, as a lack of regulation to control tourism can have adverse effects on the coastal zone in the long term. Increased development can modify land use and lead to the disruption of wider ecosystem integrity. Attention must be paid to enforcement and protection of natural resources in coastal management to ensure sustainability (Murray, 2021).

A focus on tourist areas must not come at the neglect of other areas of the coast. Caye Caulker is one of the offshore cayes which demonstrates another region of severe vulnerability due to geographic factors. This assessment fails to provide a consideration of social parameters which may act to amplify this, however. These regions are independent and self-governed islands which limit the control of tourism and discourage foreign investment. A balance between compatibility of local ideals and income diversification are inherent to the successful development of Caye Caulker. Kapucu et al. (2014) argue that resilience is high in rural regions as the maintenance of sociocultural institutions and strong community networks provide support in times of crisis. Autonomy from exploitative economies retains the control of local communities on resource production and protection and ensures these are fairly distributed across the community. This enhances the capacity for disaster management.

Bruneau et al. (2003) suggests that resilience represents the sustainability of resources through availability of alternatives. In this context, the vulnerability of rural communities is reduced as these areas have a scarcity of critical infrastructure and consistently located in highly vulnerable areas. Geographical fragmentation leads to disconnection with mainland infrastructure and access to resources is lost rapidly in systemic pressures which constrains the ability to adapt. This disproportionately impacts rural areas. Therefore, infrastructural facilities (such as increased transport networks) are an effective management strategy for these areas (Dasgupta & Shaw, 2017).

The CVI values in Caye Caulker are 48 compared with 42 in San Pedro. In rural areas, the assistance awarded per resident is often lower than that of urban areas (Seong et al., 2021) and enhances the inequality between these two regions. This is because urban areas often possess the allocation of more profitable resources and provides a higher management priority. The preservation of resources should not come at the expense of rural areas. Critical issues effecting each area should be considered alongside the intrinsic vulnerability to assist with careful prioritisation of resources to facilitate protection of people and resources (Armenio & Mossa, 2020). Resilience to natural hazards should be improved through enhancing the partnerships between urban and rural communities to aid in resource distribution in rural settings. Management authorities should consider the effect of socially disadvantaged communities and ensure strategies are accommodating of their needs. An inclusion of socio-economic variables to the CVI can incite cultural bias as these are difficult to quantify and often reflect the most developed areas (McLaughlin & Cooper, 2010). Therefore, these must be carefully chosen to characterise these discrepancies.

In Belize City, the most vulnerable segment has been shown as Sir Barry Bowen Municipal Airport. This presents an area of critical infrastructure and is highly important for transport links. Damage to critical transport hubs can directly impede the social and economic recovery of the region in a disaster (Rodrigue, 2020). Airports often provide centralised hubs for relief supplies including the delivery of food, medical and rescue services. Damage to infrastructure will result in indirect impacts including the impediment of supply chains and limits the interdependency with other nations. This can damage both the local economy and the ability to recover. This area provides a critical link to the wider area and hence is disproportionately vulnerable (Colon et al., 2021). Enhancing the resilience of critical infrastructure in severe vulnerability classes should be prioritised to ensure the capacity to restore services is rapid to cope with natural disasters.

Impacts from climate change have not been a part of the scope for this study, however, it is important to consider the additional threats these pose to the coastal zone (IPCC, 2012). These will include an increase to the frequency of high-intensity storms with rising sea-levels which provide more severe inundation risks for communities. These results provide a useful approach for monitoring of changes regularly to adapt to recurrent flooding events and mitigate the impacts through the avoidance of overwhelming critical infrastructure.

11. Supporting policy: a use in Integrated Coastal Zone Management (ICZM)?

Integrated Coastal Zone Management (ICZM) represents a governing framework to facilitate the development and management of coastal areas through an incorporation with environmental priorities and stakeholder participation. This mitigates conflicts and detrimental impediments to environmental resources.

Verutes (2016) posits that the development of an ICZM strategy in Belize has been difficult to achieve due to the absence of systematic approaches to coastal planning. The responsibility of managing the coastal region is held by the Coastal Zone Management Authority and Institute (CZMAI). Table 17 demonstrates key stakeholder considerations in Belize as outlined by CHARIM (2016). Stakeholder analysis shows that there is use for mapping vulnerability in nationalised and localised planning, emergency management and commercial concerns. Through an integration of scientific work, policy and stakeholder engagement, constructive outcomes can be achieved for each element of the management process.

These stakeholders will develop strategies underpinned by geospatial information to facilitate the implementation of individual coastal zone agendas. Cartographic data at the relevant scale will provide context on the location of resources which contribute to reduced vulnerability and necessary regions in need of planning support. There is a requirement for a centralised approach to mapping that locates spatial events with precision to assess where potential conflicts may occur. This will alleviate conflicting priorities between sectors analysing at different scales. In order to be effective in governance, these assessments must present an adequate degree of confidence resulting from high quality evidence (Azueta et al., 2020). The existing InVEST model is limited by the quality and scarcity of input data.

The current ICZM plan for Belize suggests this research is progressing but is ill-defined and not centralised (Arkema & Ruckelshaus, 2017). To be effective at national level decision making, this requires an integrated approach. The vulnerability model in this study can generate knowledge to contribute towards considerations for multi criteria decision making and provide significant parity to support sustainable development and risk mitigation. CZMAI (2016) have outlined objectives to achieve this, including: promoting sustainable use of resources, integrated development and adapting to climate change.

Table 17: Key stakeholders and relevant management issues in Belize.

Stakeholder	Information	Planning	Action
General Public	Flood awareness	Informed choices in house purchase? (general area rather than individual property level)	Community engagement and general area response to flood warnings
National and local government planning	Preparedness and resilience investment needs. National view of most likely risk	Identify new flood defence and warning schemes. Planning zone definitions.	Commission specific detailed studies in high risk areas/catchments
National and local government infrastructure	Avoidance areas for new infrastructure. Asset Management scenarios	Identify assets at highest risk and mitigation investment required. Investment in assets where economic damage is greatest	Locating and targeting post event repairs. Identify and target maintenance investment
National natural resources monitoring agencies	Sensitive regions and locations or river reaches	Identify new information, (data collection) needs e.g. gauging stations.	Install new monitoring and flood warning systems. Collect long term flood records.
National emergency management	Flood hazard communication	General location areas of evacuation centres and routes (not exact locations)	Targeting event/incident response areas
Commercial concerns (e.g. agriculture)	Exposure of existing assets	Identify less risky locations for investment	Invest in local protection/preparedness
Academia and consultancy	Areas and mechanisms to study further	Targeted research proposals. New data collection	Study, analyse, and publish findings relevant to flood risk.
Insurance	Exposure of portfolio (customers)	New markets or tailored insurance products to risk	Set premiums relative to risk

These objectives should be built upon the framework from Rosenthal et al. (figure 64, 2014). An emphasis should be placed on sustainable planning and requires an ongoing process of iteration at appropriate scales to ensure data is pertinent to decisions; especially in areas of high risk. These must also be transparent to stakeholders. Vulnerability models act to support building capacity in phase two and typically encompass a coarse analysis to understand current distributions. This can aid in the identification of data gaps or areas exhibiting strong risk for further investigation or monitoring and can be important to determine a baseline condition from which to assess impacts of storm scenarios. However, often this does not occur due to a dearth of data with insufficient timelines and budget restraints to fully characterise these. The KMeans CVI model can support this through the production of tailored reports at national and planning regional scales which can be regularly updated at a low expense (Verutes, 2016). Such a regular monitoring approach should be valuable to evaluate the impact seen in response to management strategies.

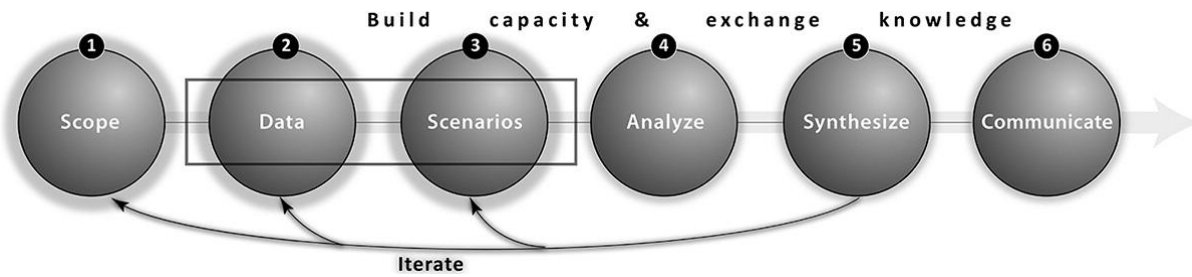


Figure 64: Iterative process for the development of management strategies (Rosenthal et al., 2014).

The economy of Belize has a dependence on environmental services present in the coastal zone which results in paradoxical agendas between stakeholders. With tourism the fastest developing industry, the dependence on the revenue generated from this grows and puts pressure on the coastal zone. This is manifested through impacts including increased development and housing demand as Belizeans migrate to coastal areas. Pressure to retain prestige to tourists results in a salient divide as politicians exert pressure for wider constitutional agendas which may be detrimental to the longevity of ecosystems (Meskell, 2013). The trevails assoicated with vulnerability can be seen as symptomatic of wider issues and discourage investment from private entities (Ablerts & Hazen, 2010). Substantial challenges can propogate from a lack of political will and a disproportionate prioritisation of economic development.

A comprehension of the distribution to vulnerability provides value in the designation of the magnitude for which services are provided by habitats. This can be influenced by the distribution of anthropogenic activities which alter ecosystem functions. New developments should utilise vulnerability assessments as a tool for determining the appropriateness of an area for development to increase economic benefits from the coastal zone. For example, development may require the clearing of mangroves or dredging of seagrass beds which exposes the area to increased wave action. This should be supported by strong regulation.

The role of ICZM ensures the protection of functional habitats through the consideration of the resources required and the proportion of a population which may benefit from development. Shoreline Management Plans (SMPs) are a technique employed to facilitate the effective use of coastal resources and are dependent on access to relevant data. In the design of SMPs, specific areas which present crucial gain for the national economy and retain a high risk to

storm surge events status could be prioritised to mitigate the degradation of the most vulnerable tourist hotspots (Brooks & Adger, 2005). Climate change will continue to increase the complexity of management with increased rates of SLR.

SMPs should not only consider economic analysis for the benefits of ecosystem services to development but also non-monetary values such as vulnerability (Spalding et al., 2014). The KMeans CVI provides value to support SMPs through a holistic consideration of the cascading impacts to coastlines. Through assessing satellite derived maps prior to clustering, these can show which areas have functional habitats that are actively contributing towards a lower vulnerability. This is evident with the identification of mangrove areas in the classifications owing to low vulnerability contributions in the final model. This is important for monitoring to avoid the destruction of functional habitats. KMeans provides a rigorous approach which is standardised and repeatable. As a result, it can be simply integrated to World Heritage processes (such as the IUCN State of Conservation Reports) and provides transparent assessments over time to assess trends. This data will be useful for a rapidly changing climate and will help make arguments for maintaining and managing coastal ecosystems.

Information on the distribution of most vulnerable areas is of crucial importance to management. Nguyen et al. (2016) show that the segmentation of coastal grids based on vulnerability is beneficial for the determination of high priority areas for resilience enhancement. Coastal managers can utilise this tool to better characterise vulnerability and define levels of risk to coastal sectors due to a clear indication of these areas. This approach aggregates multiple relevant parameters where existing CHARIM models only assess flooding with respect to elevation. Further to model outputs, a large database of physical coastal characteristics will be provided as part of this process from satellite image derivation. This data may in turn be used separately for independent coastal evaluations. Regional managers demonstrate an awareness of the cruciality of the coastal zone, although specific and simple tools are not used in the derivation of vulnerability. The CVI model developed can therefore provide a step towards a more comprehensive evaluation of vulnerability and deployed by non-experts to better regulate development in the coastal zone.

Belize is particularly susceptible to storm and hurricane hazards. The impact of natural disasters is set to become accentuated with climate change and increased rates of SLR. Disaster management focuses on short-term impacts of extreme events but also addresses long term impacts to reduce vulnerability through management. Within the ICZM strategy, the National

Emergency Management Organisation (NEMO) has the responsibility for reinforcing security and preparedness through planning initiatives. This includes empowering stakeholder's capacity to manage vulnerability and strengthen reduction information systems to reduce the exposure of new infrastructure (Azqueta et al., 2020). In order to allow sustainable development in the littoral zone, there is a need to increase the adaptive capacity of vulnerable areas (UNDP, 2022). This requires appropriate strategies to identify and reduce vulnerability.

The UNDP (2022) presents elements required for risk management, these include: anticipatory, compensatory and reactive management. Anticipatory approaches ensure development will not accentuate risk and acts to proactively reduce storm surge impacts. Compensatory approaches mitigate damages caused by existing vulnerability. Reactive management ensures vulnerability is not re-established in the aftermath of a natural disaster. KMeans CVI can support anticipatory and reactive management approaches through provision of rapid assessments that provide a high level indication of consequences. Climatic variation is diverse and subject to rapid change where frequent assessment is important. An increase with the number of assessments required demonstrates a need to reduce costs. This is especially prudent in areas where assessments may be required quickly; this could include a post-hurricane scenario or in a highly variable environment where surveys become outdated quickly.

CVI maps can also assist compensatory management through the visual communication of coastal threats to identify relative low vulnerability areas where emergency shelter could be located. These maps may also be combined with socioeconomic exposure maps to determine impacts of planning scenarios and support an integrated assessment of vulnerability (Alfieri et al., 2015).

Compensatory management tools can be used to bolster coastal protection. In Belize, the implementation of marine protected areas (MPAs) has been seen as a method for this. However, a lack of effective monitoring on ecosystem condition has resulted in a lack of understanding for the extent of habitat decline. With current rates of decline, it is arguable that the removal of the MAR from the World Heritage in Danger list was premature (Murray, 2021). Remote sensing can overcome fragmentations in sectoral management to provide harmonization of strategies. The methods suggested in this thesis can be used to construct regular change detection analysis to determine areas that are degrading at the fastest rates. These should be suggested as areas to allocate as new MPAs to prevent further destruction and enhance ecological processes.

As a SIDS, Belize is confronted with limited resources and rapid development pressures. The KMeans CVI provides a low-cost and efficient tool for coastal hazard mapping. The fast identification of vulnerable hotspots can greatly enhance the facilitation of management strategies. Remote sensing can ensure this is achieved at a high resolution (Boumboulis et al., 2021). Limiting the unnecessary expenditure of resources can be achieved through vulnerability studies. This enables the isolation of areas for which detailed assessments are subsequently required.

Coastal vulnerability assessments using remote sensing may be undertaken at a variety of spatial scales: global, regional, national, and local. The application of CVI modelling at various scales is shown in table 18. The framework demonstrated in this thesis provides a modular approach and can offer scalable solutions to different management problems for coastal nations and to meet sustainable development goals (Pereira et al., 2013). Through a range of remote sensing resolutions, this approach can provide vulnerability assessments at nested scales. Firstly through the identification of hotspots at a coarse national scale and subsequently supporting more detailed local scale studies. At macro-scales, this model can emphasise the effects of climate change to coastal communities and provide support for centralised government-level strategies. At micro-scales, the application of this model should identify specific vulnerable areas to support management authorities in the design of appropriate adaptation strategies (Torresan et al., 2008).

Application of the KMeans model to assess vulnerability over transnational scales can facilitate international cooperation in managing inter-related coastal regions (Gibson et al., 1998). The MAR extends across the meso-american countries of Belize, Honduras and Mexico. Coastal processes are not impeded by international borders and the successful management of the MAR system will depend on the consistency of initiatives between nations. This is because each individual reef is linked through bio-physical transport processes resulting in an interdependence. A holistic approach across these borders provides much more effective strategy for promoting the welfare of the entire system while reaping benefits to individual countries through enhancing coastal protection and oceanic resource productivity to fuel the blue economy. The CVI can build capacity for consistent coastal management strategies at the scale of the Yucatán coastline through highlighting priority areas and issues. There is hope to establish trans-boundary reserves linking conservation areas between areas on the coast – the CVI tool is an efficient resource to enable this.

Table 18: Appropriate scales for the application of CVI modelling (Trigg & Smith, 2016).

	Application	Scale (km ²)	Application of CVI model	Suitability	Limitations
Regional areas	National	23,000	Yes	National risk assessment.	Provides good assessment at national scale.
	Catchment	10-6,000	Yes	Identify areas with natural vulnerability.	Provides good assessment with accuracy reduced for smaller catchments.
	District	2-5	Yes	Identify specific districts vulnerable.	Provides good assessment at district scale.
	Settlement	0-22	Only largest	Identify specific settlements vulnerable.	All cities, most towns but villages too small.
Settlements	City	5-22	Yes	Which cities are most vulnerable or which areas of the city are disproportionately vulnerable.	Presence of urban artifacts in elevation models.
	Town	1-5	Only largest	Which towns are most vulnerable or which areas of the town are disproportionately vulnerable.	Small towns may not represent a full risk.
	Village	0-1	No		Not ideal at this scale as the coastal sample is too coarse to differentiate small villages.
Infrastructure	Agriculture	~0.5+	Limited	Identification of fields requiring further assessment.	General assessment of whether location is vulnerable to storm surge. Quantification of risk unlikely at this scale.
	Buildings	~10mx10m	No		Too small to be picked up by coastal sample. Could be established using Sentinel-2 or VHR images.

The goal of ICZM is to attain sustainable development of coastal and marine areas, reduce vulnerability of communities to natural hazards and to maintain essential ecological processes driven by biodiversity. The CVI has been shown to have use in supporting each of these facets. Through incorporating remote sensing and machine learning in the CVI metric, this approach provides a standardised method with ability for consistent comparison over the globe. This provides an invaluable application within ocean planning for its simple ability to integrate within existing ICZM workflows. As a result, the potential to fundamentally change coastal management in Belize is demonstrated through targeted implementation of management strategies in areas of greatest vulnerability at a low cost. Development of Belize's ICZM strategy will provide a good model for sustainable coral reef management globally due to the holistic approaches, such as those demonstrated in this study, showing clear advantages in a small country where the ability to implement management measures is simple.

12. Recommendations

An approach for multi-disciplinary vulnerability modelling has been presented in this thesis, however, further research is still required. The use of machine learning and Earth Observation have produced a robust application to identify patterns in multivariate datasets. Limitations of this approach have been highlighted in chapter nine and specific recommendations pertaining to the improvement of data quality have been suggested here. This chapter will focus on the proposition of additional studies to the application of KMeans CVI in coastal management.

Le Cozannet et al. (2020) suggest high resolution studies on coastal risk reduction are required at small scales. The current KMeans model is limited by methods of coastal aggregation and data processing. An imposition of static coastal samples has incited generalisation of continuous geographic phenomena which can result in conflicting results. Furthermore, at this 1km scale, much of the coastal zone is not considered in the vulnerability equations. Features in these regions may have a contributing effect. Resolution of assessments should be improved, especially for the use of remote sensing in localised studies. This should be achieved through sampling the coastal band using a transect-based approach as opposed to gridded 1km samples. Parameters will hence be aggregated across the foreshore at the 10m resolution afforded by Sentinel-2. In order to achieve this, higher resolution secondary datasets pertaining to wave action must be acquired. The applicability of the ESA Sea State Level 3 dataset and methods for deriving wave height from SAR (Pramudya et al., 2019) should be investigated to improve this resolution.

Sekovski et al. (2020) suggest a value to projecting models for future scenarios in the provision of evidence for proactive decision making. The KMeans CVI can be enhanced through the introduction of temporal variability and future projections. A change detection of RS imagery will provide an indication for the rates of change to habitats or bathymetry to show how land use is changing in the coastal zone. In addition, given the low-lying nature of the country, the CVI could be adapted to incorporate the RCP scenarios for global SLR rates or to include population growth metrics – factors which are rapidly changing in Belize. Hence, severity can be deduced through the assessment of CVI under two scenarios – current conditions with recent RS data and future conditions with extrapolated rates of change from time-series studies and SLR projections.

In addition to refactoring the model for use in future projections, the CVI could be adapted to provide an indication for social resilience. This will take the results from this thesis further to estimate the risk to a community in addition to its physical vulnerability. Socio-economic risks can be qualified to demonstrate the disproportionate nature of physical vulnerability. This should be achieved through the inclusion of additional metrics to the CVI pertaining to socioeconomic indicators. Hzami et al. (2021) have suggested the use of a Social Vulnerability Index (SVI) to provide a more holistic integrated vulnerability assessments. This has been combined to an Integrated Coastal Vulnerability Index (ICVI) and includes a description of socioeconomic drivers and their addition to physical vulnerability using the indicators of: land use, settlement area, transport networks and population density. These represent geospatial indicators which should be feasible to implement within the KMeans model using remote sensing assessments.

An integrated approach for CVI assessment using Earth Observation has been demonstrated for Belize. This method provides aptitude for upscaling to continental or global scales. This would be a cheap and frequent approach to ensure millions of kilometres of global coastline are surveyed to provide evidence for targeted management solutions at scale. Many coastal regions are lacking detailed information pertaining to the changes occurring in the coastal zone. Due to remote sensing variables included in the CVI, these can be produced in data-poor coastal regions, although representing different accuracies as reflected in this thesis. This would enhance the collaboration between NGOs and help consistent metrics to be adopted in reports such as the State of the Coast reports from the UN. New satellites and machine learning capabilities are in continual development so the accuracy of such assessments are only set to improve.

In order to provide evidence for such applications, the use of machine learning and EO based approaches for parameter derivation should be tested on their applicability to different typologies of coastal systems. This should include examples of different geomorphic types, underlying geologies and water column properties. Characterisation in new locations may require the inclusion of additional parameters to provide a tailored assessment (Hammar-Klose, 2000). For example, the use of shoreline change is appropriate for highly erosive coastlines and could be incorporated to the CVI model using remote sensing based approaches including the Digital Shoreline Analysis System (DSAS) (Luijendijk et al., 2018) to provide applicability in these locations.

13. Conclusions

This thesis seeks to develop and evaluate the application of Earth Observation (EO) based approaches within coastal vulnerability assessments. Specific consideration has been given to the nation of Belize to support the development of effective integrated coastal zone management (ICZM) strategies. ICZM is critical for Belize to enhance coastal protection from storm events and to encourage sustainable development. This should act to retain the conservation priorities of the region including the prestige of the Mesoamerican Barrier Reef; a UNESCO World Heritage site.

The method developed provides a modified version of the Coastal Vulnerability Index (CVI) approach. Principal modifications to the CVI include: (1) the implementation of machine learning clustering approaches to facilitate the automatic scaling of vulnerability groups for new coastlines and (2) a use of EO methods to characterise coastal geotechnical parameters. These modifications have provided a quick, efficient and regular monitoring strategy to reduce the requirement for extensive in-situ survey campaigns. This approach is simple to implement by coastal managers and does not require experienced professionals and equipment. As a result, the approach should be easy to upscale globally or to other management focuses.

Phinn et al. (2010) show the application for high resolution satellite datasets, such as Sentinel-2, for monitoring parameters in the coastal zone. Sentinel-2 has successfully provided an ability for data collection over large spatial regions with a frequent temporal extent to systematically map changes to features in Belize. The ten-metre resolution provides merit for mapping geomorphological components and a repetitive coverage is useful for the mapping of this dynamic area where surveys become dated and need updating regularly. A single image has shown functionality for analysis over a range of scales and for different applications. This data has been integrated with other supplementary layers to aid decision making with respect to vulnerability. This is more efficient than the equivalent in-situ surveys required as a prerequisite for CVI studies and to understand coastal protection. In this thesis, Sentinel-2 has been demonstrated to provide an accurate characterisation of geomorphology and marine slope parameters. These have improved upon the accuracy of existing benthic habitat maps used in Belize and, for the case of SDB, filled gaps in data coverage by producing survey results for areas which have not previously been surveyed.

Through the incorporation of KMeans, the human bias in CVI thresholding is reduced with the ability for automatic scaling. The KMeans CVI model for Belize produces significantly

improved results to that of the traditional Gornitz (1991) approach. These original thresholds suggest a homogenous risk across the coastline and are not helpful in determining the relative vulnerability of areas. Nineteen per-cent of the coastline has been assessed to retain the highest vulnerability to storm surge due to their physical geography and a seaward distribution is observed. Areas of highest vulnerability include the settlements of San Pedro and Caye Caulker; two popular and densely populated tourist areas. These areas are consistent with those identified by NEMO (2016) as areas vulnerable to the worse effects of previous hurricane events. These observations have provided a confirmation for the successful application of the KMeans CVI model in Belize.

These predictions should be improved as the model is limited by the quality and scale at which data is analysed. The use of coastal segments – of an arbitrary one kilometre – to aggregate data which does not spatially intersect imposes bias through the generalisation of continuous phenomena. This fails to capture the offshore factors contributing to vulnerability. Moreover, the use of datasets with differing spatial resolution has incited bias in the distribution of vulnerability with the highest resolution datasets having the largest impact over the degree of vulnerability in an area. This approach should be improved through two additions. The first is to fully utilise the ten metre resolution of Sentinel-2 using a transect-based approach to data aggregation. Secondly, an increase to the resolution of coarse secondary datasets, primarily to wave height, is required. This should be achieved by deriving quantities directly from SAR imagery. Higher spatial resolution data is needed to apply this method to a number of coastal processes and to transfer to new studies using different extents of coastlines.

Furthermore, to ensure the robust application of modelling, this should be applied to new coastlines with differing geotechnical properties. This study has shown how EO can provide quantification in areas with sparse data coverage but there is a need to repeat this process for an area which provides more existing data to directly validate against. This may require the addition of more pertinent parameters to the CVI such as shoreline change rates.

Machine learning and EO-based vulnerability assessments, such as that produced in this thesis, have been shown to provide a substantial role within ICZM to increase capacity for resilience. The CVI model can aid in all aspects of the UNDP (2022) framework for resilience building through anticipatory, compensatory and reactive management approaches. A provision of up-to-date information on vulnerability and contributing factors will support resource allocation and the design of holistic shoreline management plans. These are especially prevalent in Belize

due to increasing development pressures from tourism and limited resources for policy implementation. Moreover, a consistent approach acts to encourage transnational management approaches which can holistically consider the whole MAR ecosystem rather than individual regions. This is vital as the MAR reflects a dynamic and inter-related system. Consistent understanding and management action is key to avoid conflicting priorities and to maximise the effectiveness of policy outcomes. This is especially prudent with the increase to frequency and intensity of natural hazards increasing due to climate change.

REFERENCES

- Abuodha, P. and Woodroffe, C., 2010. Assessing vulnerability to sea-level rise using a coastal sensitivity index: a case study from southeast Australia. *Journal of Coastal Conservation*, 14(3), pp.189-205.
- Adams, P.N., Anderson, R.S. and Revenaugh, J. (2002) "Microseismic measurement of wave-energy delivery to a Rocky Coast," *Geology*, 30(10), p. 895.
- Ahmed, M., Seraj, R. and Islam, S.M.S., 2020. The k-means algorithm: A comprehensive survey and performance evaluation. *Electronics*, 9(8), p.1295.
- Alberts, H.C. and Hazen, H.D., 2010. Maintaining authenticity and integrity at cultural world heritage sites. *Geographical Review*, 100(1), pp.56-73.
- Alfieri, L., Feyen, L., Dottori, F. and Bianchi, A., 2015. Ensemble flood risk assessment in Europe under high end climate scenarios. *Global Environmental Change*, 35, pp.199-212.
- Andréfouët, S., Muller-Karger, F., Hochberg, E. & Hu, C., 2001. Change detection in shallow coral reef environments using Landsat 7 ETM+ data. *Remote Sensing of Environment*, 78(1-2), pp. 150-162.
- Andrés, M., Barragán, J. and Scherer, M., 2018. Urban centres and coastal zone definition: Which area should we manage?. *Land Use Policy*, 71, pp.121-128.
- Ardhuin, F., Stopa, J.E., Chapron, B., Collard, F., Husson, R., Jensen, R.E., Johannessen, J., Mouche, A., Passaro, M., Quartly, G.D. and Swail, V., 2019. Observing sea states. *Frontiers in Marine Science*, p.124.
- ARGANS Ltd., 2019. Satellite Derived Bathymetry. [Online] Available at: <https://sdb.argans.co.uk/> [Accessed 28 December 2020].
- Arkema, K.K. and Ruckelshaus, M., 2017. Transdisciplinary research for conservation and sustainable development planning in the Caribbean. In *Conservation for the Anthropocene Ocean* (pp. 333-357). Academic Press.
- Arkema, K.K., Verutes, G., Bernhardt, J.R., Clarke, C., Rosado, S., Canto, M., Wood, S.A., Ruckelshaus, M., Rosenthal, A., McField, M. and De Zegher, J., 2014. Assessing habitat risk

- from human activities to inform coastal and marine spatial planning: a demonstration in Belize. *Environmental Research Letters*, 9(11), p.114016.
- Armenio, E. and Mossa, M., 2020. On the Need for an Integrated Large-Scale Methodology of Coastal Management: A Methodological Proposal. *Journal of Marine Science and Engineering*, 8(6), p.385.
- Ashphaq, M., Srivastava, P.K. and Mitra, D., 2021. Review of near-shore satellite derived bathymetry: Classification and account of five decades of coastal bathymetry research. *Journal of Ocean Engineering and Science*, 6(4), pp.340-359.
- Aykut, N.O., Akpınar, B. and Aydın, Ö., 2013. Hydrographic data modeling methods for determining precise seafloor topography. *Computational Geosciences*, 17, pp.661-669.
- Azueta, J., Enriquez-Hernández, G., García-Flores, F. and Torres-Rodríguez, V., 2020. State of the Belize Coastal Zone Report 2014-2018. [online] Marine Conservation and Climate Adaptation Project. Available at: <<https://www.coastalzonebelize.org/wp-content/uploads/2021/02/The-State-of-the-Coast-Report-2014-2018-final-1-1.pdf>> [Accessed 27 September 2022].
- Balica, S.F., Wright, N.G. and Van der Meulen, F., 2012. A flood vulnerability index for coastal cities and its use in assessing climate change impacts. *Natural hazards*, 64(1), pp.73-105.
- Ballesteros, C. and Esteves, L.S., 2021. Integrated assessment of coastal exposure and social vulnerability to coastal hazards in East Africa. *Estuaries and Coasts*, 44(8), pp.2056-2072.
- Barbier, E.B., Hacker, S.D., Kennedy, C., Koch, E.W., Stier, A.C. and Silliman, B.R., 2011. The value of estuarine and coastal ecosystem services. *Ecological monographs*, 81(2), pp.169-193.
- Beatley, T., Brower, D. and Schwab, A.K., 2002. An introduction to coastal zone management. Island Press.
- Beijbom, O., Edmunds, P.J., Kline, D.I., Mitchell, B.G. and Kriegman, D., 2012, June. Automated annotation of coral reef survey images. In 2012 IEEE conference on computer vision and pattern recognition (pp. 1170-1177). IEEE.
- Belfiore, S., Birkmann, J., Castellan, A., Cavaletti, A., Hettiarachchi, S., Nicholls, R.J., Beirne, W., Soares, J.M.D., Stephenson, F., Trumbic, I., Villagran, J.C. and Arthurton, R.

- (2009). “Hazard awareness and risk mitigation in integrated coastal area management,” Intergovernmental Oceanographic Commission: Manuals and Guides, Dossier 5: (50):145: France, United Nations Educational, Scientific and Cultural Organization (UNESCO).
- Bender III, L.C., Guinasso Jr, N.L., Walpert, J.N. and Howden, S.D., 2010. A comparison of methods for determining significant wave heights—Applied to a 3-m discus buoy during Hurricane Katrina. *Journal of atmospheric and oceanic technology*, 27(6), pp.1012-1028.
- Benoit, G., and Comeau, A. (eds.). (2005). *A Sustainable Future for the Mediterranean. The Blue Plan’s Environment and Development Outlook*. London, UK: Earthscan.
- Bertin, X., Li, K., Roland, A., Zhang, Y.J., Breilh, J.F. and Chaumillon, E., 2014. A modeling-based analysis of the flooding associated with Xynthia, central Bay of Biscay. *Coastal Engineering*, 94, pp.80-89.
- Blagus, R. and Lusa, L., 2010. Class prediction for high-dimensional class-imbalanced data. *BMC bioinformatics*, 11(1), pp.1-17.
- Blaschke, T., Hay, G., Weng, Q. and Resch, B., 2011. Collective Sensing: Integrating Geospatial Technologies to Understand Urban Systems—An Overview. *Remote Sensing*, 3(8), pp.1743-1776.
- Bonetti, J., Fontoura Klein, A.H.D., Muler, M., Luca, C.B.D., Silva, G.V.D., Toldo, E.E. and González, M., 2013. Spatial and numerical methodologies on coastal erosion and flooding risk assessment. In *Coastal hazards* (pp. 423-442). Springer, Dordrecht.
- Boruff, B.J., Emrich, C. and Cutter, S.L., 2005. Erosion hazard vulnerability of US coastal counties. *Journal of Coastal research*, 21(5), pp.932-942.
- Boumboulis, V., Apostolopoulos, D., Depountis, N. and Nikolakopoulos, K., 2021. The Importance of Geotechnical Evaluation and Shoreline Evolution in Coastal Vulnerability Index Calculations. *Journal of Marine Science and Engineering*, 9(4), p.423.
- Brooks, J.R., Wigington Jr, P.J., Phillips, D.L., Comeleo, R. and Coulombe, R., 2012. Willamette River Basin surface water isoscape ($\delta^{18}\text{O}$ and $\delta^2\text{H}$): temporal changes of source water within the river. *Ecosphere*, 3(5), pp.1-21.
- Brooks, N. and Adger, W.N., 2005. Assessing and enhancing adaptive capacity. *Adaptation policy frameworks for climate change: Developing strategies, policies and measures*, pp.165-181.

- Bruneau, M., Chang, S.E., Eguchi, R.T., Lee, G.C., O'Rourke, T.D., Reinhorn, A.M., Shinozuka, M., Tierney, K., Wallace, W.A. and Von Winterfeldt, D., 2003. A framework to quantitatively assess and enhance the seismic resilience of communities. *Earthquake spectra*, 19(4), pp.733-752.
- Bryant, E. (2005). *Natural Hazards*. (2nd Ed). New York: Cambridge University Press.
- Caballero, I. and Stumpf, R.P., 2020. Towards routine mapping of shallow bathymetry in environments with variable turbidity: Contribution of Sentinel-2A/B satellites mission. *Remote Sensing*, 12(3), p.451.
- Calil, J., Reguero, B., Zamora, A., Losada, I. and Méndez, F., 2017. Comparative Coastal Risk Index (CCRI): A multidisciplinary risk index for Latin America and the Caribbean. *PLOS ONE*, 12(11), p.e0187011.
- Campbell, J.B. and Wynne, R.H., 2011. *Introduction to remote sensing*. Guilford Press.
- Cao, Y., Cervone, G., Barkley, Z., Lauvaux, T., Deng, A. and Taylor, A., 2017. Analysis of errors introduced by geographic coordinate systems on weather numeric prediction modeling. *Geoscientific Model Development*, 10(9), pp.3425-3440.
- Cardona, O., Ordaz, M., Mora, M., Salgado-Gálvez, M., Bernal, G., Zuloaga-Romero, D., Marulanda Fraume, M., Yamín, L. and González, D., 2014. Global risk assessment: A fully probabilistic seismic and tropical cyclone wind risk assessment. *International Journal of Disaster Risk Reduction*, 10, pp.461-476.
- Casal, G. et al., 2020. Understanding satellite-derived bathymetry using Sentinel 2 imagery and spatial prediction models. *GIScience & Remote Sensing*, 57(3).
- Casal, G., Hedley, J., Monteys, X., Harris, P., Cahalane, C. and McCarthy, T., 2020. Satellite-derived bathymetry in optically complex waters using a model inversion approach and Sentinel-2 data. *Estuarine, Coastal and Shelf Science*, 241, p.106814.
- Cea, L. and Costabile, P., 2022. Flood Risk in Urban Areas: Modelling, Management and Adaptation to Climate Change. A Review. *Hydrology*, 9(3), p.50.
- CHARIM, 2016. Belize National Flood Hazard Mapping Methodology and Validation Report (FINAL VERSION). [online] Caribbean Handbook on Risk Information Management. Available at:

<http://www.charim.net/sites/default/files/handbook/maps/BELIZE/CHARIM_Flood_Report_Belize.pdf> [Accessed 27 September 2022].

Chénier, R., Faucher, M. and Ahola, R., 2018. Satellite-Derived Bathymetry for Improving Canadian Hydrographic Service Charts. *ISPRS International Journal of Geo-Information*, 7(8), p.306.

Cherrington, E., Griffin, R., Anderson, E., Hernandez Sandoval, B., Flores-Anderson, A., Muench, R., Markert, K., Adams, E., Limaye, A. and Irwin, D., 2020. Use of public Earth observation data for tracking progress in sustainable management of coastal forest ecosystems in Belize, Central America. *Remote Sensing of Environment*, 245, p.111798.

Chiocci, F., Cattaneo, A. & Urgeles, R., 2011. Seafloor mapping for geohazard assessment: state of the art. *Marine Geophysical Research*, Volume 32, pp. 1-11.

Cho, L., 2005. Marine protected areas: a tool for integrated coastal management in Belize. *Ocean & Coastal Management*, 48(11-12), pp.932-947.

Choubin, B., Solaimani, K., Habibnejad Roshan, M. and Malekian, A., 2017. Watershed classification by remote sensing indices: A fuzzy c-means clustering approach. *Journal of Mountain Science*, 14(10), pp.2053-2063.

Cicin-Sain, B. and Belfiore, S., 2005. Linking marine protected areas to integrated coastal and ocean management: A review of theory and practice. *Ocean & Coastal Management*, 48(11-12), pp.847-868.

Cissell, J.R., Canty, S.W., Steinberg, M.K. and Simpson, L.T., 2021. Mapping national mangrove cover for Belize using Google Earth Engine and Sentinel-2 imagery. *Applied Sciences*, 11(9), p.4258.

Cogswell, A., B.J.W., Greenan, Greyson, P., 2018. *Ocean Coast Manag.* 160 (46), 51.

Collard, F., Ardhuin, F. and Chapron, B., 2005. Extraction of coastal ocean wave fields from SAR images. *IEEE Journal of Oceanic Engineering*, 30(3), pp.526-533.

Colon, C., Hallegatte, S. and Rozenberg, J., 2021. Criticality analysis of a country's transport network via an agent-based supply chain model. *Nature Sustainability*, 4(3), pp.209-215.

Copernicus, 2022. Copernicus Open Access Hub. [online] Copernicus SciHub. Available at: <<https://scihub.copernicus.eu/dhus/#/home>> [Accessed 27 September 2022].

- Corbane, C., Martino, P., Panagiotis, P., Aneta, F.J., Michele, M., Sergio, F., Marcello, S., Daniele, E., Gustavo, N. and Thomas, K., 2020. The grey-green divide: multi-temporal analysis of greenness across 10,000 urban centres derived from the Global Human Settlement Layer (GHSL). *International Journal of Digital Earth*, 13(1), pp.101-118.
- Cote, M. and Nightingale, A.J., 2012. Resilience thinking meets social theory: situating social change in socio-ecological systems (SES) research. *Progress in human geography*, 36(4), pp.475-489.
- Cui, L., Li, G., Ouyang, N., Mu, F., Yan, F., Zhang, Y. and Huang, X., 2018. Analyzing coastal wetland degradation and its key restoration technologies in the coastal area of Jiangsu, China. *Wetlands*, 38(3), pp.525-537.
- Cutter, S.L., Boruff, B.J. and Shirley, W.L., 2012. Social vulnerability to environmental hazards. In *Hazards vulnerability and environmental justice* (pp. 143-160). Routledge.
- CZMAI, 2021. GEO BON- Microsoft: EBV's on the Cloud AI for the National Belize Marine Habitat Map - Belize Coastal Zone Management. [online] Belize Coastal Zone Management. Available at: <<https://www.coastalzonebelize.org/portfolio/ai-for-belize-marine-habitat-map/>> [Accessed 27 September 2022].
- Dark, S.J. and Bram, D., 2007. The modifiable areal unit problem (MAUP) in physical geography. *Progress in Physical Geography*, 31(5), pp.471-479.
- DasGupta, R. and Shaw, R., 2017. Disaster risk reduction: A critical approach. In *The Routledge handbook of disaster risk reduction including climate change adaptation* (pp. 12-23). Routledge.
- De Dominicis, M., Wolf, J., van Hespén, R. et al. Mangrove forests can be an effective coastal defence in the Pearl River Delta, China. *Commun Earth Environ* 4, 13 (2023). <https://doi.org/10.1038/s43247-022-00672-7>
- Del Río, L. and Gracia, F.J., 2009. Erosion risk assessment of active coastal cliffs in temperate environments. *Geomorphology*, 112(1-2), pp.82-95.
- Diedrich, A., 2007. The impacts of tourism on coral reef conservation awareness and support in coastal communities in Belize. *Coral Reefs*, 26(4), pp.985-996.
- Diez, P.G., Perillo, G.M. and Piccolo, M.C., 2007. Vulnerability to sea-level rise on the coast of the Buenos Aires Province. *Journal of Coastal Research*, 23(1), pp.119-126.

- Dodet, G., Piolle, J.F., Quilfen, Y., Abdalla, S., Accensi, M., Arduin, F., Ash, E., Bidlot, J.R., Gommenginger, C., Marechal, G. and Passaro, M., 2020. The Sea State CCI dataset v1: towards a sea state climate data record based on satellite observations. *Earth System Science Data*, 12(3), pp.1929-1951.
- Doyle, C., Beach, T. and Luzzadder-Beach, S., 2021. Tropical Forest and Wetland Losses and the Role of Protected Areas in Northwestern Belize, Revealed from Landsat and Machine Learning. *Remote Sensing*, 13(3), p.379.
- Eren, F., Pe'eri, S., Rzhanov, Y. & Ward, L., 2018. Bottom characterization by using airborne lidar bathymetry (ALB) waveform features obtained from bottom return residual analysis. *Remote Sensing of Environment*, Volume 206, pp. 260-274.
- ESA, 2020. Newcomers Earth Observation Guide | ESA Business Applications. [online] European Space Agency. Available at: <<https://business.esa.int/newcomers-earth-observation-guide>> [Accessed 27 September 2022].
- European Environment Agency, 2011. Methods for assessing coastal vulnerability to climate change. Bologna: European Environment Agency.
- Farr, T.G., Rosen, P.A., Caro, E., Crippen, R., Duren, R., Hensley, S., Kobrick, M., Paller, M., Rodriguez, E., Roth, L. and Seal, D., 2007. The shuttle radar topography mission. *Reviews of geophysics*, 45(2).
- Fernandez-Macho, J., Gonzalez, P. and Virto, J., 2020. Assessing anthropogenic vulnerability of coastal regions: DEA-based index and rankings for the European Atlantic Area. *Marine Policy*, 119, p.104030.
- Foley, M. et al., 2010. Guiding ecological principles for marine spatial planning. *Marine Policy*, 34(5), pp. 955-966.
- Foody, G.M. and Arora, M.K. (1997) An Evaluation of Some Factors Affecting the Accuracy of Classification by an Artificial Neural Network. *International Journal of Remote Sensing*, 18, 799-810.
- Fuss, C.E., 2013. Digital elevation model generation and fusion (Doctoral dissertation, University of Guelph).
- Füssel, H.M. and Klein, R.J., 2006. Climate change vulnerability assessments: an evolution of conceptual thinking. *Climatic change*, 75(3), pp.301-329.

- Gamon, J.A., Wang, R., Gholizadeh, H., Zutta, B., Townsend, P.A. and Cavender-Bares, J., 2020. Consideration of scale in remote sensing of biodiversity. *Remote sensing of plant biodiversity*, pp.425-447.
- Gao, Y., Mas, J., Kerle, N. and Navarrete Pacheco, J., 2011. Optimal region growing segmentation and its effect on classification accuracy. *International Journal of Remote Sensing*, 32(13), pp.3747-3763.
- Gargiulo, C., Battarra, R. and Tremiterra, M., 2020. Coastal areas and climate change: A decision support tool for implementing adaptation measures. *Land Use Policy*, 91, p.104413.
- Gargiulo, C., Battarra, R. and Tremiterra, M.R., 2020. Coastal areas and climate change: A decision support tool for implementing adaptation measures. *Land Use Policy*, 91, p.104413.
- GFDRR, 2000. Belize Assessment of the Damage Caused by Hurricane Keith 2000 | GFDRR. [online] GFDRR. Available at: <<https://www.gfdr.org/en/publication/belize-assessment-damage-caused-hurricane-keith-2000>> [Accessed 27 September 2022].
- Ghiasian, M., Carrick, J., Rhode-Barbarigos, L., Haus, B., Baker, A.C. and Lirman, D. (2021), Dissipation of wave energy by a hybrid artificial reef in a wave simulator: implications for coastal resilience and shoreline protection. *Limnol Oceanogr Methods*, 19: 1-7. <https://doi.org/10.1002/lom3.10400>
- Gibb, J., Sheffield, A., Foster, G., 1992. A Standardized Coastal Sensitivity Index Based on an Initial Framework for Physical Coastal Hazards Information. New Zealand Department of Conservation, pp. 101 Science and Research Series, No. 55.
- Gibson, J., 2011. The Belize Barrier Reef: A World Heritage Site. *Fisheries Centre Research Reports*, 19(6), p.8.
- Gibson, J., McField, M. and Wells, S., 1998. Coral reef management in Belize: an approach through integrated coastal zone management. *Ocean & Coastal Management*, 39(3), pp.229-244.
- Gornitz, V. M., Daniels, R. C., White, T. W., & Birdwell, K. R. (1994). The Development of a Coastal Risk Assessment Database: Vulnerability to Sea-Level Rise in the U.S. Southeast. *Journal of Coastal Research*, 327–338. <http://www.jstor.org/stable/25735608>
- Gornitz, V., 1991. Global coastal hazards from future sea level rise. *Palaeogeography, Palaeoclimatology, Palaeoecology*, 89(4), pp.379-398.

- Graham, R.T., Carcamo, R., Rhodes, K.L., Roberts, C.M. and Requena, N., 2008. Historical and contemporary evidence of a mutton snapper (*Lutjanus analis* Cuvier, 1828) spawning aggregation fishery in decline. *Coral Reefs*, 27(2), pp.311-319.
- Green, E.P., Mumby, P.J., Edwards, A.J. and Clark, C.D., 1996. A review of remote sensing for the assessment and management of tropical coastal resources. *Coastal management*, 24(1), pp.1-40.
- Greig, L. A., Marmorek, D. R., Murray, C., & Robinson, D. C. E. (2013). Insight into enabling adaptive management. *Ecology and Society*, 18(3), 24.
<http://dx.doi.org/10.5751/ES-05686-180324>.
- Guannel, G., Arkema, K., Ruggiero, P. and Verutes, G., 2016. The Power of Three: Coral Reefs, Seagrasses and Mangroves Protect Coastal Regions and Increase Their Resilience. *PLOS ONE*, 11(7), p.e0158094.
- Guo, Q., Li, W., Yu, H., and Alvarez, O. (2010). Effects of topographic variability and lidar sampling density on several DEM interpolation methods. *Photogramm. Eng. Remote Sensing* 6, 701–712. doi: 10.14358/PERS.76.6.701
- Hale, L.Z., Meliane, I., Davidson, S., Sandwith, T., Beck, M., Hoekstra, J., Spalding, M., Murawski, S., Cyr, N., Osgood, K. and Hatziolos, M., 2009. Ecosystem-based adaptation in marine and coastal ecosystems. *Renewable Resources Journal*, 25(4), pp.21-28.
- Hanafin, J.A., Quilfen, Y., Arduin, F., Sienkiewicz, J., Queffeuilou, P., Obrebski, M., Chapron, B., Reul, N., Collard, F., Corman, D. and de Azevedo, E.B., 2012. Phenomenal sea states and swell from a North Atlantic storm in February 2011: A comprehensive analysis. *Bulletin of the American Meteorological Society*, 93(12), pp.1825-1832.
- Harvey, T., Krause-Jensen, D., Stæhr, P.A., Groom, G.B. and Hansen, L.B., 2018. Literature Review of Remote Sensing Technologies for Coastal Chlorophyll-a Observations and Vegetation Coverage: Part of ReSTEK-Brug Af Remote Sensing Teknologier Til Opgørelse Af Klorofyl-Koncentrationer Og Vegetationsudbredelse i Danske Kystvande. No. 112. Technical Report from DCE-Danish Centre for Environment and Energy. Aarhus University, DCE–Danish Centre for Environment and Energy,. <http://dce2.au.dk/pub/TR112.pdf>.
- Harvey, N. and Nicholls, R., 2008. Global sea-level rise and coastal vulnerability. *Sustainability Science*, 3(1), pp.5-7.

- Hayakawa, Y., Oguchi, T. and Lin, Z., 2008. Comparison of new and existing global digital elevation models: ASTER G-DEM and SRTM-3. *Geophysical Research Letters*, 35(17).
- Hedley, J., 2013. *Hyperspectral Applications*. In: J. Goodman, S. Purkis & S. Phinn, eds. *Coral Reef Remote Sensing*. New York: Springer, pp. 79-112.
- Hedley, J. D., Roelfsema, C. M., Chollett, I., Harborne, A. R., Heron, S. F., Weeks, S., et al. (2016). Remote sensing of coral reefs for monitoring and management: a review. *Remote Sens.* 8, 118–157. doi: 10.3390/rs8020118.
- Hedley, J., Roelfsema, C. & Phinn, S., 2009. Efficient radiative transfer model inversion for remote sensing applications. *Remote Sensing of Environment*, 113(11), pp. 2527-2532.
- Hedley, J., Roelfsema, C., Chollett, I., Harborne, A., Heron, S., Weeks, S., Skirving, W., Strong, A., Eakin, C., Christensen, T., Ticzon, V., Bejarano, S. and Mumby, P., 2016. *Remote Sensing of Coral Reefs for Monitoring and Management: A Review*. *Remote Sensing*, 8(2), p.118.
- Hedley, J., Roelfsema, C., Koetz, B. & Phinn, S., 2012. Capability of the Sentinel 2 mission for tropical coral reef mapping and coral bleaching detection. *Remote Sensing of Environment*, Volume 120, pp. 145-155.
- Hedley, J.D., Roelfsema, C.M., Phinn, S.R. and Mumby, P.J., 2012. Environmental and sensor limitations in optical remote sensing of coral reefs: Implications for monitoring and sensor design. *Remote Sensing*, 4(1), pp.271-302.
- Hinkel, J., Church, J., Gregory, J., Lambert, E., Le Cozannet, G., Lowe, J., McInnes, K., Nicholls, R., Pol, T. and Wal, R., 2019. Meeting User Needs for Sea Level Rise Information: A Decision Analysis Perspective. *Earth's Future*, 7(3), pp.320-337.
- Holdgate, M.W., 1979. *A perspective of environmental pollution*. Cambridge University Press.
- Hopper, T. and Meixler, M., 2016. Modeling Coastal Vulnerability through Space and Time. *PLOS ONE*, 11(10), p.e0163495.
- Horsburgh, K.J. and Wilson, C., 2007. Tide-surge interaction and its role in the distribution of surge residuals in the North Sea. *Journal of Geophysical Research: Oceans*, 112(C8).

- Huang, C., Davis, L.S. and Townshend, J.R.G., 2002. An assessment of support vector machines for land cover classification. *International Journal of remote sensing*, 23(4), pp.725-749.
- Hughes, G., 1968. On the mean accuracy of statistical pattern recognizers. *IEEE transactions on information theory*, 14(1), pp.55-63.
- Hzami, A., Heggy, E., Amrouni, O., Mahé, G., Maanan, M. and Abdeljaouad, S., 2021. Alarming coastal vulnerability of the deltaic and sandy beaches of North Africa. *Scientific reports*, 11(1), pp.1-15.
- IHO, 2021. *Status of Hydrographic Surveying and Charting Worldwide*, Monaco: International Hydrographic Organisation.
- IHO, 2022. *IHO Publication C-55 Status of Hydrographic Surveying and Charting Worldwide*. [online] INTERNATIONAL HYDROGRAPHIC ORGANIZATION. Available at: <<https://iho.int/uploads/user/pubs/cb/c-55/c55.pdf>> [Accessed 27 September 2022].
- Imamura, F., Boret, S.P., Suppasri, A. and Muhari, A., 2019. Recent occurrences of serious tsunami damage and the future challenges of tsunami disaster risk reduction. *Progress in Disaster Science*, 1, p.100009.
- IPCC, 2012: *Managing the Risks of Extreme Events and Disasters to Advance Climate Change Adaptation*. A Special Report of Working Groups I and II of the Intergovernmental Panel on Climate Change [Field, C.B., V. Barros, T.F. Stocker, D. Qin, D.J. Dokken, K.L. Ebi, M.D. Mastrandrea, K.J. Mach, G.-K. Plattner, S.K. Allen, M. Tignor, and P.M. Midgley (eds.)]. Cambridge University Press, Cambridge, UK, and New York, NY, USA, 582 pp.
- Ismail, Z. and Jaafar, J., 2013. DEM derived from photogrammetric generated DSM using morphological filter. 2013 IEEE 4th Control and System Graduate Research Colloquium,.
- Jackson, J.B.C., Donovan, M.K., Cramer, K.L. and Lam, V.V., 2014. Status and trends of Caribbean coral reefs. *Global coral reef monitoring network*, IUCN, Gland, Switzerland, pp.1970-2012.
- Jain, A.K., 2010. Data clustering: 50 years beyond K-means. *Pattern recognition letters*, 31(8), pp.651-666.

- James, N. & Ginsburg, R., 1991. *The Seaward Margin of the Belize Barrier and Atoll Reefs: Morphology, Sedimentology, Organism Distribution and Late Quaternary History*. 2nd ed. Hoboken: Wiley-Blackwell.
- Janssen, P., 2004. *The interaction of ocean waves and wind*. Cambridge University Press.
- Japan Space Systems, 2016. Features of ASTER GDEM. [online] ASTER Global Digital Elevation Model. Available at: <<https://www.jspacesystems.or.jp/ersdac/GDEM/E/2.html>> [Accessed 28 September 2022].
- Jevrejeva, S., Brichenov, L., Brown, J., Byrne, D., De Dominicis, M., Matthews, A., Rynders, S., Palanisamy, H. and Wolf, J., 2020. Quantifying processes contributing to marine hazards to inform coastal climate resilience assessments, demonstrated for the Caribbean Sea. *Natural Hazards and Earth System Sciences*, 20(10), pp.2609-2626.
- Jiang, H., 2020. Evaluation of altimeter undersampling in estimating global wind and wave climate using virtual observation. *Remote Sensing of Environment*, 245, p.111840.
- Jiang, H., Zheng, H. and Mu, L., 2020. Improving altimeter wind speed retrievals using ocean wave parameters. *IEEE Journal of Selected Topics in Applied Earth Observations and Remote Sensing*, 13, pp.1917-1924.
- Jordan, C.J., Dijkstra, T. and Grebby, S., 2016. Risk information services for Disaster Risk Management (DRM) in the Caribbean: mainstreaming opportunities. *Journal of Coastal Research*, 2012. *Remote Sensing of Coastal and Ocean Currents: An Overview*. 28(3), p.576.
- Ju, H., Niu, C., Zhang, S., Jiang, W., Zhang, Z., Zhang, X., Yang, Z. and Cui, Y., 2021. Spatiotemporal patterns and modifiable areal unit problems of the landscape ecological risk in coastal areas: A case study of the Shandong Peninsula, China. *Journal of Cleaner Production*, 310, p.127522.
- Juanes, J., Puente, A., & Ramos, E. (2017). A global approach to hierarchical classification of coastal waters at different spatial scales: The NEA case. *Journal of the Marine Biological Association of the United Kingdom*, 97(3), 465-476. doi:10.1017/S0025315416000801
- Kaab, A., 2014. Climatology of snow cover and snow water equivalent based on satellite data. [online] EuMeTrain Resources. Available at: <https://resources.eumetrain.org/data/3/358/print_2.htm> [Accessed 28 September 2022].

- Kamal, M. and Phinn, S., 2011. Hyperspectral data for mangrove species mapping: A comparison of pixel-based and object-based approach. *Remote Sensing*, 3(10), pp.2222-2242.
- Kanno, A., Tanaka, Y., Kurosawa, A. and Sekine, M., 2013. Generalized Lyzenga's Predictor of Shallow Water Depth for Multispectral Satellite Imagery. *Marine Geodesy*, 36(4), pp.365-376.
- Kapucu, N., Hawkins, C. and Rivera, F., 2013. Disaster Preparedness and Resilience for Rural Communities. *Risk, Hazards & Crisis in Public Policy*, 4(4), pp.215-233.
- Karlsson, M. and Mclean, E.L. (2020) Caribbean small-scale fishers' strategies for extreme weather events: Lessons for Adaptive Capacity from the Dominican Republic and Belize, *Coastal Management*, 48(5), pp. 456–480. Available at: <https://doi.org/10.1080/08920753.2020.1795971>.
- Karlsson, M., van Oort, B. and Romstad, B., 2015. What we have lost and cannot become: societal outcomes of coastal erosion in southern Belize. *Ecology and Society*, 20(1).
- Kearney, M.S. (2013). Coastal Risk Versus Vulnerability in an Uncertain Sea Level Future. In: Finkl, C. (eds) *Coastal Hazards*. Coastal Research Library, vol 1000. Springer, Dordrecht. https://doi.org/10.1007/978-94-007-5234-4_4
- Kelman, I., 2018. Islandness within climate change narratives of small island developing states (SIDS). *Island Studies Journal*, 13(1), pp.149-166.
- Kennedy, E., C. M. Roelfsema, M. B. Lyons, E. Kovacs, R. Borrego-Acevedo, M. Roe, S. R. Phinn, K. Larsen, N. Murray, D. Yuwono, J. Wolff and P. Tudman (2021). "Reef Cover, a coral reef classification for global habitat mapping from remote sensing." *Scientific Data*.
- Knapp, K. R., M. C. Kruk, D. H. Levinson, H. J. Diamond, and C. J. Neumann, 2010: The International Best Track Archive for Climate Stewardship (IBTrACS): Unifying tropical cyclone best track data. *Bulletin of the American Meteorological Society*, 91, 363-376. doi:10.1175/2009BAMS2755.1
- Koch, E., Barbier, E., Silliman, B., Reed, D., Perillo, G., Hacker, S., Granek, E., Primavera, J., Muthiga, N., Polasky, S., Halpern, B., Kennedy, C., Kappel, C. and Wolanski, E., 2009. Non-linearity in ecosystem services: temporal and spatial variability in coastal protection. *Frontiers in Ecology and the Environment*, 7(1), pp.29-37.

- Kopp, R., Gilmore, E., Little, C., Lorenzo-Trueba, J., Ramenzoni, V. and Sweet, W., 2019. Usable Science for Managing the Risks of Sea-Level Rise. *Earth's Future*, 7(12), pp.1235-1269.
- Koroglu, A., Ranasinghe, R., Jiménez, J.A. and Dastgheib, A., 2019. Comparison of coastal vulnerability index applications for Barcelona Province. *Ocean & coastal management*, 178, p.104799.
- Kovaleva, O., Sergeev, A. and Ryabchuk, D., 2022. Coastal vulnerability index as a tool for current state assessment and anthropogenic activity planning for the Eastern Gulf of Finland coastal zone (the Baltic Sea). *Applied Geography*, 143, p.102710.
- Kulkarni, S.C. and Rege, P.P., 2020. Pixel level fusion techniques for SAR and optical images: A review. *Information Fusion*, 59, pp.13-29.
- Lane, D., Mercer Clarke, C., Forbes, D.L. and Watson, P., 2013. The gathering storm: managing adaptation to environmental change in coastal communities and small islands. *Sustainability science*, 8(3), pp.469-489.
- Laporte, J., Dolou, H., Avis, J. & Arino, O., 2020. Thirty Years of Satellite Derived Bathymetry: The charting tool that Hydrographers can no longer ignore.. *International Hydrographic Review*, November, pp. 129-154.
- Lary, D.J., Zewdie, G.K., Liu, X., Wu, D., Levetin, E., Allee, R.J., Malakar, N., Walker, A., Mussa, H., Mannino, A. and Aurin, D., 2018. Machine learning applications for earth observation. *Earth observation open science and innovation*, 165.
- Law-Chune, S., Aouf, L., Dalphinnet, A., Levier, B., Drillet, Y. and Drevillon, M., 2021. WAVERYS: a CMEMS global wave reanalysis during the altimetry period. *Ocean Dynamics*, 71(3), pp.357-378.
- Le Cozannet, G., Kervyn, M., Russo, S., Ifejika Speranza, C., Ferrier, P., Foumelis, M., Lopez, T. and Modaressi, H., 2020. Space-based earth observations for disaster risk management. *Surveys in geophysics*, 41(6), pp.1209-1235.
- Leichenko, R., 2011. Climate change and urban resilience. *Current opinion in environmental sustainability*, 3(3), pp.164-168.

- Li, C., Wang, J., Wang, L., Hu, L. and Gong, P., 2014. Comparison of classification algorithms and training sample sizes in urban land classification with Landsat thematic mapper imagery. *Remote sensing*, 6(2), pp.964-983.
- Liang, S. and Wang, J. eds., 2019. *Advanced remote sensing: terrestrial information extraction and applications*. Academic Press.
- Lindsey, R., 2016. 2015 State of the Climate: El Niño came, saw, and conquered. [online] Climate.gov. Available at: <<https://www.climate.gov/news-features/understanding-climate/2015-state-climate-el-ni%C3%B1o-came-saw-and-conquered>> [Accessed 27 September 2022].
- Lionello, P., Nicholls, R., Umgiesser, G. and Zanchettin, D., 2021. Venice flooding and sea level: past evolution, present issues, and future projections (introduction to the special issue). *Natural Hazards and Earth System Sciences*, 21(8), pp.2633-2641.
- Lloyd, M., Peel, D. and Duck, R., 2013. Towards a social–ecological resilience framework for coastal planning. *Land Use Policy*, 30(1), pp.925-933.
- López Royo, M., Ranasinghe, R. and Jiménez, J., 2016. A Rapid, Low-Cost Approach to Coastal Vulnerability Assessment at a National Level. *Journal of Coastal Research*, 320, pp.932-945.
- Louvard, P., Cook, H., Smithers, C. and Laporte, J., 2022. A New Approach to Satellite-Derived Bathymetry: An Exercise in Seabed 2030 Coastal Surveys. *Remote Sensing*, 14(18), p.4484.
- Lu, D. and Weng, Q., 2007. A survey of image classification methods and techniques for improving classification performance. *International journal of Remote sensing*, 28(5), pp.823-870.
- Luijendijk, A., Hagenaars, G., Ranasinghe, R., Baart, F., Donchyts, G. and Aarninkhof, S., 2018. The state of the world's beaches. *Scientific reports*, 8(1), pp.1-11.
- Lyzenga, D., Malinas, N. & Tanis, F., 2006. Multispectral bathymetry using a simple physically based algorithm. *IEEE Transactions on Geoscience and Remote Sensing*, 44(8), pp. 2251-2259.

- Maguire, B., Potts, J. and Fletcher, S., 2012. The role of stakeholders in the marine planning process—Stakeholder analysis within the Solent, United Kingdom. *Marine Policy*, 36(1), pp.246-257.
- Malone, E. and Engle, N., 2011. Evaluating regional vulnerability to climate change: purposes and methods. *WIREs Climate Change*, 2(3), pp.462-474.
- Malthus, T. and Mumby, P., 2003. Remote sensing of the coastal zone: An overview and priorities for future research. *International Journal of Remote Sensing*, 24(13), pp.2805-2815.
- Marcos, M. and Woodworth, P., 2017. Spatiotemporal changes in extreme sea levels along the coasts of the North Atlantic and the Gulf of Mexico. *Journal of Geophysical Research: Oceans*, 122(9), pp.7031-7048.
- Markert, A., Griffin, R. and Sever, T., 2014, December. Using a Geographic Information System to Assess the Risk of Hurricane Hazards on the Maya Civilization. In 2014 AGU Fall Meeting. AGU.
- Masoero, A., 2016. Strong El Niño, Increased Preparedness – 2015-2016 El Niño in South America – FloodList. [online] Floodlist.com. Available at: <<https://floodlist.com/america/strong-el-nino-increased-preparedness-2015-2016-south-america>> [Accessed 27 September 2022].
- Masselink, G., Russell, P., Rennie, A., Brooks, S. and Spencer, T. (2020) Impacts of climate change on coastal geomorphology and coastal erosion relevant to the coastal and marine environment around the UK. *MCCIP Science Review 2020*, 158– 189.
- Maxwell, A., Warner, T. and Fang, F., 2018. Implementation of machine-learning classification in remote sensing: an applied review. *International Journal of Remote Sensing*, 39(9), pp.2784-2817.
- McIntosh, R. and Becker, A., 2019. Expert evaluation of open-data indicators of seaport vulnerability to climate and extreme weather impacts for U.S. North Atlantic ports. *Ocean & Coastal Management*, 180, p.104911.
- McIvor, A., Spencer, T., Möller, I. and Spalding, M., 2016. 2| Coastal defense services provided by mangroves. *Managing Coasts with Natural Solutions*, 24.
- McLaughlin, S., Cooper, A., 2010. A Multi-scale coastal vulnerability index: A tool for coastal managers? *Environ. Hazards* 9 (3), 233–248. <https://doi.org/10.3763/ehaz.2010.0052>

- McNeill, D.F., Janson, X., Bergman, K.L., Eberli, G.P. (2010). Belize: A Modern Example of a Mixed Carbonate-Siliciclastic Shelf. In: Westphal, H., Riegl, B., Eberli, G. (eds) Carbonate Depositional Systems: Assessing Dimensions and Controlling Parameters. Springer, Dordrecht. https://doi.org/10.1007/978-90-481-9364-6_3
- Meerman, J. and W. Sabido. 2004. Central American Ecosystems: Belize. Programme for Belize, Belize City. 2 volumes 50 + 88 pp.
- Meskill, L., 2013. UNESCO and the fate of the World Heritage Indigenous Peoples Council of Experts (WHIPCOE). *International Journal of Cultural Property*, 20(2), pp.155-174.
- Millard, Koreen, and Murray Richardson. 2015. On the Importance of Training Data Sample Selection in Random Forest Image Classification: A Case Study in Peatland Ecosystem Mapping. *Remote Sensing* 7, no. 7: 8489-8515.
- Misra, A. and Ramakrishnan, B., 2020. Assessment of coastal geomorphological changes using multi-temporal Satellite-Derived Bathymetry. *Continental Shelf Research*, 207, p.104213.
- Moreno, P.S. Ecotourism Along the Meso-American Caribbean Reef: The Impacts of Foreign Investment. *Hum Ecol* 33, 217–244 (2005). <https://doi.org/10.1007/s10745-005-2433-9>
- Morrow, R., Fu, L.L., Arduin, F., Benkiran, M., Chapron, B., Cosme, E., d'Ovidio, F., Farrar, J.T., Gille, S.T., Lapeyre, G. and Le Traon, P.Y., 2019. Global observations of fine-scale ocean surface topography with the Surface Water and Ocean Topography (SWOT) mission. *Frontiers in Marine Science*, 6, p.232.
- Muler, M. and Bonetti, J., 2014. An integrated approach to assess wave exposure in coastal areas for vulnerability analysis. *Marine Geodesy*, 37(2), pp.220-237.
- Mullick, M., Tanim, A. and Islam, S., 2019. Coastal vulnerability analysis of Bangladesh coast using fuzzy logic based geospatial techniques. *Ocean & Coastal Management*, 174, pp.154-169.
- Mumby, P.J., Skirving, W., Strong, A.E., Hardy, J.T., LeDrew, E.F., Hochberg, E.J., Stumpf, R.P. and David, L.T., 2004. Remote sensing of coral reefs and their physical environment. *Marine pollution bulletin*, 48(3-4), pp.219-228.

- Munich Re, 2017. Munich Re's Natural Hazards Edition. [online] Munich Re. Available at: <<https://www.munichre.com/en/solutions/for-industry-clients/location-risk-intelligence/natural-hazards-edition.html>> [Accessed 27 September 2022].
- Münnich, M. and Neelin, J.D., 2005. Seasonal influence of ENSO on the Atlantic ITCZ and equatorial South America. *Geophysical research letters*, 32(21).
- Murray, M., Zisman, S., Furley, P., Munro, D., Gibson, J., Ratter, J., Bridgewater, S., Minty, C. and Place, C., 2003. The mangroves of Belize: Part 1. distribution, composition and classification. *Forest Ecology and Management*, 174(1-3), pp.265-279.
- Murray, R., 2021. A governance analysis of three MPAs in Belize: Conservation objectives compromised by tourism development priorities?. *Marine Policy*, 127, p.104243.
- Nagendra, H. et al., 2013. Remote sensing for conservation monitoring: Assessing protected areas, habitat extent, habitat condition, species diversity, and threats. *Ecological Indicators*, Volume 33, pp. 45-59.
- Nagendra, H., Lucas, R., Honrado, J.P., Jongman, R.H., Tarantino, C., Adamo, M. and Mairota, P., 2013. Remote sensing for conservation monitoring: Assessing protected areas, habitat extent, habitat condition, species diversity, and threats. *Ecological Indicators*, 33, pp.45-59.
- Nageswara Rao, K., Subraelu, P., Venkateswara Rao, T., Hema Malini, B., Ratheesh, R., Bhattacharya, S. and Rajawat, A.S., 2008. Sea-level rise and coastal vulnerability: an assessment of Andhra Pradesh coast, India through remote sensing and GIS. *Journal of Coastal Conservation*, 12(4), pp.195-207.
- Narayan, S., Beck, M., Reguero, B., Losada, I., van Wesenbeeck, B., Pontee, N., Sanchirico, J., Ingram, J., Lange, G. and Burks-Copes, K., 2016. The Effectiveness, Costs and Coastal Protection Benefits of Natural and Nature-Based Defences. *PLOS ONE*, 11(5), p.e0154735.
- NASA, 2022. Landsat 8 | Landsat Science. [online] Landsat Science | A joint NASA/USGS Earth observation program. Available at: <<https://landsat.gsfc.nasa.gov/satellites/landsat-8/>> [Accessed 28 September 2022].
- National Oceanic and Atmospheric Administration, 2014. Deep Light. [Online] Available at: <https://oceanexplorer.noaa.gov/explorations/04deepscope/background/deeplight/deeplight.html> [Accessed 28 December 2020].

- Nature Conservancy, 2021. How Belize is Transforming the Caribbean. [online] The Nature Conservancy. Available at: <<https://www.nature.org/en-us/what-we-do/our-insights/perspectives/belize-transforming-caribbean-blue-bond/>> [Accessed 27 September 2022].
- Neil Adger, W., Arnell, N. and Tompkins, E., 2005. Successful adaptation to climate change across scales. *Global Environmental Change*, 15(2), pp.77-86.
- NEMO, 2003. BELIZE NATIONAL HAZARD MANAGEMENT PLAN. [online] NEMO. Available at: <http://site.nemo.org.bz/wp-content/publications/Search_Rescue_and_Evacuation_Plan.pdf> [Accessed 27 September 2022].
- NEMO, 2016. INITIAL DAMAGE ASSESSMENT REPORT: HURRICANE EARL. [online] Available at: <<http://site.nemo.org.bz/wp-content/uploads/2019/08/DANA-FINAL-REPORT-Hurricane-Earl-1.pdf>> [Accessed 27 September 2022].
- Nguyen, T., Bonetti, J., Rogers, K. and Woodroffe, C., 2016. Indicator-based assessment of climate-change impacts on coasts: A review of concepts, methodological approaches and vulnerability indices. *Ocean & Coastal Management*, 123, pp.18-43.
- Nicholls, R. and Small, C., 2002. Improved estimates of coastal population and exposure to hazards released. *Eos, Transactions American Geophysical Union*, 83(28), p.301.
- Nicholls, R.J., Klein, R.J. (2005). Climate change and coastal management on Europe's coast. In: Vermaat, J., Salomons, W., Bouwer, L., Turner, K. (eds) *Managing European Coasts*. Environmental Science. Springer, Berlin, Heidelberg. https://doi.org/10.1007/3-540-27150-3_11
- Nicholls, R.J., Wong, P.P., Burkett, V., Codignotto, J., Hay, J., McLean, R., Ragoonaden, S., Woodroffe, C.D., Abuodha, P.A.O., Arblaster, J. and Brown, B., 2007. Coastal systems and low-lying areas.
- Noor, N. and Abdul Maulud, K., 2022. Coastal Vulnerability: A Brief Review on Integrated Assessment in Southeast Asia. *Journal of Marine Science and Engineering*, 10(5), p.595.
- Nuridin, N., Hatta, M., Mashoreng, S., Amri, K., Pulubuhu, D., Aris, A., AS, M. and Komatsu, T., 2019. Remote Sensing of Population and Coral Destruction for Long Term on Small Islands.

- Nurse, A., McLean, R., Agard, J., Brigulio, L., Duvat-Magnan, V., Pelesikoti, N., Tompkins, E. and Webb, A., 2014. *Climate Change 2014: Impacts, Adaptation, and Vulnerability*. Cambridge: Cambridge University Press, pp.1613-1654.
- Okolie, C.J. and Smit, J.L., 2022. A systematic review and meta-analysis of Digital elevation model (DEM) fusion: pre-processing, methods and applications. *ISPRS Journal of Photogrammetry and Remote Sensing*, 188, pp.1-29.
- Onat, Y., Marchant, M., Francis, O.P. and Kim, K., 2018. Coastal exposure of the Hawaiian Islands using GIS-based index modeling. *Ocean & Coastal Management*, 163, pp.113-129.
- Orejarena-Rondón, A., Orfila, A., Restrepo, J., Ramos, I. and Hernandez-Carrasco, I., 2021. A 60 year wave hindcast dataset in the Caribbean Sea. *Data in Brief*, 37, p.107153.
- Ostfeld, R., Glass, G. & Keesing, F., 2005. Spatial epidemiology: an emerging (or re-emerging) discipline. *Trends in Ecology & Evolution*, 20(6), pp. 328-336.
- Özyurt*, G. and Ergin, A., 2010. Improving coastal vulnerability assessments to sea-level rise: a new indicator-based methodology for decision makers. *Journal of Coastal Research*, 26(2), pp.265-273.
- Pakoksung, K. and Takagi, M., 2021. Assessment and comparison of Digital Elevation Model (DEM) products in varying topographic, land cover regions and its attribute: a case study in Shikoku Island Japan. *Modeling Earth Systems and Environment*, 7, pp.465-484.
- Pal, M. and Mather, P.M. (2005) Support Vector Machines for Classification in Remote Sensing. *International Journal of Remote Sensing*, 26, 1007-1011.
- Pandey, P., Koutsias, N., Petropoulos, G., Srivastava, P. and Ben Dor, E., 2019. Land use/land cover in view of earth observation: data sources, input dimensions, and classifiers—a review of the state of the art. *Geocarto International*, 36(9), pp.957-988.
- Papathoma-Köhle, M., Neuhäuser, B., Ratzinger, K., Wenzel, H. and Dominey-Howes, D., 2007. Elements at risk as a framework for assessing the vulnerability of communities to landslides. *Natural Hazards and Earth System Sciences*, 7(6), pp.765-779.
- Papathoma-Köhle, M., Schlögl, M. and Fuchs, S., 2019. Vulnerability indicators for natural hazards: An innovative selection and weighting approach. *Scientific Reports*, 9(1), pp.1-14.

- Pendleton, E.A., 2010. Coastal vulnerability assessment of the Northern Gulf of Mexico to sea-level rise and coastal change.
- Pendleton, E.A., Thieler, E.,R., Williams, S.J., Beavers, R.S., 2004. Coastal Vulnerability Assessment of Padre Island National Seashore (PAIS) to Sea-Level Rise. USGS report No 2004-1090 Available from: <http://pubs.usgs.gov/of/2004/1090/a>.
- Peregrine, D.H. and Jonsson, I.G., 1983. Interaction of waves and currents.
- Pereira, N.D.S. and Klumb-Oliveira, L.A., 2015. Analysis of the influence of ENSO phenomena on wave climate on the central coastal zone of Rio de Janeiro (Brazil). *Revista de Gestão Costeira Integrada*, 15(3), pp.353-370.
- Perini, L., Calabrese, L., Salerno, G., Ciavola, P. and Armaroli, C., 2016. Evaluation of coastal vulnerability to flooding: comparison of two different methodologies adopted by the Emilia-Romagna region (Italy). *Natural Hazards and Earth System Sciences*, 16(1), pp.181-194.
- Pethick, J.S. and Crooks, S., 2000. Development of a coastal vulnerability index: a geomorphological perspective. *Environmental Conservation*, 27(4), pp.359-367.
- Phinn, S.R, Roelfsema, C.M. and Stumpf, R. (2010). Remote sensing: the promise and the reality. In: Dennison, W., (Ed.) *Coastal Assessment Handbook*, Chapter 15, University of Maryland.
- Piollé, J.-F.; Dodet, G.; Quilfen, Y. (2020): ESA Sea State Climate Change Initiative (Sea_State_cci) : Global remote sensing merged multi-mission monthly gridded significant wave height, L4 product, version 1.1. Centre for Environmental Data Analysis, 30 January 2020.
- Poate, T., Masselink, G., Austin, M.J., Dickson, M. and McCall, R., 2018. The role of bed roughness in wave transformation across sloping rock shore platforms. *Journal of Geophysical Research: Earth Surface*, 123(1), pp.97-123.
- Pottier, A., Catry, T., Trégarot, E., Maréchal, J., Fayad, V., David, G., Sidi Cheikh, M. and Failler, P., 2021. Mapping coastal marine ecosystems of the National Park of Banc d'Arguin (PNBA) in Mauritania using Sentinel-2 imagery. *International Journal of Applied Earth Observation and Geoinformation*, 102, p.102419.

- Poursanidis, D., Traganos, D., Reinartz, P. and Chrysoulakis, N., 2019. On the use of Sentinel-2 for coastal habitat mapping and satellite-derived bathymetry estimation using downscaled coastal aerosol band. *International Journal of Applied Earth Observation and Geoinformation*, 80, pp.58-70.
- Pramudya, F.S., Pan, J. and Devlin, A.T., 2019. Estimation of significant wave height of near-range traveling ocean waves using Sentinel-1 SAR images. *IEEE Journal of Selected Topics in Applied Earth Observations and Remote Sensing*, 12(4), pp.1067-1075.
- PSMSL, 2001. Data and Station Information for BELIZE. [online] PSMSL. Available at: <<https://www.psmsl.org/data/obtaining/stations/1085.php>> [Accessed 28 September 2022].
- Quataert, E., Storlazzi, C., Van Rooijen, A., Cheriton, O. and Van Dongeren, A., 2015. The influence of coral reefs and climate change on wave-driven flooding of tropical coastlines. *Geophysical Research Letters*, 42(15), pp.6407-6415.
- Rathore, P., Kumar, D., Bezdek, J.C., Rajasegarar, S. and Palaniswami, M., 2018. A rapid hybrid clustering algorithm for large volumes of high dimensional data. *IEEE Transactions on Knowledge and Data Engineering*, 31(4), pp.641-654.
- Rhiney, K., 2015. Geographies of Caribbean Vulnerability in a Changing Climate: Issues and Trends. *Geography Compass*, 9(3), pp.97-114.
- Roberts, C., McClean, C., Veron, J. & Hawkins, J., 2002. Marine Biodiversity Hotspots and Conservation Priorities for Tropical Reefs. *Science*, 295(5558), pp. 1280-1284.
- Rodrigue, J.P., 2020. *The geography of transport systems*. Routledge.
- Rodriguez-Galiano, V.F., Ghimire, B., Rogan, J., Chica-Olmo, M. and Rigol-Sanchez, J.P., 2012. An assessment of the effectiveness of a random forest classifier for land-cover classification. *ISPRS journal of photogrammetry and remote sensing*, 67, pp.93-104.
- Romieu, E., Welle, T., Schneiderbauer, S., Pelling, M. and Vinchon, C., 2010. Vulnerability assessment within climate change and natural hazard contexts: revealing gaps and synergies through coastal applications. *Sustainability Science*, 5(2), pp.159-170.
- Rosenthal, A., Verutes, G., McKenzie, E., Arkema, K., Bhagabati, N., Bremer, L., Olwero, N. and Vogl, A., 2014. Process matters: a framework for conducting decision-relevant assessments of ecosystem services. *International Journal of Biodiversity Science, Ecosystem Services & Management*, 11(3), pp.190-204.

- Roukounis, C. N., & Tsihrintzis, V. A. (2022). Indices of Coastal Vulnerability to Climate Change: a Review. *Environmental Processes*, 9(2), 29. <https://doi.org/10.1007/s40710-022-00577-9>
- Roy, D. and Blaschke, T., 2013. Spatial vulnerability assessment of floods in the coastal regions of Bangladesh. *Geomatics, Natural Hazards and Risk*, 6(1), pp.21-44.
- Rueda Zamora, A.C., Vitousek, S., Camus Braña, P., Tomás Sampedro, A., Espejo Hermosa, A., Losada Rodríguez, I., Barnard, P.L., Erikson, P.L., Ruggiero, P.L., Reguero, B.G. and Méndez Incera, F.J., 2017. A global classification of coastal flood hazard climates associated with large-scale oceanographic forcing.
- Sagawa, T., Yamashita, Y., Okumura, T. and Yamanokuchi, T., 2019. Satellite Derived Bathymetry Using Machine Learning and Multi-Temporal Satellite Images. *Remote Sensing*, 11(10), p.1155.
- Salichon J, Le Cozannet G, Modaressi H, Hosford S, Missotten R, McManus K, Marsh S, Paganini M, Ishida C, Plag HP, Labrecque J, Dobson C, Quick J, Giardini D, Takara K, Fukuoka H, Casagli N, Marzocchi W (2007) 2nd IGOS Geohazards Theme report, BRGM
- Saxena, A., Prasad, M., Gupta, A., Bharill, N., Patel, O.P., Tiwari, A., Er, M.J., Ding, W. and Lin, C.T., 2017. A review of clustering techniques and developments. *Neurocomputing*, 267, pp.664-681.
- Scherer, M., Andrade, J., Emerim, E., Felix, A., Oliveira, T., Mondl, H. and Lima, F., 2014. Prioritizing actions for coastal management: A methodological proposal. *Ocean Coastal Management*, 91, pp.17-22.
- Schwarz, R., Mandlburger, G., Pfennigbauer, M. and Pfeifer, N., 2019. Design and evaluation of a full-wave surface and bottom-detection algorithm for LiDAR bathymetry of very shallow waters. *ISPRS journal of photogrammetry and remote sensing*, 150, pp.1-10.
- Sekovski, I., Del Río, L. and Armaroli, C., 2020. Development of a coastal vulnerability index using analytical hierarchy process and application to Ravenna province (Italy). *Ocean & Coastal Management*, 183, p.104982.
- Seong, K., Losey, C. and Gu, D., 2021. Naturally Resilient to Natural Hazards? Urban–Rural Disparities in Hazard Mitigation Grant Program Assistance. *Housing Policy Debate*, 32(1), pp.190-210.

- Sharp, R., Tallis, H.T., Ricketts, T., Guerry, A.D., Wood, S.A., Chaplin-Kramer, R., Nelson, E., Ennaanay, D., Wolny, S., Olwero, N. and Vigerstol, K., 2016. InVEST 3.3. 3 User's Guide. The Natural Capital Project: Stanford University, University of Minnesota, The Nature Conservancy, and World Wildlife Fund.
- Shepherd, J., Bunting, P. and Dymond, J., 2019. Operational Large-Scale Segmentation of Imagery Based on Iterative Elimination. *Remote Sensing*, 11(6), p.658.
- Simpson, M.C., Mercer Clarke, C.S., Clarke, J.D., Scott, D. and Clarke, A.J., 2012. Coastal setbacks in Latin America and the Caribbean: A study of emerging issues and trends that inform guidelines for coastal planning and development.
- Sorensen, J.C. and McCreary, S.T., 1990. Institutional arrangements for managing coastal resources and environments (No. 1). National Park Service, US Department of the Interior.
- Spalding, M., Ruffo, S., Lacambra, C., Meliane, I., Hale, L., Shepard, C. and Beck, M., 2014. The role of ecosystems in coastal protection: Adapting to climate change and coastal hazards. *Ocean & Coastal Management*, 90, pp.50-57.
- Stammer, D., Wal, R., Nicholls, R., Church, J., Le Cozannet, G., Lowe, J., Horton, B., White, K., Behar, D. and Hinkel, J., 2019. Framework for High-End Estimates of Sea Level Rise for Stakeholder Applications. *Earth's Future*, 7(8), pp.923-938.
- Statistical Institute of Belize (SIB). 2017. Population and housing census. Accessed September 27, 2022. <http://sib.org.bz/statistics/>.
- Stehman, S. and Wickham, J., 2011. Pixels, blocks of pixels, and polygons: Choosing a spatial unit for thematic accuracy assessment. *Remote Sensing of Environment*, 115(12), pp.3044-3055.
- Stockdon, H.F., Holman, R.A., Howd, P.A. and Sallenger Jr, A.H., 2006. Empirical parameterization of setup, swash, and runup. *Coastal engineering*, 53(7), pp.573-588.
- Sweetman, B., Cissell, J., Rhine, S. and Steinberg, M., 2018. Land Cover Changes on Ambergris Caye, Belize: A Case Study of Unregulated Tourism Development. *The Professional Geographer*, 71(1), pp.123-134.
- Tempfli, K., Huurneman, G., Bakker, W., Janssen, L.L., Feringa, W.F., Gieske, A.S.M., Grabmaier, K.A., Hecker, C.A., Horn, J.A., Kerle, N. and Van der Meer, F.D., 2009.

- Principles of remote sensing: an introductory textbook. International Institute for Geo-Information Science and Earth Observation.
- The World Bank, 2022. Belize. [online] The World Bank Climate Change Knowledge Portal. Available at: <<https://climateknowledgeportal.worldbank.org/country/belize/vulnerability>> [Accessed 27 September 2022].
- Thia-Eng, C., 1993. Essential elements of integrated coastal zone management. *Ocean & Coastal Management*, 21(1-3), pp.81-108.
- Thieler, E.R., Hammar-Klose, E.S., 2000. National Assessment of Coastal Vulnerability to Future Sea-Level Rise: Preliminary Results for the U.S. Pacific Coast: U.S. Geological Survey, Open-File Report 00-178.
- Timmermans, B., Gommenginger, C., Dodet, G. and Bidlot, J., 2020. Global Wave Height Trends and Variability from New Multimission Satellite Altimeter Products, Reanalyses, and Wave Buoys. *Geophysical Research Letters*, 47(9).
- Toimil A, Losada IJ, Díaz-Simal P, Izaguirre C, Camus P (2017) Multi-sectoral, high-resolution assessment of climate change consequences of coastal flooding. *Clim Change* 145(3–4):431–444.
- Torresan, S., Critto, A., Dalla Valle, M., Harvey, N. and Marcomini, A., 2008. Assessing coastal vulnerability to climate change: comparing segmentation at global and regional scales. *Sustainability Science*, 3(1), pp.45-65.
- Tragaki, A., Gallousi, C. and Karymbalis, E., 2018. Coastal Hazard Vulnerability Assessment Based on Geomorphic, Oceanographic and Demographic Parameters: The Case of the Peloponnese (Southern Greece). *Land*, 7(2), p.56.
- Traganos, D. et al., 2018. Estimating Satellite-Derived Bathymetry (SDB) with the Google Earth Engine and Sentinel-2. *Remote Sensing*, 10(6), p. 859.
- Tulloch, V.J., Possingham, H.P., Jupiter, S.D., Roelfsema, C., Tulloch, A.I. and Klein, C.J., 2013. Incorporating uncertainty associated with habitat data in marine reserve design. *Biological Conservation*, 162, pp.41-51.
- Uddin, K., Matin, M.A. and Meyer, F.J., 2019. Operational flood mapping using multi-temporal Sentinel-1 SAR images: A case study from Bangladesh. *Remote Sensing*, 11(13), p.1581.

- UNDP, 2022. THE UNDP APPROACH TO RISK-INFORMED DEVELOPMENT. [online] UNDP. Available at: <https://www.undp.org/sites/g/files/zskgke326/files/2022-06/The_UNDP_Approach_to_Risk-Informed_Development.pdf> [Accessed 27 September 2022].
- UNESCO, 2022. Belize Barrier Reef Reserve System. [online] UNESCO. Available at: <<https://whc.unesco.org/en/list/764/#:~:text=The%20coastal%20area%20of%20Belize,forest%2C%20coastal%20lagoons%20and%20estuaries.>> [Accessed 27 September 2022].
- USGS and Japan ASTER Science Team (2019). ASTER Global Digital Elevation Model V003 [Data set]. NASA EOSDIS Land Processes DAAC. Accessed 2022-05-11 from <https://doi.org/10.5067/ASTER/ASTGTM.003>
- Verutes, G., Arkema, K., Clarke-Samuels, C., Wood, S., Rosenthal, A., Rosado, S., Canto, M., Bood, N. and Ruckelshaus, M., 2016. Integrated planning that safeguards ecosystems and balances multiple objectives in coastal Belize. *International Journal of Biodiversity Science, Ecosystem Services & Management*, 13(3), pp.1-17.
- Villa, F. and McLEOD, H.E.L.E.N.A., 2002. Environmental vulnerability indicators for environmental planning and decision-making: guidelines and applications. *Environmental management*, 29(3), pp.335-348.
- Wang, L., Shi, C., Diao, C., Ji, W. and Yin, D., 2016. A survey of methods incorporating spatial information in image classification and spectral unmixing. *International Journal of Remote Sensing*, 37(16), pp.3870-3910.
- Weih, R.C. and Riggan, N.D., 2010. Object-based classification vs. pixel-based classification: Comparative importance of multi-resolution imagery. *The International Archives of the Photogrammetry, Remote Sensing and Spatial Information Sciences*, 38(4), p.C7.
- Westley, K., 2021. Satellite-derived bathymetry for maritime archaeology: Testing its effectiveness at two ancient harbours in the Eastern Mediterranean. *Journal of Archaeological Science: Reports*, 38, p.103030.
- Whiteside, T., Boggs, G. and Maier, S., 2011. Comparing object-based and pixel-based classifications for mapping savannas. *International Journal of Applied Earth Observation and Geoinformation*, 13(6), pp.884-893.

- Wikipedia, 2022. k-means clustering - Wikipedia. [online] wikipedia.org. Available at: <https://en.wikipedia.org/wiki/K-means_clustering> [Accessed 27 September 2022].
- Wilson, R.J., Speirs, D.C., Sabatino, A. and Heath, M.R., 2018. A synthetic map of the north-west European Shelf sedimentary environment for applications in marine science. *Earth System Science Data*, 10(1), pp.109-130.
- WMO, 2018. Guide to Wave Analysis and Forecasting. [online] WMO. Available at: <https://library.wmo.int/doc_num.php?explnum_id=10979> [Accessed 27 September 2022].
- Werner, M., 2001. Shuttle radar topography mission (SRTM) mission overview. *Frequenz*, 55(3-4), pp.75-79.
- Wöfl, A. C. et al., 2019. Seafloor Mapping – The Challenge of a Truly Global Ocean Bathymetry. *Frontiers in Marine Science*.
- Wolters, M.L. and Kuenzer, C., 2015. Vulnerability assessments of coastal river deltas- categorization and review. *Journal of Coastal Conservation*, 19(3), pp.345-368.
- WWF, 2022. LIVING PLANET INDEX. [online] WWF. Available at: <https://wwf.panda.org/discover/knowledge_hub/all_publications/living_planet_index2/> [Accessed 27 September 2022].
- Yoo, G., Hwang, J.H. and Choi, C., 2011. Development and application of a methodology for vulnerability assessment of climate change in coastal cities. *Ocean & Coastal Management*, 54(7), pp.524-534.
- Young, C., 2008. Belize's Ecosystems: Threats and Challenges to Conservation in Belize. *Tropical Conservation Science*, 1(1), pp.18-33.
- Young, I.R. and Ribal, A., 2019. Multiplatform evaluation of global trends in wind speed and wave height. *Science*, 364(6440), pp.548-552.
- Yu, J., Rui, Y., Tang, Y.Y. and Tao, D., 2014. High-order distance-based multiview stochastic learning in image classification. *IEEE transactions on cybernetics*, 44(12), pp.2431-2442.
- Zhao, S., Cheng, W., Zhou, C., Chen, X., Zhang, S., Zhou, Z., Liu, H. and Chai, H., 2011. Accuracy assessment of the ASTER GDEM and SRTM3 DEM: an example in the Loess

Plateau and North China Plain of China. *International Journal of Remote Sensing*, 32(23), pp.8081-8093.

Zheng, Y. and Takeuchi, W., 2020. Quantitative assessment and driving force analysis of mangrove forest changes in China from 1985 to 2018 by integrating optical and radar imagery. *ISPRS International Journal of Geo-Information*, 9(9), p.513.

APPENDIX

Appendix 1 – Table of scripts written.

Script Name	Function	Inputs	Output
calculate_CVI_kmeans.py	Cluster coastal segments of 1km based on similar geotechnical properties for each parameter using KMeans. Calculate CVI value per cell.	<ul style="list-style-type: none"> • Terrestrial classification GEOTIFF • Benthic classification GEOTIFF • DEM GEOTIFF • SDB GEOTIFF • Wave climate resampled GEOTIFF • Wind speed intensity GEOTIFF • Coastline extent raster • Sentinel-2 image 	<ul style="list-style-type: none"> • Gridded GEOTIFF of CVI values.
read_netcdf.py	Read in wave data in netcdf format. Sub-sample the data and reproject. Save to GEOTIFF.	<ul style="list-style-type: none"> • WAVERYS model output netcdf 	<ul style="list-style-type: none"> • GEOTIFF sampled wave height.
supervised_classification.py	Supervised object-based image classification using Random Forests classifier.	<ul style="list-style-type: none"> • Sentinel-2 image • Training data shapefile • Number of classes 	<ul style="list-style-type: none"> • GEOTIFF 10m pixels with discrete class values.
waves_resampled.py	Resamples wave climate geotiff so pixels intersect coastline.	<ul style="list-style-type: none"> • Output raster from read_netcdf.py 	<ul style="list-style-type: none"> • GEOTIFF re-sampled wave height.

The location of all CVI scripts associated with this thesis can be found on Github @hcook24

<https://github.com/hcook24/Coastal-Vulnerability-Modelling>